USGS Awards: 03HQGR0057 and 03HQGR0106

FINAL REPORT

CORRELATION OF DAMAGE OF STEEL MOMENT-RESISTING FRAMES TO A VECTOR-VALUED GROUND MOTION PARAMETER SET THAT INCLUDES ENERGY DEMANDS

COLLABORATIVE RESEARCH WITH
THE UNIVERSITY OF TEXAS AT AUSTIN (UT) AND
AIR WORLDWIDE CORPORATION (AIR)

Nicolas Luco[a], Lance Manuel[b], Sridhar Baldava[c], Paolo Bazzurro[d]
[a]AIR Worldwide Corporation, San Francisco, CA 94111
Ph: (415) 912-3111, Fax: (415) 912-3112, E-mail: nico.luco@stanfordalumni.org
[b]Department of Civil Engineering, University of Texas, Austin, TX 78712
Ph: (512) 232-5691, Fax: (512) 471-7259, E-mail: lmanuel@mail.utexas.edu
[c]Department of Civil Engineering, University of Texas, Austin, TX 78712
Ph: (512) 293-4333, Fax: (512) 471-7259, E-mail: sridharb@mail.utexas.edu
[d]AIR Worldwide Corporation, San Francisco, CA 94111
Ph: (415) 912-3111, Fax: (415) 912-3112, E-mail: pbazzurro@air-worldwide.com

Principal investigators: Lance Manuel (UT); Paolo Bazzurro and Nicolas Luco (AIR)

NEHRP Element I: Earthquake Hazard Assessments – Products for Earthquake Loss Reduction

Research supported by the U.S. Geological Survey (USGS), Department of the Interior, under USGS award numbers 03HQGR0057 and 03HQGR0106. The views and conclusions contained in this document are those of the authors and should not be interpreted as necessarily representing the official policies, either expressed or implied, of the U.S. Government.

USGS Awards: 03HQGR0057 and 03HQGR0106

CORRELATION OF DAMAGE OF STEEL MOMENT-RESISTING FRAMES TO A VECTOR-VALUED GROUND MOTION PARAMETER SET THAT INCLUDES ENERGY DEMANDS

COLLABORATIVE RESEARCH WITH
THE UNIVERSITY OF TEXAS AT AUSTIN (UT) AND
AIR WORLDWIDE CORPORATION (AIR)

Nicolas Luco[a], Lance Manuel[b], Sridhar Baldava[c], Paolo Bazzurro[d]
[a]AIR Worldwide Corporation, San Francisco, CA 94111
Ph: (415) 912-3111, Fax: (415) 912-3112, E-mail: nico.luco@stanfordalumni.org
[b]Department of Civil Engineering, University of Texas, Austin, TX 78712
Ph: (512) 232-5691, Fax: (512) 471-7259, E-mail: lmanuel@mail.utexas.edu
[c]Department of Civil Engineering, University of Texas, Austin, TX 78712
Ph: (512) 293-4333, Fax: (512) 471-7259, E-mail: sridharb@mail.utexas.edu
[d]AIR Worldwide Corporation, San Francisco, CA 94111
Ph: (415) 912-3111, Fax: (415) 912-3112, E-mail: pbazzurro@air-worldwide.com

Principal investigators: Lance Manuel (UT); Paolo Bazzurro and Nicolas Luco (AIR)

TECHNICAL ABSTRACT

Prediction of the performance of structures in seismically active regions has traditionally been based on a single scalar ground motion parameter (GMP), most typically spectral acceleration. It is widely accepted, however, that the performance of a structure is dependent on more than a single parameter of ground shaking. Hence, performance predictions based on conventional scalar ground motion parameters are subject to a great deal of variability, which in turn requires greater effort to obtain results with a reasonable level of confidence. It is expected that by including additional information about the ground motion in a set of predictors, one might be able to predict structural performance with smaller variability or, equivalently, require less effort to predict performance with the same level of confidence. The objective of this study is to investigate whether particular vector combinations of GMPs correlate better with structural performance than does the use of a single scalar parameter like spectral acceleration. In particular, we investigate the use of displacement- and energy-based GMPs (i.e., input and absorbed energy) at the fundamental and higher frequencies of a structure in addition to or in lieu of fundamental-mode spectral acceleration. We derive these parameters using both linear elastic and nonlinear inelastic oscillators.

A total of 140 recorded ground motions are considered in this study. These motions include a "near-source" and an "ordinary" set of 70 motions each, recorded at distances (R_{close}) less than and greater than 16 km from the source, respectively. The recordings are from earthquakes of moment magnitudes (M_w) between 5.7 and 7.5, in order that the predictions of structural

response using a particular GMP can be evaluated for different values of M_w and R_{close}. Results from dynamic analyses of elastic, ductile, and brittle models of a 3-, 9-, and 20-story steel moment-resisting frame building subjected to the selected ground motion records are used to evaluate the predictive power of alternative vector-valued GMP sets.

Anticipating that the knowledge of more than a single structural performance measure can help reduce the uncertainty in predicting losses and damage levels, vectors of such performance measures (e.g., inter-story drift ratios) resulting from dynamic analyses under the selected ground motions are studied. While the emphasis is on their dependence on the selected GMPs, the degree of correlation between the structural performance measures is also evaluated for each GMP vector. This is done via multivariate multiple linear regressions (MMLRs). Such regressions are extensions of existing procedures that either consider individual structural performance measures separately or employ a single GMP. Example loss estimates based on selected vectors of correlated structural performance measures (and GMPs) are presented to demonstrate how the regression studies may be used in practice.

The energy- and displacement-based ground motion parameters considered (i.e., input and absorbed energy, and spectral acceleration, either elastic or inelastic) are found to be highly correlated with each other over the range of periods considered here, and therefore they tend to have similar predictive power for the responses of the chosen frames. In other words, including the energy-based GMPs in a vector with spectral acceleration(s) does not, in fact, appreciably improve the structural response predictions. Despite the fairly strong correlation between the inelastic and elastic counterparts of each of these GMPs, however, the use of inelastic GMPs does improve the predictions of structural response, as does the inclusion of elastic GMPs at multiple periods corresponding to the modes of vibration for each building. More specifically, the vector GMPs tend to reduce the conditional variability in structural response, as well as the remaining dependence on earthquake magnitude and source-to-site distance. Furthermore, the vector GMPs reduce the residual correlations between structural response measures, sometimes to the extent that they become negligible for loss estimation purposes. In other cases considered, however, neglecting the correlations between structural response measures (estimated via MMLR) can result in un-conservative estimates of mean losses and the range of potential losses for a given GMP level.

NON-TECHNICAL ABSTRACT

An accurate assessment of seismic building performance is of paramount importance while designing safer new structures and evaluating whether existing ones may need to be strengthened to guarantee an acceptable level of safety to occupants. In addition, better structural performance assessment capabilities can improve the prediction of earthquake-related damage and losses. The availability of reliable loss estimates is crucial to different stakeholders such as owners, tenants, insurance and reinsurance companies, and public organizations responsible for post-earthquake emergency resource management. Ideally, this problem could be solved by mining ground motion, structural damage, and loss data collected from past earthquakes and using statistical tools and engineering principles to develop a sound damage and loss estimation procedure. In the United States, however, only in the very last few years have a large network of recording stations been deployed and a significant database of ground motions recordings become available to scientists although still insufficient in number in the area very close to the rupturing fault. In addition, field data on damage and losses are not systematically collected and the sparse available data are not sufficient to establish robust statistical models for estimating earthquake-induced damage and losses.

Therefore, modern loss estimation procedures are forced to tackle this challenging problem in an alternative way that is based on engineering analysis and analytical computations rather than using empirical data. The problem is usually divided into four sequential parts that are more manageable. The *first* step of this procedure is related to establishing via computer-aided analyses which characteristics of the ground shaking are best related to the level of induced building deformation. The *second* part deals with understanding what level of physical damage may be suffered by all the structural components (e.g., beams and columns) and non-structural components (e.g., interior partitions and glazing) when subject to different levels of deformation. The *third* part deals with identifying repair strategies that may be adopted to fix each component that may be in a given state of damage (e.g., cracks of a certain size in a partition wall) after an earthquake. The *fourth* and last step quantifies the overall performance of the structure in terms of repair cost, downtime, and life safety. The core of the present study fits into the first one of these four steps, namely in the ground motion/structural response interface. The final part of our work, however, shows how, using simplified examples on a 9-story steel moment-resisting frame (SMRF) building, our findings may be used to improve loss estimation.

More specifically, this study investigates the power of several ground motion intensity parameters in predicting deformation levels for a structure. The goal is combined prediction of different but statistically correlated measures of the building response, such as the peak deformation at any story along the height of the building. The peak deformation at a story provides useful information on the state of physical damage likely to be suffered by the structural and non-structural components located at that story. The use of multiple measures of building deformation to estimate losses is an improvement over the customary use of a single measure, such as the maximum lateral deformation at the roof level alone or the peak lateral deformation at the story where it is largest, as it can lead to more precise damage and loss estimates. The novelty of this study is twofold: a) As candidate predictors of response we considered, among others, ground motion parameters that are related to the level of energy that is input into and absorbed by a structure during ground shaking. As is customarily done for other ground motion

parameters, these energy-based parameters are computed for a simple representation of the building, not for the structure itself; b) The correlation between the response measures is accounted for during the prediction exercise via a statistical technique known as multiple multivariate linear regression.

The building responses for computer models of three SMRF buildings of 3, 9, and 20 stories are computed using 140 real ground motion recordings from past earthquakes. The building deformations were computed using nonlinear dynamic analysis. Three different models of each building were considered: perfectly elastic, and inelastic with ductile beam-column connections or with brittle beam-column connections that can fracture. The first model is unrealistic (except at small levels of ground shaking) but it serves the purpose of being a simple reference point for the subsequent, more complicated analyses. The second model is intended to for newer SMRF buildings designed after the 1994 Northridge earthquake, whose beam-column connections are expected to deform beyond the elastic regime without breaking in a brittle fashion. The third model depicts SMRF buildings designed according to the Uniform Building Code before the 1994 Northridge earthquake. Several sets of structural response measures related to peak deformations at different stories were obtained from the dynamic analyses, and these were then statistically studied (jointly) as functions of various sets of ground motion intensity parameters. Results of these regression studies served to indicate which combinations of different ground motion parameters predict the building response most accurately. Finally, we showed a simplified example (for the 9-story building with ductile connections) of how a loss estimation analysis can be carried out with these different sets of ground motion intensity parameters. We also elaborated on the differences in the accuracy of the loss estimates that are obtained in the different cases.

CHAPTER 1 – INTRODUCTION

1.1 SIGNIFICANCE

For structural engineers in seismic regions, prediction of the behavior of structures during earthquakes is of prime importance. Predictions of structural performance due to ground shaking are usually based on ground motion parameters (GMPs) that are well correlated to structural response and, in turn, to damage and monetary loss. An accurate assessment of the seismic performance of buildings is of paramount importance for designing safer new structures and for evaluating whether existing ones may need to be retrofitted to guarantee an acceptable level of safety to occupants. In addition, better performance assessment capabilities can improve the prediction of earthquake-related losses. The availability of reliable loss estimates is crucial to different stakeholders such as owners, tenants, insurance and reinsurance companies, and public organizations responsible for post-earthquake emergency resource management.

The response of a structure to any input ground motion is generally thought to be well correlated with the spectral acceleration at the period of the first mode of vibration of the structure. However, the ground motion record-to-record variability in the structural response at a given spectral acceleration level can be considerable. To overcome the effects of this variability one needs to perform a sufficient number of nonlinear dynamic analyses to predict the structural response with a specified level of confidence. The goal of this study is to explore the possibility of reducing this variability of response predictions by including more than a single parameter (such as first-mode spectral acceleration) in a set of predictor variables. In particular, this study investigates the correlation of structural performance measures with vector combinations of different GMPs. We will compare the predictive power of vectors of GMPs to the predictive power of a scalar GMP used singly. This study also investigates the use of energy-based parameters (both as scalars and as parts of vector combinations), as distinct from displacement-based parameters (such as pseudo-spectral acceleration, which is proportional to spectral displacement), for correlation with the earthquake response of structures.

A unique aspect of the study is the prediction of more than a single structural response measure at a time (such as the roof drift or the maximum inter-story drift over the height of the building) – i.e., the interest is in the prediction of a vector of response measures (e.g., the peak inter-story drifts at all stories) whose components will, in general, be correlated. The knowledge of these various building performance measures simultaneously is expected to improve the accuracy of performance predictions and loss assessments (as will be demonstrated). Multivariate multiple linear regression analyses are carried out to compare the predictive power of the different GMP choices.

1.2 OBJECTIVE

The objective of this research is to investigate whether “vector” combinations of ground motion parameters might correlate better with structural damage (and therefore monetary losses) than any single scalar GMP used alone. (In passing, we note that throughout this report we shall characterize ground shaking by using the term ground motion parameter interchangeably with another commonly used term, Intensity Measure (IM).) Rather than rely on the limited structural damage data that are available from previous earthquakes, results from nonlinear dynamic analyses of model buildings subjected to suites of earthquake records will be used to evaluate the predictive power of the GMPs. Specifically, vector combinations of peak inter-story drifts resulting from each ground motion will be used as measures of structural response, as inter-story drifts are related to both structural and non-structural damage that might occur in an earthquake. Since the response measures will in general be correlated with each other, we will also estimate the covariance matrix of the damage measures given the GMP, as this information is required for estimation of losses from the damage measures (jointly).

1.3 SCOPE

This study focuses on structures and earthquake ground motions pertinent to the Southern California area, although the approach taken here may be applied to other seismic regions as well. In particular, steel moment-resisting frame (SMRF) buildings designed by practicing engineers for Los Angeles conditions (i.e., for UBC Zone 4) as part of the SAC steel project (Phase II) will be utilized. Both near-source and "ordinary" ground motions recorded during historical earthquakes of a range of magnitudes will be considered.

1.4 APPROACH

We have considered 140 real ground motion recordings from intermediate to large magnitude events (with moment magnitude, *M*, between 5.7 and 7.5) recorded at moderate distances (taken here to be less than 36 km from the causative fault). Since the selected structures are relatively symmetric in plan in the two principal directions, only two-dimensional models are considered in the study. Under the assumptions of a rigid diaphragm, the structures are represented as two-dimensional centerline models, with brittle or ductile hinge models for the connections, reflecting the state of design practice before and after the 1994 Northridge earthquake, respectively. As a basis for comparison, elastic (or infinite strength) models of the buildings are also analyzed. The dynamic analyses are carried out using the software programs RUAUMOKO (Carr, 2003) and DRAIN-2DX (Prakash et al., 1993), and the results from the two programs are compared.

Correlation between the GMP sets employed and the realized structural response (or performance) measures are assessed by carrying out a Multivariate Multiple Linear Regression (MMLR) (Johnson and Wichern, 2002) of the structural demands resulting from the dynamic

analyses and the GMP sets obtained for the suite of recorded ground motions. In multivariate multiple linear regression, 'multiple' refers to the fact that vectors of GMPs, denoted here as ***X*** (the independent variables), are to be considered; 'multivariate' refers to the fact that vector-valued measures of structural response, denoted here as ***Y*** (the dependent variables), are to be predicted. Such regressions are extensions of conventional analyses that only consider individual structural performance measures separately and/or only use a single scalar GMP. Example loss estimates based on the use of a vector of structural performance measures are presented to demonstrate how the regression studies may be used in practice.

1.5 ORGANIZATION OF REPORT

Figure 1.1 illustrates the main steps that are involved in this study. A brief summary of previous work and some related background information is presented in Chapter 2. Selection criteria for the ground motions and development of the energy-based parameters, which are not very commonly used, are discussed in Chapter 3. The results from time-history analyses of single-degree-of-freedom (SDOF) systems (i.e., response spectra) for the selected ground motion records, and comparisons between elastic and inelastic acceleration response spectra and the corresponding energy-based spectra are also presented in Chapter 3. Chapter 4 presents details on modeling of the structures and includes results from the multi-degree-of-freedom (MDOF) dynamic analyses.

The structural response measures, ***Y***, obtained from the MDOF analyses described in Chapter 4 are regressed against the ground motion parameters, ***X***, obtained from ground motion time-history analysis of SDOF systems described in Chapter 3, using MMLR (Multivariate Multiple Linear Regression). Chapter 5 describes the MMLR analysis procedure and explains the results from the numerical studies relating ground motion parameters, ***X***, and structural response measures, ***Y***.

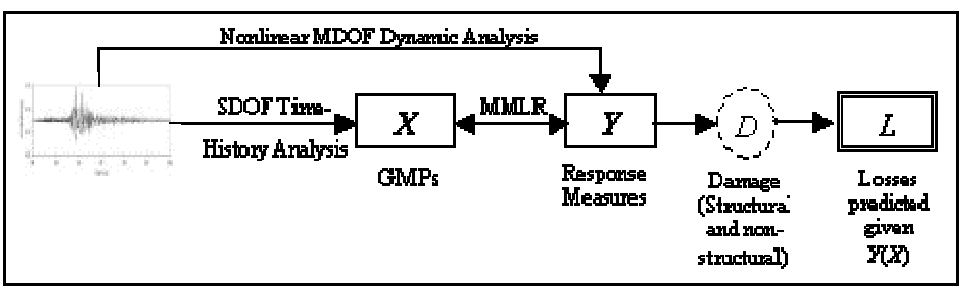

Figure 1.1 Tasks involved in this research study.

In order to illustrate the benefit of using a vector of response measures, $\boldsymbol{Y}$, to estimate monetary losses, L, examples of the use of the regression results for this purpose are presented in Chapter 6. These examples also take into consideration the use of single versus vector ground motion parameters, $\boldsymbol{X}$, as predictors. Finally, in Chapter 7, a summary of the findings from this study is presented, along with recommendations for future work.

With reference to Figure 1.1, note that all the steps of the procedure are thoroughly investigated in this study with the exception of the step that relates $\boldsymbol{Y}$ to L**,** where a fictitious functional form is assumed in order to relate damage (D) and losses (L) to structural response ($\boldsymbol{Y}$). In reality the development of these functional forms requires fragility curves that relate $\boldsymbol{Y}$ with several potential levels of physical damage (e.g., from minor to extensive) to the many structural and non-structural elements present in a building. The expected losses (and their relative dispersions) at the story level are then estimated by pricing the most appropriate repair strategy for fixing the damage to each element (e.g., a partition that is severely cracked is usually replaced not fixed) and adding up the costs for all the elements present at each story. The losses for the entire building are obtained by assembling the losses at each story. This process is lengthy and beyond the scope of this project. For an example of this procedure, see Miranda and Aslani (2003) for the methodology and Taghavi and Miranda (2003) for an implementation. From the description above, however, it should be clear that an estimate of the correlated structural response measures at each story is crucial for a realistic estimate of both physical damage and monetary losses. Accordingly, the present study focuses on prediction of this vector of correlated response measures using GMPs, and on the estimation of losses using these response predictions that in turn rely on MMLR.

CHAPTER 2 – BACKGROUND

2.1 INTRODUCTION

For design and performance assessments of new and existing structures in seismically active regions, it is important to identify ground motion parameters (GMPs) that are well correlated with structural response and, in turn, with damage or monetary loss. Once this correlation is established, engineers can, for example, efficiently estimate the likelihood that a structure at a given site will either collapse or suffer other less severe levels of structural and non-structural damage. Even with GMPs that are well correlated with response, considerable uncertainty is expected in the prediction of structural response measures (e.g., peak roof drift). As mentioned earlier, we seek to reduce the uncertainty involved in such predictions by using a vector of ground motion parameters (instead of any single parameter alone). In an attempt to capture cumulative types of damage, this vector will in some cases include energy-based GMPs in addition to conventional displacement-based GMPs, such as pseudo-spectral acceleration. In this chapter we summarize the various GMPs and damage measures used in this study.

2.2 LINEAR ELASTIC DISPLACEMENT-BASED PARAMETERS

In current design practice it is common to express the demand on a structure in terms of acceleration parameters derived from ground acceleration time histories. Two commonly considered acceleration measures are the horizontal peak ground acceleration (PGA) and the linear elastic spectral acceleration (S_a) at a specified natural period of the structure and percentage of critical damping. PGA is simply the largest (absolute) value of the ground acceleration time history. Spectral acceleration describes the maximum response of a linear elastic single-degree-of-freedom (SDOF) system subjected to a particular input motion. It is a function of the natural period (T) and damping ratio (ζ) of the SDOF system, and is defined as the largest (absolute) value of the oscillator displacement (relative to the ground), converted to acceleration terms by multiplying by $(2\pi/T)^2$. The derived acceleration parameter is more precisely the pseudo-spectral acceleration, which is the acceleration measure used in this study. Compared to PGA, several studies have shown that the period-specific $S_a(T_1)$ (i.e., the spectral acceleration at a period, T_1, close to the fundamental period of the structure of interest) is more closely related to the response of moderate to long vibration period structures (e.g., Shome *et al*., 1998). Nevertheless, $S_a(T_1)$ has also been demonstrated to be less than ideal for tall, long-period buildings, and for many structures when considering near-source ground motions (e.g., Luco, 2002; Luco *et al*., 2002). As an alternate method, it has been suggested to use parameters based on a modified $S_a(T_1)$ to account for the contribution of higher modes and the effects of inelasticity on structural demands (Luco, 2002). However, parameters based on modification of $S_a(T_1)$ require more effort to compute. Also, attenuation relationships for such modified parameters are not yet available, which makes it difficult to use them in probabilistic seismic hazard and risk analyses of interest in engineering practice.

2.3 LINEAR ELASTIC ENERGY-BASED PARAMETERS

To assess the performance of structures during an earthquake, one can also employ an energy-based approach. Several parameters based on energy principles have been employed to study structural performance. These include input energy and absorbed energy (e.g., Chou and Uang, 2000; Sari and Manuel, 2002; Mollaioli *et al*., 2004). These energy-based parameters are frequency-dependent GMPs, similar to the more conventional spectral acceleration (S_a), and establishing their values from recorded ground motions requires similar levels of effort (Sari, 2003). Such energy-based parameters are directly related to cycles of response of a SDOF system, as opposed to peak values of displacement, which is the case with S_a. Thus energy-based parameters implicitly capture the effect of ground motion duration, which is missed by the conventional spectral parameters. Input energy, for example, can be related to the work done by the base shear (net lateral force) acting through the ground displacements (Uang and Bertero, 1988). Only a few attenuation relationships for energy-based parameters currently exist (Chapman, 1999; Chou and Uang, 2000). However, if these parameters are found to be significantly better correlated to damage than conventional spectral ground motion parameters, additional attenuation relations could be easily developed. In our study, we have included elastic input and absorbed energy-equivalent acceleration as ground motion parameters. We will consider vector sets of energy-based parameters as well as combinations of energy- and displacement-based parameters in our studies. A background on estimation of these energy-based parameters from ground motion records is given in Chapter 3.

2.4 INELASTIC DISPLACEMENT- AND ENERGY-BASED PARAMETERS

For spectral acceleration (S_a), the SDOF system considered is a linear elastic oscillator of the given vibration period (T) and damping ratio (ζ, typically taken to be 5%). Alternatively, a bilinear inelastic oscillator characterized by T, ζ, a yield displacement (d_y), a post-yield strain-hardening ratio (α), non-degrading strength and stiffness, and equal loading and unloading slopes can be used to compute an *inelastic* spectral acceleration, denoted here as S_a^I. It can be expected that S_a^I will be more strongly correlated with the nonlinear response of structures than S_a, especially if the response is dominated by the first mode of vibration. Hence, in this research, S_a^I is considered as another GMP that can be coupled with S_a (or used in lieu of it) in order to improve the prediction of nonlinear structural responses. Note that a relatively simple modification of the elastic time-history analysis carried out to compute S_a is required to compute S_a^I. Also needed are values of the two additional parameters, d_y and α, which are described in more detail in Chapter 3.

Analogous to S_a^I, the input and absorbed energy (expressed as energy-equivalent accelerations) can also be computed for a bilinear inelastic SDOF system characterized by T, ζ, d_y, and α. In fact, the absorbed energy of an elastic oscillator is simply proportional to S_a and, therefore, does not provide any additional predictive power. Hence, in this report only an inelastic absorbed energy GMP is considered. The same inelastic time-history analysis carried out to compute S_a^I also results in values of the inelastic energy-based GMPs.

2.5 STRUCTURAL RESPONSE MEASURES

A major concern in earthquake engineering is the estimation of damage and losses that can occur due to ground shaking in an earthquake. In the structural engineering literature, various response measures have been proposed based on experimental and theoretical studies to explain damage observed in test structures under simulated ground motions or in actual structures struck by real earthquakes. We are interested in those response measures that are well correlated to structural and non-structural damage. Numerous studies (such as the SAC Steel Project) have indicated that peak interstory drift ratios (i.e., inter-story drift normalized by story height) are closely related to both local demands and damage and to global structural stability for steel moment-resisting frames and many other building types. Various scalar measures related to the peak interstory drift ratio have been used in research. These include, for example, the maximum peak interstory drift ratio over all stories (denoted as *MIDR*) (Giovenale *et al*., 2003; Luco, 2002) and the average peak interstory drift ratio over all stories (denoted as *AIDR*) (Luco, 2002). The response measure *MIDR* can be related to local damage (within a story) and to local instability or to story collapse. On the other hand, *AIDR* is related to overall damage in a structure and to instability of the structure as a whole. Another response measure that relates to overall structural damage and global instability is the peak roof drift ratio (*RDR*), which is the ratio of the peak lateral roof displacement to the building height.

2.6 RELATIONSHIP BETWEEN RESPONSE MEASURES AND GROUND MOTION PARAMETERS

The degree of correlation between ground motion intensity measures and the response of structures is important for the prediction of damage in earthquakes. Ground shaking intensity can be described using the displacement- or energy-based GMPs discussed earlier. The degree of correlation between response measures and GMPs is typically estimated via regression analysis. There is, however, considerable variability in the structural responses generated by accelerograms of similar GMPs due to the complexity of the dynamic response of structures and to the different characteristics of ground motion recordings. Because of this record-to-record variability, one usually needs to run a sufficient number of nonlinear dynamic analyses in order to predict response measures with specified levels of confidence. The required number of analyses is directly related to the variability (dispersion) in the response measure given the GMP (Shome *et al*., 1998), as expressed in Equation 2.1. A lower variability (dispersion) of the response measure given the GMP will require fewer nonlinear dynamic analyses to predict response with a desired level of accuracy (e.g., if the dispersion of the response measure given the GMP is reduced by a factor of two, the required number of analyses can be reduced by a factor of four to achieve the same level of accuracy). More precisely, the "dispersion in response given GMP" is the standard deviation of the (natural logarithm of the) response measure for a given value of the GMP, and the "level of accuracy" is the standard deviation of the mean of the (natural logarithms of the) response measure, also for a given value of the GMP.

$$\#\ \text{analyses} = \left[\frac{\text{Dispersion in Response} \mid GMP}{\text{Level of Accuracy}} \right]^2 \tag{2.1}$$

Choosing an appropriate set of ground motion records relevant to a given site and running the nonlinear dynamic analyses can be a time-consuming and computationally expensive process. Hence, any significant reduction in the variability of our predictions of response is helpful in limiting the number of analyses needed. This can be achieved if we identify an “efficient” GMP that predicts the desired response measure with small dispersion. Furthermore, if a GMP is "sufficient" (Luco 2002), i.e., it correlates with structural response in the same way (with the same regression results) for different types of earthquake records (e.g., near-source versus "ordinary"), the choice of an appropriate set of ground motion records relevant to a given site is simplified. In this case, a random choice of records can be adequate.

2.7 VECTOR-VALUED APPROACH

Structural response measures, in general, may be dependent on parameters other than the first-mode spectral acceleration alone. Examples of other parameters include magnitude of the causative event, duration of the ground shaking, and spectral acceleration at frequencies higher than the first mode. Since a single (scalar) GMP may not be well correlated with the response of a structure, one could consider using more than one such parameter if there is interest in reducing the uncertainty in the response prediction. In a recent study (Bazzurro and Cornell 2002), vector-valued regression analyses were carried out using spectral acceleration values at two different natural frequencies, and this was demonstrated to be beneficial for the response predictions of flexible structures dominated by multiple modes. Along these lines, in the present study we propose the use of a vector of GMPs that can jointly predict the response. The details on particular choices of vectors are discussed in Chapter 5. In general, we will limit our sets of GMPs to only those measures that can be readily computed from SDOF linear elastic or bilinear inelastic analysis, the modal vibration properties of the given structure, and an estimate of the strength of the structure. Also, we remind the reader again that instead of predicting a single response measure given the GMPs, we seek to predict *jointly* a vector of several response measures that are correlated. The knowledge of a vector of response measures is expected to improve predictions of losses in future earthquakes because it provides information about the level of drift at all stories.

CHAPTER 3 – GROUND MOTION RECORDS AND PARAMETERS

3.1 INTRODUCTION

In general, the characteristics of ground motion records that influence the seismic response of structures can be quantitatively described using various scalar parameters. Generally, the amplitude and duration of ground shaking, measures of frequency content, and the number of peaks in a ground acceleration record above a specified level are some of the characteristics that can influence structural response. Several ground motion parameters used in the literature to predict structural response were summarized in the previous chapter. To study the extent of the correlation of GMPs to structural response measures, 140 ground motion records from 20 earthquake events relevant to the Southern California region were selected. These ground motion records were analyzed using a MATLAB routine that employed Newmark's direct integration method to analyze linear elastic and bilinear inelastic SDOF systems and thus generate response spectra for pseudo-spectral acceleration and for the energy-based parameters (both elastic and inelastic). The details related to the selection of records and the definitions of the energy-based parameters are presented in this chapter. Comparisons between the energy-based approach and the conventional displacement-based approach (e.g., using pseudo-spectral acceleration) are also presented here.

3.2 STRONG GROUND MOTION RECORDS

3.2.1 INTRODUCTION

Building performance, and hence damage and losses, during an earthquake are sensitive to the input ground motion, which is characterized in a general sense by the earthquake magnitude of the causative event, the source-to-site distance, and the site conditions. To obtain results appropriate for the region of interest (Southern California in our case), one can select records pertaining to that region. Also, from the viewpoint of planned statistical analysis, it is important to consider a large number of records to make statistically significant conclusions.

3.2.2 GROUND MOTION DATA

A total of 140 ground motion records from 20 earthquakes were used for the analyses in this study. The records were obtained from the PEER database (http://peer.berkeley.edu/smcat/) assembled by Dr. Walter Silva. Only the strike-normal horizontal component of each record was included, where near-source effects were expected. For consistency, in the case of the "ordinary" (i.e., non-near-source) motions as well, only the strike-normal horizontal component was considered. For stations where a strike-normal component was not recorded, the two horizontal components were rotated to get the strike-normal component.

The ground motions used were recorded either in the free field or at the ground level of lightweight construction of no more than four stories. The selected records had a maximum

(between the two horizontal components) high-pass-filter corner frequency (f_c^{HP}) not greater than 0.20 Hz. This constraint is based on the suggestion from Dr. Walter Silva that "the usable bandwidth of the records for the purpose of engineering analysis is within a factor of 1/1.25 of the low-pass frequency and a factor of 1.25 of the high-pass frequency" (refer to http://peer.berkeley.edu/smcat/process.html); the latter corresponds to 4 seconds (or 1.25 times 0.20 Hz) in our case, which is a period range that is long enough to cover the fundamental linear elastic periods of the 3-, 9-, and 20-story SAC structures that we consider in this research (as described in the next chapter). Note that we assume here that the suggested usable bandwidth is also adequate for nonlinear structural analyses, even though the progression of damage during ground shaking may cause the effective vibration period to lengthen beyond the upper bound of the usable bandwidth. Constraining the selection of records to a lower value of f_c^{HP}, however, would eliminate enough records to impair stable statistical inferences.

3.2.3 MAGNITUDE

Strong motion records from earthquakes with moment magnitude, M_w, between 5.7 and 7.5 were used in this study. Eighty percent of the records were collected from earthquakes with M_w ranging from 6.0 to 7.0, seven percent with M_w below 6.0, and thirteen percent with M_w greater than 7.0. The selection of records was designed such that the number of records with M_w above and below 6.5 is the same. The data set is also divided into near-source and ordinary records, as described in detail in the next subsection. In Southern California, engineers are very concerned with magnitudes greater than 7.0, but not many recordings are available from such earthquakes. Nevertheless, this data set will allow us to look at the variation of structural response with magnitude, in addition to the response for large magnitude events alone.

3.2.4 SOURCE-TO-SITE DISTANCE

We have included both near-source and "ordinary" (i.e., non-near-source) ground motion records in the present study by considering values of the closest distance to the source, R_{close}, between nearly 0 and 36 km. The near-source subset contains the 70 (of 140) records with $R_{close} < 16$ km, and the "ordinary" subset contains the remainder ($16 \leq R_{close} < 36$ km). The 16 km limit for the near-source subset is motivated by the prevalent belief (e.g., in the SEAOC Blue Book) that ground motion records show "near-source" characteristics only within about 15 km of the source. The earthquake events from which the records were selected are summarized in Table 3.1. The distribution by magnitude, M_w, and distance, R_{close}, of the selected ground motions is summarized in the scatter plot shown in Figure 3.1.

No.	Earthquake Name	Year	M_w	Ordinary	Near-Source
1	Coyote Lake	1979	5.7	1	4
2	Chalfant Valley-01	1986	5.8	2	1
3	Whittier Narrows	1987	6.0	0	2
4	N. Palm Springs	1986	6.1	1	2
5	Parkfield	1966	6.2	0	4
6	Morgan Hill	1984	6.2	8	8
7	Chalfant Valley-02	1986	6.2	1	1
8	Victoria, Mexico	1980	6.3	2	2
9	Coalinga	1983	6.4	8	2
10	Imperial Valley	1979	6.5	11	18
11	Superstition Hills	1987	6.5	3	2
12	San Fernando	1971	6.6	1	0
13	Northridge	1994	6.7	9	10
14	Kobe, Japan	1995	6.9	3	1
15	Loma Prieta	1989	6.9	9	4
16	Cape Mendocino	1992	7.0	2	1
17	Duzce, Turkey	1999	7.1	0	1
18	Landers	1992	7.3	6	2
19	Tabas, Iran	1987	7.4	1	2
20	Kocaeli, Turkey	1999	7.5	2	3
	Total			70	70

Table 3.1 Distribution of the selected ground motion records from various earthquake events. Note that records from the 1999 Chi-Chi, Taiwan earthquake are not considered due to currently unresolved questions regarding their pertinence to the Southern California region and the overwhelming number of records from the event.

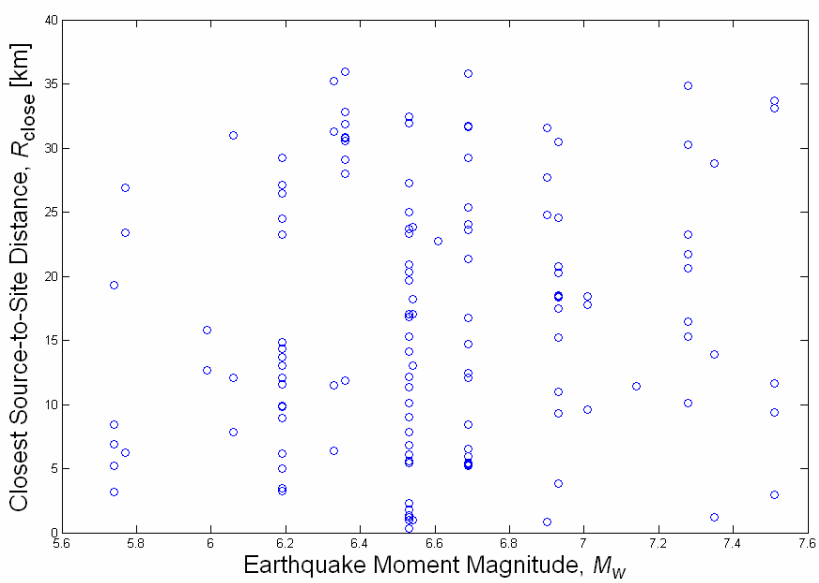

Figure 3.1 Magnitude and distance for the 140 selected ground motion records.

3.2.5 SITE CLASSIFICATION

To prevent the confounding influence of soil properties on the response, ground motions recorded only at sites classified as NEHRP D or C class ("stiff soil" or "very dense soil and soft rock"), or as Geomatrix site code (third letter) B-D when the NEHRP classification is unavailable, are considered. A list of all the selected ground motion records is presented in Appendix A.

3.3 ENERGY-BASED PARAMETERS

3.3.1 INTRODUCTION

It has long been thought that in order to evaluate seismic damage to buildings one could consider an energy-based approach in a manner similar to how a displacement-based approach uses pseudo-spectral acceleration, S_a, as the underlying parameter. Over the years, several researchers have carried out studies in order to gain a better understanding of the energy demand on structures. These studies have focused on different descriptors of such energy demands. Studies by Housner (1956), Akiyama (1985, 1988), Uang and Bertero (1988), Chou and Uang (2003), and Leelataviwat *et al*. (2002) have addressed the energy demand in multi-degree-of-freedom (MDOF) systems and have even sometimes described energy-based design procedures. Sari (2003) and Chou and Uang (2000) have considered energy-based ground motion parameters such as input energy and absorbed energy. As mentioned in Chapter 2, these energy-based parameters are frequency-dependent, similar to the more conventional S_a, and establishing their values from recorded ground motions requires similar levels of effort (Sari, 2003). Such energy-based parameters depend on the number and amplitude of the cycles of response of a single-degree-of-freedom system, as opposed to the peak values of response alone as is the case with S_a. Hence, these energy-based parameters implicitly capture the effects of duration.

3.3.2 ENERGY BALANCE EQUATIONS FOR AN SDOF SYSTEM

Consider the equation of motion for a single-degree-of-freedom (SDOF) system subjected to a horizontal ground motion:

$$m\ddot{u}_t + c\dot{u} + f_s = 0 \tag{3.1}$$

where m, c, and f_s are the mass, viscous damping coefficient, and restoring force, respectively, of the SDOF system. Also, u_t is the absolute (total) displacement of the mass, while $u = u_t - u_g$ is the relative displacement of the mass with respect to ground, and u_g is the ground displacement.

Transformation of the equation of motion into an energy balance equation is easily accomplished by integrating Equation 3.1 with respect to u from the beginning of the input ground motion (see, for example, Uang and Bertero,1988). This leads to:

$$\frac{m\dot{u}_t^2}{2} + \int_0^t c\dot{u}du + \int_0^t f_s du = \int_0^t m\ddot{u}_t du_g \tag{3.2}$$

Since the inertia force, $m\ddot{u}_t$, is numerically equal to the sum of the damping and restoring forces (as seen in Equation 3.1), it is also equal to the total force transmitted to the base of the structure. Therefore, the right-hand side of Equation 3.2 is, by definition, the energy input into the system at any time, *t*. Hereinafter, following Uang and Bertero (1988), we will define Input Energy, E_i, as the *maximum* value of the energy input into the system during ground shaking. It can also be thought of as the maximum value of the work done by the total base shear acting through the foundation/ground displacement during the ground motion (Uang and Bertero, 1988). Thus, we have:

$$E_i = \max\left\{\int_0^t m\ddot{u}_t du_g\right\} \tag{3.3}$$

It is convenient (but not necessary) to transform E_i into a parameter with units of acceleration to be included with S_a in a vector of GMPs. Thus, we define the parameter "input energy-equivalent acceleration," A_i, as follows:

$$V_i = \sqrt{\frac{2E_i}{m}}; \quad A_i = \omega V_i \tag{3.4}$$

where ω is equal to $2\pi/T_1$ and T_1 is the fundamental period of the system. Similarly, following Chou and Uang (2000), we define Absorbed Energy, E_a, as the maximum value of the third term on the left-hand side of Equation 3.2, which, in the case of an inelastic response, is composed of recoverable elastic strain energy and irrecoverable hysteretic energy. That is,

$$E_a = \max\left\{\int_0^t f_S du\right\} \tag{3.5}$$

As before, E_a is a quantity that can also be transformed into a parameter with units of acceleration, namely the "absorbed energy-equivalent acceleration," A_a:

$$V_a = \sqrt{\frac{2E_a}{m}}; \quad A_a = \omega V_a \tag{3.6}$$

Note that A_a reverts to S_a if the SDOF system is elastic (i.e., if $f_s = ku$); so, in this research we only consider A_a for an inelastic oscillator, as described in Section 3.4.

3.3.3 ENERGY RESPONSE SPECTRA

Energy-based response spectra require the same level of computational effort as conventional acceleration response spectra and are generated in a similar manner. For example, input energy

time histories for a SDOF system with specified damping can be evaluated for a particular ground motion record using Equation 3.3, for various natural periods of interest. The spectrum, in this case, is generated as a plot of the maximum values of the input energy time histories versus the corresponding periods.

In Figure 3.2, we illustrate the generation of input energy-equivalent acceleration spectra (A_i) and conventional response spectra (S_a). Note that the energy time history is converted to an equivalent acceleration time history using Equation 3.4. The time-varying input energy-equivalent acceleration and the pseudo-spectral acceleration response time history for an elastic SDOF system with a 1.0 sec natural period and 5% damping, for a single ground motion, are plotted in Figure 3.2. The maximum values from these time histories are used to obtain the spectrum ordinates at a natural period of 1.0 sec and for 5% damping. Entire response spectra are easily generated using numerous period values that cover the range from 0 to 4 sec (the period range of interest in this study).

The elastic input energy-equivalent acceleration spectra (i.e., A_i) obtained for all of the 140 ground motions are shown in Figure 3.3, along with the mean spectrum. Figure 3.4 shows the mean A_i spectra considering the entire set as well as the near-field set and the ordinary set separately. Figures 3.5 and 3.6 are analogous to Figures 3.3 and 3.4, respectively, and summarize the conventional response spectra, showing S_a versus period for the sets of ground motion records.

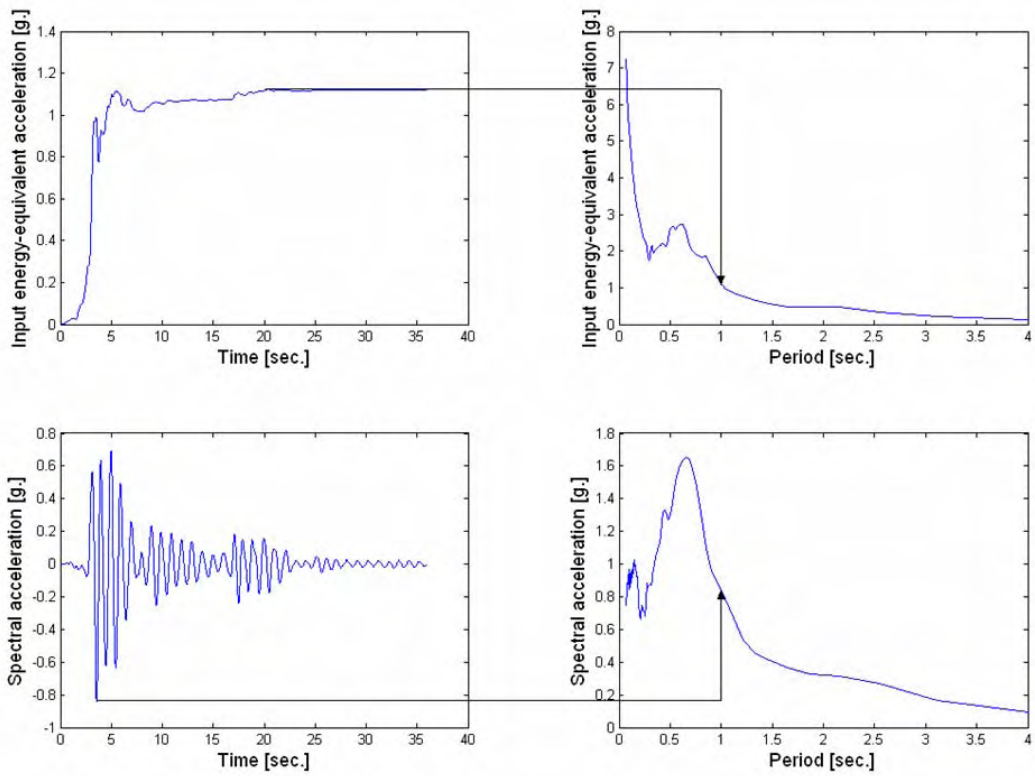

Figure 3.2 Comparison of the spectra for input energy-equivalent acceleration (A_i) and spectral acceleration (S_a) for a single ground motion record, highlighting computation for a natural period of 1 sec and 5% damping.

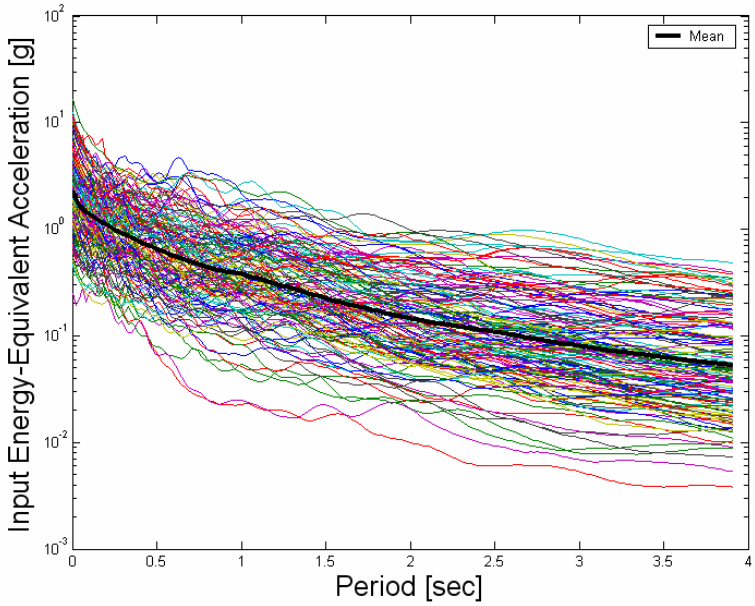

Figure 3.3 Individual input energy-equivalent acceleration (A_i) spectra for 5% damping for the 140 records, along with the mean spectrum.

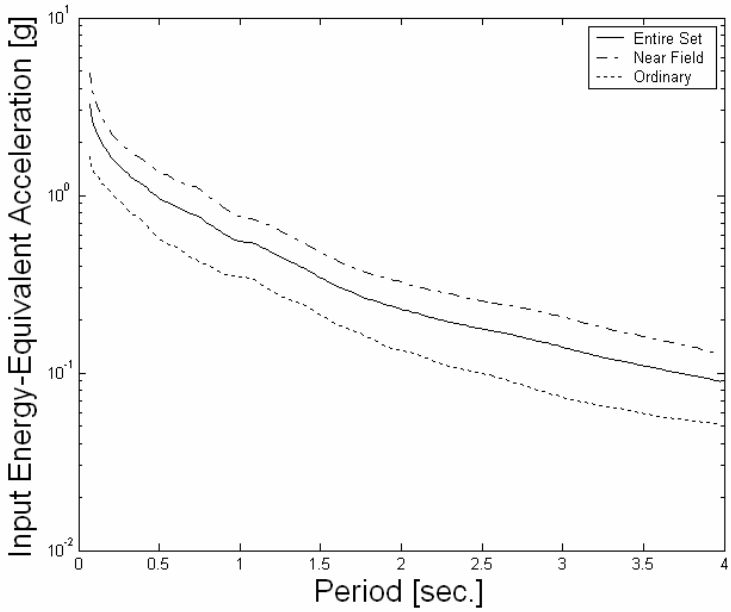

Figure 3.4 Mean input energy-equivalent acceleration (A_i) spectra based on the full set of 140 records, the near-source set, and the ordinary set of records.

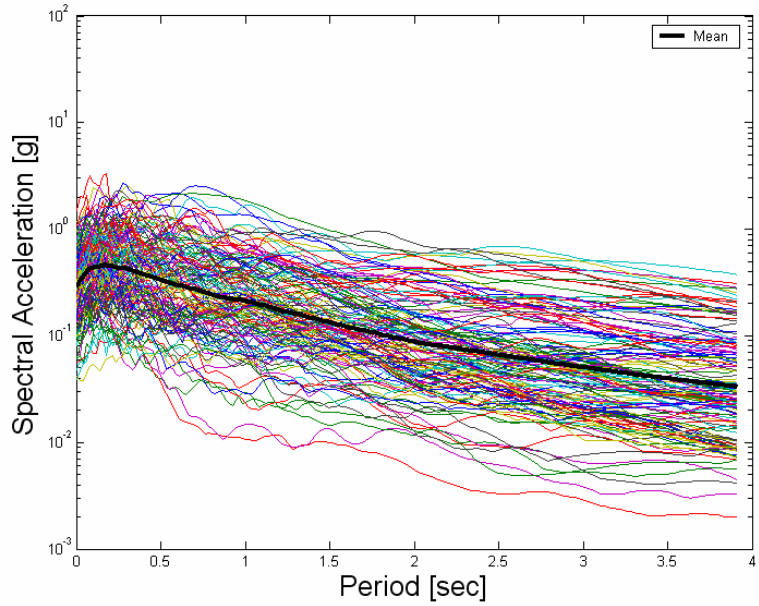

Figure 3.5 Individual acceleration spectra (S_a) for 5% damping for all 140 records, along with the mean spectrum.

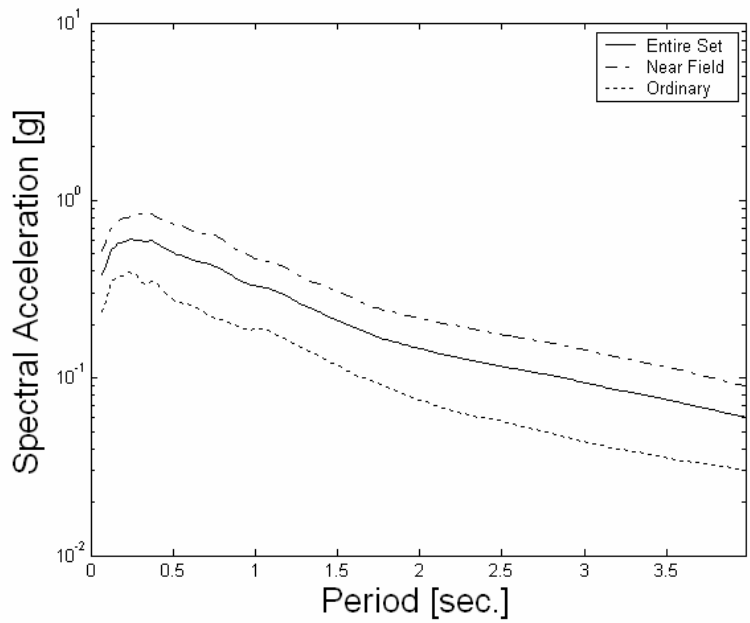

Figure 3.6 Mean response spectra (S_a) based on the full set of 140 records, the near-source set, and the ordinary set of records.

3.3.4 COMPARISON OF ELASTIC A_i AND S_a

The energy-based parameters (e.g., input energy-equivalent acceleration) convey information on the ground motion duration by virtue of the integration over time that is involved in their computation. Generally, peak values in the input energy time histories occur towards the end of the strong shaking, reflecting this cumulative effect. This is in contrast to acceleration time histories that often have their peak values during the portion of strongest shaking of the record (depending on the natural period of interest). For the ground motion record considered in Figure 3.2, for example, the peak value of the input energy occurs at about 20 seconds, whereas the peak value of the pseudo-spectral acceleration response occurs considerably earlier (at about 3.5 seconds). Spectral acceleration is a displacement-based parameter and only reflects the effects of amplitude, whereas input energy-equivalent acceleration takes into account the duration of the shaking along with the amplitude. However, we can expect the two parameters to be correlated, as we are using the same elastic SDOF system to derive both these parameters. This correlation is evident in the case shown in Figure 3.2, where a very large portion of the final input energy-equivalent acceleration has already accumulated by the time (3.5s) that the maximum value of the pseudo-spectral acceleration response occurred.

Figure 3.7 shows a plot of $A_i(T_1)$ versus $S_a(T_1)$ for a period of 2.3 sec (the fundamental period, T_1, of the 9-story steel building considered in this study that is discussed in Chapter 4). Clearly, $S_a(T_1)$ and $A_i(T_1)$ are seen to be highly correlated at this period. In general (see Figure 3.8), there is a strong correlation between S_a and A_i at most periods. This correlation is lowest at short natural periods (less than about 0.3 seconds) and it rises above 0.95 for longer periods. The high correlation suggests that the joint use of both S_a and A_i in the same response prediction model may only be justified, if at all, for short-period structures (when the correlation is lower and, therefore, the joint predictive power is potentially higher).

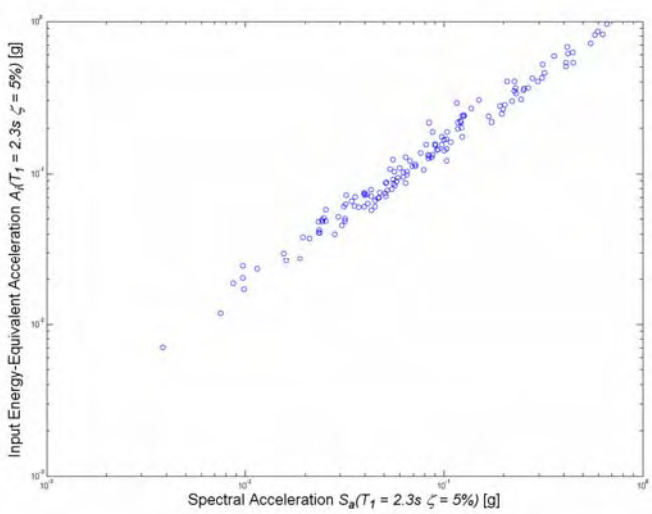

Figure 3.7 Input energy-equivalent acceleration (A_i) values plotted versus spectral acceleration (S_a) at the fundamental period of the 9-story steel building used in this study (T_1 = 2.3 sec).

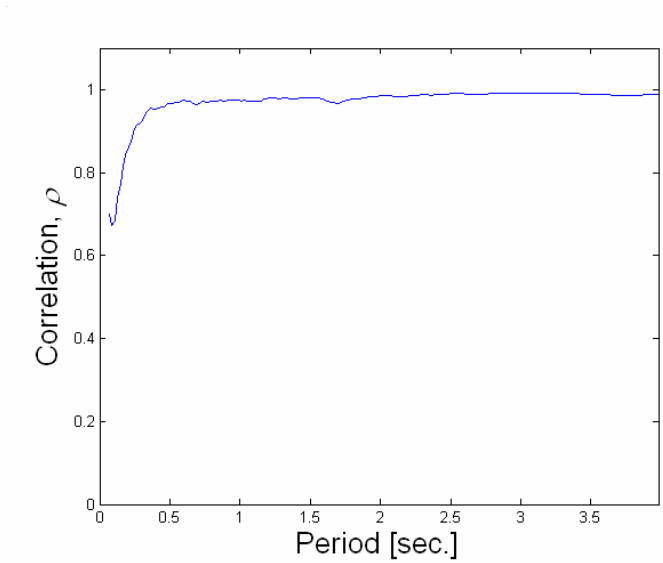

Figure 3.8 Correlation coefficient between input energy-equivalent acceleration (A_i) and spectral acceleration (S_a) versus natural period.

3.4 INELASTIC PARAMETERS

3.4.1 INTRODUCTION

Inelastic counterparts to the elastic spectral acceleration (S_a) and input energy-equivalent acceleration (A_i) ground motion parameters compared in the preceding section, as well as the inelastic absorbed energy-equivalent acceleration (A_a), can also be computed via SDOF time-history analysis (Equations 3.1 and 3.2). Given that we aim to predict the nonlinear structural response from GMPs, it is logical to consider these inelastic counterparts, denoted S_a^{I}, A_i^{I}, and A_a^{I}. Inelastic GMPs such as these are not widely used in current practice mainly because few attenuation relations for such inelastic parameters are available. The lack of available attenuation equations hinder, for the time being, the use of some of these parameters in a Probabilistic Seismic Hazard Analysis. An attenuation relation for S_a^{I} (actually, for the ratio of inelastic to elastic spectral displacement) is under development at Stanford University (Tothong & Cornell, 2004). Attenuation relations for A_i^{I}, and A_a^{I} are also available in the literature (see, for example, Chou and Uang, 2000).

In this research, a bilinear inelastic oscillator with no degrading strength and stiffness, and with identical loading and unloading slopes, is used to compute the inelastic GMPs. This bilinear oscillator is parameterized by a vibration period (T) and damping ratio (ζ), just like its elastic counterpart, but it also requires the specification of a yield displacement (d_{y}) and a post-yield strain-hardening ratio (α). We set α to be 5% in order to be consistent with the S_a^{I} attenuation relation mentioned above (i.e., Tothong & Cornell, 2004). An appropriate d_{y} level can be estimated from a nonlinear static pushover analysis of the structure of interest (e.g., Luco, 2002), but here we have based d_{y} on the inter-story (and roof) drift results for the ductile and elastic

models of each of the three steel buildings considered in this study (described in Chapter 4). For example, the ratio of the inter-story drifts from the ductile model to that from the elastic model, both computed at the first story of the 3-story building considered, is plotted in Figure 3.9 against the elastic spectral displacements for the full set of 140 ground motions. The spectral displacement at which these ductile-to-elastic ratios deviate significantly from unity provides an estimate of d_y, which in this case is about 6 cm. This value of 6 cm, then, is treated as the displacement-based "fundamental strength" of the ductile (and brittle) 3-story building.

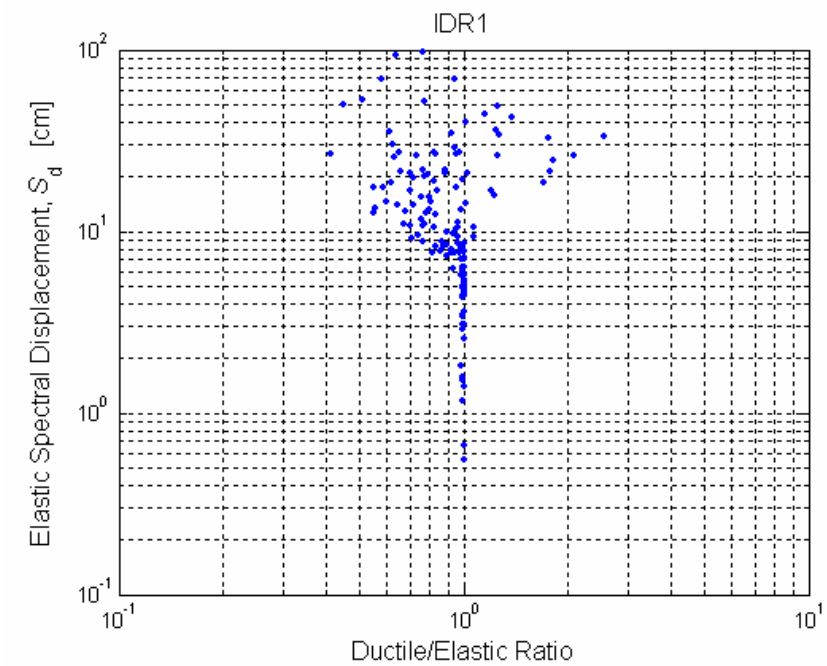

Figure 3.9 The ratio of peak interstory drifts from the ductile model to that from the elastic model at the first story of the 3-story building, plotted versus the corresponding elastic spectral displacements for the 140 ground motions. Note that the ductile model drift begins to deviate significantly from that of the elastic model at a spectral displacement of about 6 cm, namely at the "fundamental strength" of the ductile building model.

3.4.2 COMPARISON OF S_a^I AND S_a

As an example, inelastic spectral accelerations (S_a^I) for the 140 ground motions used in this study are plotted against the corresponding elastic spectral accelerations (S_a) in Figure 3.10. The period considered is the fundamental period of the 3-story building (T = 1.0 sec), and the yield displacement is also that for the 3-story building (d_y = 6 cm). Below the pseudo spectral acceleration associated with d_y (i.e., $S_a=d_y*(2\pi/T)^2=0.24g$) the two GMPs are identical, as expected. At higher ground motion levels, S_a^I is increasingly different from S_a, although the two GMPs are still highly correlated (as discussed further in Chapter 5).

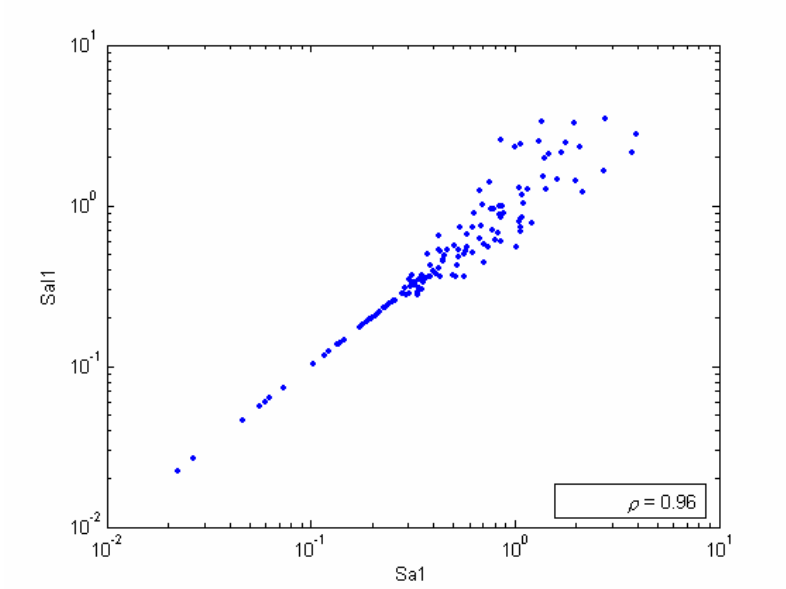

Figure 3.10 A comparison of the inelastic (ordinate) versus elastic (abscissa) spectral accelerations (both in units of *g*) at the fundamental period and strength of the 3-story building, for the 140 ground motions considered.

3.4.3 COMPARISON OF A_i^{I} AND S_a^{I}

We saw in Section 3.3.4 that the elastic input energy-equivalent acceleration (A_i) and the elastic spectral acceleration (S_a) are strongly correlated. As an analogous example, here the *inelastic* input energy-equivalent accelerations (A_i^{I}) for the 140 ground motions are plotted in Figure 3.11 against the *inelastic* spectral accelerations (S_a^{I}), again for the fundamental period and strength of the 3-story building (i.e., T = 1.0 sec and d_y = 6 cm). Similar to what was observed for their elastic counterparts, the two inelastic GMPs are highly correlated, even more so than S_a^{I} and S_a at the larger ground motion levels. This observation was also found to hold for the fundamental periods and strengths of the 9-story and 20-story buildings considered.

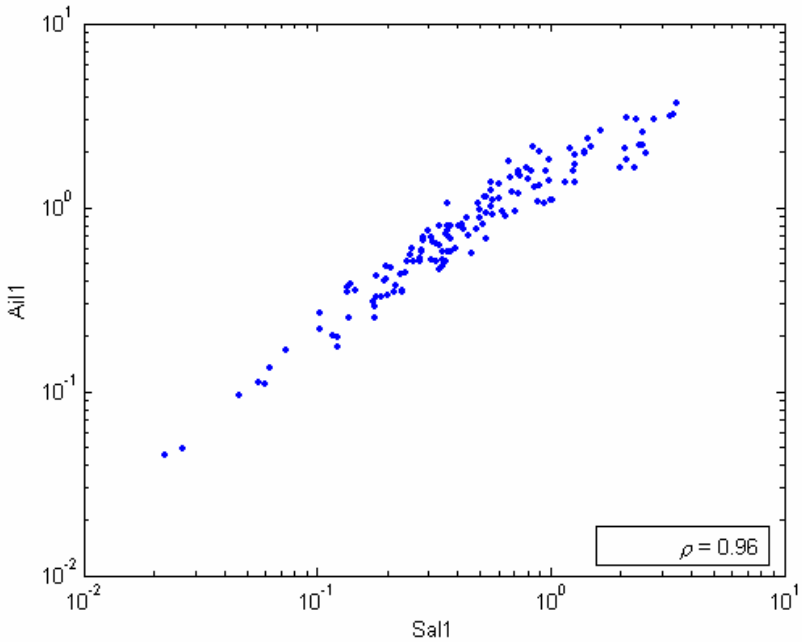

Figure 3.11 A comparison of the inelastic input energy-equivalent acceleration (ordinate) versus inelastic spectral acceleration (abscissa) (both in units of *g*) at the fundamental period and strength of the 3-story building, for the 140 ground motions considered.

3.4.4 COMPARISON OF A_a^{I} AND A_i^{I}

Recall (from Section 3.3.2) that the absorbed energy for an *elastic* oscillator is simply proportional to the elastic spectral acceleration (e.g., Chou & Uang, 2000), so A_a is not considered in this study. As demonstrated in Figure 3.12, however, again for the fundamental period and strength of the 3-story building and the 140 ground motions, the *inelastic* absorbed energy-equivalent acceleration (A_a^{I}, above the spectral acceleration corresponding to d_y) is *not* simply proportional to S_a, although the two are strongly correlated. The correlation between A_a^{I} and A_i^{I} is also very strong, as illustrated in Figure 3.13, especially at larger ground motion levels where kinetic and strain energies are relatively less important compared to hysteretic energy and, as a result, the absorbed energy there is close to the input energy. Despite the strong correlation of the inelastic energy-equivalent accelerations with inelastic S_a, one of these, A_a^{I}, is considered in Chapter 5 as an additional GMP in studying correlation with the nonlinear structural response of buildings.

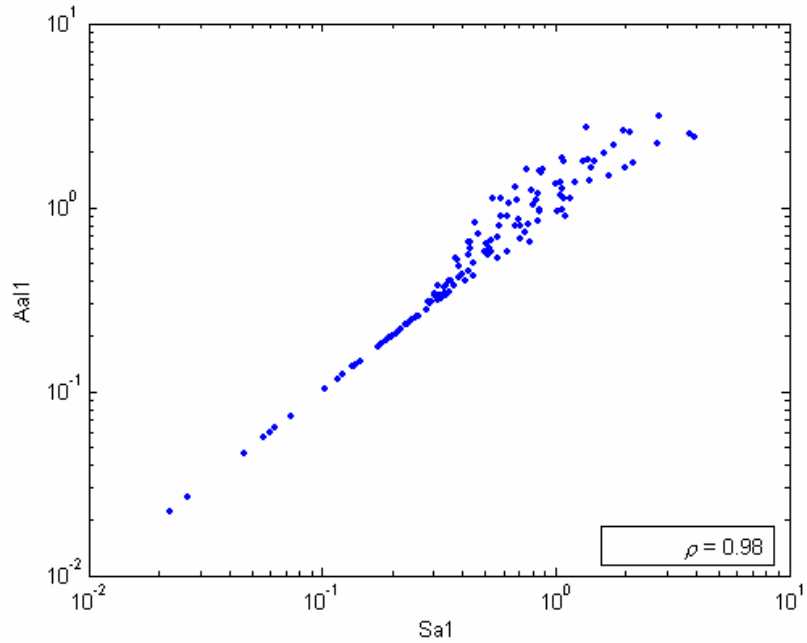

Figure 3.12 A comparison of the inelastic absorbed energy-equivalent acceleration (ordinate) versus elastic spectral acceleration (abscissa) (both in units of *g*) at the fundamental period and strength of the 3-story building, for the 140 ground motions considered.

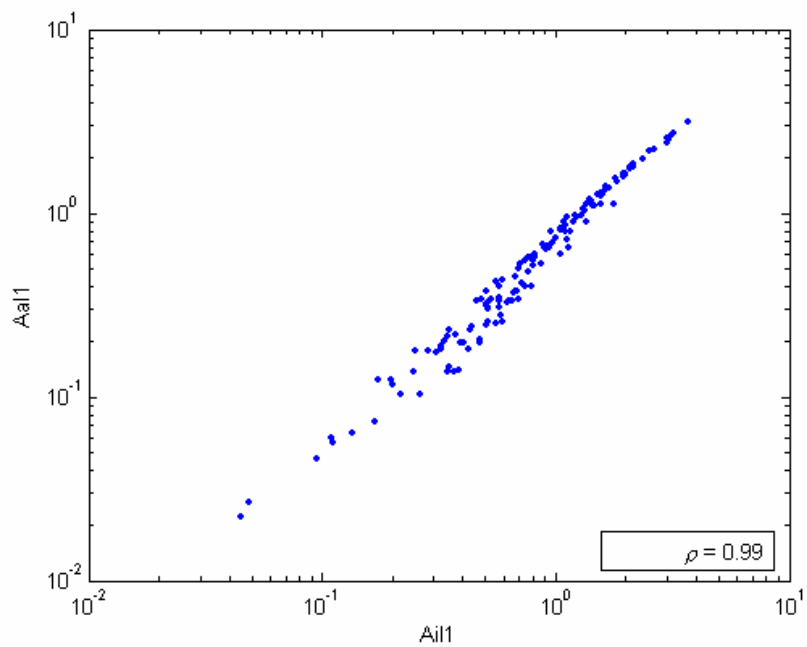

Figure 3.13 A comparison of the inelastic absorbed energy-equivalent acceleration (ordinate) versus inelastic input energy-equivalent acceleration (abscissa) (both in units of *g*) at the fundamental period and strength of the 3-story building, for the 140 ground motions considered.

CHAPTER 4 – DESCRIPTION OF THE STRUCTURES AND THE NONLINEAR DYNAMIC ANALYSES

4.1 INTRODUCTION

The structures used in this research are the 3-story, 9-story, and 20-story steel moment-resisting frame (SMRF) buildings designed for Los Angeles conditions by practicing engineers as part of the SAC Steel Project (Phase II). The building designs were carried out according to pre-Northridge earthquake practices (i.e., *UBC*, 1994). For the purpose of our analyses, centerline two-dimensional models of each structure are prepared in RUAUMOKO (Carr, 2003) and in DRAIN-2DX (Prakash *et al.*, 1993)[1]. Reflecting the state of design practice before and after the 1994 Northridge earthquake, the SMRF buildings are modeled with brittle and with ductile connections, respectively. An elastic model of each building is also considered, as a point of reference. Only details relevant to the modeling of the structures for the purposes of the dynamic analyses are presented here. A complete description of the structures can be found in FEMA 355C (2000).

4.2 DESCRIPTION OF THE STRUCTURES

All of the buildings were designed as office buildings founded on stiff soil, following the local code provisions (i.e., *UBC* 1994). The design of each building was governed by seismic loading considerations. Perimeter steel special moment-resisting frames were designed to carry all of the design lateral loads. The layout of the moment-resisting frames for the three structures is shown in Figure 4.1. Note that all of the buildings are relatively symmetric in plan in the two principal directions.

For the 3-story building, three bays of moment-resisting frames were provided in each of the four perimeter frames. These did not include the corner columns, so biaxial bending does not occur in any of the columns. For the 9-story building, each corner column has only one moment frame connection, also to prevent weak-axis bending. For the 20-story building, the entire frame was modeled as moment-resisting and box columns were used in the corners to resist biaxial bending under seismic loading.

The plan view of a typical story and the elevation of each building are shown in Figure 4.2. The 3-story building has no basement, the 9-story building has one basement level, and the 20-story building has two basement levels, each with a height of 12 feet. The column bases of the 3-story building are fixed. The column bases of the 9-story and 20-story buildings are pinned, but lateral

[1] Note that it became necessary during the course of this research to use DRAIN-2DX, in addition to RUAUMOKO, in order to adequately model brittle connection behavior (as described later). The use of both programs also allowed us to cross-check the analysis results that assumed ductile or elastic connection behavior.

movement at the basement and ground levels is restrained due to the presence of a reinforced concrete wall.

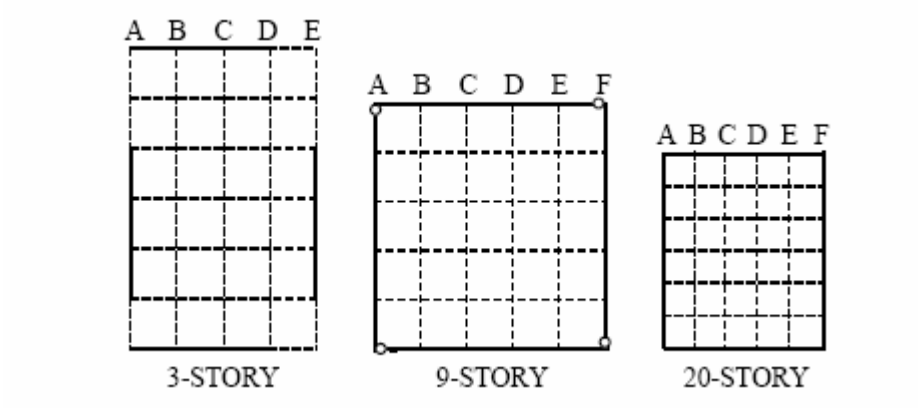

Figure 4.1 Layout of the three Moment-Resisting Frame Structures (FEMA 355C, 2000).

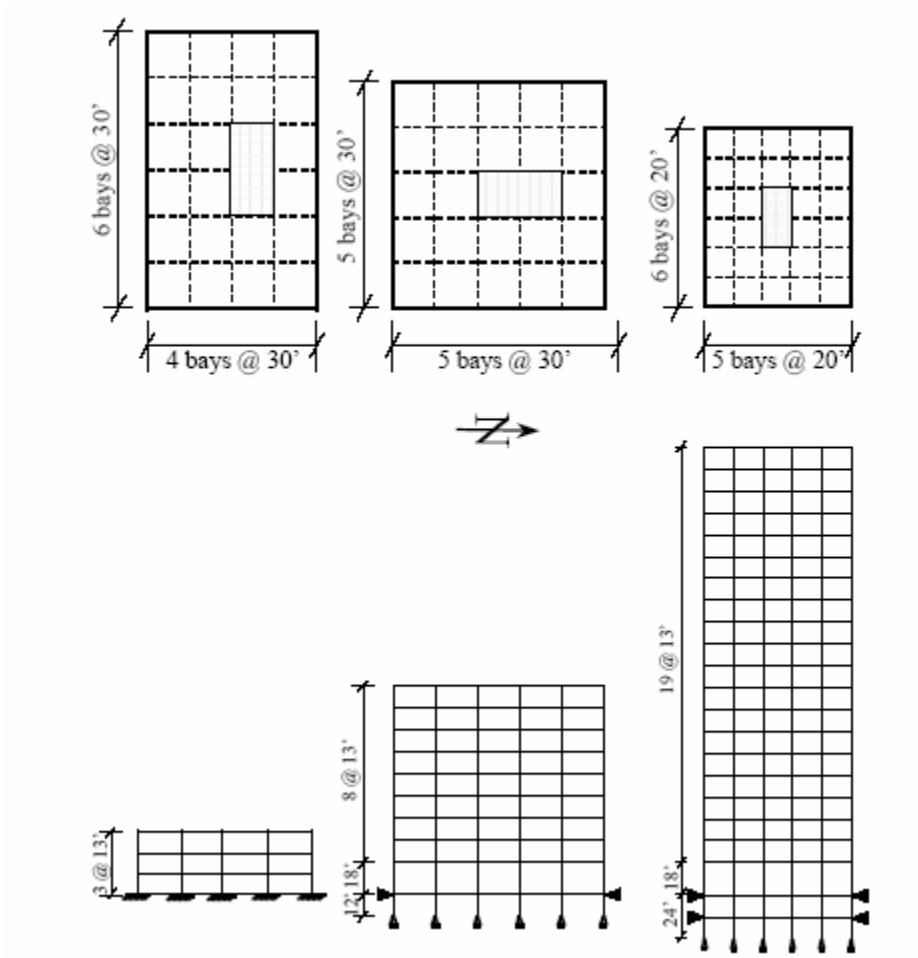

Figure 4.2 Plan View and Elevation of the three structures (FEMA 355C, 2000).

4.3 DESCRIPTION OF THE COMPUTATIONAL MODELS

Since all of the buildings are relatively symmetric in plan, only half of each structure is considered in the analyses. A 2-D centerline model of one of the N-S perimeter frames, carrying half the load in that direction, was prepared for each of the structures. A lumped mass model was used, and Rayleigh damping was assumed in the dynamic analysis. The time step used in the analyses was varied until a stable converged solution was obtained. In general, a time step of 0.001 sec was necessary.

The gravity loads used for the analysis of the frames were based on details provided in FEMA 355C (2000). The distribution of the floor dead loads (DL) and live loads (LL) is given as follows:

Load Description	Load (psf)
Floor dead load for weight calculations	96
Floor dead load for mass calculations	86
Roof dead load excluding penthouse	83
Penthouse dead load	116
Reduced live load per floor and for roof	20

Table 4.1 Distribution of gravity loads on the structures.

A load combination of 1.0DL + 0.25LL was used for the gravity loads. Based on these loading definitions, the seismic masses (from one-half of the structure) associated with the frames are given in Table 4.2 (FEMA 355C, 2000). Note that the mass was applied to only one node at each level since the horizontal displacements were coupled at each floor level (under the assumption of axially rigid beams). Live loads were not included for the purpose of calculation of the masses, but the dead load due to the penthouse was included.

Building	Floor	Mass (kips-sec^2/ft)
3-Story	Roof	35.45
	Floor 3 and Floor 2	32.71
9-Story	Roof	36.55
	Floor 9 to Floor 3	33.93
	Floor 2	34.52
20-Story	Roof	20.03
	Floor 20 to Floor 3	18.88
	Floor 2	19.31

Table 4.2 Seismic Masses applied in the Computational models of the structures.

The yield strengths of the members were taken to be the expected yield strengths for the steel used, namely 49.2 ksi for A36 steel and 57.6 ksi for Grade 50 steel. All of the elements were modeled with 3% strain hardening. This strain hardening was assumed to be maintained even at very large inelastic deformations. Other simplifications include the following: (i) torsional effects due to the penthouse on the roof of each building were ignored, (ii) panel zone deformations were not modeled, and (iii) shear deformations in beams and columns were ignored.

The authors are aware that the use of centerline models and other simplifications such as those mentioned above may sometimes result in an inaccurate evaluation of the seismic demand for SMRF buildings, mostly at the element level but possibly also at the global level. This often happens because simplified modeling assumptions can affect the mechanisms that bring the building to collapse (e.g., see Gupta and Krawinkler, 1999). In our study, however, the focus was on developing an improved methodology for estimating structural response and consequent losses based on a host of different ground motion parameters rather than on providing the best seismic demand evaluation for the three buildings, as one would strive to accomplish in a real-life practical applications. The use of more sophisticated models would have increased the already considerable computational burden without much added value to the goals of this study.

4.3.1 BEAMS

Each beam member is modeled using an elastic central frame element and inelastic plastic hinge elements at its ends. The RUAUMOKO program combines the three elements into a single one, whereas the three elements are modeled separately in DRAIN-2DX. In either case, the stiffness of each plastic hinge is governed by a specified hysteresis rule, either ductile bilinear or brittle quadrilinear, as described in the two subsections that follow. The stiffness of the hinge is such that the rotation of the hinge together with the rotation associated with the elastic curvature of the beam member over the hinge length is assumed to be the same as the rotation associated with the curvature over the hinge length with the inelastic properties in the hinge zone. If the hinge is in the elastic range, the plastic hinge has an infinite stiffness. No rigid end zones are modeled, and panel zone deformations are ignored. Where the connections are moment-resisting, the beam member is built into the joint, but where there are pinned connections (e.g., in the 9-story frame), the members are connected with pin joints. Axial and shear deformations in the beams are neglected.

4.3.1.1 DUCTILE CONNECTION BEHAVIOR

In order to model post-Northridge connections, a bilinear ductile hysteresis model is chosen. The plastic point hinges at the ends of each beam are rigid-plastic. The overall moment-rotation behavior of the beam is described in Figure 4.3, where k_o is the initial stiffness and r is the strain hardening ratio. As mentioned earlier, an assumed strain-hardening ratio of 3% is maintained throughout the hysteresis. The beams yield at the plastic moment, M_p, which is equal to ZF_{ye}, where Z is the plastic section modulus and F_{ye} is the expected yield strength of the beam material.

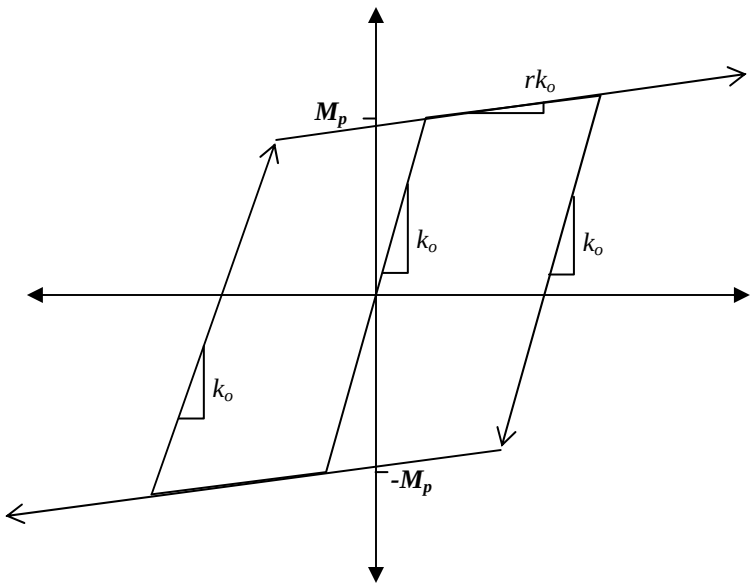

Figure 4.3 Generalized Moment-Rotation Behavior of a Ductile Connection.

4.3.1.2 BRITTLE CONNECTION BEHAVIOR

In order to model pre-Northridge connections, a quadrilinear brittle hysteresis model is chosen. At plastic rotations lower than a specified fracture threshold, the point hinges at the ends of each beam are rigid-plastic, as was the case for the ductile connections. At plastic rotations above the threshold, however, the moment capacity drops sharply to a specified fraction of M_p (the plastic moment). This fraction and the plastic rotation threshold are specified according to the FEMA 351 (2000) guidelines (Section 6.2.1.1.2 on Nonlinear Analysis), assuming a one-to-one correspondence between inter-story drifts and plastic rotations. Specifically, the plastic rotation threshold (θ_{SD} in FEMA 351) is set according to Equation (4.1), where d_b is the beam depth (in inches).

$$\theta_{SD} = 0.061 - 0.0013 d_b \tag{4.1}$$

The fraction of M_p to which the moment capacity drops upon fracture is set to 20%. An illustration of the moment-rotation behavior of a brittle hinge is provided in Figure 4.4. As was the case for the ductile hinges, the assumed strain-hardening ratio of 3% is maintained throughout the hysteresis here as well.

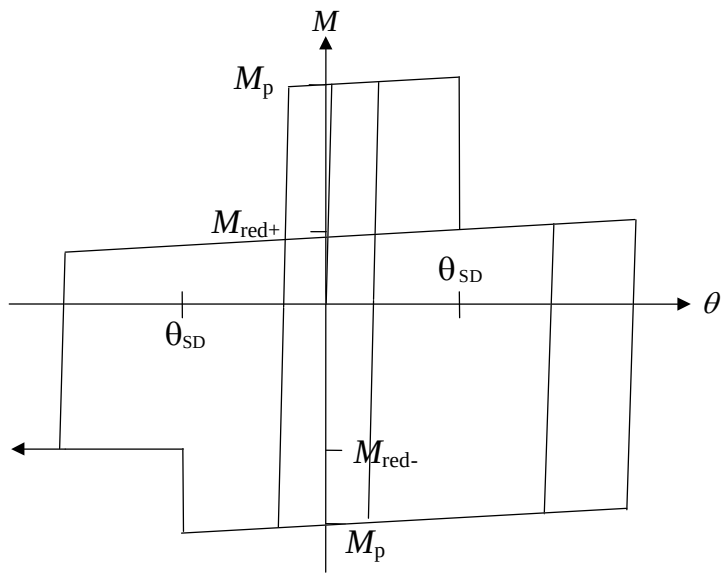

Figure 4.4 Generalized Moment-Rotation Behavior of a Brittle Connection.

Brittle connection behavior, as shown in Figure 4.4, was modeled using DRAIN-2DX. The same behavior, however, could not be modeled using RUAUMOKO, even though the program allows for strength deterioration. Hence, for the brittle model of each building, only DRAIN-2DX results have been computed.

4.3.2 COLUMNS

The columns are modeled using beam-column elements defined in RUAUMOKO and DRAIN-2DX. A ductile moment-curvature hysteresis similar to that for the beams is also used for the columns – i.e., bilinear with 3% strain hardening. The columns are not modeled with any strength-degradation or local buckling behavior. A bilinear interaction diagram for axial force and moment is used, however, as shown in Figure 4.5, where P_y is the axial load capacity equal to AF_{ye} and M_p is equal to ZF_{ye}, while A is the cross-sectional area, Z is the plastic section modulus, and F_{ye} is the expected yield strength of the material of the columns. Note that the interaction diagram is symmetric about both axes. The equation describing the interaction diagram (for strong-axis bending) displayed in Figure 4.5 is as follows:

$$M = \begin{cases} M_p & \text{for } P < 0.15P_y \\ 1.18M_p\left(1 - P/P_y\right) & \text{otherwise} \end{cases} \tag{4.2}$$

where M is the bending moment capacity of the column.

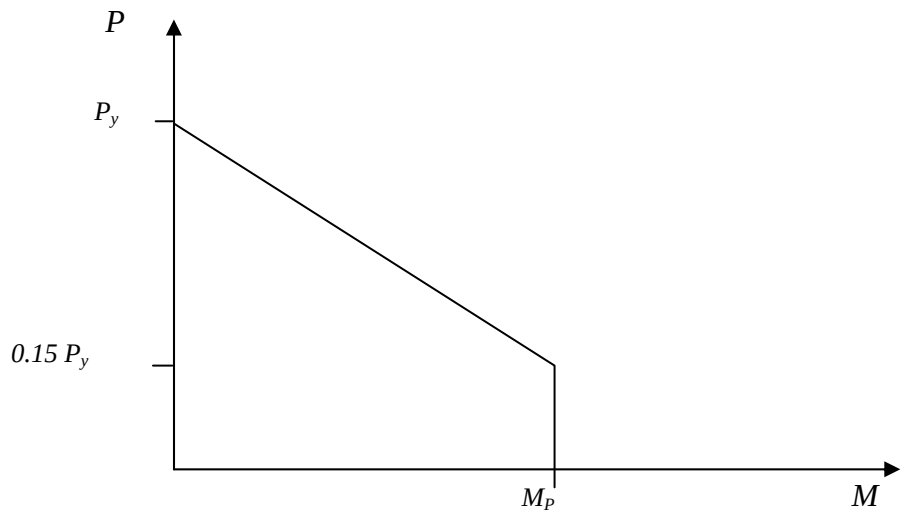

Figure 4.5 Axial Load-Moment Interaction Diagram used for the Columns.

4.3.3 OTHER MODELING CONSIDERATIONS

Since the structures are expected to undergo large displacements under seismic loading, it is important to consider P-Delta effects and the loads from interior gravity frames. A dummy axially rigid column (FEMA 355F, 2000) with zero bending stiffness was included in the model to carry the gravity loads associated with the interior gravity frames (for half of the structure). The horizontal displacement of the dummy column at each level was coupled with the horizontal displacement of the frame at that level. By doing this, the frame experiences P-Delta effects caused by the interior gravity frames, but the dummy column does not provide any lateral resistance.

4.4 DAMAGE MEASURES

In this section, we discuss some of the results obtained from the nonlinear dynamic analyses by examining various structural response measures. Most of the results are for the *ductile* 9-story building model (computed using RUAUMOKO). The response measures are briefly described before presenting the results.

The structural response measures used in the regression studies to be presented in Chapter 5 are (i) the peak inter-story drift ratio (*IDR*), (ii) the peak roof drift ratio (*RDR*), (iii) the maximum (over all stories) peak inter-story drift ratio (*MIDR*), and (iv) the average (over all stories) peak

inter-story drift ratio (*AIDR*). In order to better understand the results from the nonlinear analyses we have also studied beam moments and other drift measures. Only behavior thought to be important for this study is included in the discussion that follows.

4.4.1 ROOF DRIFT RATIO

The peak roof drift ratio (denoted as *RDR*) is defined, for a given time history, as the ratio of the peak lateral roof displacement (relative to the ground) to the building height. The *RDR* demand is a measure of the global seismic response of the structure, and is also related to the global stability of the moment-resisting frame. Figure 4.6 shows a sample ground acceleration record used in this study, and Figure 4.7 shows the time history of the roof drift ratio for the 9-story ductile model subjected to this ground motion. Figure 4.8 shows a snapshot of the displaced shape of the structure at the time instant when the peak roof drift ratio (*RDR*) is observed.

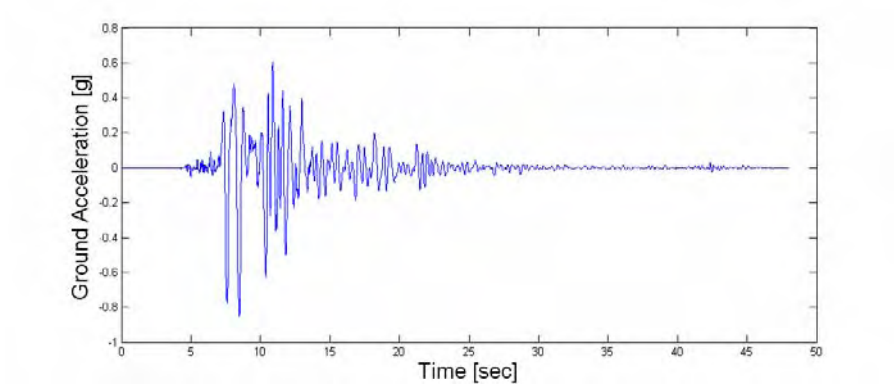

Figure 4.6 A sample input ground motion (recorded during the Kobe earthquake).

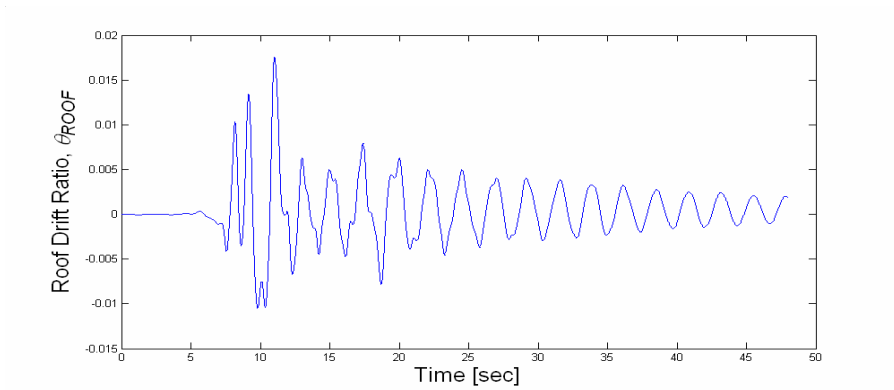

Figure 4.7 Time history of the roof drift ratio resulting from the ground motion in Figure 4.6 applied to the ductile 9-story building model.

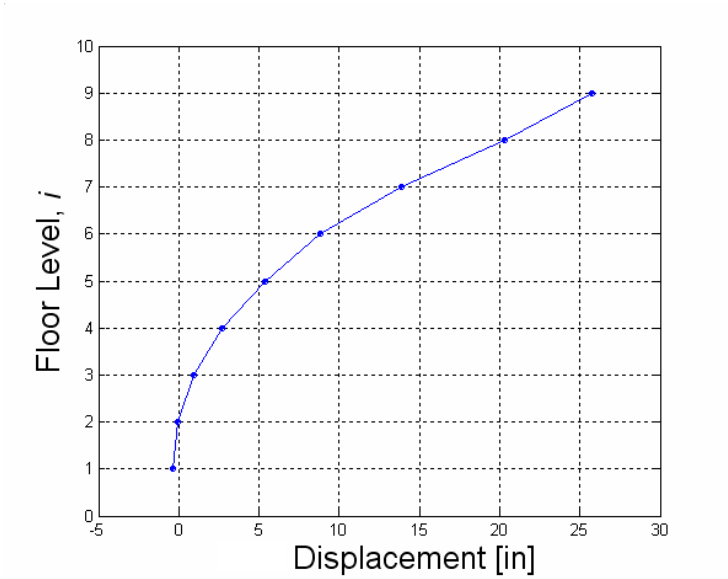

Figure 4.8 Displaced shape of the ductile 9-story structure at around 11 sec, when the lateral roof displacement is at its peak, resulting in a roof drift ratio of approximately 0.018 (see Figure 4.7).

4.4.2 PEAK INTER-STORY DRIFT RATIOS

Peak inter-story drift ratio (denoted as *IDR*) is defined, for a given time history, as the maximum (over time) difference between the lateral displacements of two adjacent floors, divided by the height of the story. Note that *IDR* will generally be closely related to both structural and non-structural damage experienced in the story during an earthquake. Inter-story drifts also tend to be about the same as the rotational demands on nearby beam-column connections. Figure 4.9 shows the time history of the inter-story drift ratio at the eighth story of the ductile 9-story building subjected to the same ground motion as before (i.e., that shown in Figure 4.6). Figure 4.10 shows a snapshot of the displaced structure at the instant when the inter-story drift ratio at the eighth story is at its peak, which is equal to 0.048. This peak value is obtained by dividing the difference between the displacement at the eighth and seventh stories (i.e., 13.2 in – 5.7 in) by the height of the story (i.e., 156 in from Figure 4.2).

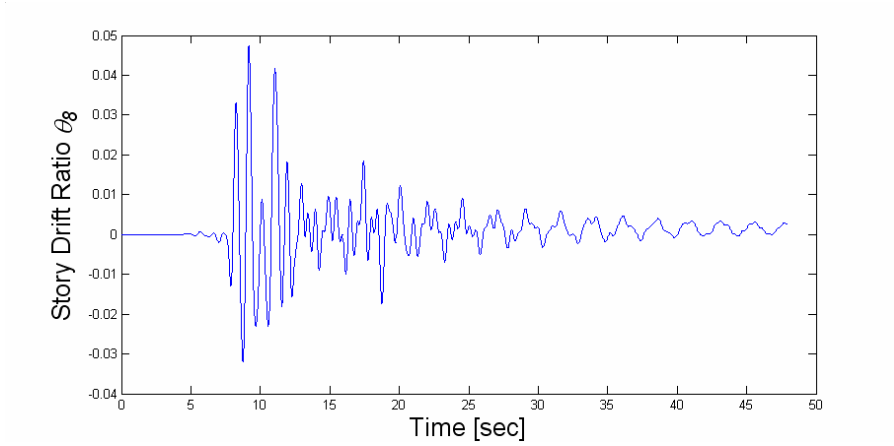

Figure 4.9 Time history of the inter-story drift ratio at the eighth floor of the ductile 9-story building model (denoted θ_8 in the figure).

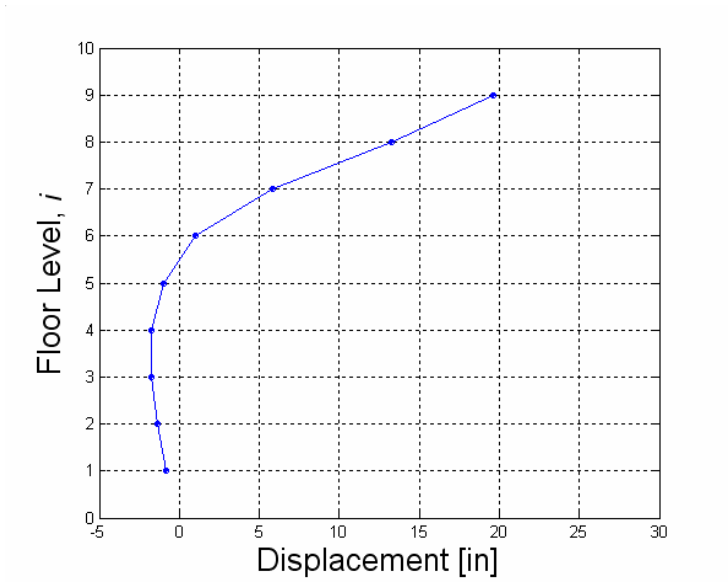

Figure 4.10 Displaced shape of the ductile 9-story structure at around 9 sec, when the inter-story drift ratio at the eighth story is at its peak, equal to approximately 0.048.

Figure 4.11 shows plots over the building height of the median *IDR* when all of the 140 selected ground motions are considered, as well as when the near-source and ordinary motions are considered separately. Similarly, Figure 4.12 shows plots of the median peak *floor displacements* over the building height. The median patterns of *IDR* and floor displacements are consistent with each other. In general, higher *IDR* values are observed at the eighth and first stories of the frame. The displacements at lower floors are smaller compared to the displacements at the higher levels.

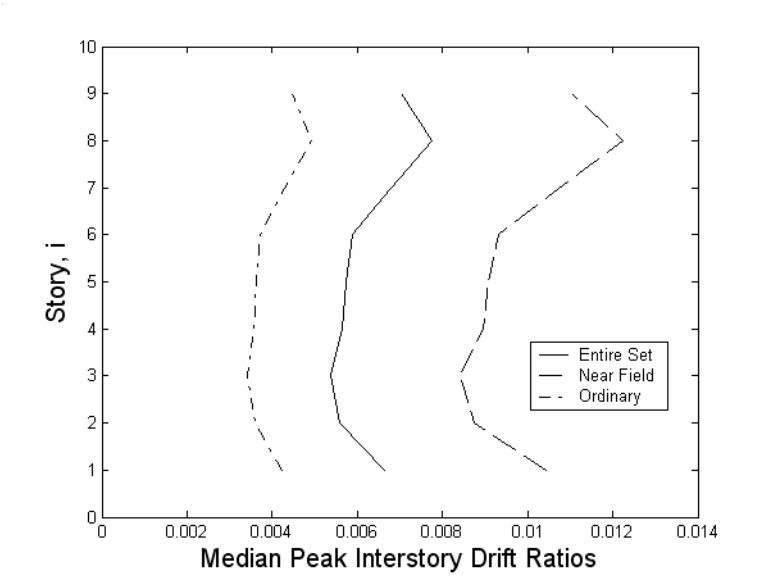

Figure 4.11 Median Peak Inter-story Drift Ratios (*IDR*) plotted over the building height for the ductile 9-story building model.

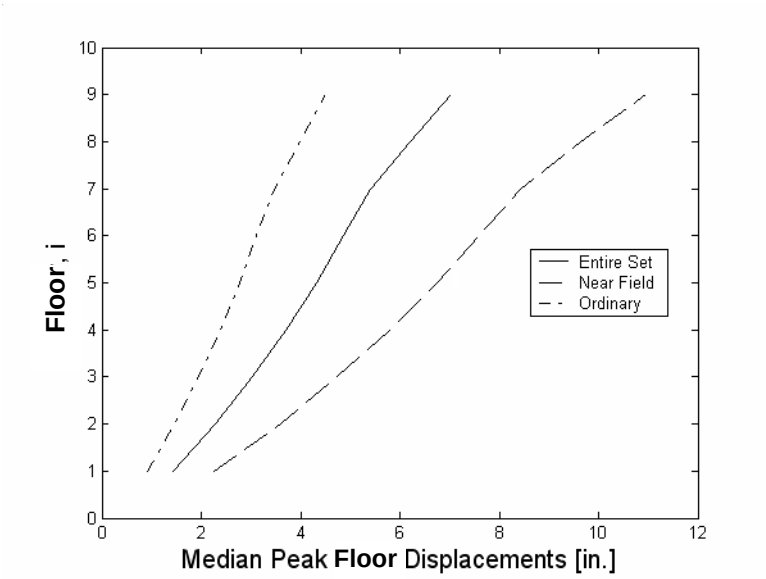

Figure 4.12 Median Peak Floor Displacements plotted over the building height for the ductile 9-story building model.

4.4.3 MAXIMUM AND AVERAGE PEAK INTER-STORY DRIFT RATIOS

Two parameters summarizing inter-story drifts are commonly used. The maximum (over all the stories) peak inter-story drift ratio (denoted as *MIDR*) is related to local damage in any single story throughout the height of the structure. It is also related to stability in terms of story collapse. The average (over all stories) peak inter-story drift ratio (*AIDR*) is related to the overall stability of the structure and also to the overall damage.

4.4.4 DRIFT LOCALIZATION

If the variation of drift throughout the height of a structure is linear, the value of *MIDR* is close to the value of *RDR*. Deviations from a linear drift variation can be caused by various factors, including the frequency content of the input ground motion. In order to study such behavior, we define a drift localization ratio given by the ratio of *MIDR* to *RDR*. This parameter is expected to be close to unity if the drift varies uniformly over the height of the structure, and significantly larger than unity if the drift is mostly concentrated at any one story. Figure 4.13 shows a plot of the drift localization ratio against the ratio of the spectral acceleration at the second-mode period, $S_a(T_2)$, to the spectral acceleration at the fundamental period, $S_a(T_1)$. Note that the localization ratio deviates significantly from unity as the ratio $S_a(T_2)/S_a(T_1)$ increases. This suggests that as higher modes grow in importance due to the increased input at these shorter periods, the inter-story drifts tend to be more variable over the height of the structure and are usually more localized.

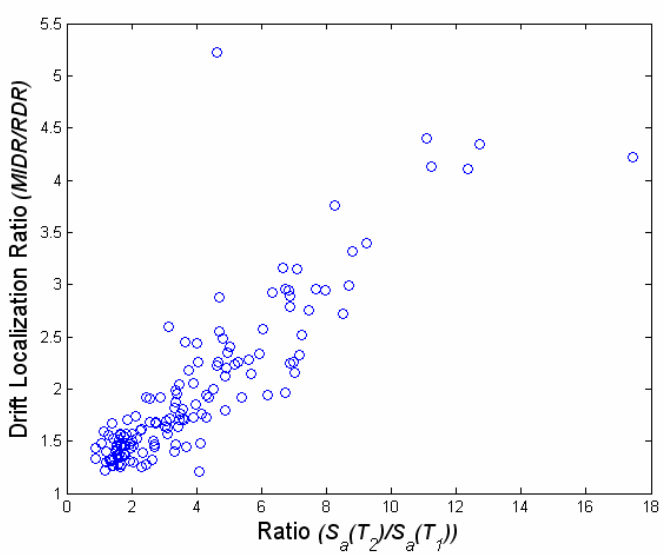

Figure 4.13 Drift localization ratios from all 140 selected ground motions plotted against the ratio of second-mode spectral acceleration to first-mode spectral acceleration for the ductile 9-story building model.

At least in terms of elastic drift response, the observed drift localization is consistent with higher-mode participation, as can be confirmed by studying the first three vibration modes of the 9-story building in Figure 4.14. The corresponding natural vibration periods are also noted in the figure. It can be seen that as modes beyond the fundamental begin to participate, deviations from a linear variation in drift grow.

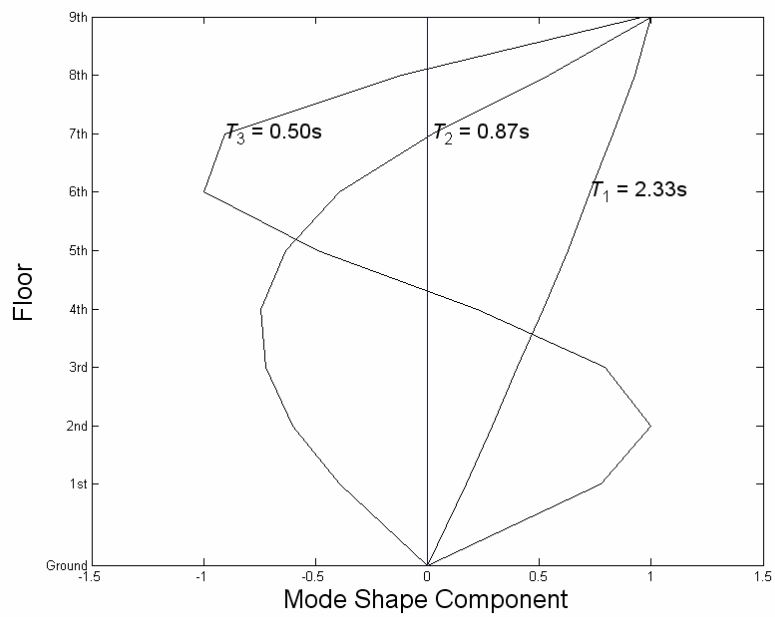

Figure 4.14 First three mode shapes and natural vibration periods of the 9-story building.

4.4.5 BEAM BEHAVIOR

The extent of inelastic behavior in the structures considered can be understood by studying the behavior of the beam connections. Figure 4.15 shows a hysteresis plot for a typical ductile connection obtained from the nonlinear dynamic analyses. Note that the strain hardening is maintained even at large rotations. This assumption is not very realistic and the results presented need to be interpreted with this consideration in mind.

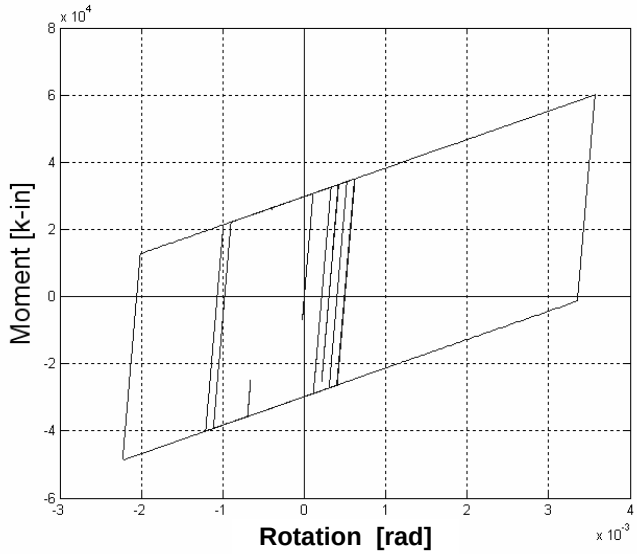

Figure 4.15 Hysteresis plot for a typical ductile connection obtained from a single nonlinear dynamic analysis of the 9-story building.

Beam-end moments at each floor, normalized with respect to the corresponding plastic moments, are also studied. Figure 4.16 shows a plot of median values of these normalized beam moments over the height of the 9-story building. The median values are based on the entire set of ground motions, as well as on the ordinary and near-source ground motion sets considered separately, and take into account all of the beam ends on a floor. These normalized moments provide an indication of the extent of yielding that occurs in the beams at each floor. Yielding in the beams can be followed by large inelastic rotations at the connections. As the moments in the beams increase due to strain hardening, the demands on the columns increase, which can cause the columns to yield and bring about larger drifts in some stories. Figure 4.17 shows time histories of the normalized beam moments at the third and the eighth floor and the corresponding normalized column moments above the joints. The beam moments at the eighth floor are as much as 3 times the plastic moment, causing yielding in the columns. The moments at the third floor reach a maximum of 1.5 times the plastic moment; as a result, there is no yielding in the columns at that floor. Figure 4.18 shows the corresponding time histories of inter-story drift ratio (*IDR*) at the third and the eighth stories. The *IDR* at the eighth story is as high as 5%, whereas that at the third story is only 2% for the particular ground motion record considered here.

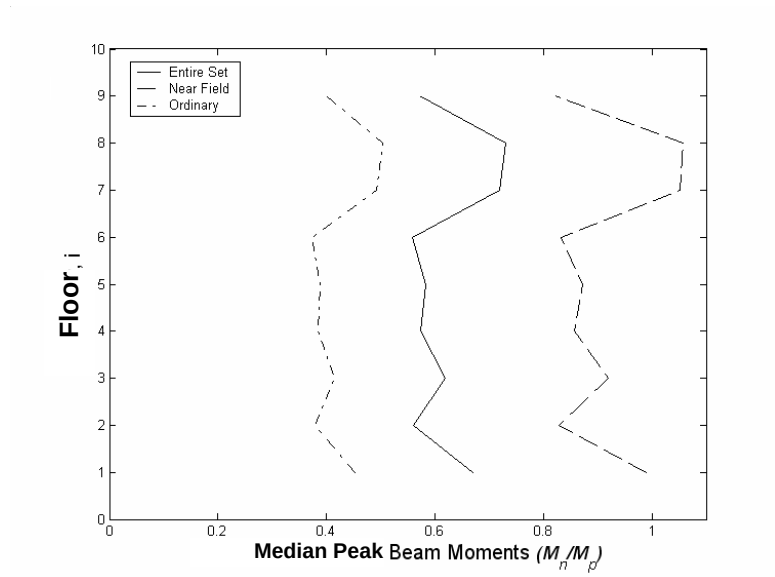

Figure 4.16 Median normalized peak beam moments at each floor plotted over the building height for the ductile 9-story building model.

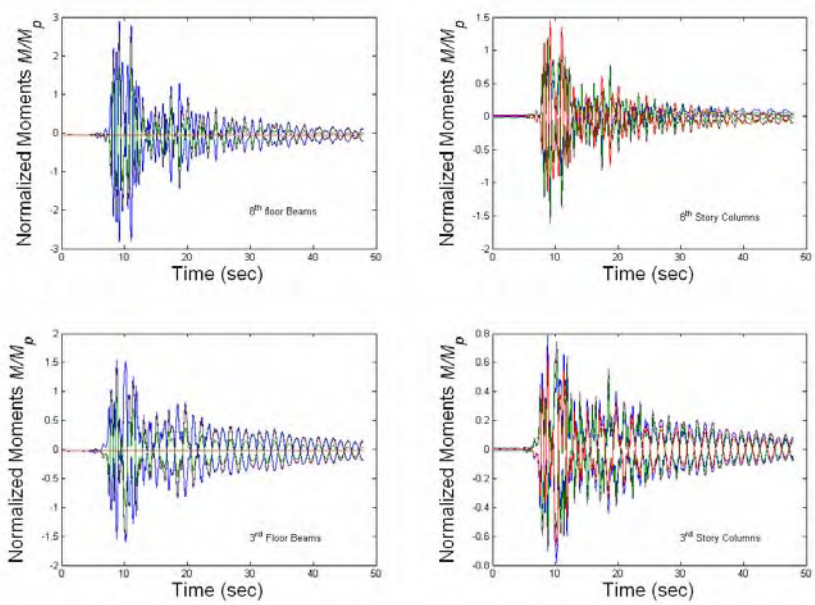

Figure 4.17 Time histories of member-end moments at the third and eighth floors of the 9-story building from a single nonlinear dynamic analysis.

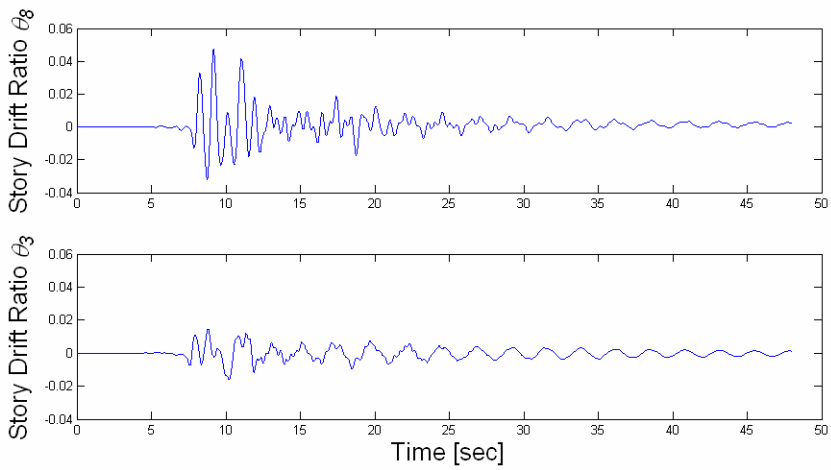

Figure 4.18 A comparison of the time histories of inter-story drift ratios at the eighth and the third stories of the ductile 9-story building for the same ground motion input considered in Figure 4.17.

4.5 RELATIONSHIP BETWEEN STRUCTURAL RESPONSE MEASURES AND GROUND MOTION PARAMETERS

Before formally presenting the method for evaluating the extent of correlation between structural response and ground motion intensity measures, let us examine the relationship between these variables graphically. Figures 4.19 through 4.21 show plots of *MIDR* and *RDR* for the three ductile building models (computed using RUAUMOKO) versus the fundamental period spectral acceleration, $S_a(T_1)$, in each case. The data points shown on each plot result from nonlinear dynamic analyses with all 140 selected ground motion records. Note that both of the response measures for the 3-story model are highly correlated with $S_a(T_1)$, even in the nonlinear range (i.e., at drift ratios above 0.01, approximately). However, the plots of *MIDR* versus $S_a(T_1)$ for the 9-story and 20-story models suggest a greater amount of variability compared to the plots of *RDR* versus $S_a(T_1)$. This is due to the contribution of higher modes to the response of mid-rise and high-rise buildings, especially in localized parts of such structures.

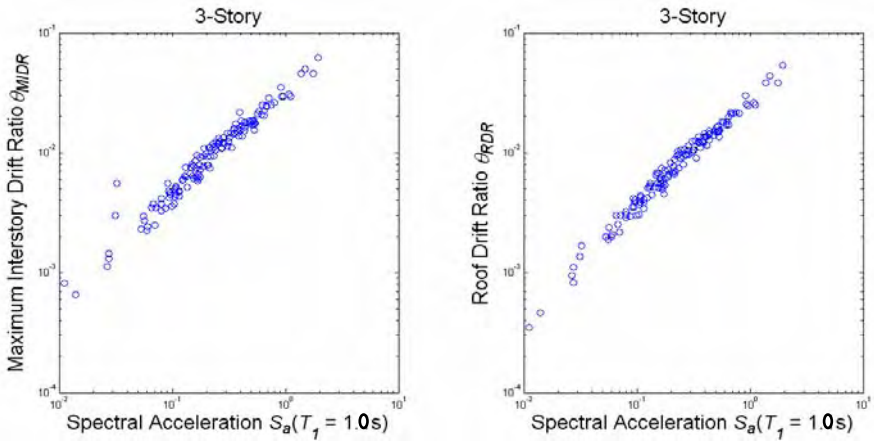

Figure 4.19 Plots of *MIDR* and *RDR* vs. the fundamental period spectral acceleration for the ductile 3-story model.

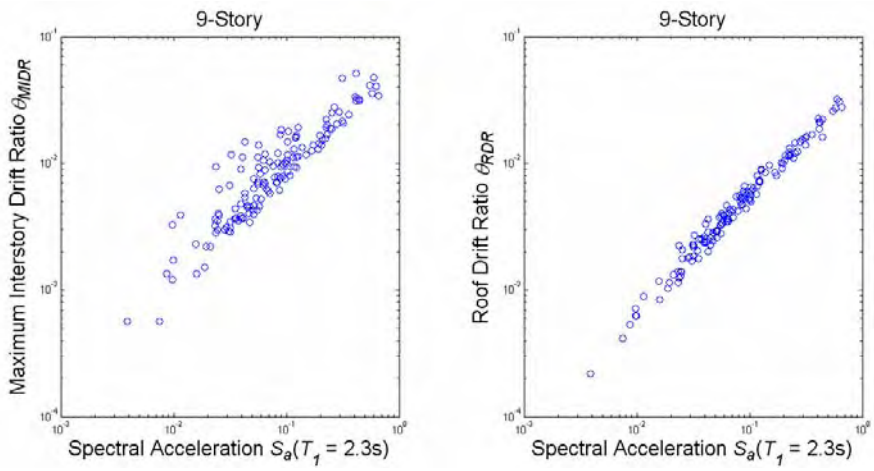

Figure 4.20 Plots of *MIDR* and *RDR* vs. the fundamental period spectral acceleration for the ductile 9-story model.

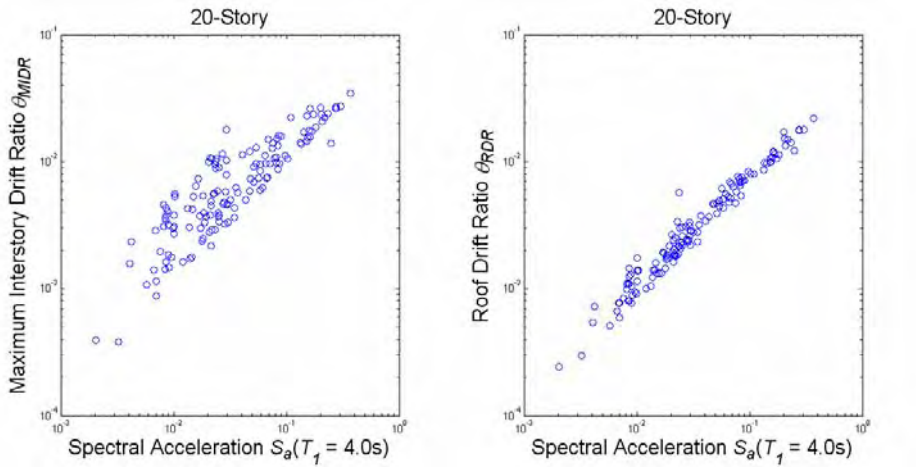

Figure 4.21 Plots of *MIDR* and *RDR* vs. the fundamental period spectral acceleration for the ductile 20-story model.

Various functional forms can be employed to describe the relationship between response measures, such as *MIDR* and *RDR*, and ground motion parameters, such as A_i and S_a. Given the practically linear log-log relationship observed between *MIDR* or *RDR* and S_a, we will employ a power law format in the regression analyses that will relate the response measures, $\boldsymbol{Y}$, to the ground motion intensity measures, $\boldsymbol{X}$. This is discussed in Chapter 5.

4.6 CONCLUDING REMARKS

A description of the structures chosen for the study was presented and details related to the computational models for the dynamic analyses were discussed. Elastic, ductile, and brittle computational models for the 3-story, 9-story, and 20-story structures have been analyzed for the 140 ground motion records, and various response measures have been computed. In particular, the peak inter-story drift ratios at all stories and the peak roof drift ratio are of interest. Whereas the response of the 3-story structure is mainly governed by its first mode, higher modes have a significant influence on the behavior of the 9- and 20-story structures. In the next chapter, regression analyses relating the computed response measures to the ground motion parameters are presented. The use of these regression results in illustrative loss estimation calculations is presented in Chapter 6.

CHAPTER 5 – MULTIVARIATE MULTIPLE LINEAR REGRESSION ANALYSES

5.1 INTRODUCTION

An important goal of engineers in seismically active regions is to be able to estimate likely damage and monetary losses that might result during an earthquake. Accordingly, our interest here is in predicting structural response measures (such as inter-story drift ratios), which can be related to damage and monetary loss, directly from ground motion parameters. The monetary loss due to damage depends on several factors – e.g., damage to connections, damage to structural members, damage to partitions, damage to equipment, etc. – all of which may vary from story to story. The accuracy of our assessment of monetary losses, therefore, is expected to improve if we use a vector of structural response measures that captures the drifts at each story of the given building. Furthermore, several studies have suggested that the nonlinear response of structures to ground motion may be explained better by using more than a single ground motion parameter (typically spectral acceleration). By including more information about the ground motion via a vector of ground motion parameters, one might expect to reduce the uncertainty involved in prediction of structural response. In order to evaluate the predictive power of vector-valued ground motion parameter sets in estimating vector-valued structural response measures, we will make use of multivariate multiple linear regression (MMLR).

A multivariate multiple linear regression (MMLR) analysis can be used to investigate the relationship between a vector of response (or "dependent") variables and a vector of predictor (or "independent") variables. MMLR is similar to the more widely used multiple linear regression (MLR), where a single response is related to several predictor variables. Computationally, MMLR yields the same regression model coefficients and the same conditional variances as one would estimate with individual MLR computations for each of the response variables separately. However, since the various response parameters are in general correlated, we need to carry out a MMLR if we wish to get information on the correlation between the different response variables conditioned on the predictor variables. This information on the cross-correlation among the response variables is needed in order to accurately estimate damage and losses that, in general, might be dependent on several response measures jointly.

5.2 METHODOLOGY

Suppose our interest is in the prediction of an n-dimensional response vector, $\boldsymbol{Y}$, from an r-dimensional ground motion parameter vector, $\boldsymbol{X}$. A multivariate multiple regression model can be described as follows (see, for example, Johnson and Wichern, 2002):

$$Y_i = b_{0i} \cdot \prod_{j=1}^{r} X_j^{b_{ji}} \cdot \varepsilon_i \qquad \text{for } i = 1 \text{ to } n. \tag{5.1}$$

where Y_i is the ith component of the response variable vector, $\boldsymbol{Y}$; each X_j is a predictor variable (GMP) that is a part of the vector, $\boldsymbol{X}$; b_{0i} and b_{ji} (with j = 1 to r) are model parameters (regression coefficients) to be determined; and ε_i is an error/residual term associated with each response variable, Y_i. Each response variable is thus assumed to follow its own regression model (we have chosen a power law, or log-log linear format in Equation 5.1), but these response variables in general may be correlated. In order to perform multivariate multiple linear regression, we take the natural log of both sides of Equation 5.1 and form the following equation written in matrix form:

$$\boldsymbol{\theta} = \mathbf{Zb} + \ln\boldsymbol{\varepsilon} \tag{5.2}$$

$$\text{where } \boldsymbol{\theta} = \ln\mathbf{Y},\ \mathbf{Z} = [\mathbf{1}\ \ \ln\mathbf{X}] \text{ and } \underset{((r+1)\times n)}{b} = \begin{bmatrix} \ln b_{01} & b_{02} & \cdots & b_{0n} \\ \ln b_{11} & b_{12} & \cdots & b_{1n} \\ \vdots & \vdots & \ddots & \vdots \\ \ln b_{r1} & \cdots & \cdots & b_{rn} \end{bmatrix} \tag{5.3}$$

The regression is said to be linear because the regression equation is linear in the coefficients, b_{ji}. Note from Equation 5.2 that $\sigma_{\ln \boldsymbol{Y}|\boldsymbol{X}}$ is equal to $\sigma_{\ln\boldsymbol{\varepsilon}}$. Each error term, $\ln\varepsilon_i$, is typically assumed to be normally distributed. Also, note that $\mathbf{E}(\ln\boldsymbol{\varepsilon}) = \mathbf{0}$, while the covariance matrix $\mathrm{Cov}(\ln\boldsymbol{\varepsilon})$ (denoted by $\boldsymbol{\Sigma}$ here) will be estimated. The design matrices for m observations are formulated as follows where the number of rows in $\boldsymbol{\theta}$ and in $\mathbf{Z}$ is equal to the number of observations:

$$\underset{(m\times n)}{\boldsymbol{\theta}} = \begin{bmatrix} \ln Y_{11} & \ln Y_{12} & \cdots & \ln Y_{1n} \\ \ln Y_{21} & \ln Y_{22} & \cdots & \ln Y_{2n} \\ \vdots & \vdots & \ddots & \vdots \\ \ln Y_{m1} & \cdots & \cdots & \ln Y_{mn} \end{bmatrix} \text{ and } \underset{(m\times(r+1))}{Z} = \begin{bmatrix} 1 & \ln X_{11} & \cdots & \ln X_{1r} \\ 1 & \ln X_{21} & \cdots & \ln X_{2r} \\ \vdots & \vdots & \ddots & \vdots \\ 1 & \ln X_{m1} & \cdots & \ln X_{mr} \end{bmatrix} \tag{5.4}$$

The unbiased least squares estimator of **b,** i.e., $\hat{\boldsymbol{\beta}}$, is given by the equation

$$\hat{\boldsymbol{\beta}} = (\mathbf{Z}'\mathbf{Z})^{-1}\mathbf{Z}'\boldsymbol{\theta} \tag{5.5}$$

where **Z'** is the transpose of **Z**. The unbiased least squares estimator of the covariance matrix, **Σ,** is given by the equation

$$\boldsymbol{\Sigma} = \mathrm{E}\left[\frac{\hat{\boldsymbol{\varepsilon}}' \cdot \hat{\boldsymbol{\varepsilon}}}{(n-r-1)}\right] \text{ where } \hat{\boldsymbol{\varepsilon}} = \boldsymbol{\theta} - \mathbf{Z}\hat{\boldsymbol{\beta}} \tag{5.6}$$

5.3 VECTORS OF STRUCTURAL RESPONSE MEASURES

Numerous studies have suggested that damage to structural components, as well as damage to many types of non-structural components (e.g., partitions, windows, interior doors and plaster ceilings), is strongly correlated with peak inter-story drift ratios (e.g., Gupta and Krawinkler, 1999; Taghavi and Miranda, 2003). Monetary losses have often been related to a single scalar drift measure that is a fairly good indicator of overall damage to the structure (e.g., *MIDR* in Miranda and Aslani, 2003). However, losses that occur in an earthquake can be related to damage at various locations in a building, making it difficult to estimate such losses using a single response measure. The accuracy in estimation of losses might improve significantly if we use more than a single response measure to capture the different aspects of damage to the structure that are in turn related to losses. Specifically, in our study, we consider two different vectors of response measures. The first one is comprised of the peak inter-story drift ratios (*IDR*s) at all the stories in the building. The other is a vector of *MIDR*, *AIDR*, and *RDR*. We have selected these vectors because we believe that the joint knowledge of the response measures in each of these vectors can help us estimate losses with higher levels of confidence than any of the measures singly. In summary, the response measures in the vector, ***Y*,** include:

Vector 1:

- IDR_j (Peak inter-story drift ratio for each story j) for j = 1 to number of stories in the building.

Vector 2:

- *RDR* (Peak roof drift ratio)
- *MIDR* (Maximum inter-story drift ratio)
- *AIDR* (Average inter-story drift ratio)

In the results presented later in this chapter (as well as in Chapter 6), a single scalar response measure, namely *RDR*, is also considered for comparison purposes.

5.4 VECTORS OF GROUND MOTION PARAMETERS

As detailed in the subsections below, the vectors of GMPs (i.e., ***X***'s) chosen are motivated by (i) the modal analysis approach to computing the response of an elastic structure to a given ground motion, (ii) the potential for energy-based GMPs to improve the prediction of nonlinear structural response, and (iii) the use of inelastic GMPs that consider the overall strength of the given structure. The GMPs investigated are grouped into three different categories, namely those that are (i) elastic and associated with the first mode of vibration, (ii) elastic but consider multiple modes of vibration, and (iii) inelastic for the first mode and elastic for higher modes.

Energy-based and displacement-based GMPs are considered within all three categories, as explained below.

5.4.1 FIRST-MODE ELASTIC GMP'S

Since the dynamic response of a structure to ground shaking is often dominated by its first mode of vibration, it is important to include a first-mode-based parameter in any vector of ground motion parameters. Currently the most widely used GMP is the elastic spectral acceleration at the fundamental period of the structure (and for a damping ratio of 5%), denoted here as $S_a(T_1)$. Recall that the fundamental periods of vibration for the 3-story, 9-story, and 20-story SMRF buildings considered in this study were 1.0, 2.3, and 4.0 seconds, as shown in Figures 4.19 to 4.21, respectively. In this study, the results of regressing different structural response measures on $S_a(T_1)$ alone will serve as a baseline for comparing the results obtained using vectors of GMPs.

As described in Chapter 3, another first-mode-based GMP is the elastic input energy-equivalent acceleration (again at the fundamental period of the structure and for 5% damping), denoted $A_i(T_1)$. Although $S_a(T_1)$ and $A_i(T_1)$ are based on the response of the same elastic oscillator, $A_i(T_1)$ implicitly includes information regarding the duration of the ground motion and structural response, unlike $S_a(T_1)$. Hence, the results of regressing structural response measures on $A_i(T_1)$ alone are also investigated in this report.

In addition to regressing structural response measures on $S_a(T_1)$ and $A_i(T_1)$ individually, these two GMPs are considered jointly in a vector GMP in order to evaluate if the combination can lead to a beneficial improvement in the quantification of the damage potential of ground motions. Recall from Section 3.3.4, however, that $S_a(T_1)$ and $A_i(T_1)$ are highly correlated (except perhaps at short T_1 values). As a result, it is difficult to distinguish between the two GMPs in the regression analyses (i.e., the problem known as multicollinearity in statistical regression jargon may arise). In this study, therefore, $A_i(T_1)$ is divided by $S_a(T_1)$ before considering it as the second element of the vector GMP with $S_a(T_1)$. As illustrated in Figure 5.1, the result is to reduce the correlation between the two elements of the vector GMP, while still maintaining information regarding both $S_a(T_1)$ and $A_i(T_1)$ in the vector GMP.

In summary, the first-mode elastic GMPs considered are:

- $S_a(T_1)$
- $A_i(T_1)$
- $\{ S_a(T_1),\ A_i(T_1) / S_a(T_{1\backslash}) \}$

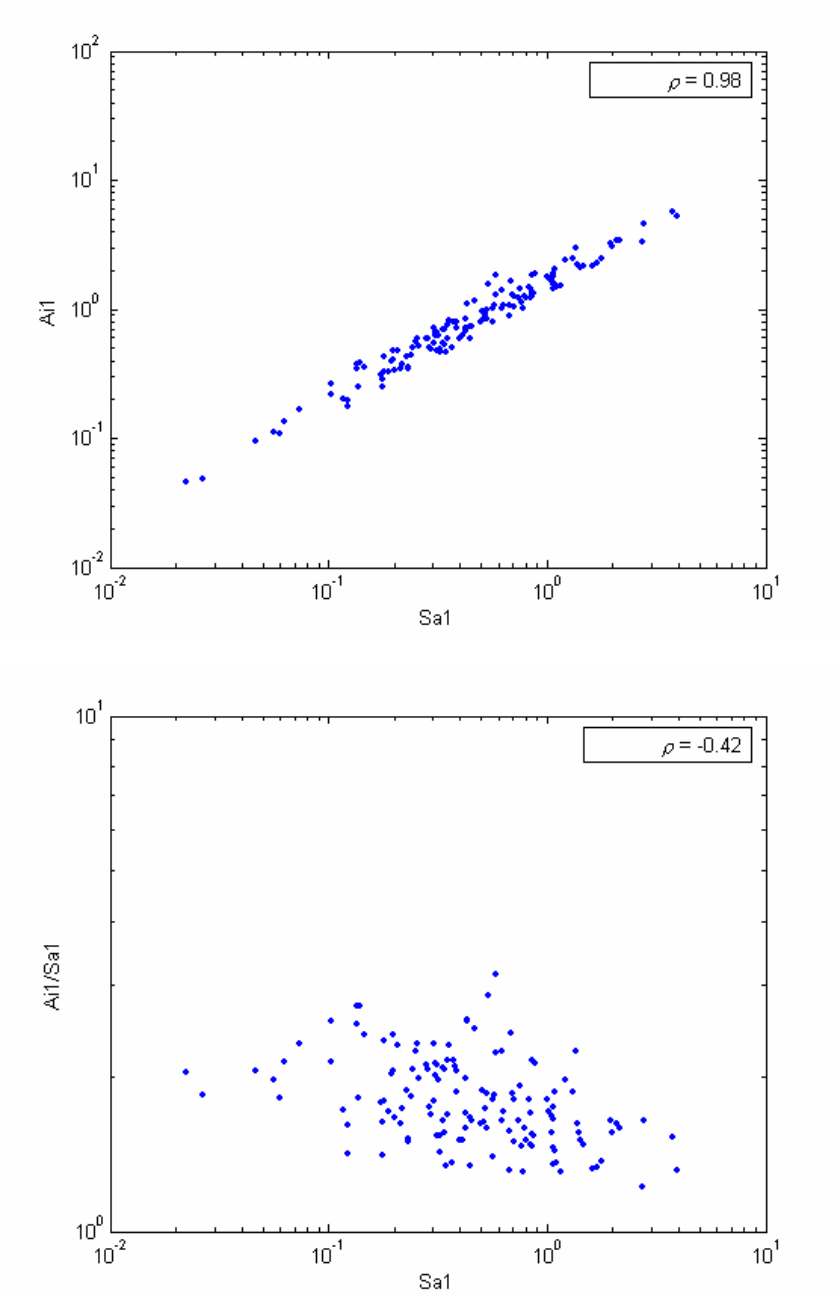

Figure 5.1 Illustration of the strong correlation between $S_a(T_1)$ and $A_i(T_1)$ (top), and the weaker correlation between $S_a(T_1)$ and $A_i(T_1)$ / $S_a(T_1)$ (bottom), for T_1=1.0 sec.

5.4.2 MULTI-MODE ELASTIC GMP'S

It is understood that, for some structures, the contribution to response from higher modes can be significant. Very often, though, the response will be mainly dominated by the first few modes. Accordingly, we consider several vector GMPs that include spectral acceleration and/or input energy-equivalent acceleration for up to four modes. In all of these vectors, either $S_a(T_1)$ or $A_i(T_1)$ is the first element.

Since modal analysis for elastic structures involves computation of the response to a given ground motion via a weighted (by participation factors) combination of the spectral accelerations at the first few modal periods, we first consider vector GMPs of spectral accelerations. The number of modal periods included in the vector is incrementally increased from two until additional modes do not improve the prediction (or reduce the dispersion) of structural response, as will be demonstrated later in this chapter. The values of the first few vibration periods of the three SMRF buildings are summarized in Table C.1 in Appendix C.

Just as was the case with $S_a(T_1)$ and $A_i(T_1)$, the spectral accelerations at consecutive modal periods (e.g., $S_a(T_1)$ and $S_a(T_2)$) can be highly correlated, especially if the periods are closely spaced, as demonstrated in Figure 5.2. Hence, before regressing structural response measures on vectors of spectral accelerations, we again normalize each higher-mode spectral acceleration by the spectral acceleration at the previous (lower) modal period. Thus, we will use $S_a(T_2)/S_a(T_1)$, $S_a(T_3)/S_a(T_2)$, etc. in our regressions. Note that if we were to instead divide all of the higher-mode spectral accelerations by $S_a(T_1)$, the (strong) correlation between, for example, $S_a(T_3)/S_a(T_1)$ and $S_a(T_2)/S_a(T_1)$ would be the same as the original correlation between $S_a(T_3)$ and $S_a(T_2)$.

Similar to the GMP vectors comprised of spectral accelerations, we consider analogous vectors involving input energy-equivalent accelerations. As will be demonstrated with the regression results that follow, however, replacing spectral acceleration with input energy-equivalent acceleration at the same period does not appear to improve the prediction of structural response. Hence, for the most part we only check whether adding to the vector GMP the input energy-equivalent acceleration at the "last" modal period considered in the regression model improves the prediction of structural response. The last modal period considered is the one whose additional consideration in the spectral acceleration GMP vector does not improve the prediction of the response measures. As before, in order to reduce correlation with other elements of the vector GMP, this higher-mode input energy-equivalent acceleration is normalized, as shown below.

In summary, the multi-mode elastic GMPs considered are:

- $\{ S_a(T_1),\ S_a(T_2)/S_a(T_1),\ \ldots,\ S_a(T_n)/S_a(T_{n-1}) \}$
- $\{ A_i(T_1),\ A_i(T_2)/A_i(T_1),\ \ldots,\ A_i(T_n)/A_i(T_{n-1}) \}$
- $\{ S_a(T_1),\ S_a(T_2)/S_a(T_1),\ \ldots,\ A_i(T_n)/S_a(T_{n-1})$ or $A_i(T_n)/S_a(T_n) \}$

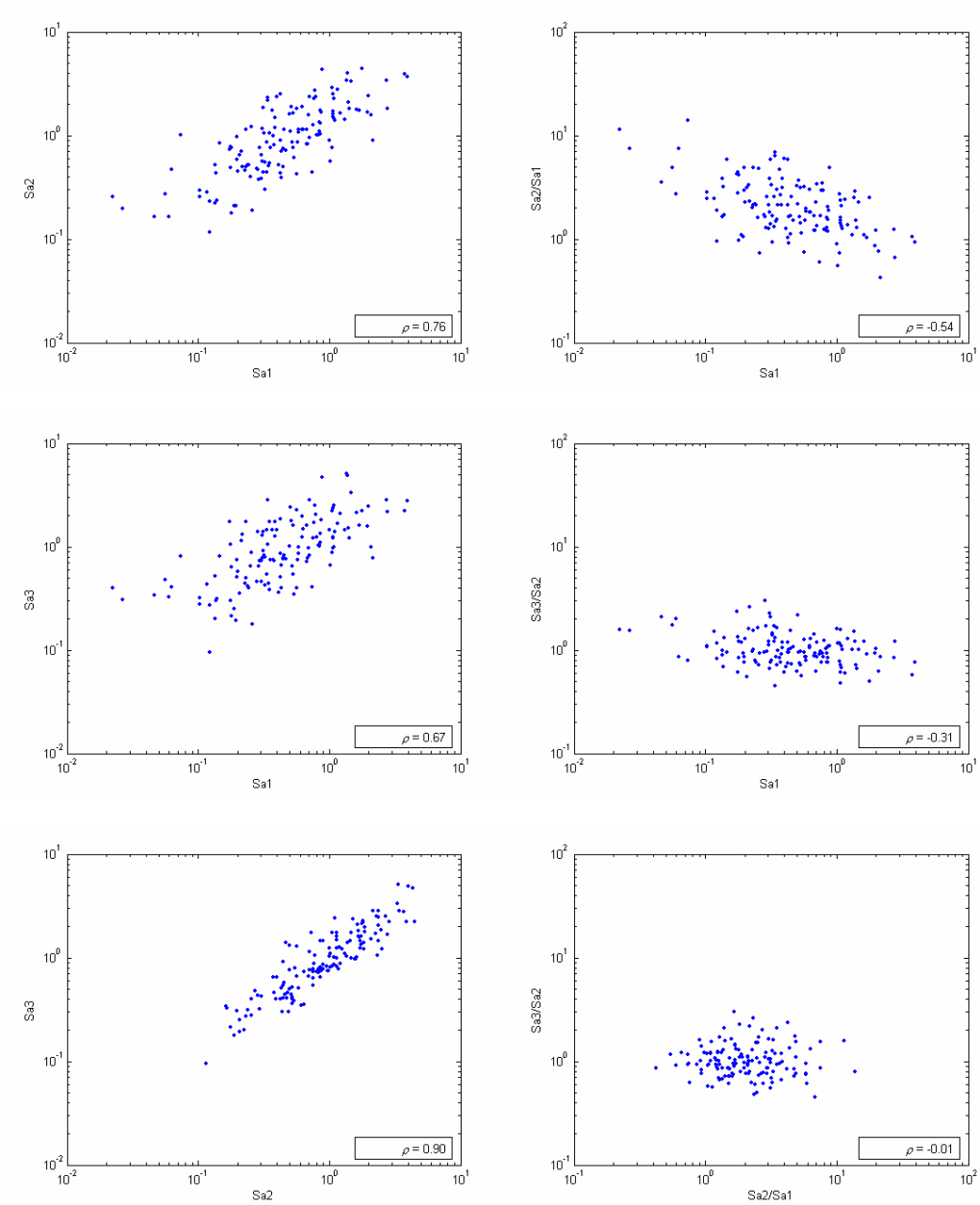

Figure 5.2 Illustration of the strong correlation between $S_a(T_1)$, $S_a(T_2)$, and $S_a(T_3)$ (left side), and the weaker correlation between $S_a(T_1)$, $S_a(T_2)/S_a(T_1)$, and $S_a(T_3)/S_a(T_2)$ (right side), for T_1=1.0 sec, T_2=0.3 sec, T_3=0.2 sec., the first three vibration periods of the 3-story SMRF building.

5.4.3 FIRST-MODE INELASTIC AND HIGHER-MODE ELASTIC GMP'S

In an attempt to improve the prediction of *nonlinear* structural response, we also consider *inelastic* analogies to spectral acceleration and input or absorbed energy-equivalent acceleration, which are all described in detail in Section 3.4. Again, because the dynamic response of a structure to ground shaking is often dominated by its first mode of vibration, it is difficult to establish the yield displacement (d_y) associated with higher modes. Hence, the inelastic GMPs considered all correspond to the first modal period – i.e., $S_a^I(T_1)$, $A_i^I(T_1)$, and $A_a^I(T_1)$. The values of d_y for the three buildings considered in this study are reported in Table C.1 in Appendix C.

As demonstrated in Chapter 3 (Figures 3.10-12), the three inelastic first-mode GMPs are strongly correlated with $S_a(T_1)$, and therefore they themselves should not be included alongside $S_a(T_1)$ in a vector GMP (in order to avoid unstable regression results due to multicollinearity of the predictors). Accordingly, we normalize the three inelastic GMPs by $S_a(T_1)$ and include them, individually, with the vectors of multi-mode elastic GMPs described in the preceding subsection.

In summary, the first-mode inelastic and higher-mode elastic GMPs considered are:

- $\{ S_a(T_1),\ S_a(T_2)/S_a(T_1),\ \ldots,\ S_a(T_n)/S_a(T_{n-1}),\ S_a^I(T_1)/S_a(T_1) \}$
- $\{ S_a(T_1),\ S_a(T_2)/S_a(T_1),\ \ldots,\ S_a(T_n)/S_a(T_{n-1}),\ A_i^I(T_1)/S_a(T_1) \}$
- $\{ S_a(T_1),\ S_a(T_2)/S_a(T_1),\ \ldots,\ S_a(T_n)/S_a(T_{n-1}),\ A_a^I(T_1)/S_a(T_1) \}$

5.4.4 OTHER COMBINATIONS OF GMP'S

It is obvious that numerous other vector combinations of GMPs can be considered, but those listed above are thought to be the most likely to improve the prediction of nonlinear structural response. Using the GMP and nonlinear structural response data provided in Appendix C with the MMLR (multivariate multiple linear regression) methodology outlined above, other vector GMPs can readily be explored.

5.5 REGRESSION RESULTS

The vectors of response measures obtained from nonlinear dynamic analyses of each of the structures are regressed on the different GMP sets detailed above using the multivariate multiple linear regression (MMLR) method described in Section 5.2. From the regression analyses we obtain unbiased estimates of the model coefficients, b_{ji} for $j = 0$ to r (see Equation 5.5), and the covariance matrix of the regression residuals, $\mathbf{\Sigma}$ (see Equation 5.6). From the estimated covariance matrix, we get the individual standard deviations, $\sigma_{\ln \varepsilon i}$, and the correlation coefficients among the residuals of the n response measures included in the vector $\boldsymbol{Y}$. The standard deviations of the residuals are directly related to uncertainty in our predictions of each

Y_i response using the ground motion parameters in $\boldsymbol{X}$, and hence they are used to compare the predictive power of the different choices of GMP vectors.

The regression results are presented here separately for each of the three categories of ground motion parameters considered: (i) first-mode elastic, (ii) multi-mode elastic, and (iii) first-mode inelastic and higher-mode elastic GMPs. Within each of the three categories, results are presented for the structural response measures, (i) {*MIDR*, *AIDR*, *RDR*}, (ii) *IDR*s at all stories (also a vector), and (iii) *RDR* (a scalar). The specific combinations considered and the subsections where they are discussed are included in the list below:

Subsection	Ground Motion Parameter (GMP)	Structural Response Measures	Building Models
5.5.1.1	$S_a(T_1)$	*IDR*	Ductile 9-Story
5.5.1.2	$S_a(T_1)$	{*MIDR*, *AIDR*, *RDR*}	Ductile 9-Story
5.5.1.3	$A_i(T_1)$ vs. $S_a(T_1)$	*IDR*	Ductile 3-, 9-, and 20-Story
5.5.1.4	$A_i(T_1)$	{*MIDR*, *AIDR*, *RDR*}	Ductile 3-, 9-, and 20-Story
5.5.1.5	$\{S_a(T_1), A_i(T_1)/S_a(T_1)\}$	*IDR* and {*MIDR*, *AIDR*, *RDR*}	Ductile 3-, 9-, and 20-Story
5.5.2.1	$\{S_a(T_1), S_a(T_2)/S_a(T_1)\}$	*IDR*	Ductile 9-Story
5.5.2.2	$\{S_a(T_1), S_a(T_2)/S_a(T_1)\}$	{*MIDR*, *AIDR*, *RDR*}	Ductile 9-Story
5.5.2.3	$\{A_i(T_1), A_i(T_2)/A_i(T_1)\}$ vs. $\{S_a(T_1), S_a(T_2)/S_a(T_1)\}$	*IDR*	Ductile 3-, 9-, and 20-Story
5.5.2.4	$\{A_i(T_1), A_i(T_2)/A_i(T_1)\}$ vs. $\{S_a(T_1), S_a(T_2)/S_a(T_1)\}$	{*MIDR*, *AIDR*, *RDR*}	Ductile 3-, 9-, and 20-Story
5.5.2.5	$\{S_a(T_1), A_i(T_2)/S_a(T_1)\}$ and $\{S_a(T_1), A_i(T_2)/S_a(T_2)\}$	*IDR* and *RDR*	Elastic, Ductile, and Brittle 3-Story
"	$\{S_a(T_1), S_a(T_2)/S_a(T_1), S_a(T_3)/S_a(T_2)\}$ and $\{S_a(T_1), S_a(T_2)/S_a(T_1), A_i(T_3)/S_a(T_3)\}$	*IDR* and *RDR*	Elastic, Ductile, and Brittle 9-Story
"	$\{S_a(T_1), S_a(T_2)/S_a(T_1), S_a(T_3)/S_a(T_2)\}$, $\{S_a(T_1), S_a(T_2)/S_a(T_1), S_a(T_3)/S_a(T_2), S_a(T_4)/S_a(T_3)\}$, and $\{S_a(T_1), S_a(T_2)/S_a(T_1), S_a(T_3)/S_a(T_2), A_i(T_4)/S_a(T_4)\}$	*IDR* and *RDR*	Elastic, Ductile, and Brittle 20-Story
5.5.3.1	$\{S_a(T_1), \ldots, S_a(T_n)/S_a(T_{n-1}), S_a^I(T_1)/S_a(T_1)\}$	*IDR* and *RDR*	Ductile and Brittle 3-, 9-, and 20-Story
5.5.3.2	$\{S_a(T_1), \ldots, S_a(T_n)/S_a(T_{n-1}), A_i^I(T_1)/S_a(T_1)\}$ and $\{S_a(T_1), \ldots, S_a(T_n)/S_a(T_{n-1}), A_a^I(T_1)/S_a(T_1)\}$	*IDR* and *RDR*	Ductile and Brittle 3-, 9-, and 20-Story

5.5.1 REGRESSIONS ON FIRST-MODE ELASTIC GMP'S

5.5.1.1 USE OF $S_a(T_1)$ IN PREDICTING *IDR*'S FOR THE DUCTILE 9-STORY BUILDING

The regression coefficients and the standard deviations of the errors obtained from regressing the vector of response measures IDR_i (i = 1 to 9) on $S_a(T_1)$ alone are given in Table 5.1 for the ductile 9-story building, while the error correlations for the nine response measures are given in Table 5.2. Analogous results for the 3- and 20-story ductile buildings are provided in Appendix A (Tables A.1 to A.2 and A.13 to A.14, respectively).

IDR_i	b_{0i}	b_{1i}	$\sigma_{ln\varepsilon}$
1	0.060	0.848	0.215
2	0.054	0.877	0.175
3	0.054	0.892	0.145
4	0.055	0.877	0.164
5	0.054	0.864	0.181
6	0.053	0.847	0.233
7	0.059	0.836	0.284
8	0.059	0.784	0.355
9	0.044	0.711	0.392

Table 5.1 Regression coefficients and standard deviations of the residuals for the ductile 9-story building peak inter-story drift ratios regressed on $S_a(T_1)$.

ρ	1	2	3	4	5	6	7	8	9
1	1.00	0.93	0.74	0.63	0.75	0.84	0.80	0.80	0.77
2	*	1.00	0.82	0.59	0.65	0.74	0.75	0.73	0.67
3	*	*	1.00	0.77	0.63	0.67	0.63	0.60	0.59
4	*	*	*	1.00	0.84	0.65	0.48	0.51	0.55
5	*	*	*	*	1.00	0.84	0.65	0.68	0.70
6	*	*	*	*	*	1.00	0.91	0.88	0.86
7	*	*	*	*	*	*	1.00	0.96	0.90
8	*	*	*	*	*	*	*	1.00	0.96
9	*	*	*	*	*	*	*	*	1.00

Table 5.2 Error correlation matrix for the ductile 9-story building peak inter-story drift ratios regressed on $S_a(T_1)$.

It appears from the results in Table 5.1 that *IDR* values in the lower floors (below, say, the 5th floor) are well predicted by the first-mode $S_a(T_1)$. At higher floors, however, the standard deviations of the residuals are larger, indicating that $S_a(T_1)$ alone is ineffective in predicting *IDR* values there. Note that the increase in the response measures with $S_a(T_1)$ is less than proportional,

i.e., b_{1i} is less than unity for each Y_i. This means that the equal displacement rule (Veletsos and Newmark, 1960; Veletsos *et al*., 1965) is not very accurate for this 9-story building.

As might be expected, the residuals from the *IDR* values at adjacent stories are highly correlated with each other, as can be confirmed from Table 5.2. Certain other pairs of residuals are also highly correlated with each other – e.g., residuals of the first and the sixth story *IDR* values. These correlations among residuals of inter-story drifts at non-adjacent stories likely result from the contribution to these drifts by factors other than the first-mode type of vibration (i.e., contribution from higher modes).

5.5.1.2 USE OF $S_a(T_1)$ IN PREDICTING {*MIDR, AIDR, RDR*} FOR THE DUCTILE 9-STORY BUILDING

The regression coefficients and the standard deviations of the errors obtained from regressing the vector of response measures {*MIDR*, *AIDR*, *RDR*} on $S_a(T_1)$ alone are given in Table 5.3 for the ductile 9-story building, while the error correlations for the response measures are given in Table 5.4. Analogous results for the 3- and 20-story ductile buildings are provided in Appendix A (Tables A.19 to A.20 and A.31 to A.32, respectively).

Y_i	b_{0i}	b_{1i}	$\sigma_{ln\varepsilon}$
MIDR	0.064	0.796	0.336
AIDR	0.055	0.832	0.228
RDR	0.047	0.922	0.133

Table 5.3 Regression coefficients and standard deviations of the residuals for the ductile 9-story building response regressed on $S_a(T_1)$.

ρ	*MIDR*	*AIDR*	*RDR*
MIDR	1.00	0.97	0.47
AIDR	*	1.00	0.57
RDR	*	*	1.00

Table 5.4 Error correlation matrix for the ductile 9-story building response regressed on $S_a(T_1)$.

The error correlation matrix suggests that the residuals for the response measures *MIDR* and *AIDR* are highly correlated with each other, but not as highly correlated with *RDR*. We expect this, due to the influence of the higher modes on the response measures *MIDR* and *AIDR*. As evidenced by its relatively low $\sigma_{\ln\varepsilon}$ (in Table 5.3), *RDR* is quite adequately predicted by the first-mode-based parameter $S_a(T_1)$ alone, and hence the residuals for *RDR* are not as highly correlated with *MIDR* and *AIDR*.

5.5.1.3 USE OF $A_i(T_1)$ VS. $S_a(T_1)$ IN PREDICTING *IDR*'S

Here, the results of regressing vectors of peak inter-story drift ratios (*IDR*s) on the scalar ground motion parameter $A_i(T_1)$ are compared to the results of regression on $S_a(T_1)$. Figure 5.3 shows plots of the *IDR* values for the ductile 9-story building against the fundamental-period spectral acceleration, $S_a(T_1)$. Figure 5.4 shows similar plots using the fundamental-period input energy-equivalent acceleration, $A_i(T_1)$. As expected given the high correlation between $S_a(T_1)$ and $A_i(T_1)$ shown in Figure 3.7, the fits to the data based on regression on $A_i(T_1)$ are very similar to the fits obtained for $S_a(T_1)$ at all the stories. This can be seen not only by studying the regression lines and the data, but also by comparing the standard deviations of the residuals, which are given in the figures and are summarized in Table 5.6. Note that the relatively large scatter at higher stories in *IDR* for a given $S_a(T_1)$, which was mentioned in Subsection 5.5.1.1, is clearly visible in Figure 5.3.

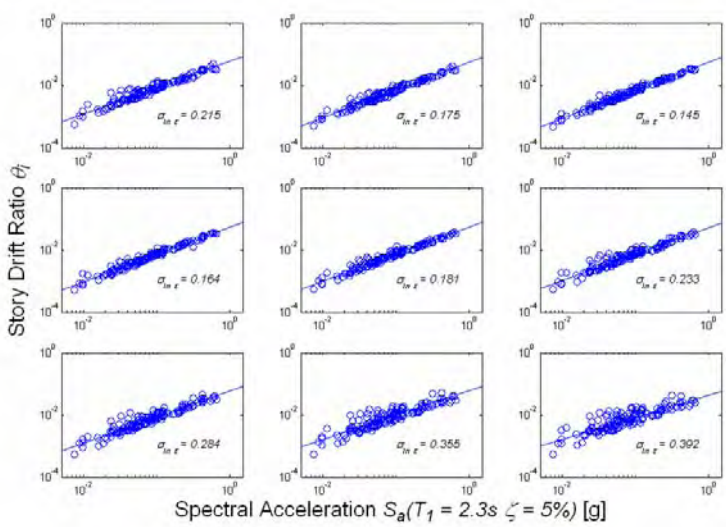

Figure 5.3 Plots of peak inter-story drift ratio versus first-mode spectral acceleration, ordered from top to bottom and left to right (i.e., story 1 is at the top left-hand corner; story 9 is at the bottom right-hand corner).

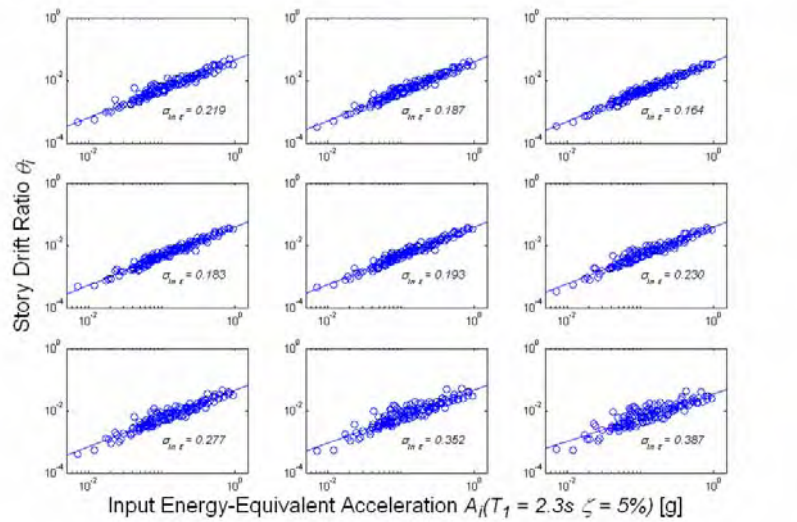

Figure 5.4 Plots of peak inter-story drift ratio versus first-mode input energy-equivalent acceleration, ordered from top to bottom and left to right (i.e., story 1 is at the top left-hand corner; story 9 is at the bottom right-hand corner).

For all three of the ductile building models, the standard deviations of the residuals from the regressions of the vector of peak inter-story drift ratios (*IDR*s) on the scalar ground motion parameter ($A_i(T_1)$ versus $S_a(T_1)$) are presented in Tables 5.5 through 5.7. Also presented in the tables (here and in subsequent subsections) are the standard deviations of the response measures *before* regressing on any GMP. These standard deviations are much larger, emphasizing the usefulness of GMPs for predicting nonlinear structural response. Although not discussed until later (in Section 5.5.1.5), for the sake of conciseness in presentation, results of regressing on a vector that includes information regarding both scalar GMPs, i.e., $\{S_a(T_1), S_a(T_1)/A_i(T_1)\}$, are also included in these tables.

Story	$\sigma_{\ln Y}$	$\sigma_{\ln Y \mid Sa(T1)}$	$\sigma_{\ln Y \mid Ai(T1)}$	$\sigma_{\ln Y \mid Sa(T1), Ai(T1)/Sa(T1)}$
1	0.833	0.168	0.194	0.161
2	0.863	0.121	0.163	0.112
3	0.804	0.194	0.218	0.190

Table 5.5 Summary of the standard deviations of residuals from regressions of *IDR* on first-mode elastic GMPs for the ductile 3-story building.

Story	$\sigma_{\ln Y}$	$\sigma_{\ln Y \mid Sa(T1)}$	$\sigma_{\ln Y \mid Ai(T1)}$	$\sigma_{\ln Y \mid Sa(T1), Ai(T1)/Sa(T1)}$
1	0.894	0.215	0.219	0.209
2	0.914	0.175	0.187	0.168
3	0.924	0.145	0.164	0.139
4	0.912	0.164	0.183	0.160
5	0.903	0.181	0.193	0.175
6	0.897	0.233	0.230	0.223
7	0.900	0.284	0.277	0.274
8	0.877	0.355	0.352	0.350
9	0.825	0.392	0.387	0.387

Table 5.6 Summary of the standard deviations of residuals from regressions of *IDR* on first-mode elastic GMPs for the ductile 9-story building.

Story	$\sigma_{\ln Y}$	$\sigma_{\ln Y \mid Sa(T1)}$	$\sigma_{\ln Y \mid Ai(T1)}$	$\sigma_{\ln Y \mid Sa(T1), Ai(T1)/Sa(T1)}$
1	0.880	0.340	0.312	0.312
2	0.915	0.329	0.301	0.302
3	0.926	0.304	0.274	0.274
4	0.928	0.276	0.246	0.247
5	0.931	0.257	0.232	0.233
6	0.924	0.245	0.226	0.226
7	0.928	0.245	0.225	0.225
8	0.925	0.246	0.224	0.224
9	0.906	0.252	0.229	0.229
10	0.882	0.254	0.233	0.234
11	0.870	0.282	0.260	0.261
12	0.864	0.309	0.287	0.288
13	0.860	0.332	0.310	0.311
14	0.852	0.355	0.333	0.334
15	0.840	0.389	0.365	0.365
16	0.828	0.415	0.391	0.389
17	0.819	0.441	0.417	0.415
18	0.817	0.474	0.451	0.447
19	0.803	0.497	0.475	0.471
20	0.781	0.501	0.483	0.480

Table 5.7 Summary of the standard deviations of residuals from regressions of *IDR* on first-mode elastic GMPs for the ductile 20-story building.

Overall, the standard deviations of the *IDR* residuals are comparable when the scalar GMP is $A_i(T_1)$ versus $S_a(T_1)$. The standard deviations are slightly larger for $A_i(T_1)$ in the case of the 3-story building and the lower five stories of the 9-story building, whereas they are slightly smaller for $A_i(T_1)$ in the case of the 20-story building and the upper four stories of the 9-story building.

It should be pointed out that the standard deviations of the residuals when using $S_a(T_1)$ or $A_i(T_1)$ for the 3-story model are not very different between stories, as is to be expected for a low-rise building whose response is governed mostly by the fundamental mode of vibration. For the 9-story and the 20-story models, however, the standard deviations of the residuals at the higher stories are greater than at the lower stories. This suggests that response predictions at higher stories of mid-rise and high-rise frame buildings will generally require a greater number of analyses to achieve levels of confidence similar to those at lower stories or for low-rise buildings (if such predictions are based on an elastic first-mode GMP).

5.5.1.4 USE OF $A_i(T_1)$ IN PREDICTING {*MIDR*, *AIDR*, *RDR*}

The standard deviations of the residuals for the response vector comprised of the summary drift measures {*MIDR*, AIDR, *RDR*} are presented in Tables 5.8 through 5.10 for all three ductile building models, based on regression on the scalar ground motion parameters $A_i(T_1)$ or, as a basis for comparison, $S_a(T_1)$. Again, note that the results of regressing on the vector {$S_a(T_1)$, $S_a(T_1)/A_i(T_1)$} are also included in these tables, but their discussion is deferred until the next subsection.

Response Variable	$\sigma_{\ln Y}$	$\sigma_{\ln Y \mid Sa(T1)}$	$\sigma_{\ln Y \mid Ai(T1)}$	$\sigma_{\ln Y \mid Sa(T1),\, Ai(T1)/Sa(T1)}$
MIDR	0.820	0.175	0.203	0.170
AIDR	0.827	0.144	0.176	0.137
RDR	0.866	0.129	0.163	0.118

Table 5.8 Summary of the standard deviations of residuals from regressions of the vector {*MIDR*, *AIDR*, *RDR*} on first-mode elastic GMPs for the ductile 3-story building.

Response Variable	$\sigma_{\ln Y}$	$\sigma_{\ln Y \mid Sa(T1)}$	$\sigma_{\ln Y \mid Ai(T1)}$	$\sigma_{\ln Y \mid Sa(T1),\, Ai(T1)/Sa(T1)}$
MIDR	0.881	0.336	0.332	0.329
AIDR	0.881	0.228	0.229	0.221
RDR	0.953	0.133	0.143	0.120

Table 5.9 Summary of the standard deviations of residuals from regressions of the vector {*MIDR*, *AIDR*, *RDR*} on first-mode elastic GMPs for the ductile 9-story building.

Response Variable	$\sigma_{\ln Y}$	$\sigma_{\ln Y \mid Sa(T1)}$	$\sigma_{\ln Y \mid Ai(T1)}$	$\sigma_{\ln Y \mid Sa(T1),\, Ai(T1)/Sa(T1)}$
MIDR	0.883	0.414	0.390	0.390
AIDR	0.858	0.320	0.293	0.293
RDR	0.949	0.177	0.162	0.157

Table 5.10 Summary of the standard deviations of residuals from regressions of the vector {*MIDR*, *AIDR*, *RDR*} on first-mode elastic GMPs for the ductile 20-story building.

As was observed in the preceding subsection for the response vector *IDR*, the standard deviations of the residuals for the three response measures are similar whether the regressions are on $S_a(T_1)$ or $A_i(T_1)$. For the ductile 3-story building, the standard deviations are slightly larger for $A_i(T_1)$, whereas the opposite is true for the ductile 20-story building.

Note that the standard deviations for *RDR* are at similar levels across the three buildings. However, the standard deviations for *MIDR* and *AIDR* (conditional on either scalar GMP) are significantly higher for the 9- and 20-story structures compared to the 3-story structure. This suggests that if one uses only a scalar first-mode elastic GMP as the predictor variable, response predictions (other than those of *RDR*) for mid- and high-rise frame structures will in general require a greater number of analyses to achieve levels of confidence similar to those for low-rise frame buildings.

5.5.1.5 USE OF $\{S_a(T_1), A_i(T_1)/S_a(T_1)\}$ IN PREDICTING *IDR*'S OR {*MIDR, AIDR, RDR*}

As one might expect, given that the results of regressing on $S_a(T_1)$ versus $A_i(T_1)$ are very similar (as demonstrated above), the standard deviations of the residuals reported in Tables 5.5 through 5.10 above indicate that there is little advantage in using the vector $\{S_a(T_1), S_a(T_1)/A_i(T_1)\}$ to predict any of the structural response measures considered, over the use of either $S_a(T_1)$ or $A_i(T_1)$ alone as a scalar GMP. If there is any benefit at all, the standard deviations of the residuals are only very slightly smaller when the vector GMP is used in lieu of the scalar $S_a(T_1)$ or $A_i(T_1)$. However, the complication of using two predictor variables instead of one is not worth this negligible prediction gain.

5.5.1.6 MEDIAN LEVELS OF *MIDR, AIDR, RDR,* AND *IDR*

Before investigating the standard deviations of residuals from regressions on (i) multi-mode elastic GMPs and (ii) first-mode inelastic and higher-mode elastic GMPs, median response estimates as obtained from regressions on $S_a(T_1)$ and $A_i(T_1)$ are presented here. Tables 5.11 and 5.12 compare the median response of the ductile 9-story frame for five bins of 28 earthquake records that have been organized (from the complete set of 140 earthquake records described in Chapter 3) based on increasing values of the first-mode elastic ground motion parameters, $S_a(T_1)$ and $A_i(T_1)$. The median response values of *MIDR*, *AIDR*, and *RDR* calculated directly from the data (resulting from nonlinear dynamic analyses) are compared against estimates based on the regression equation (by setting the predictor variable to the same median value as in the data – see the first column in Tables 5.11 and 5.12). It can be seen that the predicted response values closely match the values from the data over all levels of input motion and for both of the ground motion parameters.

Median $S_a(T_1)$ (g) for Bin	*MIDR*		*AIDR*		Roof Drift Ratio	
	Data	Predicted	Data	Predicted	Data	Predicted
0.02	0.0030	0.0032	0.0022	0.0024	0.0013	0.0015
0.04	0.0046	0.0054	0.0038	0.0041	0.0026	0.0027
0.07	0.0078	0.0078	0.0065	0.0060	0.0043	0.0041
0.12	0.0117	0.0118	0.0101	0.0093	0.0071	0.0067
0.31	0.0251	0.0255	0.0201	0.0208	0.0157	0.0163

Table 5.11 Median response values of *MIDR*, *AIDR*, and *RDR* for 5 bins of 28 earthquake records each, sorted according to $S_a(T_1)$, and corresponding predicted values based on regression on $S_a(T_1)$.

Median $A_i(T_1)$ (g) for Bin	*MIDR*		*AIDR*		Roof Drift Ratio	
	Data	Predicted	Data	Predicted	Data	Predicted
0.04	0.0030	0.0032	0.0022	0.0024	0.0013	0.0015
0.07	0.0046	0.0052	0.0038	0.0039	0.0026	0.0026
0.12	0.0081	0.0079	0.0064	0.0061	0.0043	0.0042
0.22	0.0122	0.0132	0.0101	0.0104	0.0071	0.0076
0.44	0.0251	0.0244	0.0201	0.0198	0.0157	0.0154

Table 5.12 Median response values of *MIDR*, *AIDR*, and *RDR* for 5 bins of 28 earthquake records each, sorted according to $A_i(T_1)$, and corresponding predicted values based on regression on $A_i(T_1)$.

Note that the predictions (and the data) based on $S_a(T_1)$ versus $A_i(T_1)$ are very similar because of the high degree of correlation ($\rho = 0.98$) between the two GMPs (as was seen in Figure 3.7).

Figure 5.5 shows median peak inter-story drift ratios (*IDR*s) predicted by the regression model based on $S_a(T_1)$ alone, again for median values of the 5 bins of 28 records sorted according to increasing $S_a(T_1)$. Note that these regression predictions compare well with the median deformed shapes obtained empirically from the nonlinear dynamic analyses for each set of records directly. Also, note that the response at higher stories grows with $S_a(T_1)$ at different rates than does the response at lower stories.

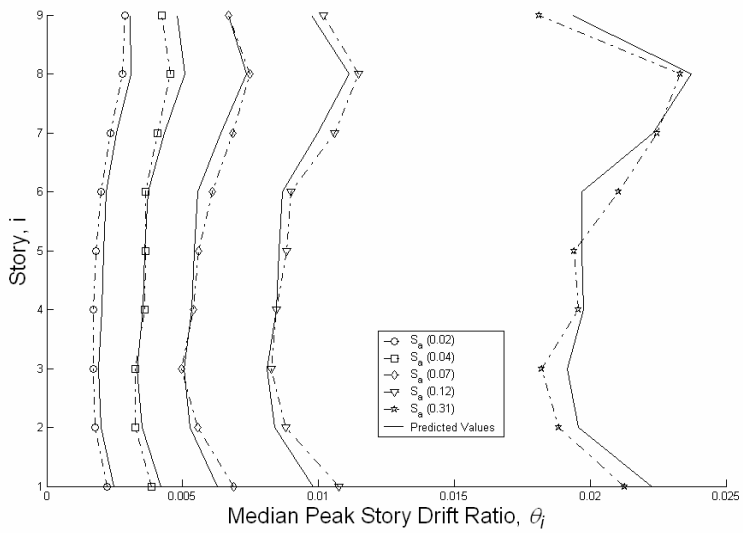

Figure 5.5 Median peak inter-story drift response of the ductile 9-story building model for 5 bins of 28 earthquake records each, sorted according to $S_a(T_1)$.

5.5.1.7 SUMMARY OF RESULTS USING FIRST-MODE ELASTIC GMP'S

The predictions of response measures based on $S_a(T_1)$ or $A_i(T_1)$ (or on the vector $\{S_a(T_1), A_i(T_1)/S_a(T_1)\}$) are very similar for the building frames under consideration, most likely due to the high degree of correlation between the two scalar GMPs (see Figure 3.8). Overall, the response prediction using either of the parameters is good. However, we see significant variability in the response at higher stories (e.g., for *IDR* at the sixth story and above in the 9- and 20-story structures). Also, the variability in *MIDR* and *AIDR* is greater when compared to that in *RDR* for mid- and high-rise buildings. Next we discuss results from regression based on vectors of elastic GMPs at multiple modes. By including more variables in our predictor set we expect to achieve lower variability in our response measures, as we shall see.

5.5.2 REGRESSIONS ON MULTI-MODE ELASTIC GMP'S

5.5.2.1 USE OF $\{S_a(T_1), S_a(T_2)/S_a(T_1)\}$ IN PREDICTING *IDR* FOR THE DUCTILE 9-STORY BUILDING

The regression coefficients and the standard deviations of the residuals obtained from regressing the vector of response measures IDR_i (i = 1 to 9) on the vector GMP $\{S_a(T_1), S_a(T_2)/S_a(T_1)\}$ are given in Table 5.13 for the ductile 9-story building, while the error correlations for the response measures are given in Table 5.14. Analogous results for the 3- and 20-story ductile buildings are provided in Appendix A (Tables A.37 to A.38 and A.45 to A.46, respectively).

IDR_i	b_{0i}	b_{1i}	b_{2i}	$\sigma_{ln\varepsilon}$
1	0.053	0.908	0.235	0.167
2	0.050	0.919	0.165	0.146
3	0.051	0.918	0.100	0.133
4	0.052	0.899	0.088	0.156
5	0.050	0.903	0.153	0.158
6	0.045	0.919	0.285	0.164
7	0.048	0.937	0.399	0.163
8	0.045	0.919	0.528	0.176
9	0.033	0.858	0.577	0.201

Table 5.13 Regression coefficients and standard deviations of the residuals for the ductile 9-story building peak inter-story drift ratios regressed on $S_a(T_1)$ and the ratio $S_a(T_2)/S_a(T_1)$.

ρ	1	2	3	4	5	6	7	8	9
1	1.00	0.90	0.68	0.59	0.65	0.71	0.64	0.65	0.56
2	*	1.00	0.78	0.53	0.52	0.60	0.62	0.61	0.47
3	*	*	1.00	0.74	0.54	0.59	0.57	0.55	0.52
4	*	*	*	1.00	0.83	0.64	0.41	0.51	0.59
5	*	*	*	*	1.00	0.80	0.50	0.59	0.62
6	*	*	*	*	*	1.00	0.81	0.74	0.70
7	*	*	*	*	*	*	1.00	0.87	0.65
8	*	*	*	*	*	*	*	1.00	0.85
9	*	*	*	*	*	*	*	*	1.00

Table 5.14 Error correlation matrix for the ductile 9-story building peak inter-story drift ratios regressed on $S_a(T_1)$ and the ratio $S_a(T_2)/S_a(T_1)$.

Overall, we see significant reduction in the standard deviation of the residuals that results from adding the second-mode GMP (compare Table 5.13 with Table 5.1), especially at the higher stories. Note also that the response is closer to being proportional with $S_a(T_1)$ (i.e., $b_{1i} \cong 1$) compared to when $S_a(T_1)$ was the sole predictor (see Table 5.1).

Table 5.15 shows the decrease in the error correlations for the inter-story drift ratios of the ductile 9-story building when regressed first on $S_a(T_1)$ (see Table 5.2) and then on the vector $\{S_a(T_1), S_a(T_2)/S_a(T_1)\}$ (see Table 5.14). Note that for most pairs of stories the correlation is reduced by including the second-mode parameter. This is indicative of the contribution of the second mode in improved prediction, *simultaneously*, of the response at different stories that was not achieved as effectively by regression on $S_a(T_1)$ alone.

ρ	1	2	3	4	5	6	7	8	9
1	0.00	0.03	0.06	0.04	0.10	0.13	0.17	0.15	0.21
2	*	0.00	0.04	0.06	0.13	0.15	0.13	0.12	0.21
3	*	*	0.00	0.03	0.09	0.07	0.06	0.05	0.07
4	*	*	*	0.00	0.01	0.01	0.07	0.00	-0.03
5	*	*	*	*	0.00	0.04	0.15	0.10	0.08
6	*	*	*	*	*	0.00	0.10	0.13	0.17
7	*	*	*	*	*	*	0.00	0.09	0.24
8	*	*	*	*	*	*	*	0.00	0.11
9	*	*	*	*	*	*	*	*	0.00

Table 5.15 Reduction in the error correlations for the ductile 9-story building response (*IDR*) when first regressed on $S_a(T_1)$ and then on the vector $\{S_a(T_1), S_a(T_2)/S_a(T_1)\}$.

5.5.2.2 USE OF $\{S_a(T_1), S_a(T_2)/S_a(T_1)\}$ IN PREDICTING {*MIDR*, *AIDR*, *RDR*} FOR THE DUCTILE 9-STORY BUILDING

The regression coefficients and the standard deviations of the errors obtained from regressing the vector of response measures {*MIDR*, *AIDR*, *RDR*} on the vector of GMPs $\{S_a(T_1), S_a(T_2)/S_a(T_1)\}$ are given in Table 5.16 for the ductile 9-story building, while the error correlations for the response measures are given in Table 5.17. Analogous results for the 9- and 20-story ductile buildings are provided in Appendix A (Tables A.49 to A.50 and A.57 to A.58, respectively).

Note that the standard deviations of the residuals for *MIDR* and *AIDR* in Table 5.16 are reduced significantly compared to those found when $S_a(T_1)$ was the sole GMP (as we saw in Table 5.3). There is almost no similar beneficial effect, however, on the standard deviation of the residuals for *RDR*, again because *RDR* is mostly driven by the first mode.

Y_i	b_{0i}	b_{1i}	b_{2i}	$\sigma_{ln\varepsilon}$
MIDR	0.050	0.917	0.474	0.191
AIDR	0.047	0.910	0.307	0.141
RDR	0.046	0.936	0.053	0.130

Table 5.16 Regression coefficients and standard deviations of the residuals for the ductile 9-story building response regressed on $S_a(T_1)$ and the ratio $S_a(T_2)/S_a(T_1)$.

ρ	*MIDR*	*AIDR*	*RDR*
MIDR	1.00	0.93	0.51
AIDR	*	1.00	0.64
RDR	*	*	1.00

Table 5.17 Error correlation matrix for the ductile 9-story building response regressed on $S_a(T_1)$ and the ratio $S_a(T_2)/S_a(T_1)$.

Despite the predictive power gained from including $S_a(T_2)/S_a(T_1)$ with $S_a(T_1)$ in a vector GMP, it can be seen from Table 5.17 that the residuals for the response measures *MIDR* and *AIDR* are still highly correlated, perhaps due to the contributions of even higher modes of vibration and/or the effects of nonlinearity.

5.5.2.3 USE OF $\{A_i(T_1), A_i(T_2)/A_i(T_1)\}$ vs. $\{S_a(T_1), S_a(T_2)/S_a(T_1)\}$ IN PREDICTING *IDR*

The results of regressing the vector of peak inter-story drift ratios (*IDR*) on the vector GMP $\{A_i(T_1), A_i(T_2)/A_i(T_1)\}$ for each of the three ductile structures (3-, 9-, and 20-story) are summarized in Tables 5.18 to 5.20. Also shown in the tables for comparison purposes are the results for the GMP vector, $\{S_a(T_1), S_a(T_2)/S_a(T_1)\}$, and the GMP scalars, $S_a(T_1)$ and $A_i(T_1)$, separately.

As was the case when we studied the differences resulting from regressions on $A_i(T_1)$ alone versus $S_a(T_1)$ alone, there is only a slight difference between the standard deviations of the residual *IDR* values resulting from regressions on $\{A_i(T_1), A_i(T_2)/A_i(T_1)\}$ versus $\{S_a(T_1), S_a(T_2)/S_a(T_1)\}$. Furthermore, here we see that for the 3-story building there is little reduction in the standard deviation of the residuals (at any story) brought about by the use of either of the two GMP vectors instead of a single scalar first-mode GMP. This is again because the response of the 3-story model is mainly governed by the first mode. The standard deviations of the residuals for the 9-story and 20-story structures, however, are reduced significantly by including a second-mode based GMP, especially at the higher stories. In fact, when a second-mode GMP is used, the standard deviations of the residuals for the 9- and 20-story buildings are comparable to those for the 3-story building at almost all levels, including the higher stories. Hence, about the same number of analyses would be required to achieve similar levels of confidence in our response predictions for mid-rise and high-rise frame buildings if a multi-mode elastic GMP vector is used in predictions of response.

Story	Multi-mode GMPs		First-mode GMPs	
	$\sigma_{\ln Y \mid Sa(T1),\, Sa(T2)/Sa(T1)}$	$\sigma_{\ln Y \mid Ai(T1),\, Ai(T2)/Ai(T1)}$	$\sigma_{\ln Y \mid Sa(T1)}$	$\sigma_{\ln Y \mid Ai(T1)}$
1	0.152	0.179	0.168	0.194
2	0.121	0.163	0.121	0.163
3	0.151	0.186	0.194	0.218

Table 5.18 Summary of standard deviations of residuals based on first- and multi-mode elastic GMPs for the ductile 3-story building.

Story	Multi-mode GMPs		First-mode GMPs	
	$\sigma_{\ln Y \mid Sa(T1),\ Sa(T2)/Sa(T1)}$	$\sigma_{\ln Y \mid Ai(T1),\ Ai(T2)/Ai(T1)}$	$\sigma_{\ln Y \mid Sa(T1)}$	$\sigma_{\ln Y \mid Ai(T1)}$
1	0.167	0.178	0.215	0.219
2	0.146	0.165	0.175	0.187
3	0.133	0.157	0.145	0.164
4	0.156	0.179	0.164	0.183
5	0.158	0.177	0.181	0.193
6	0.164	0.166	0.233	0.230
7	0.163	0.159	0.284	0.277
8	0.176	0.182	0.355	0.352
9	0.201	0.202	0.392	0.387

Table 5.19 Summary of standard deviations of residuals based on first- and multi-mode elastic GMPs for the ductile 9-story building.

Story	Multi-mode GMPs		First-mode GMPs	
	$\sigma_{\ln Y \mid Sa(T1),\ Sa(T2)/Sa(T1)}$	$\sigma_{\ln Y \mid Ai(T1),\ Ai(T2)/Ai(T1)}$	$\sigma_{\ln Y \mid Sa(T1)}$	$\sigma_{\ln Y \mid Ai(T1)}$
1	0.223	0.211	0.340	0.312
2	0.227	0.213	0.329	0.301
3	0.225	0.207	0.304	0.274
4	0.214	0.197	0.276	0.246
5	0.207	0.196	0.257	0.232
6	0.211	0.206	0.245	0.226
7	0.218	0.212	0.245	0.225
8	0.212	0.207	0.246	0.224
9	0.204	0.202	0.252	0.229
10	0.179	0.184	0.254	0.233
11	0.171	0.179	0.282	0.260
12	0.169	0.175	0.309	0.287
13	0.170	0.169	0.332	0.310
14	0.172	0.166	0.355	0.333
15	0.174	0.168	0.389	0.365
16	0.179	0.175	0.415	0.391
17	0.192	0.192	0.441	0.417
18	0.214	0.222	0.474	0.451
19	0.243	0.256	0.497	0.475
20	0.267	0.286	0.501	0.483

Table 5.20 Summary of standard deviations of residuals based on first- and multi-mode elastic GMPs for the ductile 20-story building.

5.5.2.4 USE OF $\{A_i(T_1), A_i(T_2)/A_i(T_1)\}$ vs. $\{S_a(T_1), S_a(T_2)/S_a(T_1)\}$ IN PREDICTING {*MIDR, AIDR, RDR*}

The results of regressing the vector {*MIDR*, *AIDR*, *RDR*} on the vector GMP $\{A_i(T_1), A_i(T_2)/A_i(T_1)\}$ for the three ductile structures are given in Tables 5.22 to 5.24. Also shown in the tables, for comparison purposes, are the results for the GMP vector, $\{S_a(T_1), S_a(T_2)/S_a(T_1)\}$, and the GMP scalars, $S_a(T_1)$ and $A_i(T_1)$, separately.

As was seen for the *IDR* response in the preceding subsection, there is little difference between the standard deviations of the residuals resulting from regressions on $\{A_i(T_1), A_i(T_2)/A_i(T_1)\}$ versus $\{S_a(T_1), S_a(T_2)/S_a(T_1)\}$, especially for the 9- and 20-story buildings. For the 3-story structure, there is little reduction in the standard deviation of the residuals (for any of the response variables) caused by the use of either of the two GMP vectors instead of the corresponding scalar first-mode GMP. For the 9- and 20-story models, there is also insignificant reduction in the standard deviation of the residuals for *RDR* caused by going to a GMP vector for regression. This is because, as mentioned before, *RDR* is dominated by the first mode of vibration of the structure. The standard deviations of the residuals for the response variables *MIDR* and *AIDR* for the 9- and 20-story structures are reduced significantly, however, by adding a second-mode GMP, whether it be $A_i(T_2)/A_i(T_1)$ or $S_a(T_2)/S_a(T_1)$. For the 20-story structure, for example, there is a reduction by almost a factor of two in the standard deviation of the residuals, which translates to a reduction by a factor of four in the number of nonlinear dynamic analyses that would be required to predict the response with a comparable level of accuracy.

Finally, note that *MIDR* and *AIDR* are derived from the *IDR*s and hence the lower variability in the *IDR* values when multi-mode elastic GMPs are used is what leads to smaller variations in the *MIDR* and *AIDR* as well. In light of this, when inelastic first-mode and elastic higher-mode GMPs are investigated next (in Sections 5.5.3), only the vector response measure *IDR* and the scalar *RDR* will be considered.

Response Variable	Multi-mode GMPs		First-mode GMPs	
	$\sigma_{\ln Y \mid Sa(T1),\, Sa(T2)/Sa(T1)}$	$\sigma_{\ln Y \mid Ai(T1),\, Ai(T2)/Ai(T1)}$	$\sigma_{\ln Y \mid Sa(T1)}$	$\sigma_{\ln Y \mid Ai(T1)}$
MIDR	0.148	0.184	0.175	0.203
AIDR	0.125	0.163	0.144	0.176
RDR	0.129	0.163	0.129	0.163

Table 5.22 Summary of standard deviations of residuals based on first- and multi-mode elastic GMPs for the ductile 3-story building.

Response Variable	Multi-mode GMPs		First-mode GMPs	
	$\sigma_{\ln Y \mid Sa(T1), Sa(T2)/Sa(T1)}$	$\sigma_{\ln Y \mid Ai(T1), Ai(T2)/Ai(T1)}$	$\sigma_{\ln Y \mid Sa(T1)}$	$\sigma_{\ln Y \mid Ai(T1)}$
MIDR	0.191	0.195	0.336	0.332
AIDR	0.141	0.153	0.228	0.229
RDR	0.130	0.141	0.133	0.143

Table 5.23 Summary of standard deviations of residuals based on first- and multi-mode elastic GMPs for the ductile 9-story building.

Response Variable	Multi-mode GMPs		First-mode GMPs	
	$\sigma_{\ln Y \mid Sa(T1), Sa(T2)/Sa(T1)}$	$\sigma_{\ln Y \mid Ai(T1), Ai(T2)/Ai(T1)}$	$\sigma_{\ln Y \mid Sa(T1)}$	$\sigma_{\ln Y \mid Ai(T1)}$
MIDR	0.237	0.245	0.414	0.390
AIDR	0.173	0.170	0.320	0.293
RDR	0.165	0.160	0.177	0.162

Table 5.24 Summary of standard deviations of residuals based on first- and multi-mode elastic GMPs for the ductile 20-story building.

5.5.2.5 USE OF OTHER MULTI-MODE ELASTIC GMP'S

Besides $\{S_a(T_1), S_a(T_2)/S_a(T_1)\}$ and $\{A_i(T_1), A_i(T_2)/A_i(T_1)\}$, several other multi-mode elastic GMP combinations were considered for the 3-, 9-, and 20-story buildings. The standard deviations of the *IDR* and *RDR* residuals for not only the ductile models of these building, but for models that consider (i) elastic behavior and (ii) brittle beam-column connection behavior, are reported in Appendix B. For reasons discussed later, the results presented in Appendix B make use of building models that are approximately half as strong as the ductile models considered so far. Nevertheless, the observations above based on the ductile building models, related to the differences between various first-mode elastic and multi-mode elastic GMPs, also apply to the results in Appendix B. Here we merely summarize the regression results for those multi-mode elastic GMPs that have not been considered in the preceding sections.

For the 3-story building models (elastic, ductile, and brittle), two additional multi-mode elastic ground motion parameters were considered: $\{S_a(T_1), A_i(T_2)/S_a(T_1)\}$ and $\{S_a(T_1), A_i(T_2)/S_a(T_2)\}$. Neither of these GMP vectors, however, reduces the standard deviations of the *IDR* and *RDR* residuals appreciably, if at all, relative to the vector, $\{S_a(T_1), S_a(T_2)/S_a(T_1)\}$. This supports our observation that, when considering the 3-story building, none of the second-mode GMPs improved on the predictive power of $S_a(T_1)$ alone.

For the 9-story building models, the following additional multi-mode elastic GMPs were considered: $\{S_a(T_1),\ S_a(T_2)/S_a(T_1),\ S_a(T_3)/S_a(T_2)\}$ and $\{S_a(T_1),\ S_a(T_2)/S_a(T_1),\ A_i(T_3)/S_a(T_3)\}$. Again, neither of these two GMP vectors reduces the standard deviation of the *IDR* and *RDR* residuals appreciably, if at all, relative to the vector $\{S_a(T_1),\ S_a(T_2)/S_a(T_1)\}$. Recall, however, that the inclusion of $S_a(T_2)/S_a(T_1)$ in a vector in addition to the first-mode scalar GMP, $S_a(T_1)$, did improve the predictive power for the *IDR* (but not *RDR*) response of the 9-story building.

Finally, for the 20-story building models, three additional multi-mode elastic GMP vectors were considered:

- $\{S_a(T_1),\ S_a(T_2)/S_a(T_1),\ S_a(T_3)/S_a(T_2)\}$,
- $\{S_a(T_1),\ S_a(T_2)/S_a(T_1),\ S_a(T_3)/S_a(T_2),\ S_a(T_4)/S_a(T_3)\}$, and
- $\{S_a(T_1),\ S_a(T_2)/S_a(T_1),\ S_a(T_3)/S_a(T_2),\ A_i(T_4)/S_a(T_4)\}$.

In a few of the highest stories, the first of the three GMP vectors listed above does indeed reduce the standard deviations of the *IDR* residuals relative to the results based on regression on $\{S_a(T_1),\ S_a(T_2)/S_a(T_1)\}$. Neither of the other two GMP vectors, however, provides any additional predictive power. For the first-mode-dominated *RDR* response, recall that even $\{S_a(T_1),\ S_a(T_2)/S_a(T_1)\}$ does not improve on the prediction relative to the scalar $S_a(T_1)$.

5.5.2.6 SUMMARY OF RESULTS USING MULTI-MODE ELASTIC GMP'S

For the 3-story models studied, there is little reduction in the structural response variation that results from including a second-mode GMP, in addition to a first-mode GMP, in the regression studies carried out. This is because the response of the 3-story building is dominated by the first mode. However, by including a second-mode GMP in our set of predictor variables, we are able to better predict the response for the 9- and 20-story building models, especially at the higher stories, where higher-mode effects contribute significantly to the building deformation. In fact, for the 20-story building models, including $S_a(T_3)/S_a(T_2)$ in the multi-mode elastic vector GMP further improves the prediction at a few of the highest stories. The improvement in the level of prediction at lower stories is not significant compared to that at the higher stories. This can be attributed to the fact that there is relatively little contribution to the response from higher modes at the lower stories. The variation in *MIDR* is significantly reduced by using multi-mode elastic GMPs for the cases in which the maximum inter-story drift occurs at higher stories. There is little improvement in the prediction of *RDR*, which depends mainly on the first mode of vibration of the structure.

Finally, it is important to note that there is little improvement in response prediction achieved by combining the spectral acceleration and energy-based parameters, or by using energy-based GMPs in lieu of spectral accelerations. Hence, given the greater familiarity with spectral accelerations, in the next subsection we build upon the use of $S_a(T_1)$ for the 3-story building models, $\{S_a(T_1),\ S_a(T_2)/S_a(T_1)\}$ for the 9-story building models, and $\{S_a(T_1),\ S_a(T_2)/S_a(T_1),$

$S_a(T_3)/S_a(T_2)$} for the the 20-story building models. In all three cases, we add *inelastic* first-mode GMPs to obtain vectors of ground motion parameters.

5.5.3 REGRESSIONS ON FIRST-MODE INELASTIC AND HIGHER-MODE ELASTIC GMP'S

Building upon the multi-mode elastic GMP vectors that were found (in the preceding subsection) to best predict the nonlinear structural response of each of the three buildings (3-, 9-, and 20-story) considered, we investigate whether addition of the first-mode *inelastic* GMPs described in Section 5.4.3 can further improve the predictions. The standard deviations of the residual *IDR* and *RDR* responses are listed in Appendix B for the elastic, ductile, and brittle models of each building. The regression results confirm that for the elastic models there is no benefit in including the inelastic first-mode GMPs; hence, only the ductile and brittle models are discussed here.

As mentioned earlier, the results presented in Appendix B make use of building models that are each half as strong as the corresponding ductile building model used to obtain the results that were tabulated and illustrated earlier in this chapter. Weaker versions of the three buildings are considered because, as is evident from Figure 5.3, for example, the response of the original buildings for a large portion of the 140 ground motions considered is, in fact, elastic (i.e., *IDR* values less than about 0.01). Instead of actually halving the strength of each structure, we take the approximate (but exact for single-degree-of-freedom structures – see, for example, page 250 of Chopra, 1995) approach of doubling the amplitude of the ground motion records. By this approach, the stiffness of each structure remains unchanged, whereas in reality the stiffness would also be affected by a change in strength. Nevertheless, the regression results for these weaker versions of the buildings are consistent with those presented above for the first-mode elastic and multi-mode elastic GMPs.

5.5.3.1 USE OF {$S_a(T_1)$, …, $S_a(T_n)/S_a(T_{n-1})$, $S_a^I(T_1)/S_a(T_1)$} IN PREDICTING *IDR* AND *RDR*

The standard deviations of the residuals resulting from regressing (i) the vector of *IDR* responses and (ii) the scalar *RDR* response on the vector ground motion parameter {$S_a(T_1)$, …, $S_a(T_n)/S_a(T_{n-1})$, $S_a^I(T_1)/S_a(T_1)$} are reported in Appendix B.

For the ductile and brittle 3-story building models, adding the ground motion parameter $S_a^I(T_1)/S_a(T_1)$ decreases the standard deviation and thereby increases the predictive power relative to the regression on $S_a(T_1)$ alone. This is true for both the *IDR* and *RDR* response measures.

For the ductile 9-story building model, the addition of $S_a^I(T_1)/S_a(T_1)$ to the multi-mode elastic ground motion parameter {$S_a(T_1)$, $S_a(T_2)/S_a(T_1)$} does significantly improve the prediction (i.e., it reduces the standard deviations) of the *IDR* responses at lower stories (say, 1st through 3rd), but the improvement is minimal at the higher stories (where the higher modes dominate) and for the *RDR* response. As a result, the predictive power of the first-mode *inelastic* ground motion parameter {$S_a(T_1)$, $S_a(T_2)/S_a(T_1)$, $S_a^I(T_1)/S_a(T_1)$} is comparable across all stories. For the brittle 9-

story model, $S_a^I(T_1)/S_a(T_1)$ also improves the predictive power of the vector GMP, but to a lesser extent. Again the biggest improvements are at the lowest stories.

For the ductile and brittle models of the 20-story building, the addition of the first-mode inelastic GMP, $S_a^I(T_1)/S_a(T_1)$, to the multi-mode elastic vector $\{S_a(T_1), S_a(T_2)/S_a(T_1), S_a(T_3)/S_a(T_2)\}$ does not appreciably improve the predictive power of the GMP vector for either the vector *IDR* (at any story level) or the scalar *RDR*. This is likely due to the fact that $S_a^I(T_1)$ is roughly equal to $S_a(T_1)$ at the long fundamental period of the 20-story building (T_1 = 4.0 sec).

5.5.3.2 USE OF $\{S_a(T_1), \ldots, S_a(T_n)/S_a(T_{n-1}), A_i^I(T_1)/S_a(T_1)$ OR $A_a^I(T_1)/S_a(T_1)\}$ IN PREDICTING *IDR* AND *RDR*

The standard deviations of the residuals resulting from regressing (i) the vector of *IDR* responses and (ii) the scalar *RDR* response on the vector ground motion parameters $\{S_a(T_1), \ldots, S_a(T_n)/S_a(T_{n-1}), A_i^I(T_1)/S_a(T_1)$ or $A_a^I(T_1)/S_a(T_1)\}$ are also reported in Appendix B. In no cases (across buildings and stories) does the introduction of $A_i^I(T_1)/S_a(T_1)$ or $A_a^I(T_1)/S_a(T_1)$ in lieu of $S_a^I(T_1)/S_a(T_1)$ reduce the standard deviation of the residuals by more than two percentage points. In some cases (e.g., for the *RDR* response of the brittle 3-story model), the predictive power of the GMP vector containing $S_a^I(T_1)/S_a(T_1)$ is superior, and hence overall it is preferred.

5.5.3.3 SUMMARY OF RESULTS USING FIRST-MODE INELASTIC AND HIGHER-MODE ELASTIC GMP'S

For ductile and brittle models of the three buildings considered that are roughly half as strong as the original building designed, we have found that the addition of a first-mode inelastic GMP to a multi-mode elastic GMP vector can indeed improve the predictive power of the resulting vector GMP. The improvement, however, may be minimal for long-period structures (such as for the 20-story building) because of the "equal displacements rule" (Veletsos and Newmark, 1960; Veletsos *et al*., 1965), which indicates that the inelastic GMP will be roughly equal to its elastic counterpart. The use of inelastic energy-based GMPs does not appear to have any advantage over inelastic spectral acceleration.

5.6 "SUFFICIENCY" OF FIRST-MODE ELASTIC VS. FIRST-MODE INELASTIC AND HIGHER-MODE ELASTIC GMP'S

Recall that the regressions of nonlinear structural response measures (e.g., *IDR*) on ground motion parameters (GMPs) result in estimates of (i) the median (or geometric mean) response, via the regression coefficients, and (ii) the logarithmic standard deviation of the response ($\sigma_{ln\varepsilon}$), both for a given level of ground motion. Assuming that the response conditional on a given level of ground motion is lognormally distributed, the regression results can be used to compute the probability of exceeding a specified response conditioned on the ground motion level, denoted here as $G[IDR|\text{GMP}]$ for *IDR* response. Note that this conditional complementary cumulative distribution function (CDF) for all ground motion levels can be convolved with the ground

motion hazard to obtain a hazard curve in terms of nonlinear structural response (e.g., Bazzurro and Cornell, 1994).

For some ground motion parameters more so than for others, the regression results, and therefore $G[IDR|\text{GMP}]$, can depend on the set of earthquake records used – e.g., "near-source" versus "ordinary," as described in Chapter 3 – even if the record sample size is very large. A "sufficient" GMP, however, will provide approximately the same regression results regardless of the types of ground motions considered (Luco, 2002). A major advantage of the use of a sufficient GMP is that regression of nonlinear structural response on such a GMP can be carried out for an arbitrary set of earthquake records, rather than for a set of records whose characteristics match those for the earthquake scenarios that control the hazard at the particular building site.

The sufficiency of $S_a(T_1)$ and $\{S_a(T_1), S_a(T_2)/S_a(T_1), S_a^I(T_1)/S_a(T_1)\}$ with respect to (i) near-source versus "ordinary" ground motions, and (ii) ground motions from relatively large versus small magnitude earthquakes, is illustrated in Figures 5.6 and 5.7, respectively. Recall (from Chapter 3) that the near-source ground motions are defined as those with $R_{\text{close}} < 16$km, and the large magnitude earthquakes are taken to be those with $M_{\text{w}} > 6.5$. The $G[IDR|\text{GMP}]$ results are shown for *IDR* responses at only the first and ninth stories of the ductile 9-story building model, but the results at the other stories exhibit similar trends. The ground motion level considered for these figures is the median level across the full set of 140 earthquake records.

Note from Figures 5.6 and 5.7 that the $G[IDR|\text{GMP}]$ results are more similar across distance (nearby vs. non-nearby) and magnitude (small vs. large) ranges when the GMP is comprised of the first-mode inelastic and higher-mode elastic vector $\{S_a(T_1), S_a(T_2)/S_a(T_1), S_a^I(T_1)/S_a(T_1)\}$. Hence, not only does this vector GMP better predict nonlinear structural response than the conventional $S_a(T_1)$, as demonstrated earlier, it appears to be more "sufficient" as well.

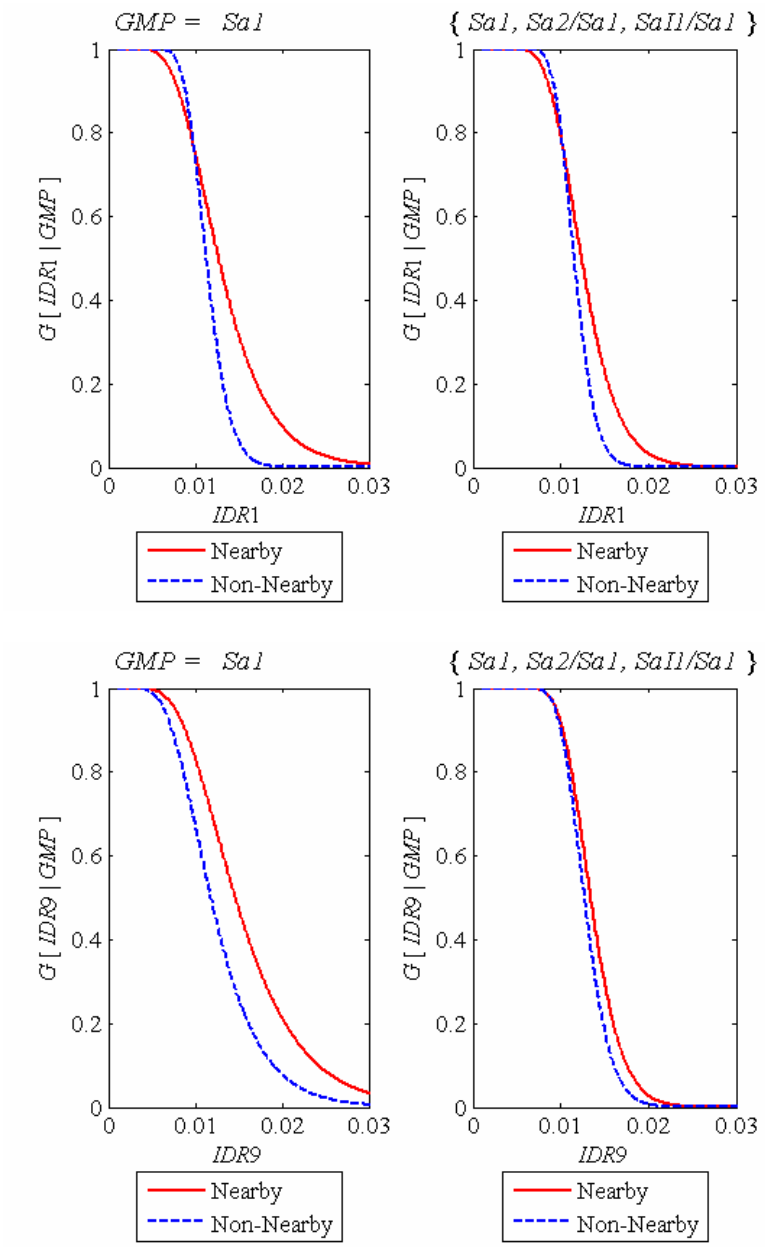

Figure 5.6 Complementary CDFs of first- and ninth-story *IDR* for the ductile 9-story building, conditioned on the median ground motion level defined in terms of $S_a(T_1)$ and $\{S_a(T_1), S_a(T_2)/S_a(T_1), S_a^I(T_1)/S_a(T_1)\}$ and for the near-source (or "nearby") versus ordinary (or "non-nearby") subsets of earthquake records.

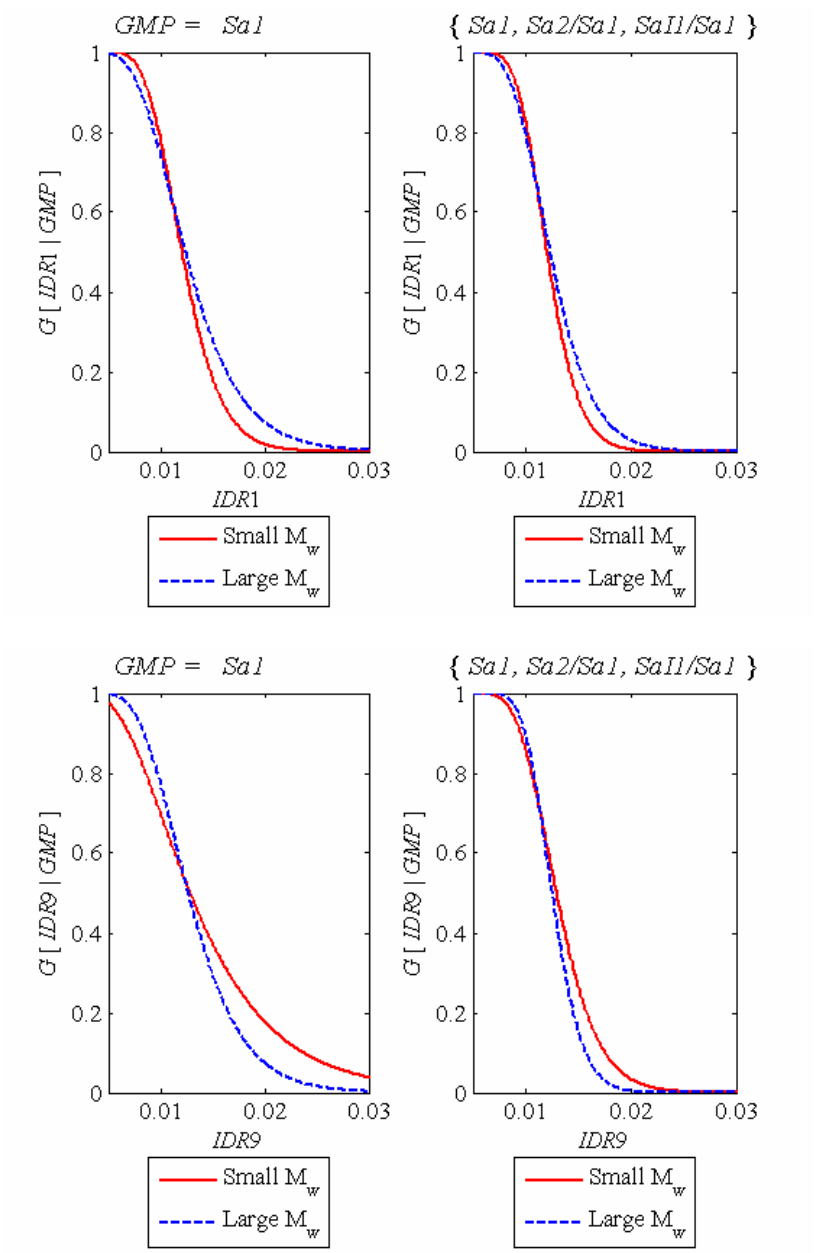

Figure 5.7 Complementary CDFs of first- and ninth-story *IDR* for the ductile 9-story building, conditioned on the median ground motion level defined in terms of $S_a(T_1)$ and $\{S_a(T_1), S_a(T_2)/S_a(T_1), S_a^I(T_1)/S_a(T_1)\}$ and for the smaller versus larger magnitude subsets of earthquake records.

5.7 CONCLUDING REMARKS

Using elastic, ductile, and brittle models of three different steel moment-resisting frame structures (3-, 9-, and 20-story buildings) and 140 earthquake ground motion records, different scalar and vector ground motion parameter (GMP) sets were used as predictor variables to estimate various response measure vectors that included (i) maximum (over all stories) peak inter-story drift ratio (*MIDR*), (ii) average (over all stories) peak inter-story drift ratio (*AIDR*), (iii) peak roof drift ratio (*RDR*), and (iv) peak inter-story drift ratios for individual stories (*IDR*). The two response vectors considered were {*MIDR*, *AIDR*, *RDR*} and {IDR_i; i = 1 to number of stories}. In general, we have found that a GMP vector that includes a higher-mode elastic spectral acceleration [e.g., $S_a(T_2)/S_a(T_1)$] and first-mode *inelastic* spectral acceleration [e.g., $S_a^I(T_1)/S_a(T_1)$], in addition to the first-mode elastic spectral acceleration [i.e., $S_a(T_1)$], better predicts nonlinear structural response than $S_a(T_1)$ alone. The response prediction is especially improved for the 9-story building. Energy-based GMPs [e.g., $A_i(T_1)$], however, do not appreciably improve the predictive power of such vectors due, in part, to the strong correlation of $A_i(T_1)$ with $S_a(T_1)$.

CHAPTER 6 – SIMPLIFIED ILLUSTRATIONS OF LOSS ESTIMATION

6.1 INTRODUCTION

A reasonable and commonly sought goal is to estimate building damage and associated monetary losses in the face of future earthquake events. Accurate and reliable estimates of monetary losses can form the basis for rational decision making related to risk management. For example, accurate loss estimates guide insurers in selecting fair earthquake insurance premiums and owners in adopting risk mitigation strategies, such as embarking on preemptive structural retrofitting or buying earthquake insurance, or a combination of both. Monetary losses due to damage to buildings can be related to several factors – e.g., damage to connections, damage to structural members, and damage to partitions and other non-structural components. Loss estimation studies are usually carried out from knowledge of the response of the structures involved.

In this chapter, we will attempt to demonstrate by means of intentionally simple illustrations how the MMLR-based studies resulting in predictions of structural response given ground motion parameters can be employed in loss estimation studies. There are three main reasons why the illustrations that we present here are simplified ones. First, data from past earthquakes on structural and non-structural damage observed in buildings and on monetary losses due to the need to repair or replace damaged components are very rare and, for liability reasons, extremely difficult to obtain. Even when available, they are insufficient for making any statistical inference on losses from physical damage for buildings of different characteristics (e.g., material, lateral-force resisting system, and number of stories). Hence, in research studies such as this one, the missing empirical loss data are simply "simulated" from the levels of deformation computed by nonlinear dynamic analyses of the buildings subject to ground motions of different intensity. The loss data are sometimes inferred using a detailed approach (e.g., see the methodology pursued by the Pacific Earthquake Engineering Research Center) that links the level of story deformation to the damage state of each element present at that story and from there to the appropriate repair strategy and, finally, to repair costs. The global loss is then computed by adding the losses from all stories. In this study, however, we derived functional relationships between building responses and loss in a simplified way that will be discussed later in this chapter. Second, for the sake of simplicity, we restrict our illustrations only to the ductile models of the three buildings discussed in Chapter 5 and, in fact, mostly to the 9-story building. Third, though MMLR studies in Chapter 5 suggested that not only multi-mode elastic GMPs but also first-mode inelastic mode GMPs can lead to better predictions of structural performance (e.g., IDRs), we restrict our illustrations to ones where only elastic GMPs are employed including only up to second-mode elastic S_a. No inelastic GMPs and no energy-related GMPs are included.

Note that our first simplification (namely that of needing to simulate loss data for steel MRF buildings, which is explained later) implies that our conclusions regarding which structural performance measures (***Y***) predicted from which GMPs (***X***) leads to loss estimates with least uncertainty are often not realistic. In other words, the procedure that we outline here is what we wish to emphasize, not the findings in the hypothetical cases studied. Notwithstanding these problems, we present results on estimates for losses and uncertainty on such estimates using simulated loss data; if we had real damage data to use in the illustrations, the procedures that we outline below for loss estimation would stay the same but the findings would be intuitively more in line with engineering intuition.

Our second and third simplifications – those of confining the loss estimation studies to elastic one- and two-mode GMPs and to the use of the 9-story ductile building model – are made despite indications that inelastic first-mode GMPs can lead to better predictions of structural response, ***Y***. This is done merely so that we could focus on the procedure involved in the loss estimation. The procedure described can be easily repeated for all of the buildings with brittle connection models and where the most efficient and sufficient MMLR-based models are employed instead. The extension to those cases from the simpler case presented here would be direct.

6.2 A MODEL FOR LOSS ESTIMATION

In Section 5.2, we have seen that the prediction of an *n*-dimensional response vector, ***Y***, (e.g., the maximum interstory drift and the peak roof drift) from an *r*-dimensional ground motion parameter vector, ***X*,** (e.g., the spectral accelerations at multiple oscillator frequencies) may be carried using the following model for regression:

$$Y_i(\boldsymbol{X}) = b_{0i}\left(\prod_{j=1}^{r} X_j^{b_{ji}}\right)\varepsilon_i = b_{0i}\exp\left(\sum_{j=1}^{r} b_{ji}\ln X_j\right)\cdot\varepsilon_i \qquad \text{for } i = 1 \text{ to } n. \tag{6.1}$$

where b_{ji} and the covariance matrix of the residual error terms, ε_i, (denoted hereafter as $\boldsymbol{\Sigma}$) are estimated by carrying out multiple multivariate regression analyses as described in Section 5.2. Estimates of b_{ji} and $\boldsymbol{\Sigma}$ obtained for different choices of the ground motion parameter vector, ***X***, and the response vector, ***Y***, are given in Appendix A. If the model in Equation 6.1 leads to unbiased estimates of $Y_i(\boldsymbol{X})$, then ε_i has a median value of unity.

Consider now a loss or damage function that is related to a vector, ***Y***, comprised of *n* structural response measures. Depending on the choice of elements included in ***Y***, the loss function, L_n, is subject to uncertainty. Assume that L_n can be predicted as follows:

$$L_n(\boldsymbol{Y}(\boldsymbol{X})) = \alpha_0 \cdot \prod_{i=1}^{n} Y_i(\boldsymbol{X})^{\alpha_i} \cdot \varepsilon_{L_n} \tag{6.2}$$

where α_0 and α_i (i = 1 to n) are regression coefficients for the loss model and the variable ε_{Ln} is introduced to account for the uncertainty in predicting losses given $\boldsymbol{Y}$. For unbiased predictions of losses given $\boldsymbol{Y}$, ε_{Ln} may be modeled as a log-normal random variable with a median value of unity. The coefficient of variation, CoV, of ε_{Ln} will, in general, be estimated from data on losses and studies relating losses to structural performance. Unless the response measures included in $\boldsymbol{Y}$ are highly correlated, it is expected that the inclusion of a larger number of response measures in $\boldsymbol{Y}$ will, in general, reduce standard errors in the model of Equation 6.2 or, equivalently, lead to smaller CoV estimates for ε_{Ln}. Estimation of losses is greatly affected by the variability due to an inadequate model, which is associated with a large CoV for the model error random variable, ε_{L_n}, in Equation 6.2. Loss estimation is also influenced by the underlying variability in $\boldsymbol{Y}$ given $\boldsymbol{X}$ (the vector of GMPs) for the structure(s) and site under consideration. If we are interested in estimating losses for structures at a site that is characterized by the various ground motions likely to be experienced there, it is useful to be able to estimate $\boldsymbol{Y}$ efficiently and without bias from parameters, $\boldsymbol{X}$, that describe those ground motions. The GMPs that comprise $\boldsymbol{X}$ ideally should:

- be easy to compute given an earthquake record,
- "efficiently" allow prediction of $\boldsymbol{Y}$ – i.e., it is important that the uncertainty in predicting $\boldsymbol{Y}$ from $\boldsymbol{X}$ be small so that both a small number of structural analyses will suffice (see Equation 2.1) *and* errors propagating to prediction of losses do not get excessively large, thereby leading to large uncertainty in loss estimation, and
- be "predictable" given the characteristics of the causative earthquake (e.g., magnitude, M, and source-to-site distance, R). If uncertainty in predicting the parameters in $\boldsymbol{X}$ is large given M and R, then this uncertainty propagates to the loss estimates for a structure located at a given site. Note that this source of uncertainty is not considered in what follows, because only conditional losses (on $\boldsymbol{X}$) are estimated.

Taking into account the dependency of the n-dimensional $\boldsymbol{Y}$ on the r-dimensional $\boldsymbol{X}$, we can rewrite Equation 6.2 as follows:

$$\begin{aligned} L_{nr}(\boldsymbol{X}) &= \alpha_0 \cdot \prod_{i=1}^{n} \left[b_{0i} \exp(\sum_{j=1}^{r} b_{ji} \ln X_j) \cdot \varepsilon_i \right]^{\alpha_i} \cdot \varepsilon_{L_n} \\ &= \alpha_0 \cdot \prod_{i=1}^{n} \left[b_{0i} \exp(\sum_{j=1}^{r} b_{ji} \ln X_j) \right]^{\alpha_i} \cdot \prod_{i=1}^{n} \varepsilon_i^{\alpha_i} \cdot \varepsilon_{L_n} \\ &= \hat{L}_{nr}(\boldsymbol{X}) \cdot \varepsilon_{L_{nr}|\boldsymbol{X}} \end{aligned} \tag{6.3}$$

where the median loss is given by $\hat{L}_{nr}(\boldsymbol{X}) = \alpha_0 \cdot \prod_{i=1}^{n} \left[b_{0i} \exp(\sum_{j=1}^{r} b_{ji} \ln X_j) \right]^{\alpha_i}$ and the unit-median random error term in the expression for L_{nr} given $\boldsymbol{X}$ is $\varepsilon_{L_{nr}|\boldsymbol{X}} = \prod_{i=1}^{n} \varepsilon_i^{\alpha_i} \cdot \varepsilon_{L_n}$.

Note that if the ε_i's and ε_{L_n} are assumed to be lognormal, then $L_{nr}(\boldsymbol{X})$ is also a lognormal random variable. Statistics of ln $L_{nr}(\boldsymbol{X})$ can be written as follows:

$$\begin{aligned} &\mathrm{E}[\ln L_{nr}(\boldsymbol{X})] = \ln \alpha_0 + \sum_{i=1}^{n} \alpha_i \left(\ln b_{0i} + \sum_{j=1}^{r} b_{ji} \ln X_j \right); \\ &\mathrm{Var}[\ln L_{nr}(\boldsymbol{X})] = \mathrm{Var}[\ln \varepsilon_{L_{nr}|\boldsymbol{X}}] \cong \mathrm{CoV}(L_{nr})^2 \end{aligned} \tag{6.4}$$

where the approximation for Var[ln $L_{nr}(\boldsymbol{X})$] is good if the CoV of L_{nr} (given $\boldsymbol{X}$) is less than say 30%. For unbiased estimates of losses, conditioned on $\boldsymbol{X}$, we have (since the individual error terms are all unit-median lognormal random variables)

$$\mathrm{E}[\ln \varepsilon_{L_{nr}|\boldsymbol{X}}] = 0 \tag{6.5}$$

The variance of the losses, conditioned on $\boldsymbol{X}$, can be written in terms of the loss model parameters in Equation 6.2 and the covariance matrix $\boldsymbol{\Sigma}$ of the individual error terms (from regression of $\boldsymbol{Y}$ on $\boldsymbol{X}$) as follows:

$$\begin{aligned} \mathrm{Var}[\ln \varepsilon_{L_{nr}|\boldsymbol{X}}] &= \sum_{i,j=1}^{n} \alpha_i \alpha_j \Sigma_{i,j} + \mathrm{Var}[\ln \varepsilon_{L_n}] \\ &= \sum_{i=1}^{n} \alpha_i^2 \sigma^2_{\ln \varepsilon_i} + \sum_{\substack{i=1 \\ i \neq j}}^{n} \sum_{j=1}^{n} \alpha_i \alpha_j \rho_{\ln \varepsilon_i \ln \varepsilon_j} \sigma_{\ln \varepsilon_i} \sigma_{\ln \varepsilon_j} + \sigma^2_{\ln \varepsilon_{Ln}} \end{aligned} \tag{6.6}$$

It is clear that the uncertainty in predicting losses is directly related to the variance, $\mathrm{Var}[\ln \varepsilon_{L_{nr}|\boldsymbol{X}}]$. For two alternative unbiased loss models, we will have greater confidence in loss estimates based on the model with the smaller variance.

Equation 6.6 shows the contribution of different factors towards the total uncertainty (variance) in loss estimates. The first term is related to the uncertainty in predicting each response variable, Y_i (i = 1 to n), from knowledge of the selected ground motion parameter vector, $\boldsymbol{X}$. Smaller uncertainty in predicting each response variable, Y_i (by using a suitable choice for the ground motion parameter vector, $\boldsymbol{X}$), will propagate to smaller errors in estimating losses. The second term on the right hand side of Equation 6.6 takes into account the cross-correlation among the different response measures, Y_i. Neglecting the correlation among the various response measures can lead to unconservative estimates of confidence bounds on, say, mean losses. Note that this needed information on the cross-correlation of the response measures is obtained as a direct

result of multivariate multiple linear regressions (MMLR), as was demonstrated in Chapter 5. The last term on the right hand side of Equation 6.6 is related to the model uncertainty resulting from estimating losses based upon knowledge of the structural response, ***Y***. In the optimal situation where structural response data and loss data are available, the use of a larger number of response measures in ***Y*** to correlate with monetary losses would likely reduce this model uncertainty. (In our case, where simulated loss data are employed, this reduction in uncertainty, when present, is very small, as we shall see.)

Note that in the illustrations that follow, we ensure that the alternative loss models lead to the same median losses at a given level of the GMP vector, ***X*** as that of a Base Case (0) unbiased model by enforcing the following:

$$\alpha_{0,\mathrm{I}} \cdot \prod_{i=1}^{n(\mathrm{I})} \left[b_{0i,\mathrm{I}} \exp\left(\sum_{j=1}^{r(\mathrm{I})} b_{ji,\mathrm{I}} \ln X_{j,\mathrm{I}} \right) \right]^{\alpha_{i,\mathrm{I}}} = \alpha_{0,0} \cdot \prod_{i=1}^{n(0)} \left[b_{0i,0} \exp\left(\sum_{j=1}^{r(0)} b_{ji,0} \ln X_{j,0} \right) \right]^{\alpha_{i,0}} \tag{6.7}$$

where $\alpha_{0,\mathrm{I}}$ refers to the α_0 parameter for a generic Model I and $\alpha_{0,0}$ is the α_0 parameter for the unbiased Base Case model. The trailing ",I" and ",0" on the b_{0i} and b_{ji} parameters also refer to the alternate models (I and 0, respectively) while n(I) and r(I) are the size of the vector, ***Y***, included in computing losses and the size of the vector, ***X***, included in computing ***Y*** for model I, and n(0) and r(0) are defined similarly for the Base Case (0) model. The calibration of the various loss models suggested by Equation (6.7) results in unbiased losses only at the level selected for ***X***. In the illustrations that follow, we ensure unbiased models only at the median level of ***X***. Alternative loss models are understood to mean that both n and r as well as the constituent structural response parameters (Y_i, i = 1 to n) and the constituent GMPs (X_j, j = 1 to r) can vary.

For a lognormal random variable, the mean losses can be written as follows:

$$\mu_{L_{nr}}(\boldsymbol{X}) = \hat{L}_{nr}(\boldsymbol{X}) e^{\frac{1}{2}\mathrm{Var}[\ln \varepsilon_{L_{nr}|\boldsymbol{X}}]} \tag{6.8}$$

Note that the mean losses $\mu_{L_{nr}}(\boldsymbol{X})$ are dependent (see Equation 6.3) on the loss model parameters, α_i, the model parameters for predicting response from ground motion parameters, b_{ji}, the variance of the random error terms, $\mathrm{Var}[\ln \varepsilon_{L_{nr}|\boldsymbol{X}}]$, and the levels of intensity for each of the GMPs in the vector, ***X***. In addition to estimates of the mean losses, it is also of interest to estimate the range of values of losses that can result for a given ***X***. This can be done by studying specific percentile confidence intervals of losses. We will present results of the 95% (central) confidence intervals on losses that are computed using the 2.5% non-exceedance losses, $L_{nr,2.5}(\boldsymbol{X})$, and the 97.5% non-exceedance losses, $L_{nr,97.5}(\boldsymbol{X})$, for a given ***X***:

$$\begin{aligned} L_{nr,2.5}(\boldsymbol{X}) &= \hat{L}_{nr}(\boldsymbol{X}) e^{-1.96\sigma_{\ln \varepsilon_{Lnr|\boldsymbol{X}}}} \\ L_{nr,97.5}(\boldsymbol{X}) &= \hat{L}_{nr}(\boldsymbol{X}) e^{+1.96\sigma_{\ln \varepsilon_{Lnr|\boldsymbol{X}}}} \end{aligned} \tag{6.9}$$

The 95% confidence interval on losses, $L_{95}(\boldsymbol{X})$, is computed as:

$$L_{95}(\boldsymbol{X}) = L_{nr,97.5}(\boldsymbol{X}) - L_{nr,2.5}(\boldsymbol{X}) \tag{6.10}$$

In the following, we compare estimates of the mean losses and the 95% confidence intervals on losses conditioned on $\boldsymbol{X}$ for various choices of the response variable vector, $\boldsymbol{Y}$, and the ground motion parameter vector, $\boldsymbol{X}$.

6.3 SIMULATED DATA ON LOSSES

In order to compare the predictive power of different choices of the response measure vector, $\boldsymbol{Y}$, and the ground motion parameter vector, $\boldsymbol{X}$, we need loss models that are consistent for the different choices of $\boldsymbol{Y}$. As mentioned earlier, such models could be easily developed if we had real data on losses and corresponding response measures. However, since such data do not currently exist, we rely here on losses that are not a result of actual documentation of quantitative losses that followed earthquakes, but rather are "simulated" based on nonlinear dynamic time-history analyses performed on steel MRF buildings. In particular, we used the ductile model of the 9-story building subject to the 140 ground motions presented in Chapter 3. These simulated losses as developed for this study represent a composite but fictitious indication of damage that is related to the following different performance measures that are obtained from the nonlinear analyses:

- peak inter-story drift ratios (at all stories);
- peak roof drift ratio;
- ratio of plastic hinges formed to the total number of possible hinge locations;
- state of stress (degree of inelastic behavior) of individual structural members.

In plain words, every one of the 140 ground motions is run through the building model and, in each case, the building response quantities itemized above are monitored and recorded. The "loss" is a function of those four quantities.

The various performance measures are combined to yield the composite simulated "loss" measure. In addition, these simulated losses are best studied only in relative terms, not in absolute values such as repair costs in dollars. In the following studies, then, it is most useful to compare loss estimates from the various loss models discussed in relative terms – for example, relative to the base case model to be discussed first. As was stated in Section 6.1, a limitation of this brief study on the use of MMLR results from Chapter 5 in loss estimation illustrations is that we are forced to employ simulated loss data instead of real data. Moreover, recognizing that we are merely developing a procedure for loss estimation here, the nonlinear dynamic analyses from which we simulate loss data are the same analyses that were performed on one of the buildings (the 9-story building ductile model) using the 140 ground motions described in Chapter 3.

Note that while there are obvious limitations to using simulated loss data in lieu of actual data from the field, or even simulated data obtained from an accurate analysis of the repair or replacement cost of each building component in different damage states, it is reasonable to expect that the performance indicators used to arrive at the simulated data are likely to be correlated with damage and, thus, with losses. The main purpose for using simulated loss data that are based on realistic structural performance indicators associated with damage is so that we can have consistent loss estimates to be studied in our examples. In particular, once such loss data are simulated, regression of these losses on any single scalar or vector of response variables, $\boldsymbol{Y}$, can yield estimates of α_0 and α_i in Equation 6.2 as well as coefficient of variation estimates of losses, $V(L_n)$, for a model where n structural response measures are employed. Table 6.1 summarizes results for the 9-story building from regressions of loss data on four different choices of $\boldsymbol{Y}$: {*MIDR*}, {*RDR*}, {*MIDR, RDR*}, and {IDR_1, IDR_5, IDR_8}. These four loss models are discussed in the examples that follow.

It is also worth noting at this point that the loss data were not based on use of the brittle models for the structures and as such will not be applied to those cases. Moreover, only a single building (i.e., the 9-story one) was considered in the loss data simulation. As such, we limit our illustrative studies of loss estimation to such ductile 9-story buildings (except for one very brief case where we apply the same loss model definition to the 3-, 9- and 20-story ductile building models in the Base Case model with $\boldsymbol{Y}$ = {*MIDR*}).

From Table 6.1, it may be noted that the uncertainty levels (characterized by the coefficient of variation of losses given $\boldsymbol{Y}$) in the four loss models presented there are remarkably similar. This is a result of the approach followed here for simulating loss data from engineering analyses. In reality, one might expect that there would be significant benefit and thus a greatly reduced $V(L_n)$ for a 9-story building from using a model where Y = {IDR_1, IDR_5, IDR_8} versus one where $\boldsymbol{Y}$ = {*RDR*}, for example. Another important point to note is that the levels of uncertainty associated with loss estimation in more realistic cases are expected to be a lot higher than is seen here with these simulated data where the coefficients of variation are never greater than 20%.

Response Vector, *Y*	n	α_0	α_i (i = 1 to n)	$\boldsymbol{V(L_n)}$
{*MIDR*}	1	5.346	0.538	0.181
{*RDR*}	1	6.066	0.499	0.177
{*MIDR, RDR*}	2	6.192	0.263, 0.270	0.159
{IDR_1, IDR_5, IDR_8}	3	6.300	0.114, 0.217, 0.218	0.156

Table 6.1 Estimates of loss model parameters and coefficient of variation for losses based on different selections of $\boldsymbol{Y}$ in regressions of losses on $\boldsymbol{Y}$.

Next we study estimates of mean losses and 95% confidence intervals on losses based on different loss models and different MMLR regression choices involving $\boldsymbol{Y}$ and $\boldsymbol{X}$. While any of the regression models for $\boldsymbol{Y}$ on $\boldsymbol{X}$ presented in Chapter 5 could have been chosen, our illustrations are only for the ductile building models, only for the loss models shown in Table 6.1, and only for elastic first- and higher-mode displacement-based GMPs in $\boldsymbol{X}$ (i.e., $\boldsymbol{X}$ does not include any of the inelastic GMPs discussed in Chapter 5, nor any of the energy-based GMPs discussed there). Furthermore, as mentioned earlier, in the illustrations that follow, losses are not in real monetary terms but are best discussed in relative terms – for instance, with direct comparisons with a Base Case model that we present first.

6.4 LOSS ESTIMATION USING A FIRST-MODE ELASTIC GMP

Base Case: $n = 1$; $r = 1$; $\boldsymbol{Y} = \{MIDR\}$; $\boldsymbol{X} = \{S_a(T_1)\}$

Most types of damage in framed structures, and some non-structural damage as well (e.g., damage to partitions), are known to be related to inter-story drifts. The maximum (over all stories) peak inter-story drift ratio (*MIDR*) is commonly thought to be related to local collapse. As a result, *MIDR* is often used as a response measure related to damage and, hence, monetary losses resulting from an earthquake. Figure 6.1 shows a plot of non-dimensional mean losses versus first-mode spectral acceleration for all the three buildings assuming ductile behavior at connections. As we discussed in Section 6.3, all the loss estimation studies that we will discuss presently will apply to the 9-story building alone. However, in this first very brief case at the outset, we assume that the same loss model (developed from data on the ductile 9-story building) is applicable to all three building types with the same level of uncertainty. This may not be the case in general – for example, the uncertainty in predicting losses might increase with number of stories due to increased variability in the response. An increased variability in the response for taller buildings would tend to raise the curves for the 9- and 20-story buildings in Figure 6.1 even more. If data were available, such plots could also be prepared for buildings of other types and sizes and for different locations. Then from knowledge of the levels of ground motion intensity likely to be experienced, one could estimate a probabilistic distribution of losses resulting from an earthquake with appropriate weightings for different GMP (intensity) levels based on their likelihood of occurrence. As was discussed earlier, the mean losses conditional on $\boldsymbol{X}$ (see Equation 6.8) are directly related to the regression parameters obtained in Section 5.5, to the variability in predicting response from ground motion parameters, to the variability in the loss model, and to the loss model parameters.

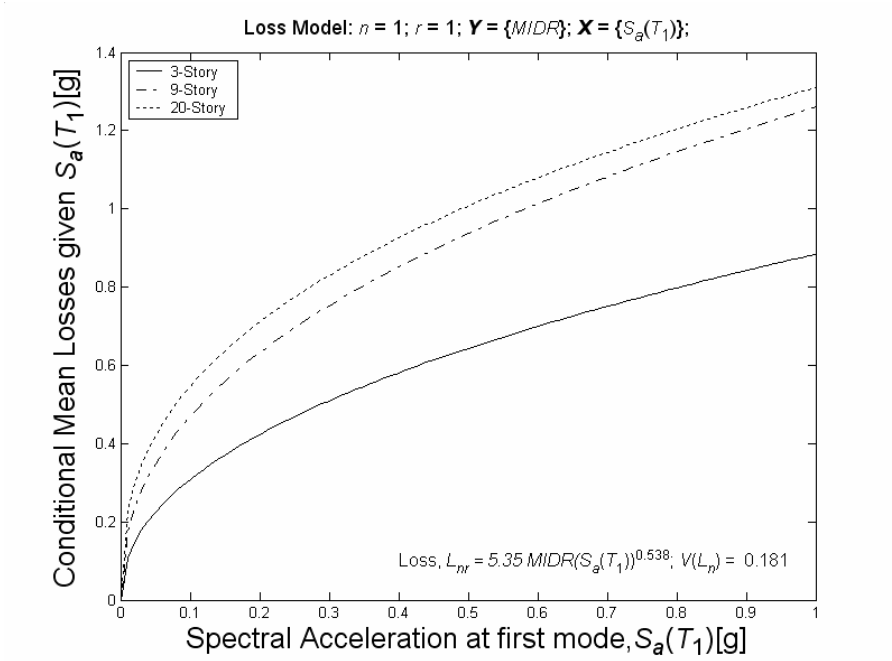

Figure 6.1 Plots of mean losses versus first-mode elastic spectral acceleration for the 3-, 9-, and 20-story buildings.

Figure 6.1 suggests that the mean losses predicted for the 9- and 20-story buildings are considerably higher than for the 3-story building. This is due to the greater variability in response predictions for the 9- and 20-story structures (see Table 6.2). There is greater variability in predicting *MIDR* based on first-mode spectral acceleration, $S_a(T_1)$, for the 9- and 20-story structures, as this response measure is contributed to significantly by higher modes for these structures. This is different for the 3-story structure where the response measure (*MIDR*) is mainly dominated by the first mode.

Building	b_{0i}	b_{1i}	$\sigma_{\ln \varepsilon_{MIDR\|Sa1}}$
3-Story	0.034	0.850	0.175
9-Story	0.064	0.796	0.336
20-Story	0.068	0.705	0.414

Table 6.2 Model parameters and standard deviation of residuals for the response measure *MIDR* regressed on $S_a(T_1)$ for the 3-, 9-, and 20-story buildings (ductile models). (See Tables A.19, A. 25, and A.31.)

To compare the uncertainty in loss estimates based on different choices of the ground motion parameter vector, $\boldsymbol{X}$, and the response measure vector, $\boldsymbol{Y}$, with the uncertainty for the base case model, we study the mean loss and the 95% confidence interval on losses predicted with each model with respect to the corresponding loss predictions for the base case. The extent of the reduction (if any) in the 95% confidence interval for any given model over the base case 95% confidence interval will indicate the effectiveness of that model in estimating losses.

Case 1: $n = 1$; $r = 1$; $\boldsymbol{Y} = \{RDR\}$; $\boldsymbol{X} = \{S_a(T_1)\}$;

The peak roof drift ratio (*RDR*) is often used as a measure of global damage to structures and is also related to the global stability of the structure. Hence, we consider the use of *RDR* as a response measure to estimate losses. Figure 6.2 shows comparative plots of the mean losses and the 95% confidence intervals on losses for the ductile 9-story building using two models, the Base Case and Case 1. The mean losses are close to each other for small levels of $S_a(T_1)$ (< 0.2g), and are only slightly different at higher levels. However, the confidence intervals (indicated by the vertical separation between the top and bottom curves for each set) for loss estimates based on *RDR* are smaller than those based on *MIDR*. For example, at the median level of $S_a(T_1)$ of 0.08g, based on the 140 selected ground motions, the ratio of the 95% confidence intervals for Case1 to that for the Base Case is 0.72. This is mainly due to the smaller errors in predicting *RDR* from knowledge of $S_a(T_1)$ versus the errors in predicting *MIDR* (see Table 5.3), as the peak roof drift ratio is dominated by the first-mode response of the structure. It is worth pointing out that though it can be agreed that *RDR* is in fact better predicted using $S_a(T_1)$ than is *MIDR*, the uncertainty in loss estimates using *RDR* instead of *MIDR* may not be lower if actual loss data were used rather than the simulated loss data that led to smaller standard errors for the *RDR*-based model relative to the *MIDR*-based model (see Table 6.1). It is reasonable to expect that the maximum inter-story drift ratio could be a better predictor of damage and losses than the roof drift ratio. Nevertheless, for the simulated loss data used here, the results are as discussed above.

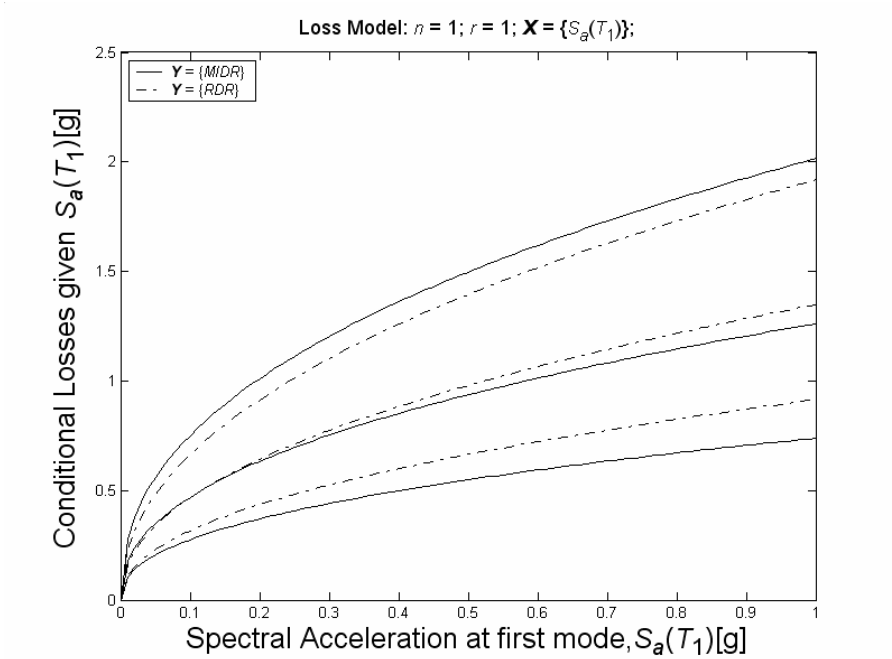

Figure 6.2 Mean losses and 95% confidence intervals on losses predicted by using {*MIDR*} and {*RDR*} for the ductile 9-story structure following regression on the fundamental-mode spectral acceleration, $S_a(T_1)$.

Case 2: $n = 2$; $r = 1$; $\boldsymbol{Y} = \{MIDR, RDR\}$; $\boldsymbol{X} = \{S_a(T_1)\}$;

The maximum (over all stories) peak inter-story drift ratio (*MIDR*) is related more to local damage, whereas the peak roof drift ratio (*RDR*) is related more to global damage and overall stability of the structure. The two measures when taken together can represent two different damage aspects (e.g., the structure may have a low overall drift but may have a large localized story drift or vice versa). By considering either of the two measures singly we may not be able to capture the true state of damage to the structure. By combining these two measures to estimate losses we could expect to improve our confidence in the results (i.e., obtain smaller confidence intervals). Figure 6.3 shows comparative plots of the mean losses and the 95% confidence intervals on losses for the ductile 9-story building using two models, the Base Case and Case 2. As expected we have a smaller 95% confidence interval in Case 2 (e.g., at the median level of $S_a(T_1)$ of 0.08g, the ratio of the 95% confidence interval for Case 2 to that for the Base Case is 0.74). When we consider a vector of response measures for estimating losses, we need to take into account the correlation among the response measures involved. The normalized 95% confidence intervals for Case 2, with and without consideration for correlation among the response measures, are presented in Table 6.3. It can be clearly seen that, if we ignore the effect of correlation among the different response measures, we would unconservatively estimate smaller confidence intervals on losses. However, these differences in this case are not very great here – this, however, is partly due to the fact that we had

unrealistically small standard errors in our loss models (as can be confirmed from Table 6.1). Also, though, the correlation between *MIDR* and *RDR* is only 0.47 (see Table 5.4) and hence the additional uncertainty in loss estimates due to the second term on the right hand side of Equation 6.6 is not significant.

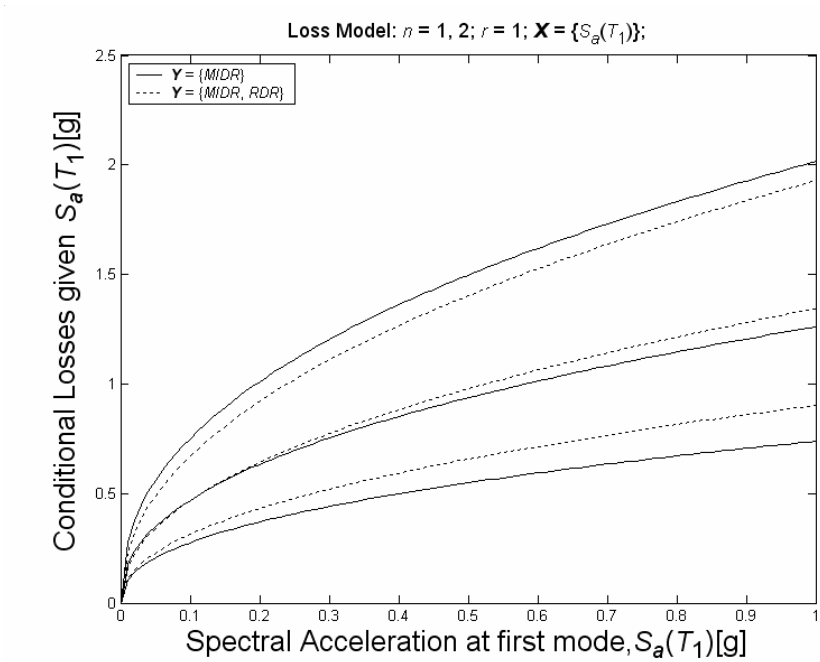

Figure 6.3 Mean losses and 95% confidence intervals on losses predicted by using {*MIDR*} and {*MIDR*, *RDR*} for the ductile 9-story structure following regression on the fundamental-mode spectral acceleration, $S_a(T_1)$.

Case 2	With Correlation	Without Correlation
Normalized 95% Confidence interval	0.74	0.71

Table 6.3 Normalized 95% confidence intervals on losses predicted by using a vector of response measures {*MIDR*, *RDR*} with and without consideration for the correlation among the response measures for the ductile 9-story building at the median level of $S_a(T_1)$ equal to 0.08g.

Case 3: $n = 3$; $r = 1$; $\boldsymbol{Y} = \{IDR_1, IDR_5, IDR_8\}$; $\boldsymbol{X} = \{S_a(T_1)\}$;

Since most types of structural damage as well as some non-structural damage (e.g., damage to partitions) are known to be related to inter-story drifts, by employing a response vector that includes several peak inter-story drift ratios over the height of the structure we might expect to reduce the uncertainty in estimating losses (see Table 6.1). Figure 6.4 shows comparative plots of the mean losses and the 95% confidence intervals on losses for the ductile 9-story building using two models, the Base Case and Case 3. As expected we have a smaller 95% confidence interval in the latter case (e.g., at the median level of $S_a(T_1)$ of 0.08g, the ratio of the 95% confidence intervals for Case 3 to that for the Base Case is 0.78). The normalized 95% confidence intervals for this case, with and without consideration for the correlation among the different response measures, are presented in Table 6.4. As we have a greater number of response measures here (relative to Case 2), we see an even greater underestimation of the confidence intervals if we ignore the effect of correlation among the response measures. As pointed out before, this error due to neglecting correlation is often unconservative. The correlation coefficients needed here are obtained directly using multivariate multiple linear regression (MMLR). Unlike in Case 2, here the correlations between the three *IDR* values are significantly larger (between 0.68 and 0.80, as can be verified from Table 5.2) and hence, the omission of the second term on the right hand side of Equation leads to significant reduction in the confidence interval.

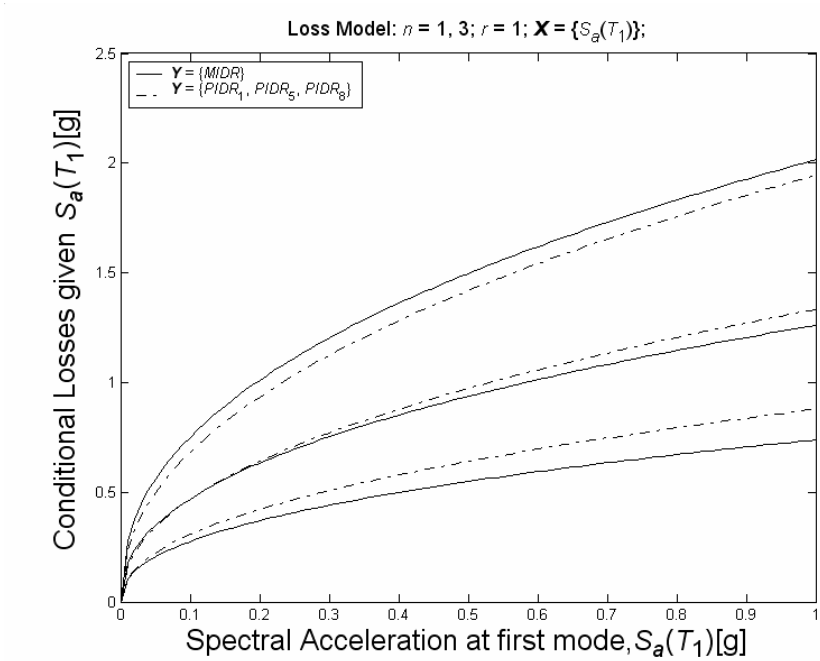

Figure 6.4 Mean losses and 95% confidence intervals on losses predicted by using {*MIDR*} and $\{IDR_1, IDR_5, IDR_8\}$ for the ductile 9-story structure following regression on the fundamental-mode spectral acceleration, $S_a(T_1)$.

Case 3	With Correlation	Without Correlation
Normalized 95% Confidence interval	0.78	0.68

Table 6.4 Normalized 95% confidence intervals on losses predicted by using a vector of response measures, $\{IDR_1, IDR_5, IDR_8\}$, with and without consideration for the correlation among the response measures for the ductile 9-story building at the median level of $S_a(T_1)$ equal to 0.08g.

Loss Model	GMP $\boldsymbol{X}$	Response Measure $\boldsymbol{Y}$	Normalized 95% Confidence Interval
Base Case	$S_a(T_1)$	$\{MIDR\}$	1.00
Case 1	$S_a(T_1)$	$\{RDR\}$	0.72
Case 2	$S_a(T_1)$	$\{MIDR; RDR\}$	0.74
Case 3	$S_a(T_1)$	$\{IDR_1, IDR_5, IDR_8\}$	0.78

Table 6.5 Normalized 95% confidence intervals on losses predicted for the ductile 9-story building for different cases at the median level of $S_a(T_1)$ of 0.08g.

Table 6.5 summarizes the normalized 95% confidence intervals for Cases 1 through 3. We see that the confidence interval is smallest for predictions based on *RDR* alone as the response measure (Case 1). This is due to the smaller variability in predicting *RDR* and the greater variability in predicting peak inter-story drift ratios (and *MIDR*) from knowledge of the first-mode-based parameter, $S_a(T_1)$, alone (see Tables 5.1 and 5.3).

We point out again that any suggestion resulting from the results summarized in Table 6.5 such as that the use of *RDR* alone leads to models for losses that have the least uncertainty may not be true in general when one employs real data on losses. Only because the conditional uncertainty on losses, L_{nr}, given $\boldsymbol{Y}$ is fairly comparable in the four models (see Table 6.1), the net uncertainty is driven by the ability to predict $\boldsymbol{Y}$ from $S_a(T_1)$, and here *RDR* is best predicted from knowledge of $S_a(T_1)$.

6.5 LOSS ESTIMATION USING FIRST- AND SECOND-MODE ELASTIC GMP'S

As was explained earlier (see Equation 6.6), the uncertainty in loss estimation is influenced by the uncertainty in predicting $\boldsymbol{Y}$ from $\boldsymbol{X}$. It was shown in Section 5.5 that the uncertainty in prediction of response variables can be reduced significantly if we use a vector of GMPs (such as a vector comprising of $S_a(T_1)$ and the ratio $S_a(T_2)/S_a(T_1)$) instead of a single scalar GMP.

Therefore, if we use a vector of ground motion parameters, we might expect to reduce the errors that propagate towards uncertainty in loss estimation. In this section, we consider loss estimation based on the use of two ground motion parameters. First, we consider the estimation of losses using a single scalar response measure and later we consider estimation of losses based on the use of a vector of response measures.

Case 1': $n = 1$; $r = 2$; $\boldsymbol{Y} = \{MIDR\}$; $\boldsymbol{X} = \{S_a(T_1), S_a(T_2)/S_a(T_1)\}$;

Figure 6.5 shows a 3-D plot of mean losses versus $\{S_a(T_1), S_a(T_2)/S_a(T_1)\}$ for the ductile 9-story building. Note that such a plot would in general need to be combined with the joint likelihood of $\{S_a(T_1), S_a(T_2)/S_a(T_1)\}$ pairs at a given site to evaluate a probabilistic distribution on losses. In general, large $S_a(T_1)$ values are not associated with large $S_a(T_2)/S_a(T_1)$ values. Intuitively, when $S_a(T_1)$ is on a peak of a response spectrum, it is relatively unlikely that $S_a(T_2)$ is also on a peak. For example, based on the 140 selected ground motions of this study, the joint distribution of $S_a(T_1)$ and $S_a(T_2)/S_a(T_1)$ is plotted in Figure 6.6. It is clear that the joint occurrence of large values of $S_a(T_1)$ and $S_a(T_2)/S_a(T_1)$ is not very likely. Therefore, mean losses are expected to remain at lower levels than those suggested by the peak of the graph in Figure 6.5.

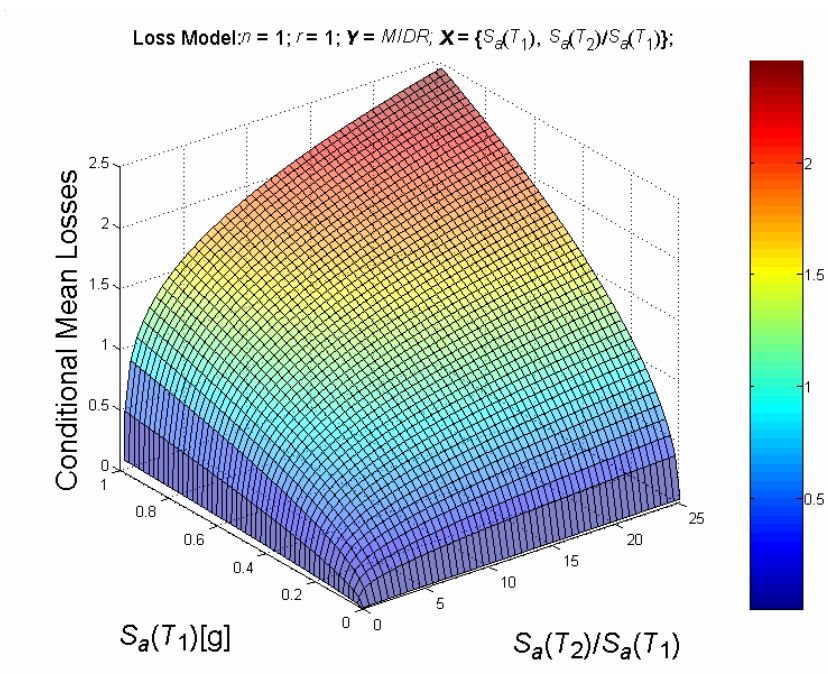

Figure 6.5 Plot of mean losses versus the vector $\{S_a(T_1), S_a(T_2)/S_a(T_1)\}$ for the ductile 9-story building.

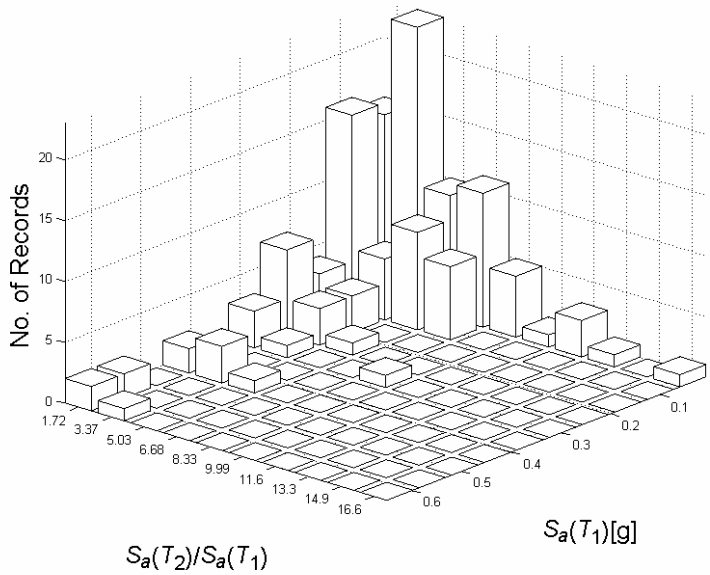

Figure 6.6 Joint distribution of spectral acceleration at the first mode, $S_a(T_1)$, and the ratio of spectral accelerations at the first two modes, $S_a(T_2)/S_a(T_1)$, for the ductile 9-story building, based on the 140 selected ground motions.

Loss Model	$\boldsymbol{X} = \{S_a(T_1), S_a(T_2)/S_a(T_1)\}$	$\boldsymbol{X} = \{S_a(T_1)\}$
Normalized 95% Confidence interval	0.80	1.0

Table 6.6 Normalized 95% confidence intervals on losses estimated from {*MIDR*} using different ground motion parameter vectors, $\boldsymbol{X}$, at median levels of $S_a(T_1)$ and $S_a(T_2)/S_a(T_1)$.

Table 6.6 shows the normalized 95% confidence interval on losses for this case (Case 1') evaluated at the median values of the variables in the ground motion parameter vector, $\boldsymbol{X}$. As expected, this confidence interval is significantly tighter (by 20%) than the corresponding interval for the Base Case (reported in the last column of the table) since the GMP vector includes second-mode consideration, which reduces uncertainty in predicting *MIDR*. This can be explained by studying Tables 5.3 and 5.16 where standard errors are seen to be greatly reduced upon adding $S_a(T_2)/S_a(T_1)$ to $S_a(T_1)$ in $\boldsymbol{X}$ for predicting *MIDR*.

Case 2': $n = 1$; $r = 2$; $\boldsymbol{Y} = \{RDR\}$; $\boldsymbol{X} = \{S_a(T_1), S_a(T_2)/S_a(T_1)\}$;

This case differs from Case 1' only in the use of *RDR* rather than *MIDR* as the response parameter of choice for estimating losses. Table 6.7 presents normalized confidence intervals at the median values of the variables in the ground motion parameter vector, $\boldsymbol{X}$. As expected there is not much improvement in the accuracy of loss predictions by including a second-mode parameter when the response measure employed is the peak roof drift ratio. Peak roof drift ratio, being dominated by the first-mode response of the structure, is very well correlated with the first-mode spectral acceleration and little is gained from using a vector of GMPs that includes second-mode spectral acceleration instead of the first-mode spectral acceleration (e.g., standard errors in predicting *RDR* are only slightly decreased by addition of $S_a(T_2)/S_a(T_1)$ to $S_a(T_1)$ in $\boldsymbol{X}$, as can be verified from Tables 5.3 and 5.16).

	$\boldsymbol{X} = \{S_a(T_1), S_a(T_2)/S_a(T_1)\}$	$\boldsymbol{X} = \{S_a(T_1)\}$
Normalized 95% Confidence interval	0.722	0.724

Table 6.7 Normalized 95% confidence intervals on losses estimated from {*RDR*} using different ground motion parameter vectors, $\boldsymbol{X}$, at median levels of $S_a(T_1)$ and $S_a(T_2)/ S_a(T_1)$.

Case 3': $n = 2$; $r = 2$; $\boldsymbol{Y} = \{MIDR, RDR\}$; $\boldsymbol{X} = \{S_a(T_1), S_a(T_2)/S_a(T_1)\}$;

Table 6.8 presents normalized confidence intervals at the median values of the variables in the ground motion parameter vector, $\boldsymbol{X}$. Since the maximum inter-story drift ratio (*MIDR*) is better correlated with a vector of ground motion parameters that includes second-mode spectral acceleration (as we saw in Case 1'), we see an improvement in the accuracy of loss estimations in this case compared to Case 2. As seen in Table 6.9, the error due to neglecting correlation among the two response variables (*MIDR* and *RDR*) is small because overall uncertainty is artificially small in this case where simulated loss data were used. We commented about reasons for this when discussing Case 2 and Table 6.3 before.

	$\boldsymbol{X} = \{S_a(T_1), S_a(T_2)/S_a(T_1)\}$	$\boldsymbol{X} = \{S_a(T_1)\}$
Normalized 95% Confidence interval	0.67	0.74

Table 6.8 Normalized 95% confidence intervals on losses estimated by using {*MIDR*, *RDR*} with different ground motion parameter vectors, $\boldsymbol{X}$, at median levels of $S_a(T_1)$ and $S_a(T_2)/ S_a(T_1)$.

Case 3’	With Correlation	Without Correlation
Normalized 95% Confidence interval	0.67	0.65

Table 6.9 Normalized 95% confidence intervals on losses predicted by using a vector of response measures {*MIDR*, *RDR*} with and without consideration for the correlation among the response measures for the ductile 9-story building at median levels of $S_a(T_1)$ and $S_a(T_2)/ S_a(T_1)$.

Case 4’: $n = 3$; $r = 2$; $\boldsymbol{Y} = \{IDR_1, IDR_5, IDR_8\}$; $\boldsymbol{X} = \{S_a(T_1), S_a(T_2)/S_a(T_1)\}$;

Table 6.10 presents normalized confidence intervals at the median values of the variables in the ground motion parameter vector, $\boldsymbol{X}$. The errors in predicting the peak inter-story drift ratios are smaller, particularly at the eighth story level (compare standard errors in Tables 5.1 and 5.13), resulting in a smaller confidence interval for the losses relative to Case 3. Also, as seen in Table 6.11, the error due to neglecting correlation among the three response measures is not very large here.

The normalized 95% confidence intervals for Cases 1’, 2’, 3’ and 4’ where first- and second-mode elastic GMPs were used to estimate losses are summarized in Table 6.12. The smallest confidence intervals are for the loss models predicted from two or more response measures (Cases 3’ and 4’) that are in turn predicted from a vector comprised of two elastic ground motion parameters, $S_a(T_1)$ and $S_a(T_2)/S_a(T_1)$.

	$\boldsymbol{X} = \{S_a(T_1), S_a(T_2)/S_a(T_1)\}$	$\boldsymbol{X} = \{S_a(T_1)\}$
Normalized 95% Confidence interval	0.67	0.78

Table 6.10 Normalized 95% confidence intervals on losses estimated by using {IDR_1, IDR_5, IDR_8} with different ground motion parameter vectors, $\boldsymbol{X}$ at median levels of $S_a(T_1)$ and $S_a(T_2)/ S_a(T_1)$.

Case 4’	With Correlation	Without Correlation
Normalized 95% Confidence interval	0.67	0.63

Table 6.11 Normalized 95% confidence intervals on losses predicted by using a vector of response measures {IDR_1, IDR_5, IDR_8} with and without consideration for the correlation among the response measures for the ductile 9-story building at median levels of $S_a(T_1)$ and $S_a(T_2)/ S_a(T_1)$.

Loss Model	GMP $\boldsymbol{X}$	Response Measure $\boldsymbol{Y}$	Normalized 95% Confidence Interval
Case 1'	$S_a(T_1)$, $S_a(T_2)/S_a(T_1)$	$\{MIDR\}$	0.80
Case 2'	$S_a(T_1)$, $S_a(T_2)/S_a(T_1)$	$\{RDR\}$	0.72
Case 3'	$S_a(T_1)$, $S_a(T_2)/S_a(T_1)$	$\{MIDR; RDR\}$	0.67
Case 4'	$S_a(T_1)$, $S_a(T_2)/S_a(T_1)$	$\{IDR_1, IDR_5, IDR_8\}$	0.67

Table 6.12 Normalized 95% confidence intervals on losses predicted for the ductile 9-story building for different cases and at the median levels of the ground motion parameter vector, $\boldsymbol{X}$.

6.6 SUMMARY

Loss models were developed that relate losses to various structural response measures. This was achieved by means of nonlinear dynamic analyses of ductile building models because field data on structural response and associated damage/loss pairs are unavailable. Several consistent loss models were developed using the simulated data. The response measures considered were the maximum (over all stories) peak inter-story drift ratio (*MIDR*), the peak roof drift ratio (*RDR*), and a group of individual peak inter-story drift ratios (*IDR*s). Studies were focused on the 9-story building with ductile connections.

Results summarizing mean losses and 95% confidence intervals on losses were presented for various models. There are several sources of uncertainty that arise in predicting losses. One source relates to the number and type of response measures used to predict losses. Another source relates to the GMP set used to predict the response measures. A third source was shown to be directly related to simultaneous estimation of pairs of response measures (and hence their correlation) that are involved in the loss model.

While the loss estimation examples are merely illustrative and were based on simulated loss data, the benefit of using multivariate multiple linear regression (MMLR) and thus of estimating the correlation between different response measures involved, as well as the benefit of using a GMP vector (over a scalar, even though only illustrated for elastic GMPs) was demonstrated in the loss estimation examples. Such studies need to expand to consider real data, whenever available, or loss data simulated using a more refined approach than that adopted here, and to include alternative response measures in $\boldsymbol{Y}$ and other elastic and inelastic ground motion parameters in $\boldsymbol{X}$. As long as nonlinear dynamics analyses can be carried out for the class of structures of interest so that MMLR studies can relate structural performance to ground motion parameters, available loss data and correlations within a subset of the structural response variables can help establish the loss model. Then, the methodology presented here could be of considerable use if implemented in decision making and planning against earthquake-related losses.

CHAPTER 7 – CONCLUSIONS

7.1 GENERAL SUMMARY

The objectives of this research were (i) to investigate whether vector combinations of ground motion parameters (GMPs) (also referred to as intensity measures or IMs in the literature) could more accurately predict vector and scalar measures of structural response than the use of a single scalar GMP (e.g., spectral acceleration); and (ii) to study the predictive power of energy- versus displacement-based GMPs. The derivation of input and absorbed energy-based parameters was presented and differences between the conventional spectral acceleration and the energy-equivalent accelerations were also discussed. Inelastic GMPs, both energy- and displacement-based, were also defined.

A total of 140 ground motions relevant to the Southern California region were obtained from the Pacific Earthquake Engineering Research (PEER) Center Strong Motion Database assembled by Dr. Walter Silva. The records included "near-source" and "ordinary" ground motions from small and large (M_w>6.5) magnitude earthquakes. Elastic and inelastic time-history analysis of SDOF oscillators subject to these records produced GMPs for a range of periods of interest for the three buildings that were considered. Two-dimensional computational models of the three moment-resisting frame buildings were analyzed, again for all 140 records, using the non-linear dynamic analysis programs RUAUMOKO and DRAIN-2DX. Three different models were considered for each building that assumed (i) elastic, (ii) ductile, and (iii) brittle beam-column connection behavior.

Multivariate multiple linear regressions (MMLRs) were carried out for various vector and scalar choices of ground motion parameters ($\boldsymbol{X}$) and response measures ($\boldsymbol{Y}$). Estimates of the regression model parameters and the covariance matrix of the residuals were obtained. The predictive power of the various GMPs was measured in terms of the standard deviations of the residuals, since uncertainty in response predictions based on regression models is directly related to them.

Results from the regression analyses were used to illustrate loss estimation calculations and the benefit of the MMLR analyses with vector GMPs and vector structural response measures.

7.2 CONCLUSIONS

The energy- and displacement-based ground motion parameters considered (i.e., input and absorbed energy-equivalent acceleration, and spectral acceleration) were found to be highly correlated with each other over the range of periods of interest, and therefore they tend to have similar predictive power for the responses of the chosen frames. In other words, including the energy-based GMPs in a vector with spectral acceleration(s) did not appreciably improve the structural response predictions. Despite the fairly strong correlation between the inelastic and elastic counterparts of these GMPs, however, the use of inelastic GMPs did improve the

predictions of structural response, as did the inclusion of elastic GMPs at multiple periods corresponding to the modes of vibration for each building.

The response of the 3-story frame considered was dominated by the first mode. As a result, the response measures were very highly correlated with first-mode-based intensity measures. By including a second-mode-based parameter in our response regressions for the 3-story building, little reduction was achieved in the standard deviation of the residuals. However, consideration of an *inelastic* GMP in lieu of an elastic one did significantly improve the prediction of nonlinear structural response.

In contrast to the 3-story building, as expected the response of the 9- and 20-story structures was significantly influenced by higher modes. Standard deviations of the residuals of the peak interstory drift ratios (*IDR*s) regressed on first-mode-based parameters were, in general, larger at the higher stories where higher modes were important. Also, standard deviations of the residuals for maximum peak interstory drift ratio (*MIDR*) and the average peak interstory drift ratio (*AIDR*) were higher than that for the peak roof drift ratio (*RDR*), which was more highly dominated by the first mode. There was strong correlation among the residuals of adjacent stories, as well as between pairs of stories whose response was significantly influenced by higher modes. By including higher-mode-based parameters in a vector-valued GMP set, the response predictions of the 9- and 20-story frames were improved. The standard deviations of the residuals of the response measures (especially *MIDR*, *AIDR* and the higher-floor *IDR*s) were smaller. For example, for the 20-story frame, these standard deviations were sometimes reduced by a factor of two, which would translate into a four-fold reduction in the number of analyses required to achieve results with similar levels of confidence (as compared to when one uses a single scalar first-mode GMP to predict response). The use of inelastic GMPs also improved the prediction of some *IDR*s in the 9-story building, but for the long-period 20-story building, the inelastic GMPs were comparable to their elastic counterparts (as expected based on the "equal displacements rule"), and hence did little to improve the predictions.

In summary, for all three buildings considered here a vector of GMPs that includes higher-mode and/or inelastic terms has proven to be superior to single scalar GMPs in predicting localized structural responses such as IDRs. The gain is not significant, however, when trying to estimate more global response measures such as the RDR.

The benefits of using MMLR analyses to predict a vector of response measures using a vector of GMPs as predictor variables was demonstrated in the loss estimation examples. The use of a vector GMP instead of a scalar, and the availability of correlation information among the response measures (obtained directly through MMLR analyses), both improved loss estimates.

7.3 RECOMMENDATIONS FOR FUTURE WORK

An important element missing from the current study is that actual recorded data on losses correlated with structural response measures were not available. Regression studies using well-documented data from past earthquakes need to be carried out to establish more realistic

relationships between loss and response measures that can then be used in loss estimation studies.

This study could be easily extended to other regions and structure types. Uncertainty in material strength and other modeling assumptions can also be considered. Other ground motion parameters could be included in addition to the ones considered here.

If a GMP vector is useful in predicting the response of structures, as was true for the cases considered in this study, it follows that ground motion studies will need to be carried to establish the joint occurrence of these ground motion parameters as a function of magnitude, distance, and other pertinent quantities, as is customarily done in attenuation models. Then to estimate the joint likelihood of a vector of ground motion parameters at a particular site, we will need to perform a vector-valued probabilistic seismic hazard analysis. Even though such vector-valued seismic hazard analyses are not routinely carried out in practice, the methodology and software for carrying out such analyses are available to the earthquake engineering community, and these hazard analyses can usefully complement studies such as this one that focus on correlation of structural performance and losses with vectors of GMPs. The present study using MMLR with vectors of GMPs as predictors of vectors of structural response measures (ultimately linking them to loss models) is, in fact, one example of the type of study that motivates the need for vector-valued seismic hazard analyses. By combining such studies, either site-specific or region-specific loss studies can be carried out that employ probabilistic information on a suitable GMP vector together with robust models of structural performance vectors to yield probabilistic distributions on damage/losses.

Specifically, then, one can efficiently compute, for example, the annual likelihood that earthquake-induced losses exceeding any specified amount are suffered by a building at a given site. This can be done by convolving the site hazard, either in terms of a vector of GMPs or of a scalar GMP, with the loss versus response measure(s) relationships mentioned at the beginning of this subsection. Such fully probabilistic loss estimation analyses are key studies for the different stakeholders, such as property owners, insurance and reinsurance companies, capital lending institutions, local government agencies, and structural engineers, all of whom strive to make informed decisions regarding earthquake risk mitigation strategies.

REFERENCES

1. Akiyama, H., 1985, *Earthquake-resistant Limit-State Design for Buildings*, University Tokyo Press, Japan.
2. Akiyama, H., 1988, *A Prospect for Future Earthquake-Resistant Design, Engineering Structures*, Vol. 20, 4-6, pp. 447-451.
3. Bazzurro, P., and Cornell, C. A., 1994, *Seismic Hazard Analysis of Nonlinear Structures. I: Methodology. II: Applications*, Journal of Structural Engineering, ASCE, Vol. 120, No. 11, pp. 3320-3365.
4. Bazzurro, P., and Cornell, C. A., 2002, *Vector-valued probabilistic seismic hazard analysis (VPSHA)*, Proceedings of the Seventh U.S. National Conference on Earthquake Engineering, Boston, MA.
5. Carr, A. J., 2003, *Ruaumoko User Manual*, University of Canterbury, New Zealand.
6. Chapman, M. C., 1999, *On the Use of Elastic Input Energy for Seismic Hazard Analysis*, Earthquake Spectra, V. 15, No. 4, pp. 607-635.
7. Chopra, A.K., 1995, *Dynamic of Structures: Theory and Applications to Earthquake Engineering*, Prentice Hall, Inc., New Jersey.
8. Chou, C.-C., and Uang, C.-M., 2000, *Establishing absorbed energy spectra-an attenuation approach*, Earthquake Engineering and Structural Dynamics, 29, pp. 1441-1455.
9. Chou, C.-C., and Uang, C.-M., 2003, *A procedure for evaluating seismic energy demand of framed structures*, Earthquake Engineering and Structural Dynamics, Vol. 32, No. 2, pp. 229-244.
10. Giovenale P., Ciampoli M., and Jalayer, F., 2003, *Comparison of ground motion intensity measures using the incremental dynamic analysis*, Applications of Statistics and Probability in Civil Engineering, Der Kiureghian, Madanat & Pestana (eds).
11. FEMA 351, 2000, *Recommended Seismic Evaluation and Upgrade Criteria for Welded Steel Moment-Frame Buildings*, Federal Emergency Management Agency.
12. FEMA-355C, 2000, *State of the Art Report on Systems Performance of Steel Moment Frames Subject to Earthquake Ground Shaking*, Federal Emergency Management Agency.
13. FEMA-355F, 2000, *State of the Art Report on Performance Prediction and Evaluation of Steel Moment-Frame Buildings*, Federal Emergency Management Agency.
14. Gupta, A., and Krawinkler, H., 1999, *Seismic Demands for Performance Evaluation of Moment-Resisting Frame Structures (SAC Task 5.4.3)*, The John A. Blume Earthquake Engineering Center, Rept. No. 132, Dept. of Civil and Environmental Engineering, Stanford, University, Stanford, CA.
15. Housner, G. W., (1956) *Limit Design of Structures to Resist Earthquakes*, First Conference on Earthquake Engineering, EERI, Berkeley, CA.
16. Johnson, R.A., and Wichern, D. W., 2002, *Applied Multivariate Statistical Analysis*, 5th Edition, Prentice Hall, Inc., New Jersey.
17. Leelataviwat, S., Goel, S. C., and Stojadinovic, B., 2002, *Energy-based Seismic Design of Structures using Yield Mechanism and Target Drift*, Journal of Structural Engineering, ASCE, Vol. 128, No. 8.

18. Luco, N., 2002, *Probabilistic seismic demand analysis, SMRF Connection Fractures, and Near-Source Effects, Ph. D. Thesis*, Department of Civil and Environmental Engineering, Stanford University, California.
19. Luco, N., Mai, P. M., Cornell, C. A., Beroza, G.C., 2002, *Probabilistic seismic demand analysis at a near-fault site using ground motion simulations based on a stochastic-kinematic earthquake source model*, Proceedings of the Seventh U.S. National Conference on Earthquake Engineering, Boston, MA.
20. Miranda, E., and H. Aslani, 2003, *Probabilistic Response Assessment for Building-Specific Loss Estimation*, Pacific Earthquake Engineering Research Center, PEER Rept. No. 2003/03.
21. Page: 97
Mollaioli, F., Bruno, S., Decanini, L., and R. Saragoni (2004). *On the Correlation Between Energy and Displacement*, Proceedings of the 13th World Conference on Earthquake Engineering, Paper 161, Vancouver, Canada, August 1-6.
22. Prakash, V., Powell, G.H., Campbell, S., 1993, *DRAIN-2DX Base Program Description and User Guide, Version 1.10*, Report No. UCB/SEMM-93/17, Department of Civil Engineering, University of California at Berkeley, California.
23. Sari, A., 2003, *Energy Considerations in Ground Motion Attenuation and Probabilistic Seismic Hazard Studies*, Ph. D. Thesis, Department of Civil Engineering, The University of Texas at Austin, Texas.
24. Sari, A., and Manuel, L., 2002, *Strength and Energy Demands from the August 1999 Kocaeli Earthquake Ground Motions*, Proceedings of the 7th U.S. National Conference on Earthquake Engineering, Boston, MA
25. Shome, N., Cornell, C. A., Bazzurro, P., Carballo, J. E., 1998, *Earthquakes, records, and non-linear responses*, Earthquake Spectra, 14(3), pp. 469-500.
26. Taghavi, S., and Miranda, E., 2003, *Response Assessment of Nonstructural Building Elements*, Pacific Earthquake Engineering Research Center, PEER Rept. No. 2003/05.
27. Tothong, P., and Cornell, C. A., 2004, *Personal Communication*.
28. Uang, C.-M., and Bertero, V. V., 1988, *Use of Energy as a Design Criterion in Earthquake-Resistant Design*, Report No: UCB/EERC-88/18, Earthquake Engineering Research Center, College of Engineering, University of California at Berkeley.
29. UBC, 1994, *Structural Engineering Design Provisions*, Uniform Building Code, Vol. 2, International Conference of Building Officials.
30. Veletsos A.S., Newmark, N.M., 1960, *Effect of Inelastic Behavior on the Response of Simple Systems to Earthquake Motions*, Proceedings of the 2nd World Conference on Earthquake Engineering, Japan, Vol. 2, pp. 895–912.
31. Veletsos A.S., Newmark, N.M., and Chelapati, C.V., 1965, *Deformation Spectra for Elastic and Elastoplastic Systems Subjected to Ground Shock and Earthquake Motions*, Proceedings of the 3rd World Conference on Earthquake Engineering, New Zealand, Vol. II, pp. 663–682.

APPENDIX A

Presented here are the results of all the regression analyses for the ductile 3-, 9-, and 20-story buildings, modeled with the RUAUMOKO program and subjected to the 140 ground motion records considered. They are organized into sections based on the structural response vector and the GMP set on which the response vector is regressed.

A.1 REGRESSIONS OF PEAK INTER-STORY DRIFT RATIOS (*IDR*'S) ON FIRST-MODE ELASTIC GMP'S

i	b_{0i}	b_{1i}	$\sigma_{ln\varepsilon}$
1	0.025	0.866	0.168
2	0.034	0.907	0.121
3	0.031	0.829	0.194

Table A.1 Regression coefficients and standard deviations of the residuals for the *IDR* response of the 3-story model regressed on $S_a(T_1)$.

ρ	1	2	3
1	1.00	0.62	0.70
2	*	1.00	0.51
3	*	*	1.00

Table A.2 Error correlation matrix for the *IDR* response of the 3-story model regressed on $S_a(T_1)$.

i	b_{0i}	b_{1i}	$\sigma_{ln\varepsilon}$
1	0.016	0.916	0.194
2	0.021	0.959	0.163
3	0.020	0.876	0.218

Table A.3 Regression coefficients and standard deviations of the residuals for the *IDR* response of the 3-story model regressed on $A_i(T_1)$.

ρ	1	2	3
1	1.00	0.74	0.77
2	*	1.00	0.65
3	*	*	1.00

Table A.4 Error correlation matrix for the *IDR* response of the 3-story model regressed on $A_i(T_1)$.

i	b_{0i}	b_{1i}	b_{2i}	$\sigma_{ln\varepsilon}$
1	0.022	0.888	0.287	0.161
2	0.030	0.928	0.274	0.112
3	0.028	0.848	0.245	0.190

Table A.5 Regression coefficients and standard deviations of the residuals for the *IDR* response of the 3-story model regressed on $S_a(T_1)$ and the ratio $A_i(T_1)/S_a(T_1)$.

ρ	1	2	3
1	1.00	0.58	0.68
2	*	1.00	0.48
3	*	*	1.00

Table A.6 Error correlation matrix for the *IDR* response of the 3-story model regressed $S_a(T_1)$ and the ratio $A_i(T_1)/S_a(T_1)$.

i	b_{0i}	b_{1i}	$\sigma_{ln\varepsilon}$
1	0.060	0.848	0.215
2	0.054	0.877	0.175
3	0.054	0.892	0.145
4	0.055	0.877	0.164
5	0.054	0.864	0.181
6	0.053	0.847	0.233
7	0.059	0.836	0.284
8	0.059	0.784	0.355
9	0.044	0.711	0.392

Table A.7 Regression coefficients and standard deviations of the residuals for the *IDR* response of the 9-story model regressed on $S_a(T_1)$.

ρ	1	2	3	4	5	6	7	8	9
1	1.00	0.93	0.74	0.63	0.75	0.84	0.80	0.80	0.77
2	*	1.00	0.82	0.59	0.65	0.74	0.75	0.73	0.67
3	*	*	1.00	0.77	0.63	0.67	0.63	0.60	0.59
4	*	*	*	1.00	0.84	0.65	0.48	0.51	0.55
5	*	*	*	*	1.00	0.84	0.65	0.68	0.70
6	*	*	*	*	*	1.00	0.91	0.88	0.86
7	*	*	*	*	*	*	1.00	0.96	0.90
8	*	*	*	*	*	*	*	1.00	0.96
9	*	*	*	*	*	*	*	*	1.00

Table A.8 Error correlation matrix for the *IDR* response of the 9-story model regressed on $S_a(T_1)$.

i	b_{0i}	b_{1i}	$\sigma_{ln\varepsilon}$
1	0.044	0.909	0.219
2	0.040	0.939	0.187
3	0.039	0.954	0.164
4	0.040	0.938	0.183
5	0.040	0.925	0.193
6	0.039	0.910	0.230
7	0.044	0.899	0.277
8	0.045	0.843	0.352
9	0.035	0.765	0.387

Table A.9 Regression coefficients and standard deviations of the residuals for the *IDR* response of the 9-story model regressed on $A_i(T_1)$.

ρ	1	2	3	4	5	6	7	8	9
1	1.00	0.93	0.75	0.66	0.76	0.84	0.79	0.79	0.75
2	*	1.00	0.84	0.65	0.69	0.74	0.72	0.70	0.63
3	*	*	1.00	0.82	0.69	0.66	0.59	0.56	0.53
4	*	*	*	1.00	0.86	0.65	0.46	0.49	0.51
5	*	*	*	*	1.00	0.83	0.63	0.66	0.66
6	*	*	*	*	*	1.00	0.90	0.87	0.85
7	*	*	*	*	*	*	1.00	0.96	0.89
8	*	*	*	*	*	*	*	1.00	0.96
9	*	*	*	*	*	*	*	*	1.00

Table A.10 Error correlation matrix for the *IDR* response of the 9-story model regressed on $A_i(T_1)$.

i	b_{0i}	b_{1i}	b_{2i}	$\sigma_{ln\varepsilon}$
1	0.053	0.880	0.408	0.209
2	0.049	0.905	0.347	0.168
3	0.049	0.917	0.321	0.139
4	0.050	0.900	0.291	0.160
5	0.049	0.891	0.335	0.175
6	0.046	0.885	0.492	0.223
7	0.050	0.879	0.553	0.274
8	0.051	0.823	0.496	0.350
9	0.038	0.750	0.509	0.387

Table A.11 Regression coefficients and standard deviations of the residuals for the *IDR* response of the 9-story model regressed on $S_a(T_1)$ and the ratio $A_i(T_1)/S_a(T_1)$.

ρ	1	2	3	4	5	6	7	8	9
1	1.00	0.93	0.72	0.61	0.73	0.82	0.79	0.79	0.76
2	*	1.00	0.80	0.56	0.62	0.72	0.73	0.72	0.66
3	*	*	1.00	0.76	0.60	0.64	0.59	0.58	0.57
4	*	*	*	1.00	0.83	0.63	0.44	0.49	0.53
5	*	*	*	*	1.00	0.83	0.63	0.67	0.69
6	*	*	*	*	*	1.00	0.90	0.88	0.86
7	*	*	*	*	*	*	1.00	0.96	0.90
8	*	*	*	*	*	*	*	1.00	0.96
9	*	*	*	*	*	*	*	*	1.00

Table A.12 Error correlation matrix for the *IDR* response of the 9-story model regressed on $S_a(T_1)$ and the ratio $A_i(T_1)/S_a(T_1)$.

i	b_{0i}	b_{1i}	$\sigma_{ln\varepsilon}$
1	0.052	0.733	0.340
2	0.071	0.772	0.329
3	0.070	0.791	0.304
4	0.068	0.800	0.276
5	0.066	0.809	0.257
6	0.063	0.805	0.245
7	0.062	0.808	0.245
8	0.061	0.806	0.246
9	0.058	0.786	0.252
10	0.055	0.763	0.254
11	0.055	0.744	0.282
12	0.056	0.730	0.309
13	0.054	0.717	0.332
14	0.052	0.701	0.355
15	0.049	0.673	0.389
16	0.044	0.648	0.415
17	0.041	0.624	0.441
18	0.039	0.602	0.474
19	0.035	0.571	0.497
20	0.030	0.543	0.501

Table A.13 Regression coefficients and standard deviations of the residuals for the *IDR* response of the 20-story model regressed on $S_a(T_1)$.

	1	2	3	4	5	6	7	8	9	10	11	12	13	14	15	16	17	18	19	20
1	1.00	0.99	0.96	0.92	0.87	0.85	0.83	0.84	0.86	0.86	0.82	0.77	0.75	0.71	0.70	0.72	0.73	0.75	0.79	0.83
2	*	1.00	0.99	0.95	0.91	0.89	0.86	0.87	0.89	0.87	0.83	0.78	0.74	0.70	0.70	0.75	0.76	0.78	0.83	0.86
3	*	*	1.00	0.99	0.95	0.93	0.90	0.90	0.90	0.88	0.84	0.77	0.72	0.68	0.70	0.76	0.78	0.81	0.85	0.88
4	*	*	*	1.00	0.98	0.96	0.92	0.91	0.90	0.88	0.84	0.76	0.69	0.65	0.70	0.77	0.79	0.82	0.86	0.89
5	*	*	*	*	1.00	0.99	0.95	0.93	0.91	0.88	0.82	0.73	0.66	0.63	0.69	0.76	0.78	0.82	0.85	0.88
6	*	*	*	*	*	1.00	0.98	0.95	0.92	0.88	0.80	0.71	0.64	0.61	0.67	0.74	0.77	0.81	0.84	0.86
7	*	*	*	*	*	*	1.00	0.99	0.95	0.89	0.80	0.69	0.61	0.58	0.65	0.74	0.77	0.81	0.84	0.85
8	*	*	*	*	*	*	*	1.00	0.98	0.94	0.85	0.73	0.65	0.61	0.67	0.75	0.78	0.81	0.84	0.86
9	*	*	*	*	*	*	*	*	1.00	0.98	0.90	0.80	0.72	0.67	0.71	0.77	0.79	0.82	0.84	0.86
10	*	*	*	*	*	*	*	*	*	1.00	0.96	0.87	0.79	0.73	0.77	0.80	0.81	0.82	0.85	0.86
11	*	*	*	*	*	*	*	*	*	*	1.00	0.95	0.87	0.79	0.79	0.80	0.81	0.81	0.82	0.84
12	*	*	*	*	*	*	*	*	*	*	*	1.00	0.96	0.88	0.82	0.78	0.77	0.76	0.76	0.78
13	*	*	*	*	*	*	*	*	*	*	*	*	1.00	0.95	0.88	0.79	0.75	0.72	0.72	0.74
14	*	*	*	*	*	*	*	*	*	*	*	*	*	1.00	0.94	0.82	0.75	0.70	0.70	0.72
15	*	*	*	*	*	*	*	*	*	*	*	*	*	*	1.00	0.94	0.87	0.81	0.79	0.80
16	*	*	*	*	*	*	*	*	*	*	*	*	*	*	*	1.00	0.97	0.92	0.88	0.88
17	*	*	*	*	*	*	*	*	*	*	*	*	*	*	*	*	1.00	0.98	0.94	0.92
18	*	*	*	*	*	*	*	*	*	*	*	*	*	*	*	*	*	1.00	0.98	0.96
19	*	*	*	*	*	*	*	*	*	*	*	*	*	*	*	*	*	*	1.00	0.99
20	*	*	*	*	*	*	*	*	*	*	*	*	*	*	*	*	*	*	*	1.00

Table A.14 Error correlation matrix for the *IDR* response of the 20-story model regressed on $S_a(T_1)$.

i	b_{0i}	b_{1i}	$\sigma_{ln\varepsilon}$
1	0.043	0.780	0.312
2	0.057	0.819	0.301
3	0.056	0.839	0.274
4	0.054	0.848	0.246
5	0.052	0.855	0.232
6	0.049	0.850	0.226
7	0.049	0.853	0.225
8	0.048	0.851	0.224
9	0.046	0.831	0.229
10	0.044	0.806	0.233
11	0.045	0.787	0.260
12	0.045	0.773	0.287
13	0.044	0.760	0.310
14	0.043	0.744	0.333
15	0.041	0.718	0.365
16	0.037	0.692	0.391
17	0.035	0.668	0.417
18	0.034	0.646	0.451
19	0.031	0.614	0.475
20	0.026	0.583	0.483

Table A.15 Regression coefficients and standard deviations of the residuals for the *IDR* response of the 20-story model regressed on $A_i(T_1)$.

	1	2	3	4	5	6	7	8	9	10	11	12	13	14	15	16	17	18	19	20
1	1.00	0.99	0.95	0.91	0.86	0.84	0.81	0.82	0.84	0.83	0.78	0.73	0.70	0.65	0.64	0.68	0.69	0.72	0.77	0.82
2	*	1.00	0.98	0.95	0.90	0.87	0.84	0.85	0.86	0.84	0.79	0.73	0.68	0.62	0.63	0.69	0.72	0.75	0.80	0.85
3	*	*	1.00	0.98	0.95	0.92	0.88	0.88	0.88	0.85	0.79	0.72	0.65	0.60	0.63	0.70	0.74	0.78	0.83	0.86
4	*	*	*	1.00	0.98	0.95	0.91	0.90	0.88	0.85	0.79	0.70	0.62	0.58	0.63	0.71	0.75	0.80	0.84	0.87
5	*	*	*	*	1.00	0.99	0.94	0.91	0.89	0.85	0.78	0.67	0.58	0.54	0.61	0.70	0.74	0.78	0.83	0.86
6	*	*	*	*	*	1.00	0.97	0.94	0.91	0.85	0.76	0.65	0.56	0.53	0.60	0.69	0.73	0.78	0.82	0.84
7	*	*	*	*	*	*	1.00	0.98	0.94	0.87	0.77	0.63	0.54	0.50	0.58	0.69	0.73	0.78	0.81	0.83
8	*	*	*	*	*	*	*	1.00	0.98	0.92	0.82	0.68	0.59	0.53	0.61	0.70	0.74	0.78	0.81	0.83
9	*	*	*	*	*	*	*	*	1.00	0.98	0.88	0.76	0.67	0.61	0.66	0.72	0.76	0.78	0.82	0.84
10	*	*	*	*	*	*	*	*	*	1.00	0.95	0.85	0.75	0.68	0.72	0.76	0.78	0.79	0.82	0.84
11	*	*	*	*	*	*	*	*	*	*	1.00	0.94	0.84	0.75	0.76	0.76	0.76	0.76	0.78	0.80
12	*	*	*	*	*	*	*	*	*	*	*	1.00	0.95	0.85	0.79	0.73	0.71	0.70	0.70	0.73
13	*	*	*	*	*	*	*	*	*	*	*	*	1.00	0.95	0.85	0.74	0.68	0.65	0.65	0.68
14	*	*	*	*	*	*	*	*	*	*	*	*	*	1.00	0.93	0.78	0.69	0.63	0.63	0.65
15	*	*	*	*	*	*	*	*	*	*	*	*	*	*	1.00	0.92	0.83	0.76	0.74	0.75
16	*	*	*	*	*	*	*	*	*	*	*	*	*	*	*	1.00	0.96	0.89	0.86	0.84
17	*	*	*	*	*	*	*	*	*	*	*	*	*	*	*	*	1.00	0.97	0.93	0.91
18	*	*	*	*	*	*	*	*	*	*	*	*	*	*	*	*	*	1.00	0.98	0.95
19	*	*	*	*	*	*	*	*	*	*	*	*	*	*	*	*	*	*	1.00	0.99
20	*	*	*	*	*	*	*	*	*	*	*	*	*	*	*	*	*	*	*	1.00

Table A.16 Error correlation matrix for the *IDR* response of the 20-story model regressed on $A_i(T_1)$.

i	b_{0i}	b_{1i}	b_{2i}	$\sigma_{ln\varepsilon}$
1	0.054	0.842	0.934	0.274
2	0.053	0.849	0.888	0.247
3	0.053	0.852	0.786	0.233
4	0.052	0.844	0.695	0.226
5	0.051	0.848	0.710	0.225
6	0.050	0.846	0.728	0.224
7	0.047	0.828	0.752	0.229
8	0.045	0.803	0.718	0.234
9	0.045	0.785	0.757	0.261
10	0.045	0.775	0.815	0.288
11	0.042	0.764	0.848	0.311
12	0.041	0.750	0.887	0.334
13	0.038	0.728	0.984	0.365
14	0.033	0.705	1.046	0.389
15	0.031	0.684	1.082	0.415
16	0.028	0.665	1.144	0.447
17	0.026	0.635	1.157	0.471
18	0.022	0.602	1.076	0.480
19	0.054	0.842	0.934	0.274
20	0.053	0.849	0.888	0.247

Table A.17 Regression coefficients and standard deviations of the residuals for the *IDR* response of the 20-story model regressed on $S_a(T_1)$ and the ratio $A_i(T_1)/S_a(T_1)$.

	1	2	3	4	5	6	7	8	9	10	11	12	13	14	15	16	17	18	19	20
1	1.00	0.99	0.95	0.91	0.86	0.84	0.81	0.83	0.85	0.84	0.80	0.75	0.72	0.67	0.67	0.69	0.69	0.72	0.77	0.82
2	*	1.00	0.98	0.95	0.90	0.87	0.84	0.86	0.87	0.86	0.81	0.75	0.70	0.65	0.66	0.71	0.72	0.75	0.80	0.85
3	*	*	1.00	0.98	0.95	0.92	0.88	0.88	0.89	0.87	0.81	0.74	0.68	0.63	0.66	0.72	0.74	0.78	0.83	0.86
4	*	*	*	1.00	0.98	0.95	0.91	0.90	0.89	0.87	0.81	0.72	0.64	0.60	0.66	0.73	0.76	0.80	0.84	0.87
5	*	*	*	*	1.00	0.99	0.94	0.92	0.90	0.86	0.79	0.68	0.60	0.56	0.64	0.72	0.74	0.79	0.83	0.86
6	*	*	*	*	*	1.00	0.97	0.94	0.91	0.86	0.77	0.66	0.58	0.54	0.62	0.70	0.73	0.78	0.82	0.84
7	*	*	*	*	*	*	1.00	0.98	0.94	0.88	0.77	0.64	0.55	0.51	0.59	0.69	0.73	0.78	0.81	0.83
8	*	*	*	*	*	*	*	1.00	0.98	0.93	0.82	0.68	0.59	0.54	0.61	0.70	0.74	0.78	0.81	0.83
9	*	*	*	*	*	*	*	*	1.00	0.98	0.89	0.76	0.67	0.61	0.66	0.73	0.76	0.78	0.82	0.84
10	*	*	*	*	*	*	*	*	*	1.00	0.95	0.85	0.75	0.68	0.72	0.76	0.78	0.79	0.82	0.84
11	*	*	*	*	*	*	*	*	*	*	1.00	0.94	0.84	0.75	0.76	0.76	0.76	0.77	0.79	0.81
12	*	*	*	*	*	*	*	*	*	*	*	1.00	0.95	0.85	0.79	0.73	0.71	0.70	0.71	0.74
13	*	*	*	*	*	*	*	*	*	*	*	*	1.00	0.95	0.85	0.74	0.69	0.65	0.66	0.69
14	*	*	*	*	*	*	*	*	*	*	*	*	*	1.00	0.93	0.78	0.69	0.64	0.64	0.67
15	*	*	*	*	*	*	*	*	*	*	*	*	*	*	1.00	0.93	0.84	0.77	0.75	0.76
16	*	*	*	*	*	*	*	*	*	*	*	*	*	*	*	1.00	0.96	0.90	0.86	0.85
17	*	*	*	*	*	*	*	*	*	*	*	*	*	*	*	*	1.00	0.97	0.93	0.91
18	*	*	*	*	*	*	*	*	*	*	*	*	*	*	*	*	*	1.00	0.98	0.95
19	*	*	*	*	*	*	*	*	*	*	*	*	*	*	*	*	*	*	1.00	0.99
20	*	*	*	*	*	*	*	*	*	*	*	*	*	*	*	*	*	*	*	1.00

Table A.18 Error correlation matrix for the *IDR* response of the 20-story model regressed on $S_a(T_1)$ and ratio $A_i(T_1)/S_a(T_1)$.

A.2 REGRESSIONS OF {MIDR, AIDR, RDR} ON FIRST-MODE ELASTIC GMP'S

i	b_{0i}	b_{1i}	$\sigma_{ln\varepsilon}$
MIDR	0.034	0.850	0.175
AIDR	0.030	0.864	0.144
RDR	0.030	0.909	0.129

Table A.19 Regression coefficients and standard deviations of the residuals for the 3-story model responses regressed on $S_a(T_1)$.

ρ	MIDR	AIDR	RDR
MIDR	1.00	0.96	0.66
AIDR	*	1.00	0.76
RDR	*	*	1.00

Table A.20 Error correlation matrix for the 3-story model responses regressed on $S_a(T_1)$.

i	b_{0i}	b_{1i}	$\sigma_{ln\varepsilon}$
MIDR	0.022	0.898	0.203
AIDR	0.019	0.914	0.176
RDR	0.019	0.962	0.163

Table A.21 Regression coefficients and standard deviations of the residuals for the 3-story model responses regressed on $A_i(T_1)$.

ρ	MIDR	AIDR	RDR
MIDR	1.00	0.97	0.76
AIDR	*	1.00	0.85
RDR	*	*	1.00

Table A.22 Error correlation matrix for the 3-story model responses regressed on $A_i(T_1)$.

i	b_{0i}	b_{1i}	b_{2i}	$\sigma_{ln\varepsilon}$
MIDR	0.030	0.870	0.252	0.170
AIDR	0.027	0.886	0.270	0.137
RDR	0.026	0.933	0.311	0.118

Table A.23 Regression coefficients and standard deviations of the residuals for the 3-story model responses regressed on $S_a(T_1)$ and the ratio $A_i(T_1)/S_a(T_1)$.

ρ	MIDR	AIDR	RDR
MIDR	1.00	0.96	0.63
AIDR	*	1.00	0.73
RDR	*	*	1.00

Table A.24 Error correlation matrix for the 3-story model responses regressed $S_a(T_1)$ and the ratio $A_i(T_1)/S_a(T_1)$.

i	b_{0i}	b_{1i}	$\sigma_{ln\varepsilon}$
MIDR	0.064	0.796	0.336
AIDR	0.055	0.832	0.228
RDR	0.047	0.922	0.133

Table A.25 Regression coefficients and standard deviations of the residuals for the 9-story model responses regressed on $S_a(T_1)$.

ρ	MIDR	AIDR	RDR
MIDR	1.00	0.97	0.47
AIDR	*	1.00	0.57
RDR	*	*	1.00

Table A.26 Error correlation matrix for the 9-story model responses regressed on $S_a(T_1)$.

i	b_{0i}	b_{1i}	$\sigma_{ln\varepsilon}$
MIDR	0.049	0.857	0.332
AIDR	0.041	0.893	0.229
RDR	0.035	0.988	0.143

Table A.27 Regression coefficients and standard deviations of the residuals for the 9-story model responses regressed on $A_i(T_1)$.

ρ	MIDR	AIDR	RDR
MIDR	1.00	0.96	0.43
AIDR	*	1.00	0.57
RDR	*	*	1.00

Table A.28 Error correlation matrix for the 9-story model responses regressed on $A_i(T_1)$.

i	b_{0i}	b_{1i}	b_{2i}	$\sigma_{ln\varepsilon}$
MIDR	0.055	0.837	0.525	0.329
AIDR	0.048	0.866	0.431	0.221
RDR	0.042	0.956	0.429	0.120

Table A.29 Regression coefficients and standard deviations of the residuals for the 9-story model responses regressed on $S_a(T_1)$ and the ratio $A_i(T_1)/S_a(T_1)$.

ρ	MIDR	AIDR	RDR
MIDR	1.00	0.97	0.43
AIDR	*	1.00	0.52
RDR	*	*	1.00

Table A.30 Error correlation matrix for the 9-story model responses regressed on $S_a(T_1)$ and the ratio $A_i(T_1)/S_a(T_1)$.

i	b_{0i}	b_{1i}	$\sigma_{ln\varepsilon}$
MIDR	0.068	0.705	0.414
AIDR	0.050	0.719	0.320
RDR	0.053	0.842	0.177

Table A.31 Regression coefficients and standard deviations of the residuals for the 20-story model responses regressed on $S_a(T_1)$.

ρ	MIDR	AIDR	RDR
MIDR	1.00	0.97	0.49
AIDR	*	1.00	0.61
RDR	*	*	1.00

Table A.32 Error correlation matrix for the 20-story model responses regressed on $S_a(T_1)$.

i	b_{0i}	b_{1i}	$\sigma_{ln\varepsilon}$
MIDR	0.056	0.751	0.390
AIDR	0.040	0.764	0.293
RDR	0.041	0.886	0.162

Table A.33 Regression coefficients and standard deviations of the residuals for the 20-story model responses regressed on $A_i(T_1)$.

ρ	MIDR	AIDR	RDR
MIDR	1.00	0.97	0.36
AIDR	*	1.00	0.48
RDR	*	*	1.00

Table A.34 Error correlation matrix for the 20-story model responses regressed on $A_i(T_1)$.

i	b_{0i}	b_{1i}	b_{2i}	$\sigma_{ln\varepsilon}$
MIDR	0.052	0.761	1.019	0.390
AIDR	0.039	0.770	0.915	0.293
RDR	0.045	0.874	0.584	0.157

Table A.35 Regression coefficients and standard deviations of the residuals for the 20-story model responses regressed on $S_a(T_1)$ and the ratio $A_i(T_1)/S_a(T_1)$.

ρ	MIDR	AIDR	RDR
MIDR	1.00	0.97	0.40
AIDR	*	1.00	0.52
RDR	*	*	1.00

Table A.36 Error correlation matrix for the 20-story model responses regressed on $S_a(T_1)$ and the ratio $A_i(T_1)/S_a(T_1)$.

A.3 REGRESSIONS OF PEAK INTER-STORY DRIFT RATIOS (*IDR*'S) ON MULTI-MODE ELASTIC GMP'S

i	b_{0i}	b_{1i}	b_{2i}	$\sigma_{ln\varepsilon}$
1	0.024	0.911	0.142	0.152
2	0.034	0.914	0.022	0.121
3	0.030	0.905	0.239	0.151

Table A.37 Regression coefficients and standard deviations of the residuals for the *IDR* response of the 3-story model regressed on $S_a(T_1)$ and the ratio $S_a(T_2)/S_a(T_1)$.

ρ	1	2	3
1	1.00	0.65	0.61
2	*	1.00	0.59
3	*	*	1.00

Table A.38 Error correlation matrix for the *IDR* response of the 3-story model regressed on $S_a(T_1)$ and the ratio $S_a(T_2)/S_a(T_1)$.

i	b_{0i}	b_{1i}	b_{2i}	$\sigma_{ln\varepsilon}$
1	0.014	0.965	0.173	0.179
2	0.021	0.964	0.017	0.163
3	0.017	0.951	0.266	0.186

Table A.39 Regression coefficients and standard deviations of the residuals for the *IDR* response of the 3-story model regressed on $A_i(T_1)$ and the ratio $A_i(T_2)/A_i(T_1)$.

ρ	1	2	3
1	1.00	0.78	0.72
2	*	1.00	0.74
3	*	*	1.00

Table A.40 Error correlation matrix for the *IDR* response of the 3-story model regressed on $A_i(T_1)$ and the ratio $A_i(T_2)/A_i(T_1)$.

i	b_{0i}	b_{1i}	b_{2i}	$\sigma_{ln\varepsilon}$
1	0.053	0.908	0.235	0.167
2	0.050	0.919	0.165	0.146
3	0.051	0.918	0.100	0.133
4	0.052	0.899	0.088	0.156
5	0.050	0.903	0.153	0.158
6	0.045	0.919	0.285	0.164
7	0.048	0.937	0.399	0.163
8	0.045	0.919	0.528	0.176
9	0.033	0.858	0.577	0.201

Table A.41 Regression coefficients and standard deviations of the residuals for the *IDR* response of the 9-story model regressed on $S_a(T_1)$ and the ratio $S_a(T_2)/S_a(T_1)$.

ρ	1	2	3	4	5	6	7	8	9
1	1.00	0.90	0.68	0.59	0.65	0.71	0.64	0.65	0.56
2	*	1.00	0.78	0.53	0.52	0.60	0.62	0.61	0.47
3	*	*	1.00	0.74	0.54	0.59	0.57	0.55	0.52
4	*	*	*	1.00	0.83	0.64	0.41	0.51	0.59
5	*	*	*	*	1.00	0.80	0.50	0.59	0.62
6	*	*	*	*	*	1.00	0.81	0.74	0.70
7	*	*	*	*	*	*	1.00	0.87	0.65
8	*	*	*	*	*	*	*	1.00	0.85
9	*	*	*	*	*	*	*	*	1.00

Table A.42 Error correlation matrix for the *IDR* response of the 9-story model regressed on $S_a(T_1)$ and the ratio $S_a(T_2)/S_a(T_1)$.

i	b_{0i}	b_{1i}	b_{2i}	$\sigma_{ln\varepsilon}$
1	0.036	0.963	0.261	0.178
2	0.034	0.976	0.179	0.165
3	0.036	0.976	0.104	0.157
4	0.037	0.955	0.082	0.179
5	0.035	0.958	0.160	0.177
6	0.030	0.976	0.323	0.166
7	0.030	0.994	0.461	0.159
8	0.027	0.969	0.610	0.182
9	0.020	0.903	0.669	0.202

Table A.43 Regression coefficients and standard deviation of the residuals for the *IDR* response of the 9-story model regressed on $A_i(T_1)$ and the ratio $A_i(T_2)/A_i(T_1)$.

	1	2	3	4	5	6	7	8	9
1	1.00	0.91	0.73	0.67	0.71	0.74	0.67	0.68	0.58
2	*	1.00	0.83	0.64	0.62	0.64	0.66	0.64	0.49
3	*	*	1.00	0.81	0.65	0.64	0.61	0.59	0.53
4	*	*	*	1.00	0.87	0.71	0.50	0.59	0.63
5	*	*	*	*	1.00	0.84	0.57	0.65	0.65
6	*	*	*	*	*	1.00	0.81	0.75	0.69
7	*	*	*	*	*	*	1.00	0.87	0.65
8	*	*	*	*	*	*	*	1.00	0.85
9	*	*	*	*	*	*	*	*	1.00

Table A.44 Error correlation matrix for the *IDR* response of the 9-story model regressed on $A_i(T_1)$ and the ratio $A_i(T_2)/A_i(T_1)$.

i	b_{0i}	b_{1i}	b_{2i}	$\sigma_{ln\varepsilon}$
1	0.047	0.886	0.395	0.223
2	0.064	0.913	0.367	0.227
3	0.064	0.912	0.314	0.225
4	0.063	0.904	0.269	0.214
5	0.062	0.900	0.237	0.207
6	0.059	0.880	0.195	0.211
7	0.059	0.876	0.175	0.218
8	0.058	0.881	0.194	0.212
9	0.054	0.875	0.229	0.204
10	0.051	0.870	0.278	0.179
11	0.050	0.876	0.344	0.171
12	0.050	0.883	0.398	0.169
13	0.048	0.886	0.439	0.170
14	0.046	0.885	0.478	0.172
15	0.043	0.879	0.535	0.174
16	0.038	0.870	0.576	0.179
17	0.035	0.859	0.610	0.192
18	0.033	0.853	0.649	0.214
19	0.030	0.828	0.665	0.243
20	0.025	0.794	0.653	0.267

Table A.45 Regression coefficients and standard deviations of the residuals for the *IDR* response of the 20-story model regressed on $S_a(T_1)$ and the ratio $S_a(T_2)/S_a(T_1)$.

	1	2	3	4	5	6	7	8	9	10	11	12	13	14	15	16	17	18	19	20
1	1.00	0.95	0.83	0.66	0.47	0.40	0.33	0.42	0.53	0.57	0.58	0.64	0.68	0.66	0.58	0.51	0.46	0.45	0.49	0.55
2	*	1.00	0.94	0.79	0.59	0.49	0.41	0.49	0.58	0.61	0.62	0.67	0.70	0.67	0.60	0.57	0.54	0.53	0.58	0.64
3	*	*	1.00	0.92	0.75	0.64	0.53	0.56	0.62	0.64	0.64	0.67	0.68	0.66	0.63	0.62	0.61	0.61	0.65	0.70
4	*	*	*	1.00	0.91	0.79	0.65	0.62	0.63	0.63	0.64	0.64	0.61	0.61	0.64	0.65	0.65	0.67	0.70	0.72
5	*	*	*	*	1.00	0.93	0.76	0.69	0.65	0.62	0.59	0.56	0.53	0.54	0.60	0.62	0.63	0.65	0.67	0.69
6	*	*	*	*	*	1.00	0.90	0.80	0.71	0.62	0.53	0.49	0.46	0.49	0.54	0.58	0.60	0.63	0.63	0.64
7	*	*	*	*	*	*	1.00	0.94	0.81	0.67	0.53	0.44	0.40	0.40	0.47	0.54	0.58	0.61	0.60	0.60
8	*	*	*	*	*	*	*	1.00	0.94	0.81	0.65	0.54	0.48	0.46	0.51	0.56	0.60	0.61	0.62	0.62
9	*	*	*	*	*	*	*	*	1.00	0.94	0.80	0.69	0.63	0.58	0.60	0.61	0.62	0.62	0.63	0.65
10	*	*	*	*	*	*	*	*	*	1.00	0.93	0.82	0.74	0.68	0.68	0.66	0.66	0.64	0.64	0.66
11	*	*	*	*	*	*	*	*	*	*	1.00	0.93	0.83	0.74	0.71	0.66	0.65	0.63	0.63	0.65
12	*	*	*	*	*	*	*	*	*	*	*	1.00	0.95	0.84	0.75	0.66	0.63	0.60	0.59	0.63
13	*	*	*	*	*	*	*	*	*	*	*	*	1.00	0.94	0.83	0.70	0.63	0.58	0.58	0.63
14	*	*	*	*	*	*	*	*	*	*	*	*	*	1.00	0.92	0.77	0.66	0.60	0.59	0.64
15	*	*	*	*	*	*	*	*	*	*	*	*	*	*	1.00	0.92	0.81	0.73	0.71	0.73
16	*	*	*	*	*	*	*	*	*	*	*	*	*	*	*	1.00	0.95	0.87	0.82	0.81
17	*	*	*	*	*	*	*	*	*	*	*	*	*	*	*	*	1.00	0.96	0.91	0.88
18	*	*	*	*	*	*	*	*	*	*	*	*	*	*	*	*	*	1.00	0.97	0.93
19	*	*	*	*	*	*	*	*	*	*	*	*	*	*	*	*	*	*	1.00	0.98
20	*	*	*	*	*	*	*	*	*	*	*	*	*	*	*	*	*	*	*	1.00

Table A.46 Error correlation matrix for the *IDR* response of the 20-story model regressed on $S_a(T_1)$ and ratio $S_a(T_2)/S_a(T_1)$.

i	b_{0i}	b_{1i}	b_{2i}	$\sigma_{ln\varepsilon}$
1	0.034	0.923	0.393	0.211
2	0.046	0.953	0.364	0.213
3	0.046	0.951	0.306	0.207
4	0.046	0.941	0.254	0.197
5	0.046	0.933	0.214	0.196
6	0.045	0.908	0.160	0.206
7	0.045	0.901	0.131	0.212
8	0.044	0.905	0.147	0.207
9	0.041	0.899	0.186	0.202
10	0.038	0.896	0.246	0.184
11	0.037	0.905	0.323	0.179
12	0.036	0.915	0.389	0.175
13	0.034	0.923	0.444	0.169
14	0.032	0.924	0.493	0.166
15	0.030	0.920	0.553	0.168
16	0.026	0.910	0.596	0.175
17	0.024	0.899	0.631	0.192
18	0.022	0.891	0.668	0.222
19	0.021	0.864	0.683	0.256
20	0.017	0.826	0.664	0.286

Table A.47 Regression coefficients and standard deviations of the residuals for the *IDR* response of the 20-story model regressed on $A_i(T_1)$ and the ratio $A_i(T_2)/A_i(T_1)$.

	1	2	3	4	5	6	7	8	9	10	11	12	13	14	15	16	17	18	19	20
1	1.00	0.96	0.86	0.71	0.53	0.44	0.36	0.45	0.56	0.60	0.60	0.67	0.70	0.67	0.57	0.48	0.43	0.42	0.47	0.55
2	*	1.00	0.94	0.81	0.61	0.50	0.40	0.48	0.59	0.62	0.63	0.70	0.71	0.67	0.58	0.52	0.48	0.48	0.54	0.61
3	*	*	1.00	0.93	0.76	0.64	0.51	0.55	0.62	0.65	0.66	0.71	0.70	0.66	0.61	0.56	0.54	0.55	0.60	0.66
4	*	*	*	1.00	0.91	0.78	0.61	0.60	0.64	0.66	0.67	0.69	0.66	0.63	0.63	0.60	0.58	0.61	0.65	0.69
5	*	*	*	*	1.00	0.93	0.73	0.67	0.66	0.65	0.63	0.62	0.57	0.57	0.60	0.58	0.56	0.59	0.62	0.65
6	*	*	*	*	*	1.00	0.89	0.79	0.72	0.66	0.59	0.56	0.52	0.52	0.56	0.55	0.53	0.57	0.58	0.61
7	*	*	*	*	*	*	1.00	0.94	0.83	0.71	0.59	0.50	0.45	0.43	0.49	0.52	0.53	0.55	0.56	0.56
8	*	*	*	*	*	*	*	1.00	0.95	0.84	0.70	0.59	0.53	0.48	0.52	0.54	0.54	0.56	0.57	0.58
9	*	*	*	*	*	*	*	*	1.00	0.95	0.82	0.71	0.65	0.59	0.60	0.58	0.57	0.57	0.59	0.62
10	*	*	*	*	*	*	*	*	*	1.00	0.93	0.83	0.75	0.67	0.67	0.63	0.62	0.60	0.62	0.64
11	*	*	*	*	*	*	*	*	*	*	1.00	0.94	0.83	0.73	0.70	0.64	0.62	0.60	0.61	0.64
12	*	*	*	*	*	*	*	*	*	*	*	1.00	0.94	0.83	0.74	0.64	0.60	0.58	0.59	0.63
13	*	*	*	*	*	*	*	*	*	*	*	*	1.00	0.94	0.82	0.69	0.61	0.56	0.58	0.63
14	*	*	*	*	*	*	*	*	*	*	*	*	*	1.00	0.92	0.76	0.64	0.58	0.58	0.63
15	*	*	*	*	*	*	*	*	*	*	*	*	*	*	1.00	0.92	0.80	0.72	0.69	0.72
16	*	*	*	*	*	*	*	*	*	*	*	*	*	*	*	1.00	0.94	0.85	0.80	0.78
17	*	*	*	*	*	*	*	*	*	*	*	*	*	*	*	*	1.00	0.95	0.89	0.86
18	*	*	*	*	*	*	*	*	*	*	*	*	*	*	*	*	*	1.00	0.97	0.92
19	*	*	*	*	*	*	*	*	*	*	*	*	*	*	*	*	*	*	1.00	0.98
20	*	*	*	*	*	*	*	*	*	*	*	*	*	*	*	*	*	*	*	1.00

Table A.48 Error correlation matrix for the *IDR* response of the 20-story model regressed on $A_i(T_1)$ and ratio $A_i(T_2)/A_i(T_1)$.

A.4 REGRESSIONS OF (MIDR, AIDR, RDR) ON MULTI-MODE ELASTIC GMP'S

i	b_{0i}	b_{1i}	b_{2i}	$\sigma_{ln\varepsilon}$
MIDR	0.032	0.908	0.184	0.148
AIDR	0.029	0.909	0.141	0.125
RDR	0.030	0.915	0.021	0.129

Table A.49 Regression coefficients and standard deviations of the residuals for the 3-story model responses regressed on $S_a(T_1)$ and the ratio $S_a(T_2)/S_a(T_1)$.

ρ	MIDR	AIDR	RDR
MIDR	1.00	0.95	0.73
AIDR	*	1.00	0.83
RDR	*	*	1.00

Table A.50 Error correlation matrix for the 3-story model responses regressed on $S_a(T_1)$ and the ratio $S_a(T_2)/S_a(T_1)$.

i	b_{0i}	b_{1i}	b_{2i}	$\sigma_{ln\varepsilon}$
MIDR	0.019	0.956	0.203	0.184
AIDR	0.017	0.960	0.161	0.163
RDR	0.018	0.966	0.014	0.163

Table A.51 Regression coefficients and standard deviations of the residuals for the 3-story model responses regressed on $A_i(T_1)$ and the ratio $A_i(T_2)/A_i(T_1)$.

ρ	MIDR	AIDR	RDR
MIDR	1.00	0.96	0.83
AIDR	*	1.00	0.91
RDR	*	*	1.00

Table A.52 Error correlation matrix for the 3-story model responses regressed on $A_i(T_1)$ and the ratio $A_i(T_2)/A_i(T_1)$.

i	b_{0i}	b_{1i}	b_{2i}	$\sigma_{ln\varepsilon}$
MIDR	0.050	0.917	0.474	0.191
AIDR	0.047	0.910	0.307	0.141
RDR	0.046	0.936	0.053	0.130

Table A.53 Regression coefficients and standard deviations of the residuals for the 9-story model responses regressed on $S_a(T_1)$ and the ratio $S_a(T_2)/S_a(T_1)$.

ρ	MIDR	AIDR	RDR
MIDR	1.00	0.93	0.51
AIDR	*	1.00	0.64
RDR	*	*	1.00

Table A.54 Error correlation matrix for the 9-story model responses regressed on $S_a(T_1)$ and the ratio $S_a(T_2)/S_a(T_1)$.

i	b_{0i}	b_{1i}	b_{2i}	$\sigma_{ln\varepsilon}$
MIDR	0.031	0.968	0.544	0.195
AIDR	0.031	0.964	0.348	0.153
RDR	0.033	0.998	0.045	0.141

Table A.55 Regression coefficients and standard deviation of the residuals for the 9-story model responses regressed on $A_i(T_1)$ and the ratio $A_i(T_2)/A_i(T_1)$.

ρ	MIDR	AIDR	RDR
MIDR	1.00	0.92	0.53
AIDR	*	1.00	0.70
RDR	*	*	1.00

Table A.56 Error correlation matrix for the 9-story model responses regressed on $A_i(T_1)$ and the ratio $A_i(T_2)/A_i(T_1)$.

i	b_{0i}	b_{1i}	b_{2i}	$\sigma_{ln\varepsilon}$
MIDR	0.059	0.907	0.522	0.237
AIDR	0.044	0.879	0.413	0.173
RDR	0.052	0.880	0.099	0.165

Table A.57 Regression coefficients and standard deviations of the residuals for the 20-story model responses regressed on $S_a(T_1)$ and the ratio $S_a(T_2)/S_a(T_1)$.

ρ	MIDR	AIDR	RDR
MIDR	1.00	0.90	0.36
AIDR	*	1.00	0.61
RDR	*	*	1.00

Table A.58 Error correlation matrix for the 20-story model responses regressed on $S_a(T_1)$ and the ratio $S_a(T_2)/S_a(T_1)$.

i	b_{0i}	b_{1i}	b_{2i}	$\sigma_{ln\varepsilon}$
MIDR	0.041	0.941	0.519	0.245
AIDR	0.032	0.913	0.407	0.170
RDR	0.040	0.907	0.056	0.160

Table A.59 Regression coefficients and standard deviations of the residuals for the 20-story model responses regressed on $A_i(T_1)$ and the ratio $A_i(T_2)/A_i(T_1)$.

ρ	MIDR	AIDR	RDR
MIDR	1.00	0.91	0.32
AIDR	*	1.00	0.56
RDR	*	*	1.00

Table A.60 Error correlation matrix for the 20-story model responses regressed on $A_i(T_1)$ and the ratio $A_i(T_2)/A_i(T_1)$.

APPENDIX B

The standard deviations of the residual inter-story and roof drift ratios (*IDR*s and *RDR*s) from multivariate multiple linear regression (MMLR) analysis on (i) first-mode elastic, (ii) multi-mode elastic, and (iii) inelastic first-mode and elastic higher-mode ground motion parameters (GMPs) are listed in Tables B.1 through B.9. Also noted in the tables are the standard deviations of the *IDR*s and *RDR*s, before considering any GMP. These results are for the elastic and "weaker" ductile and brittle models (using the DRAIN-2DX program) of the 3-, 9-, and 20-story buildings, obtained by doubling the amplitude of each of the 140 records considered.

σ for 03E	No *GMP* (1)	*Sa1* (2)	*Ai1* (3)	*Sa1 Ai1/Sa1* (4)	*Sa1 Sa2/Sa1* (5)	*Sa1 Ai2/Sa1* (6)	*Sa1 Ai2/Sa2* (7)	*Sa1 SaI1/Sa1* (8)	*Sa1 AiI1/Sa1* (9)	*Sa1 AaI1/Sa1* (10)
Story 1	0.88	0.18	0.21	0.17	0.17	0.17	0.18	0.18	0.18	0.18
Story 2	0.92	0.14	0.17	0.13	0.14	0.14	0.14	0.14	0.14	0.14
Story 3	0.87	0.20	0.23	0.19	0.18	0.18	0.19	0.20	0.20	0.20
Roof	0.92	0.15	0.17	0.13	0.15	0.15	0.15	0.15	0.15	0.15

Table B.1 Standard deviations of the residual *IDR*s and *RDR* from regressions on various GMPs for the *elastic* 3-story model (0 collapses).

σ for 03D	No *GMP* (1)	*Sa1* (2)	*Ai1* (3)	*Sa1 Ai1/Sa1* (4)	*Sa1 Sa2/Sa1* (5)	*Sa1 Ai2/Sa1* (6)	*Sa1 Ai2/Sa2* (7)	*Sa1 SaI1/Sa1* (8)	*Sa1 AiI1/Sa1* (9)	*Sa1 AaI1/Sa1* (10)
Story 1	0.85	0.26	0.28	0.26	0.25	0.24	0.26	0.19	0.25	0.25
Story 2	0.84	0.20	0.22	0.19	0.20	0.19	0.20	0.14	0.18	0.18
Story 3	0.80	0.23	0.25	0.23	0.20	0.19	0.23	0.20	0.22	0.22
Roof	0.86	0.21	0.23	0.20	0.21	0.20	0.21	0.14	0.19	0.19

Table B.2 Standard deviations of the residual *IDR*s and *RDR* from regressions on various GMPs for the *ductile* 3-story model (0 collapses).

σ for 03B	No *GMP* (1)	*Sa1* (2)	*Ai1* (3)	*Sa1 Ai1/Sa1* (4)	*Sa1 Sa2/Sa1* (5)	*Sa1 Ai2/Sa1* (6)	*Sa1 Ai2/Sa2* (7)	*Sa1 SaI1/Sa1* (8)	*Sa1 AiI1/Sa1* (9)	*Sa1 AaI1/Sa1* (10)
Story 1	1.04	0.41	0.43	0.41	0.40	0.39	0.40	0.34	0.40	0.40
Story 2	1.05	0.36	0.39	0.36	0.36	0.36	0.36	0.29	0.35	0.36
Story 3	1.04	0.41	0.43	0.41	0.39	0.37	0.41	0.35	0.40	0.40
Roof	1.08	0.39	0.41	0.38	0.39	0.38	0.38	0.31	0.38	0.38

Table B.3 Standard deviations of the residual *IDR*s and *RDR* from regressions on various GMPs for the *brittle* 3-story model (0 collapses).

σ for 09E	No *GMP* (1)	*Sa1* (2)	*Ai1* (3)	*Sa1* *Ai1/Sa1* (4)	*Sa1* *Sa2/Sa1* (5)	*Sa1* *Sa2/Sa1* *Sa3/Sa2* (6)	*Sa1* *Sa2/Sa1* *Ai3/Sa3* (7)	*Sa1* *Sa2/Sa1* *SaI1/Sa1* (8)	*Sa1* *Sa2/Sa1* *AiI1/Sa1* (9)	*Sa1* *Sa2/Sa1* *AaI1/Sa1* (10)
Story 1	0.95	0.22	0.22	0.21	0.17	0.17	0.17	0.17	0.17	0.17
Story 2	0.96	0.18	0.19	0.17	0.15	0.15	0.15	0.15	0.15	0.15
Story 3	0.96	0.15	0.17	0.14	0.14	0.14	0.14	0.14	0.14	0.14
Story 4	0.94	0.16	0.18	0.15	0.15	0.14	0.15	0.15	0.15	0.15
Story 5	0.94	0.18	0.20	0.18	0.16	0.14	0.16	0.16	0.16	0.16
Story 6	0.93	0.23	0.23	0.22	0.16	0.16	0.16	0.16	0.16	0.16
Story 7	0.94	0.28	0.28	0.27	0.17	0.17	0.17	0.17	0.17	0.17
Story 8	0.93	0.34	0.35	0.34	0.18	0.18	0.18	0.18	0.18	0.18
Story 9	0.88	0.39	0.39	0.38	0.21	0.19	0.21	0.21	0.21	0.20
Roof	0.98	0.13	0.14	0.12	0.13	0.13	0.13	0.13	0.13	0.13

Table B.4 Standard deviations of the residual *IDR*s and *RDR* from regressions on various GMPs for the *elastic* 9-story model (0 collapses).

σ for 09D	No *GMP*	*Sa1*	*Ai1*	*Sa1* *Ai1/Sa1*	*Sa1* *Sa2/Sa1*	*Sa1* *Sa2/Sa1* *Sa3/Sa2*	*Sa1* *Sa2/Sa1* *Ai3/Sa3*	*Sa1* *Sa2/Sa1* *SaI1/Sa1*	*Sa1* *Sa2/Sa1* *AiI1/Sa1*	*Sa1* *Sa2/Sa1* *AaI1/Sa1*
	(1)	(2)	(3)	(4)	(5)	(6)	(7)	(8)	(9)	(10)
Story 1	0.93	0.29	0.30	0.29	0.28	0.28	0.28	0.22	0.28	0.28
Story 2	1.00	0.26	0.28	0.26	0.26	0.26	0.26	0.19	0.26	0.26
Story 3	0.99	0.22	0.26	0.22	0.22	0.22	0.22	0.17	0.22	0.22
Story 4	0.94	0.20	0.24	0.20	0.20	0.19	0.20	0.17	0.20	0.20
Story 5	0.83	0.21	0.23	0.21	0.19	0.18	0.19	0.19	0.19	0.19
Story 6	0.74	0.26	0.26	0.25	0.21	0.20	0.21	0.21	0.20	0.20
Story 7	0.75	0.32	0.31	0.31	0.20	0.20	0.20	0.20	0.19	0.19
Story 8	0.75	0.37	0.37	0.37	0.20	0.20	0.20	0.20	0.19	0.18
Story 9	0.73	0.41	0.40	0.40	0.22	0.20	0.22	0.22	0.21	0.21
Roof	0.90	0.18	0.21	0.18	0.18	0.18	0.18	0.16	0.17	0.18

Table B.5 Standard deviations of the residual *IDR*s and *RDR* from regressions on various GMPs for the *ductile* 9-story model (0 collapses).

σ for 09B	No *GMP* (1)	*Sa1* (2)	*Ai1* (3)	*Sa1* *Ai1/Sa1* (4)	*Sa1* *Sa2/Sa1* (5)	*Sa1* *Sa2/Sa1* *Sa3/Sa2* (6)	*Sa1* *Sa2/Sa1* *Ai3/Sa3* (7)	*Sa1* *Sa2/Sa1* *SaI1/Sa1* (8)	*Sa1* *Sa2/Sa1* *AiI1/Sa1* (9)	*Sa1* *Sa2/Sa1* *AaI1/Sa1* (10)
Story 1	1.08	0.40	0.42	0.41	0.40	0.40	0.40	0.36	0.40	0.39
Story 2	1.20	0.40	0.44	0.40	0.40	0.40	0.40	0.36	0.40	0.40
Story 3	1.21	0.39	0.43	0.39	0.39	0.39	0.39	0.35	0.39	0.39
Story 4	1.14	0.36	0.40	0.36	0.36	0.36	0.36	0.33	0.36	0.36
Story 5	0.98	0.35	0.37	0.35	0.33	0.33	0.33	0.32	0.33	0.33
Story 6	0.78	0.37	0.36	0.36	0.31	0.31	0.31	0.31	0.31	0.31
Story 7	0.74	0.39	0.39	0.39	0.30	0.30	0.30	0.29	0.30	0.30
Story 8	0.75	0.43	0.43	0.43	0.29	0.29	0.29	0.29	0.29	0.29
Story 9	0.73	0.47	0.46	0.46	0.31	0.29	0.31	0.30	0.30	0.30
Roof	1.06	0.28	0.31	0.28	0.28	0.28	0.28	0.25	0.28	0.28

Table B.6 Standard deviations of the residual *IDR*s and *RDR* from regressions on various GMPs for the *brittle* 9-story model (4 collapses).

σ for 20E	No *GMP* (1)	*Sa1* (2)	*Ai1* (3)	*Sa1* *Ai1/Sa1* (4)	*Sa1* *Sa2/Sa1* (5)	*Sa1* *Sa2/Sa1* *Sa3/Sa2* (6)	*Sa1* *Sa2/Sa1* *Sa3/Sa2* *Sa4/Sa3* (7)	*Sa1* *Sa2/Sa1* *Sa3/Sa2* *Ai4/Sa4* (8)	*Sa1* *Sa2/Sa1* *Sa3/Sa2* *SaI1/Sa1* (9)	*Sa1* *Sa2/Sa1* *Sa3/Sa2* *AiI1/Sa1* (10)	*Sa1* *Sa2/Sa1* *Sa3/Sa2* *AaI1/Sa1* (11)
Story 1	0.96	0.34	0.32	0.32	0.19	0.18	0.18	0.18	0.18	0.18	0.18
Story 2	0.97	0.33	0.30	0.30	0.18	0.18	0.18	0.18	0.18	0.18	0.18
Story 3	0.98	0.30	0.27	0.27	0.18	0.18	0.18	0.18	0.18	0.17	0.18
Story 4	0.99	0.27	0.24	0.24	0.17	0.17	0.17	0.17	0.16	0.16	0.17
Story 5	1.00	0.24	0.21	0.21	0.16	0.15	0.15	0.15	0.15	0.15	0.15
Story 6	1.00	0.22	0.20	0.20	0.17	0.15	0.15	0.15	0.14	0.15	0.15
Story 7	1.01	0.22	0.20	0.20	0.18	0.14	0.14	0.14	0.14	0.14	0.14
Story 8	1.01	0.22	0.21	0.20	0.18	0.14	0.14	0.14	0.14	0.14	0.14
Story 9	1.00	0.24	0.22	0.22	0.18	0.15	0.15	0.15	0.15	0.15	0.15
Story 10	0.97	0.25	0.23	0.23	0.16	0.15	0.15	0.15	0.15	0.15	0.15
Story 11	0.96	0.28	0.26	0.26	0.16	0.15	0.15	0.15	0.15	0.15	0.15
Story 12	0.95	0.32	0.29	0.29	0.17	0.16	0.16	0.16	0.16	0.16	0.16
Story 13	0.94	0.34	0.32	0.32	0.17	0.17	0.17	0.17	0.17	0.17	0.17
Story 14	0.94	0.37	0.34	0.34	0.17	0.17	0.17	0.17	0.17	0.17	0.17
Story 15	0.93	0.40	0.38	0.38	0.17	0.17	0.17	0.17	0.17	0.17	0.17
Story 16	0.93	0.43	0.41	0.41	0.17	0.17	0.17	0.17	0.17	0.17	0.17
Story 17	0.92	0.46	0.44	0.44	0.18	0.17	0.17	0.17	0.17	0.17	0.17
Story 18	0.91	0.49	0.47	0.46	0.20	0.17	0.17	0.17	0.17	0.17	0.17
Story 19	0.89	0.51	0.49	0.49	0.22	0.17	0.17	0.17	0.17	0.17	0.17
Story 20	0.87	0.52	0.50	0.50	0.25	0.18	0.17	0.18	0.18	0.18	0.18
Roof	1.04	0.17	0.15	0.14	0.14	0.14	0.14	0.14	0.14	0.14	0.14

Table B.7 Standard deviations of the residual *IDR*s and *RDR* for the *elastic* 20-story model (0 collapses).

σ for 20D	No *GMP*	*Sa1*	*Ai1*	*Sa1* *Ai1/Sa1*	*Sa1* *Sa2/Sa1*	*Sa1* *Sa2/Sa1* *Sa3/Sa2*	*Sa1* *Sa2/Sa1* *Sa3/Sa2* *Sa4/Sa3*	*Sa1* *Sa2/Sa1* *Sa3/Sa2* *Ai4/Sa4*	*Sa1* *Sa2/Sa1* *Sa3/Sa2* *SaI1/Sa1*	*Sa1* *Sa2/Sa1* *Sa3/Sa2* *AiI1/Sa1*	*Sa1* *Sa2/Sa1* *Sa3/Sa2* *AaI1/Sa1*
	(1)	(2)	(3)	(4)	(5)	(6)	(7)	(8)	(9)	(10)	(11)
Story 1	0.96	0.40	0.41	0.40	0.33	0.33	0.33	0.32	0.32	0.32	0.30
Story 2	1.04	0.38	0.37	0.37	0.29	0.29	0.29	0.29	0.28	0.29	0.28
Story 3	1.08	0.36	0.36	0.35	0.28	0.29	0.29	0.28	0.28	0.28	0.27
Story 4	1.09	0.34	0.34	0.33	0.28	0.28	0.28	0.28	0.27	0.27	0.26
Story 5	1.07	0.32	0.34	0.32	0.28	0.28	0.28	0.28	0.27	0.27	0.25
Story 6	0.94	0.27	0.29	0.27	0.24	0.23	0.24	0.23	0.22	0.23	0.22
Story 7	0.85	0.25	0.26	0.25	0.23	0.20	0.20	0.20	0.19	0.21	0.20
Story 8	0.78	0.25	0.24	0.24	0.22	0.20	0.20	0.20	0.19	0.20	0.20
Story 9	0.71	0.26	0.25	0.25	0.21	0.21	0.20	0.21	0.20	0.19	0.20
Story 10	0.67	0.26	0.26	0.26	0.20	0.20	0.20	0.20	0.20	0.19	0.19
Story 11	0.66	0.29	0.28	0.28	0.21	0.21	0.21	0.21	0.21	0.20	0.19
Story 12	0.67	0.32	0.31	0.31	0.22	0.22	0.21	0.22	0.22	0.20	0.20
Story 13	0.67	0.34	0.33	0.32	0.21	0.21	0.21	0.21	0.21	0.20	0.20
Story 14	0.66	0.36	0.35	0.35	0.21	0.21	0.21	0.21	0.21	0.19	0.20
Story 15	0.64	0.38	0.36	0.36	0.21	0.21	0.21	0.22	0.21	0.20	0.20
Story 16	0.64	0.41	0.39	0.38	0.23	0.23	0.23	0.23	0.23	0.22	0.22
Story 17	0.66	0.43	0.41	0.41	0.24	0.23	0.23	0.23	0.23	0.22	0.22
Story 18	0.68	0.47	0.45	0.44	0.25	0.22	0.22	0.22	0.22	0.21	0.21
Story 19	0.67	0.48	0.46	0.45	0.27	0.22	0.21	0.22	0.22	0.21	0.21
Story 20	0.63	0.47	0.45	0.45	0.28	0.23	0.21	0.23	0.23	0.22	0.22
Roof	0.90	0.20	0.22	0.20	0.18	0.18	0.18	0.18	0.18	0.18	0.18

Table B.8 Standard deviations of the residual *IDR*s and *RDR* for the *ductile* 20-story model (3 collapses).

σ for 20B	No *GMP*	*Sa1*	*Ai1*	*Sa1* *Ai1/Sa1*	*Sa1* *Sa2/Sa1*	*Sa1* *Sa2/Sa1* *Sa3/Sa2*	*Sa1* *Sa2/Sa1* *Sa3/Sa2* *Sa4/Sa3*	*Sa1* *Sa2/Sa1* *Sa3/Sa2* *Ai4/Sa4*	*Sa1* *Sa2/Sa1* *Sa3/Sa2* *SaI1/Sa1*	*Sa1* *Sa2/Sa1* *Sa3/Sa2* *AiI1/Sa1*	*Sa1* *Sa2/Sa1* *Sa3/Sa2* *AaI1/Sa1*
	(1)	(2)	(3)	(4)	(5)	(6)	(7)	(8)	(9)	(10)	(11)
Story 1	0.69	0.34	0.33	0.33	0.22	0.22	0.22	0.22	0.22	0.22	0.22
Story 2	0.79	0.35	0.34	0.34	0.23	0.23	0.23	0.23	0.23	0.23	0.23
Story 3	0.84	0.35	0.33	0.33	0.24	0.24	0.24	0.24	0.24	0.24	0.24
Story 4	0.83	0.32	0.31	0.31	0.24	0.24	0.24	0.24	0.24	0.24	0.24
Story 5	0.79	0.30	0.30	0.29	0.23	0.23	0.23	0.23	0.22	0.23	0.22
Story 6	0.69	0.25	0.25	0.24	0.20	0.18	0.18	0.18	0.18	0.18	0.19
Story 7	0.67	0.25	0.25	0.24	0.21	0.18	0.18	0.18	0.17	0.18	0.18
Story 8	0.66	0.25	0.25	0.24	0.21	0.19	0.18	0.19	0.18	0.18	0.18
Story 9	0.64	0.24	0.24	0.24	0.20	0.19	0.19	0.19	0.18	0.18	0.19
Story 10	0.62	0.24	0.24	0.23	0.17	0.17	0.17	0.17	0.16	0.17	0.17
Story 11	0.63	0.27	0.26	0.26	0.17	0.17	0.17	0.17	0.17	0.17	0.17
Story 12	0.64	0.30	0.29	0.29	0.18	0.18	0.18	0.18	0.17	0.18	0.18
Story 13	0.65	0.34	0.32	0.32	0.18	0.18	0.18	0.18	0.18	0.18	0.18
Story 14	0.64	0.36	0.34	0.34	0.18	0.18	0.18	0.18	0.18	0.18	0.18
Story 15	0.62	0.38	0.36	0.36	0.19	0.19	0.19	0.19	0.19	0.18	0.19
Story 16	0.63	0.41	0.39	0.39	0.21	0.20	0.20	0.20	0.20	0.20	0.20
Story 17	0.65	0.44	0.42	0.42	0.22	0.20	0.20	0.20	0.20	0.20	0.20
Story 18	0.68	0.48	0.46	0.45	0.23	0.20	0.20	0.20	0.20	0.19	0.20
Story 19	0.67	0.49	0.47	0.46	0.26	0.20	0.19	0.20	0.20	0.19	0.20
Story 20	0.64	0.48	0.47	0.46	0.28	0.21	0.20	0.21	0.21	0.21	0.21
Roof	0.71	0.18	0.20	0.18	0.17	0.17	0.17	0.17	0.16	0.17	0.17

Table B.9 Standard deviations of the residual *IDR*s and *RDR* for the *brittle* 20-story model (21 collapses).

APPENDIX C

The modal vibration periods (T_i) and first-mode yield displacement (d_y) for the three building models are given in Table C.1. Recall that the damping ratio and the post-yield strain-hardening ratio are set equal to 5%.

The earthquake ground motion records selected for this study are listed in Table C.2. Note that the first 70 records in the list are the "near-source" records, and the second 70 are the "ordinary" records (see definitions in Chapter 3). Within these two subsets the records are listed in order of increasing earthquake magnitude.

The various elastic and inelastic spectral and energy-based accelerations computed for all 140 records, each scaled by a factor of two, are listed in Table C.3 through C.5 for the 3-, 9-, and 20-story buildings, respectively.

Finally, the peak inter-story and roof drift ratios (*IDR*s and *RDR*s), as well the maximum and average *IDR* across stories (*MIDR*s and *AIDR*s), are listed in Tables C.6 through C.14 for the elastic, ductile, and brittle models of the 3-, 9-, and 20-story buildings. These are the results of nonlinear dynamic analyses for the 140 records listed in Table C.2, each scaled by a factor of two.

Building	T_1 (sec)	T_2 (sec)	T_3 (sec)	T_4 (sec)	d_y (cm)
3-Story	1.0	0.3	0.2	--	6
9-Story	2.3	0.9	0.5	0.3	12
20-Story	4.0	1.4	0.8	0.6	16

Table C.1 Modal vibration periods and first-mode yield displacement (explained in Chapter 3) for each of the three buildings considered.

ID #	Earthquake Name	Station Name	Year	Mw	Closest Dist. (km)	Geomatrix Site Code	NEHRP Site Class	Max fcHP	Min fcLP	Strike
1	Coyote Lake	Gilroy Array #2	1979	5.7	8.5	IQD	D	0.20	40.0	336
2	Coyote Lake	Gilroy Array #3	1979	5.7	6.9	IHD	D	0.20	40.0	336
3	Coyote Lake	Gilroy Array #4	1979	5.7	5.2	AHD	D	0.20	25.0	336
4	Coyote Lake	Gilroy Array #6	1979	5.7	3.2	IKB	C	0.20	25.0	336
5	Chalfant Valley-01	Zack Brothers Ranch	1986	5.8	6.2	AAD	-	0.11	30.0	48
6	Whittier Narrows-01	Garvey Res. - Control Bldg	1987	6.0	12.7	APB	-	0.20	40.0	280
7	Whittier Narrows-01	Norwalk - Imp Hwy, S Grnd	1987	6.0	15.8	IHD	-	0.15	40.0	280
8	N. Palm Springs	Cabazon	1986	6.1	7.8	AHD	-	0.15	40.0	287
9	N. Palm Springs	Morongo Valley	1986	6.1	12.1	AHC	C	0.08	50.0	287
10	Parkfield	Cholame - Shandon Array #12	1966	6.2	14.4	IQD	C	0.20	20.0	143
11	Parkfield	Cholame - Shandon Array #5	1966	6.2	5.0	IHC	D	0.20	17.4	143
12	Parkfield	Cholame - Shandon Array #8	1966	6.2	9.0	IQD	D	0.20	20.0	143
13	Parkfield	Temblor pre-1969	1966	6.2	9.8	IJA	C	0.20	14.7	143
14	Morgan Hill	Anderson Dam (Downstream)	1984	6.2	3.3	AFD	C	0.10	30.0	148
15	Morgan Hill	Gilroy - Gavilan Coll.	1984	6.2	14.8	AFB	C	0.10	30.0	148
16	Morgan Hill	Gilroy Array #2	1984	6.2	13.7	IQD	D	0.20	31.0	148
17	Morgan Hill	Gilroy Array #3	1984	6.2	13.0	IHD	D	0.10	32.0	148
18	Morgan Hill	Gilroy Array #4	1984	6.2	11.5	AHD	D	0.10	25.0	148
19	Morgan Hill	Gilroy Array #6	1984	6.2	9.9	IKB	C	0.10	27.0	148
20	Morgan Hill	Gilroy Array #7	1984	6.2	12.1	AHB	D	0.10	30.0	148
21	Morgan Hill	Halls Valley	1984	6.2	3.5	IFC	D	0.20	26.0	148
22	Chalfant Valley-02	Zack Brothers Ranch	1986	6.2	6.2	AAD	-	0.10	33.0	148
23	Victoria, Mexico	Cerro Prieto	1980	6.3	6.4	AVA	C	0.20	62.5	130
24	Victoria, Mexico	Chihuahua	1980	6.3	11.5	IQD	D	0.20	22.0	130
25	Coalinga-01	Pleasant Valley P.P. - bldg	1983	6.4	11.8	AHD	-	0.20	20.0	145
26	Coalinga-01	Pleasant Valley P.P. - yard	1983	6.4	11.8	AHD	-	0.20	31.0	145
27	Imperial Valley-06	Aeropuerto Mexicali	1979	6.5	1.4	I-D	D	0.05	-11.0	143
28	Imperial Valley-06	Agrarias	1979	6.5	1.2	IQD	-	0.05	-11.0	143
29	Imperial Valley-06	Bonds Corner	1979	6.5	1.0	AQD	D	0.10	40.0	143
30	Imperial Valley-06	Brawley Airport	1979	6.5	10.1	AQD	D	0.10	40.0	143
31	Imperial Valley-06	Calexico Fire Station	1979	6.5	12.2	AQD	D	0.20	40.0	143
32	Imperial Valley-06	EC Meloland Overpass FF	1979	6.5	1.8	IDD	D	0.10	40.0	143
33	Imperial Valley-06	El Centro Array #10	1979	6.5	7.9	AQD	D	0.10	40.0	143
34	Imperial Valley-06	El Centro Array #11	1979	6.5	14.2	AQD	D	0.20	40.0	143
35	Imperial Valley-06	El Centro Array #4	1979	6.5	5.5	IQD	D	0.10	40.0	143
36	Imperial Valley-06	El Centro Array #5	1979	6.5	2.3	IQD	D	0.10	40.0	143
37	Imperial Valley-06	El Centro Array #6	1979	6.5	0.3	IQD	D	0.10	40.0	143
38	Imperial Valley-06	El Centro Array #7	1979	6.5	2.3	AQD	D	0.10	40.0	143
39	Imperial Valley-06	El Centro Array #8	1979	6.5	5.6	AQD	D	0.10	40.0	143
40	Imperial Valley-06	El Centro Differential Array	1979	6.5	6.8	IQD	D	0.10	40.0	143
41	Imperial Valley-06	El Centro Imp. Co. Cent	1979	6.5	9.0	AQD	D	0.10	35.0	143
42	Imperial Valley-06	Holtville Post Office	1979	6.5	6.1	AQD	D	0.10	40.0	143
43	Imperial Valley-06	Parachute Test Site	1979	6.5	15.3	AQD	C	0.10	40.0	143
44	Imperial Valley-06	SAHOP Casa Flores	1979	6.5	11.4	I-C	D	0.20	-11.0	143
45	Superstition Hills-02	Parachute Test Site	1987	6.5	1.0	AQD	C	0.12	20.0	127
46	Superstition Hills-02	Westmorland Fire Sta	1987	6.5	13.0	ADD	D	0.10	35.0	127
47	Northridge-01	Canoga Park - Topanga Can	1994	6.7	14.7	--D	D	0.05	30.0	122
48	Northridge-01	Canyon Country - W Lost Cany	1994	6.7	12.4	--D	D	0.10	30.0	122
49	Northridge-01	Jensen Filter Plant	1994	6.7	5.4	--D	C	0.20	-11.0	122
50	Northridge-01	Newhall - Fire Sta	1994	6.7	5.9	AQD	D	0.12	23.0	122
51	Northridge-01	Northridge - 17645 Saticoy St	1994	6.7	12.1	--D	D	0.10	30.0	122
52	Northridge-01	Rinaldi Receiving Sta	1994	6.7	6.5	--C	D	11.00	-11.0	122
53	Northridge-01	Sepulveda VA	1994	6.7	8.4	--D	D	0.10	-11.0	122
54	Northridge-01	Sylmar - Converter Sta	1994	6.7	5.4	--D	D	11.00	-11.0	122
55	Northridge-01	Sylmar - Converter Sta East	1994	6.7	5.2	--D	D	11.00	-11.0	122

Table C.2 List of the ground motion records selected for this study according to the criteria described in Chapter 3.

ID #	Earthquake Name	Station Name	Year	Mw	Closest Dist. (km)	Geomatrix Site Code	NEHRP Site Class	Max fcHP	Min fcLP	Strike
56	Northridge-01	Sylmar - Olive View Med FF	1994	6.7	5.3	AQD	C	0.12	23.0	122
57	Kobe, Japan	KJMA	1995	6.9	0.8	--B	C	0.05	-11.0	230
58	Loma Prieta	Capitola	1989	6.9	15.2	AQC	D	0.20	40.0	128
59	Loma Prieta	Corralitos	1989	6.9	3.9	APB	C	0.20	40.0	128
60	Loma Prieta	Gilroy - Historic Bldg.	1989	6.9	11.0	BQD	-	0.20	38.0	128
61	Loma Prieta	Saratoga - W Valley Coll.	1989	6.9	9.3	AQD	C	0.10	38.0	128
62	Cape Mendocino	Petrolia	1992	7.0	9.6	IMD	D	0.07	23.0	340
63	Duzce, Turkey	Duzce	1999	7.1	11.4	A-D	D	0.08	50.0	265
64	Landers	Joshua Tree	1992	7.3	10.1	AGC	C	0.07	23.0	355
65	Landers	Morongo Valley	1992	7.3	15.3	AHC	C	11.00	-11.0	355
66	Tabas, Iran	Dayhook	1978	7.4	13.9	ABB	-	0.10	-11.0	330
67	Tabas, Iran	Tabas	1978	7.4	1.2	ABC	-	0.05	-11.0	330
68	Kocaeli, Turkey	Arcelik	1999	7.5	11.7	B-B	C	0.07	50.0	274
69	Kocaeli, Turkey	Duzce	1999	7.5	9.4	A-D	D	11.00	15.0	274
70	Kocaeli, Turkey	Yarimca	1999	7.5	3.0	B-D	D	0.07	50.0	274
71	Coyote Lake	San Juan Bautista, 24 Polk St	1979	5.7	19.3	AQD	C	0.20	20.0	336
72	Chalfant Valley-01	Bishop - LADWP South St	1986	5.8	23.4	AQD	-	0.11	20.0	48
73	Chalfant Valley-01	Lake Crowley - Shehorn Res.	1986	5.8	26.9	AAB	-	0.16	25.0	48
74	N. Palm Springs	San Jacinto Vall. Cem	1986	6.1	31.0	AQD	D	0.20	31.0	287
75	Morgan Hill	Agnews State Hospital	1984	6.2	24.5	AQD	D	0.20	13.0	148
76	Morgan Hill	Corralitos	1984	6.2	23.2	APB	C	0.20	24.0	148
77	Morgan Hill	Hollister Diff Array #1	1984	6.2	26.4	IQD	D	0.20	30.0	148
78	Morgan Hill	Hollister Diff Array #3	1984	6.2	26.4	IQD	D	0.20	30.0	148
79	Morgan Hill	Hollister Diff Array #4	1984	6.2	26.4	IQD	D	0.20	30.0	148
80	Morgan Hill	Hollister Diff Array #5	1984	6.2	26.4	IQD	D	0.20	30.0	148
81	Morgan Hill	Hollister Diff. Array	1984	6.2	26.4	IQD	D	0.20	23.0	148
82	Morgan Hill	San Juan Bautista, 24 Polk St	1984	6.2	27.2	AQD	C	0.10	21.0	148
83	Chalfant Valley-02	McGee Creek - Surface	1986	6.2	29.2	IQC	-	0.10	35.0	148
84	Victoria, Mexico	SAHOP Casa Flores	1980	6.3	31.3	I-C	D	0.20	27.0	130
85	Victoria, Mexico	Victoria Hospital Sotano	1980	6.3	35.2	--D	-	0.20	26.0	130
86	Coalinga-01	Parkfield - Fault Zone 12	1983	6.4	30.5	IHC	-	0.20	20.0	145
87	Coalinga-01	Parkfield - Fault Zone 14	1983	6.4	30.8	IHC	-	0.20	23.0	145
88	Coalinga-01	Parkfield - Fault Zone 15	1983	6.4	30.8	IQB	-	0.20	20.0	145
89	Coalinga-01	Parkfield - Fault Zone 16	1983	6.4	29.1	IQC	-	0.20	26.0	145
90	Coalinga-01	Parkfield - Fault Zone 9	1983	6.4	32.8	IPB	-	0.20	23.0	145
91	Coalinga-01	Parkfield - Vineyard Cany 1E	1983	6.4	28.0	IQC	-	0.20	23.0	145
92	Coalinga-01	Parkfield - Vineyard Cany 2W	1983	6.4	31.9	IHC	-	0.20	30.0	145
93	Coalinga-01	Parkfield - Vineyard Cany 4W	1983	6.4	35.9	IMB	-	0.20	27.0	145
94	Imperial Valley-06	Calipatria Fire Station	1979	6.5	25.0	BQD	D	0.10	40.0	143
95	Imperial Valley-06	Cerro Prieto	1979	6.5	23.3	AVA	C	0.10	-11.0	143
96	Imperial Valley-06	Chihuahua	1979	6.5	17.1	IQD	D	0.05	-11.0	143
97	Imperial Valley-06	Compuertas	1979	6.5	20.9	IQD	D	0.20	-11.0	143
98	Imperial Valley-06	Delta	1979	6.5	31.9	IQD	D	0.05	-11.0	143
99	Imperial Valley-06	El Centro Array #1	1979	6.5	20.3	AQD	D	0.10	40.0	143
100	Imperial Valley-06	El Centro Array #12	1979	6.5	19.7	IQD	D	0.10	40.0	143
101	Imperial Valley-06	El Centro Array #13	1979	6.5	23.7	AQD	D	0.20	40.0	143
102	Imperial Valley-06	Plaster City	1979	6.5	32.4	AQD	D	0.10	40.0	143
103	Imperial Valley-06	Superstition Mtn Camera	1979	6.5	27.3	AGB	C	0.10	40.0	143
104	Imperial Valley-06	Westmorland Fire Sta	1979	6.5	16.8	ADD	D	0.10	40.0	143
105	Superstition Hills-02	Brawley Airport	1987	6.5	17.0	AQD	D	0.13	20.0	127
106	Superstition Hills-02	El Centro Imp. Co. Cent	1987	6.5	18.2	AQD	D	0.10	38.0	127
107	Superstition Hills-02	Wildlife Liquef. Array	1987	6.5	23.9	IQD	-	0.10	40.0	127
108	San Fernando	LA - Hollywood Stor FF	1971	6.6	22.8	IPD	D	0.20	35.0	290
109	Northridge-01	Lake Hughes #1	1994	6.7	35.8	APC	C	0.12	23.0	122
110	Northridge-01	Lake Hughes #12A	1994	6.7	21.4	IHC	C	0.12	46.0	122

Table C.2 (continued) List of the ground motion records selected for this study according to the criteria described in Chapter 3.

ID #	Earthquake Name	Station Name	Year	Mw	Closest Dist. (km)	Geomatrix Site Code	NEHRP Site Class	Max fcHP	Min fcLP	Strike
111	Northridge-01	Lake Hughes #4 - Camp Mend	1994	6.7	31.7	IGB	C	0.12	23.0	122
112	Northridge-01	Lake Hughes #4B - Camp Mend	1994	6.7	31.7	IGB	C	0.12	23.0	122
113	Northridge-01	Lake Hughes #9	1994	6.7	25.4	AGA	C	0.08	-11.0	122
114	Northridge-01	Pacific Palisades - Sunset	1994	6.7	24.1	--B	C	0.05	30.0	122
115	Northridge-01	Santa Susana Ground	1994	6.7	16.7	--A	C	11.00	-11.0	122
116	Northridge-01	Stone Canyon	1994	6.7	29.2	---	C	0.03	-11.0	122
117	Northridge-01	Vasquez Rocks Park	1994	6.7	23.6	IBA	C	0.08	-11.0	122
118	Kobe, Japan	Abeno	1995	6.9	24.8	--D	D	0.05	40.0	230
119	Kobe, Japan	Tadoka	1995	6.9	31.6	--D	D	0.05	40.0	230
120	Kobe, Japan	Yae	1995	6.9	27.7	--D	-	0.05	-11.0	230
121	Loma Prieta	Agnews State Hospital	1989	6.9	24.6	AQD	D	0.20	30.0	128
122	Loma Prieta	Anderson Dam (Downstream)	1989	6.9	20.3	AFD	C	0.20	40.0	128
123	Loma Prieta	Anderson Dam (L Abut)	1989	6.9	20.3	AQA	C	0.10	32.0	128
124	Loma Prieta	Coyote Lake Dam (Downst)	1989	6.9	20.8	IHD	C	0.10	29.0	128
125	Loma Prieta	Gilroy Array #6	1989	6.9	18.3	IKB	C	0.20	31.0	128
126	Loma Prieta	Halls Valley	1989	6.9	30.5	IFC	D	0.20	22.0	128
127	Loma Prieta	UCSC	1989	6.9	18.5	--B	-	0.10	-11.0	128
128	Loma Prieta	UCSC Lick Observatory	1989	6.9	18.4	AKA	C	0.20	40.0	128
129	Loma Prieta	WAHO	1989	6.9	17.5	AQD	-	0.10	-11.0	128
130	Cape Mendocino	Fortuna - Fortuna Blvd	1992	7.0	18.5	IQD	C	0.07	23.0	340
131	Cape Mendocino	Rio Dell Overpass - FF	1992	7.0	17.8	APC	C	0.07	23.0	340
132	Landers	Barstow	1992	7.3	34.9	IQD	C	0.07	23.0	355
133	Landers	Desert Hot Springs	1992	7.3	16.4	AQD	C	0.07	23.0	355
134	Landers	Mission Creek Fault	1992	7.3	20.6	---	C	11.00	-11.0	355
135	Landers	North Palm Springs	1992	7.3	21.7	AHD	C	11.00	-11.0	355
136	Landers	Palm Springs Airport	1992	7.3	30.3	IQD	D	0.07	23.0	355
137	Landers	Yermo Fire Station	1992	7.3	23.3	AQD	D	0.07	23.0	355
138	Tabas, Iran	Boshrooyeh	1978	7.4	28.8	--C	-	0.04	20.0	330
139	Kocaeli, Turkey	Goynuk	1999	7.5	33.7	--B	-	0.15	25.0	274
140	Kocaeli, Turkey	Iznik	1999	7.5	33.1	A-D	D	0.10	25.0	274

Table C.2 (continued) List of the ground motion records selected for this study according to the criteria described in Chapter 3.

ID #	Sa(T1)	Sa(T2)	Sa(T3)	SaI(T1)	Ai(T1)	Ai(T2)	Ai(T3)	AiI(T1)	AaI(T1)
1	0.332	0.851	1.452	0.276	0.545	1.904	2.848	0.530	0.337
2	0.705	0.953	0.821	0.439	1.051	1.900	1.793	0.880	0.680
3	0.495	1.605	1.000	0.371	0.801	2.702	2.079	0.793	0.577
4	1.099	1.385	1.386	1.023	1.496	3.432	3.750	1.085	0.889
5	0.316	1.048	0.825	0.322	0.621	1.894	2.143	0.635	0.331
6	0.626	1.139	1.243	0.510	1.025	2.266	2.882	0.817	0.568
7	0.444	0.495	0.763	0.456	0.594	1.231	1.768	0.558	0.422
8	0.177	0.778	1.048	0.177	0.287	1.493	2.542	0.287	0.177
9	0.855	1.020	1.106	0.600	1.321	1.896	2.347	1.126	0.952
10	0.103	0.254	0.275	0.103	0.264	0.572	0.780	0.264	0.103
11	0.313	1.833	1.387	0.371	0.657	3.091	2.443	0.669	0.378
12	0.308	0.563	1.286	0.336	0.617	1.487	2.070	0.620	0.329
13	0.367	1.734	1.460	0.354	0.499	2.461	2.588	0.507	0.378
14	0.339	2.314	1.045	0.306	0.697	3.370	2.863	0.684	0.373
15	0.060	0.165	0.329	0.060	0.110	0.426	0.776	0.110	0.060
16	0.197	0.968	0.742	0.197	0.405	1.759	1.713	0.405	0.197
17	0.307	1.170	0.776	0.316	0.651	2.055	1.995	0.649	0.335
18	0.620	1.878	1.978	0.735	1.388	3.307	3.481	1.193	0.890
19	1.070	1.511	2.359	0.684	1.444	2.440	4.190	1.206	0.978
20	0.073	1.012	0.807	0.073	0.169	2.665	1.501	0.169	0.073
21	0.846	1.087	1.016	0.878	1.437	2.281	3.571	1.082	0.834
22	0.772	2.691	2.519	0.707	1.010	5.428	5.082	0.944	0.643
23	1.208	1.652	2.110	0.785	2.373	3.056	3.995	1.636	1.361
24	0.244	0.520	0.396	0.244	0.503	1.534	1.707	0.504	0.244
25	1.069	1.721	1.241	0.734	1.863	3.672	2.736	1.523	1.250
26	1.986	2.385	2.445	1.410	3.093	5.252	5.364	2.002	1.637
27	0.835	1.348	1.035	0.990	1.230	3.261	3.273	1.392	1.195
28	0.678	0.826	0.720	1.244	1.057	2.714	3.654	1.566	1.300
29	0.884	4.310	4.706	0.902	1.878	7.892	9.306	1.989	1.598
30	0.425	0.903	0.865	0.534	0.674	2.530	2.695	0.674	0.451
31	0.385	1.198	1.260	0.424	0.791	2.655	2.657	0.760	0.479
32	1.060	1.601	0.973	2.404	1.545	5.598	7.569	2.158	1.856
33	0.372	0.989	0.750	0.497	0.797	2.335	3.058	0.873	0.528
34	0.426	2.502	1.857	0.646	0.724	3.802	4.890	0.893	0.650
35	0.997	0.900	1.440	2.304	1.799	3.920	5.490	1.638	1.332
36	1.397	2.095	1.512	1.979	2.165	5.289	6.329	1.639	1.399
37	0.859	1.751	1.342	2.551	1.846	5.857	7.516	1.969	1.565
38	1.314	1.436	1.447	2.485	2.442	5.224	7.461	2.162	1.793
39	0.677	1.134	1.619	0.623	0.888	3.003	4.695	0.955	0.786
40	0.766	2.251	1.699	0.945	1.122	3.658	4.735	1.044	0.801
41	0.378	0.803	0.730	0.361	0.792	2.648	3.693	0.801	0.523
42	0.697	1.577	0.974	1.006	1.289	3.628	3.989	1.094	0.867
43	0.249	0.397	0.650	0.249	0.558	1.059	1.722	0.556	0.249
44	0.562	1.807	2.285	0.497	1.011	3.532	6.408	0.975	0.695
45	1.948	1.688	1.570	3.261	3.204	5.914	7.504	3.112	2.595
46	0.807	1.002	1.229	0.606	1.216	2.367	3.125	1.328	1.039
47	0.874	1.664	1.827	0.985	1.337	3.397	4.976	1.816	1.541
48	1.087	2.287	2.521	1.156	1.560	3.176	5.106	1.365	1.112
49	2.096	1.590	0.989	2.326	3.388	4.889	7.058	3.005	2.566
50	2.751	3.403	2.847	1.639	3.347	6.699	9.469	2.634	2.234
51	1.616	1.769	2.124	1.450	2.141	4.608	4.818	2.355	1.970
52	3.943	3.673	2.792	2.769	5.181	8.271	12.163	2.990	2.422
53	1.371	3.979	4.861	1.503	2.223	8.218	9.709	2.151	1.803
54	2.771	1.820	2.187	3.487	4.557	5.920	8.702	3.711	3.128
55	1.460	3.316	3.352	2.100	2.152	6.357	8.022	2.097	1.768

Table C.3 Ground motion parameters for the 3-story building.

ID #	Sa(T1)	Sa(T2)	Sa(T3)	SaI(T1)	Ai(T1)	Ai(T2)	Ai(T3)	AiI(T1)	AaI(T1)
56	1.790	4.453	2.215	2.478	2.441	7.358	8.841	2.534	2.186
57	3.739	3.906	2.229	2.112	5.691	6.247	7.283	3.038	2.497
58	0.796	2.364	2.037	0.957	1.261	5.351	4.513	1.578	1.225
59	1.052	2.886	2.238	1.278	1.760	4.625	4.663	1.701	1.369
60	0.449	1.144	0.829	0.490	0.736	2.143	2.446	1.046	0.821
61	1.416	1.825	1.207	1.264	2.122	3.827	4.841	1.944	1.655
62	1.689	1.753	1.594	2.118	2.255	3.441	5.840	1.828	1.484
63	1.068	2.507	1.200	0.827	1.764	5.081	4.899	1.588	1.262
64	1.087	1.465	0.986	0.842	2.020	4.568	4.673	2.153	1.768
65	0.465	0.711	0.762	0.529	1.148	2.592	2.162	1.129	0.719
66	0.508	1.097	2.388	0.563	0.956	2.445	4.520	0.913	0.639
67	1.352	3.374	5.068	3.340	3.015	8.886	13.959	3.202	2.709
68	0.216	0.499	1.310	0.216	0.375	1.352	2.600	0.375	0.216
69	0.849	1.311	1.097	0.850	1.242	3.441	4.250	1.289	0.974
70	0.751	1.257	1.220	1.409	1.436	3.524	3.847	1.954	1.599
71	0.200	0.453	0.579	0.200	0.333	0.905	0.982	0.333	0.200
72	0.241	0.523	0.412	0.241	0.440	0.970	0.876	0.440	0.241
73	0.026	0.198	0.304	0.026	0.049	0.360	0.479	0.049	0.026
74	0.103	0.293	0.320	0.103	0.219	0.705	0.852	0.219	0.103
75	0.135	0.224	0.202	0.135	0.371	0.533	0.592	0.371	0.135
76	0.233	0.494	0.498	0.233	0.348	0.770	0.893	0.348	0.233
77	0.289	0.374	0.644	0.309	0.502	0.898	1.693	0.517	0.302
78	0.322	0.302	0.423	0.323	0.493	0.822	1.168	0.503	0.321
79	0.345	0.513	0.439	0.346	0.462	1.083	1.366	0.479	0.342
80	0.305	0.382	0.462	0.344	0.547	0.893	1.357	0.576	0.331
81	0.315	0.442	0.922	0.326	0.482	1.080	2.441	0.507	0.316
82	0.181	0.177	0.213	0.181	0.323	0.468	0.622	0.323	0.181
83	0.022	0.253	0.398	0.022	0.045	0.537	0.987	0.045	0.022
84	0.116	0.285	0.428	0.116	0.200	0.822	0.981	0.200	0.116
85	0.123	0.116	0.095	0.123	0.197	0.403	0.418	0.197	0.123
86	0.742	0.442	0.405	0.553	1.220	1.253	1.147	1.010	0.737
87	2.142	0.903	0.777	1.205	3.409	2.250	2.796	2.071	1.741
88	0.533	0.754	0.542	0.531	0.983	1.644	1.759	0.928	0.657
89	0.523	0.855	0.642	0.420	0.908	1.923	1.728	0.810	0.595
90	0.258	0.189	0.176	0.258	0.511	0.459	0.664	0.511	0.258
91	1.026	0.562	0.655	0.552	1.757	1.245	1.645	1.226	0.947
92	0.137	0.436	0.303	0.137	0.248	1.103	0.917	0.248	0.137
93	0.196	0.207	0.193	0.196	0.395	0.511	0.541	0.395	0.196
94	0.181	0.756	0.640	0.181	0.423	1.605	1.783	0.423	0.181
95	0.580	1.145	0.982	0.556	1.285	2.529	3.580	1.357	0.893
96	0.828	1.001	1.041	0.675	1.494	2.676	3.461	1.453	1.104
97	0.197	0.584	0.504	0.197	0.475	1.000	1.585	0.475	0.197
98	0.583	1.083	0.867	0.668	1.840	3.877	3.045	1.772	1.118
99	0.136	0.523	0.517	0.136	0.343	1.256	1.532	0.343	0.136
100	0.306	0.647	0.727	0.283	0.705	1.905	2.095	0.691	0.340
101	0.146	0.850	0.802	0.146	0.350	1.670	1.914	0.350	0.146
102	0.046	0.163	0.342	0.046	0.095	0.454	0.726	0.095	0.046
103	0.057	0.274	0.476	0.057	0.111	0.714	1.115	0.111	0.057
104	0.140	0.238	0.313	0.140	0.383	1.210	1.885	0.383	0.140
105	0.335	0.445	0.543	0.287	0.694	1.261	1.636	0.663	0.372
106	0.634	1.140	1.470	0.898	1.082	3.008	3.961	1.309	1.050
107	0.576	0.863	0.744	0.521	1.059	2.256	2.490	1.149	0.791
108	0.294	0.757	0.729	0.277	0.495	1.580	2.323	0.513	0.307
109	0.567	0.423	0.402	0.361	0.792	0.987	1.213	0.708	0.526
110	0.174	0.733	1.730	0.174	0.309	1.622	2.780	0.309	0.174

Table C.3 (continued) Ground motion parameters for the 3-story building.

ID #	Sa(T1)	Sa(T2)	Sa(T3)	SaI(T1)	Ai(T1)	Ai(T2)	Ai(T3)	AiI(T1)	AaI(T1)
111	0.178	0.492	0.302	0.178	0.249	1.068	0.745	0.249	0.178
112	0.123	0.233	0.270	0.123	0.174	0.474	0.658	0.174	0.123
113	0.063	0.473	0.404	0.063	0.134	1.147	1.026	0.134	0.063
114	0.339	2.160	2.823	0.346	0.527	5.287	6.704	0.519	0.331
115	0.532	1.657	1.620	0.480	0.846	3.664	3.499	0.769	0.576
116	0.396	2.365	1.451	0.390	0.593	4.211	3.167	0.597	0.436
117	0.326	0.547	0.790	0.334	0.465	1.196	1.827	0.461	0.333
118	0.354	0.757	0.746	0.333	0.813	1.966	1.920	0.786	0.397
119	0.389	1.478	1.745	0.358	0.723	2.815	4.227	0.719	0.412
120	0.538	0.612	0.344	0.735	1.546	1.440	1.543	1.566	1.107
121	0.255	1.211	0.873	0.255	0.592	2.524	2.601	0.592	0.255
122	0.350	1.056	1.738	0.299	0.753	2.349	3.180	0.740	0.399
123	0.189	0.208	0.249	0.189	0.323	0.608	0.864	0.323	0.189
124	0.283	0.467	1.404	0.281	0.584	1.366	2.646	0.570	0.304
125	0.444	0.747	0.771	0.449	0.739	1.636	1.946	0.696	0.496
126	0.230	0.458	0.443	0.230	0.431	1.119	1.353	0.431	0.230
127	0.232	1.131	1.760	0.232	0.352	2.384	4.535	0.352	0.232
128	0.510	1.877	1.794	0.359	0.832	4.563	4.477	0.745	0.552
129	0.705	2.379	2.824	0.569	1.273	4.930	7.495	1.102	0.799
130	0.422	0.432	0.509	0.403	0.835	1.197	1.738	0.798	0.548
131	1.162	2.781	1.678	1.272	1.514	4.549	4.004	1.359	1.129
132	0.412	0.518	0.359	0.376	0.620	1.528	2.156	0.570	0.396
133	0.680	0.823	0.773	0.739	1.652	2.103	2.342	1.471	1.089
134	0.206	0.644	0.353	0.206	0.473	1.753	1.772	0.473	0.206
135	0.429	0.698	0.666	0.519	1.102	2.000	2.625	1.140	0.653
136	0.429	0.393	0.397	0.361	1.100	1.253	1.674	1.046	0.602
137	1.044	0.765	0.884	0.801	1.624	3.195	3.905	1.424	1.159
138	0.280	0.483	0.461	0.283	0.590	1.168	2.049	0.586	0.280
139	0.214	0.708	1.146	0.214	0.346	1.303	2.513	0.346	0.214
140	0.349	0.536	0.382	0.365	0.587	1.383	1.470	0.575	0.348

Table C.3 (continued) Ground motion parameters for the 3-story building.

ID #	Sa(T1)	Sa(T2)	Sa(T3)	Sa(T4)	SaI(T1)	Ai(T1)	Ai(T2)	Ai(T3)	Ai(T4)	AiI(T1)	AaI(T1)
1	0.085	0.278	0.329	0.851	0.085	0.123	0.478	0.663	1.904	0.123	0.085
2	0.156	0.637	0.386	0.953	0.139	0.277	0.965	0.632	1.900	0.249	0.165
3	0.084	0.736	1.215	1.605	0.084	0.152	1.187	2.069	2.702	0.152	0.084
4	0.213	1.346	1.620	1.385	0.222	0.251	1.696	2.349	3.432	0.216	0.182
5	0.093	0.350	0.849	1.048	0.093	0.124	0.533	1.561	1.894	0.125	0.093
6	0.050	0.789	0.810	1.139	0.050	0.088	1.157	1.418	2.266	0.088	0.050
7	0.104	0.579	1.227	0.495	0.103	0.145	0.737	1.825	1.231	0.144	0.105
8	0.085	0.142	0.357	0.778	0.085	0.133	0.291	0.608	1.493	0.133	0.085
9	0.169	0.679	0.825	1.020	0.161	0.222	1.045	1.373	1.896	0.227	0.169
10	0.063	0.101	0.148	0.254	0.063	0.120	0.273	0.382	0.572	0.120	0.063
11	0.147	0.257	1.253	1.833	0.120	0.231	0.562	2.030	3.091	0.218	0.142
12	0.053	0.251	0.473	0.563	0.053	0.120	0.495	1.182	1.487	0.120	0.053
13	0.096	0.304	0.922	1.734	0.096	0.144	0.499	1.254	2.461	0.143	0.096
14	0.110	0.555	1.867	2.314	0.106	0.202	0.909	2.545	3.370	0.199	0.119
15	0.019	0.066	0.097	0.165	0.019	0.040	0.118	0.200	0.426	0.040	0.019
16	0.064	0.236	0.442	0.968	0.064	0.104	0.360	1.016	1.759	0.104	0.064
17	0.138	0.364	0.777	1.170	0.121	0.249	0.651	1.201	2.055	0.239	0.141
18	0.078	0.707	1.437	1.878	0.078	0.150	1.283	3.045	3.307	0.150	0.078
19	0.118	1.235	1.026	1.511	0.119	0.170	1.727	1.612	2.440	0.179	0.116
20	0.021	0.093	0.531	1.012	0.021	0.050	0.210	1.043	2.665	0.050	0.021
21	0.130	1.125	1.327	1.087	0.132	0.178	1.716	2.219	2.281	0.184	0.126
22	0.185	1.101	2.398	2.691	0.122	0.280	1.487	3.473	5.428	0.266	0.183
23	0.186	1.235	1.892	1.652	0.153	0.322	2.217	3.006	3.056	0.294	0.196
24	0.260	0.243	0.394	0.520	0.172	0.490	0.667	0.914	1.534	0.414	0.323
25	0.173	0.809	2.333	1.721	0.183	0.257	1.228	4.830	3.672	0.280	0.183
26	0.213	1.443	4.166	2.385	0.237	0.370	2.226	7.347	5.252	0.398	0.277
27	0.402	0.805	1.144	1.348	0.231	0.502	1.264	2.024	3.261	0.388	0.316
28	0.503	0.877	1.295	0.826	0.451	0.645	1.601	2.304	2.714	0.422	0.342
29	0.287	1.309	2.614	4.310	0.162	0.515	2.351	5.596	7.892	0.432	0.309
30	0.339	0.382	0.300	0.903	0.441	0.480	0.740	1.089	2.530	0.436	0.367
31	0.115	0.385	1.351	1.198	0.115	0.177	0.724	2.865	2.655	0.186	0.113
32	1.105	1.199	1.345	1.601	1.270	1.451	1.875	3.702	5.598	0.848	0.686
33	0.409	0.365	1.146	0.989	0.618	0.570	0.755	1.906	2.335	0.537	0.461
34	0.203	0.472	1.586	2.502	0.267	0.350	0.879	2.635	3.802	0.354	0.255
35	0.646	0.890	1.279	0.900	1.312	0.923	1.748	2.399	3.920	0.879	0.736
36	0.882	1.380	2.003	2.095	1.507	1.075	2.069	3.400	5.289	0.985	0.809
37	0.823	1.021	1.343	1.751	1.220	1.229	2.157	3.170	5.857	0.972	0.800
38	0.830	2.011	1.634	1.436	1.216	1.063	3.189	3.094	5.224	0.844	0.693
39	0.376	0.895	1.374	1.134	0.531	0.551	1.148	2.099	3.003	0.507	0.435
40	0.465	0.807	1.522	2.251	0.725	0.678	1.164	2.741	3.658	0.565	0.481
41	0.434	0.615	1.255	0.803	0.749	0.600	1.276	2.335	2.648	0.641	0.546
42	0.341	0.735	1.258	1.577	0.476	0.438	1.427	1.944	3.628	0.543	0.463
43	0.159	0.251	0.593	0.397	0.213	0.266	0.459	1.168	1.059	0.245	0.197
44	0.067	0.756	1.612	1.807	0.067	0.148	1.539	2.401	3.532	0.148	0.067
45	1.283	1.783	1.598	1.688	0.641	1.652	3.454	4.026	5.914	0.844	0.673
46	0.191	0.757	0.901	1.002	0.202	0.293	1.199	2.162	2.367	0.352	0.273
47	0.674	1.024	1.238	1.664	0.392	1.107	1.655	2.845	3.397	0.639	0.528
48	0.423	1.025	2.600	2.287	0.283	0.551	1.516	3.787	3.176	0.380	0.313
49	1.155	1.629	1.232	1.590	0.821	1.588	2.884	2.991	4.889	0.953	0.789
50	0.561	2.746	3.968	3.403	0.695	0.785	3.385	6.519	6.699	0.776	0.618
51	0.736	1.435	2.374	1.769	0.500	1.179	2.453	3.994	4.608	0.690	0.555
52	0.874	4.164	3.638	3.673	0.992	1.463	5.834	5.497	8.271	0.822	0.640
53	0.481	1.676	2.621	3.979	0.374	0.702	3.217	3.859	8.218	0.584	0.475
54	1.188	3.189	2.083	1.820	1.183	1.691	4.728	3.911	5.920	1.125	0.880
55	0.833	1.837	2.581	3.316	0.927	1.027	3.238	4.315	6.357	0.846	0.701

Table C.4 Ground motion parameters for the 9-story building.

ID #	Sa(T1)	Sa(T2)	Sa(T3)	Sa(T4)	SaI(T1)	Ai(T1)	Ai(T2)	Ai(T3)	Ai(T4)	AiI(T1)	AaI(T1)
56	1.322	1.605	2.147	4.453	0.802	1.925	2.607	3.722	7.358	0.849	0.693
57	0.653	4.625	3.522	3.906	0.542	0.874	6.566	7.013	6.247	0.790	0.624
58	0.207	0.811	1.682	2.364	0.176	0.297	1.587	2.888	5.351	0.322	0.219
59	0.261	1.297	1.875	2.886	0.260	0.371	2.597	3.009	4.625	0.330	0.238
60	0.215	0.431	1.328	1.144	0.204	0.298	0.707	2.262	2.143	0.271	0.207
61	0.466	1.497	0.871	1.825	0.490	0.811	1.871	2.096	3.827	0.661	0.550
62	0.602	1.930	2.586	1.753	0.698	0.828	3.167	5.146	3.441	0.556	0.438
63	0.465	1.518	2.185	2.507	0.560	0.737	2.135	4.442	5.081	0.783	0.689
64	0.293	1.171	0.830	1.465	0.290	0.606	2.266	2.096	4.568	0.566	0.425
65	0.185	0.522	0.969	0.711	0.154	0.336	1.064	1.844	2.592	0.322	0.195
66	0.149	0.669	0.979	1.097	0.136	0.226	1.235	2.043	2.445	0.254	0.171
67	0.915	2.621	3.169	3.374	1.029	1.298	5.456	5.649	8.886	0.929	0.758
68	0.071	0.277	0.430	0.499	0.071	0.123	0.487	0.652	1.352	0.123	0.071
69	0.583	0.894	1.403	1.311	0.556	0.879	1.674	2.895	3.441	0.717	0.611
70	0.442	0.824	1.131	1.257	0.610	0.687	1.675	2.413	3.524	0.771	0.654
71	0.045	0.217	0.502	0.453	0.045	0.079	0.374	0.938	0.905	0.079	0.045
72	0.114	0.279	0.273	0.523	0.114	0.165	0.406	0.497	0.970	0.160	0.115
73	0.016	0.024	0.107	0.198	0.016	0.025	0.047	0.217	0.360	0.025	0.016
74	0.018	0.132	0.241	0.293	0.018	0.039	0.231	0.433	0.705	0.039	0.018
75	0.100	0.160	0.214	0.224	0.100	0.146	0.430	0.396	0.533	0.146	0.100
76	0.024	0.251	0.585	0.494	0.024	0.049	0.344	1.032	0.770	0.049	0.024
77	0.048	0.313	0.313	0.374	0.048	0.083	0.553	0.570	0.898	0.083	0.048
78	0.051	0.343	0.361	0.302	0.051	0.101	0.531	0.718	0.822	0.101	0.051
79	0.051	0.405	0.413	0.513	0.051	0.098	0.525	0.687	1.083	0.098	0.051
80	0.050	0.332	0.322	0.382	0.050	0.104	0.626	0.844	0.893	0.104	0.050
81	0.047	0.325	0.361	0.442	0.047	0.097	0.489	0.665	1.080	0.097	0.047
82	0.056	0.161	0.135	0.177	0.056	0.078	0.278	0.290	0.468	0.078	0.056
83	0.008	0.024	0.109	0.253	0.008	0.015	0.048	0.227	0.537	0.015	0.008
84	0.097	0.160	0.345	0.285	0.097	0.145	0.297	0.766	0.822	0.145	0.097
85	0.066	0.137	0.125	0.116	0.066	0.106	0.246	0.337	0.403	0.106	0.066
86	0.130	0.505	0.490	0.442	0.120	0.206	0.988	1.038	1.253	0.222	0.127
87	0.251	1.679	0.970	0.903	0.280	0.478	2.511	1.975	2.250	0.456	0.318
88	0.173	0.481	0.948	0.754	0.176	0.264	0.928	1.640	1.644	0.256	0.171
89	0.093	0.397	0.697	0.855	0.093	0.139	0.686	1.362	1.923	0.139	0.093
90	0.076	0.262	0.266	0.189	0.076	0.147	0.483	0.449	0.459	0.147	0.076
91	0.133	0.927	0.504	0.562	0.118	0.199	1.503	0.927	1.245	0.200	0.141
92	0.064	0.157	0.279	0.436	0.064	0.102	0.254	0.581	1.103	0.102	0.064
93	0.078	0.203	0.235	0.207	0.078	0.124	0.436	0.486	0.511	0.124	0.078
94	0.124	0.183	0.244	0.756	0.128	0.229	0.376	0.663	1.605	0.227	0.132
95	0.108	0.587	0.562	1.145	0.108	0.256	1.552	1.954	2.529	0.265	0.123
96	0.194	0.945	1.476	1.001	0.136	0.328	1.859	2.352	2.676	0.335	0.227
97	0.067	0.214	0.493	0.584	0.067	0.131	0.555	1.070	1.000	0.131	0.067
98	0.245	0.772	1.435	1.083	0.245	0.600	2.200	3.756	3.877	0.606	0.428
99	0.098	0.144	0.286	0.523	0.098	0.150	0.314	0.662	1.256	0.150	0.098
100	0.161	0.294	0.394	0.647	0.151	0.293	0.660	1.051	1.905	0.300	0.192
101	0.097	0.177	0.324	0.850	0.097	0.166	0.358	0.853	1.670	0.166	0.097
102	0.037	0.068	0.109	0.163	0.037	0.055	0.108	0.299	0.454	0.055	0.037
103	0.031	0.072	0.174	0.274	0.031	0.050	0.147	0.414	0.714	0.050	0.031
104	0.234	0.198	0.202	0.238	0.321	0.407	0.421	0.832	1.210	0.393	0.319
105	0.083	0.294	0.504	0.445	0.083	0.135	0.550	1.088	1.261	0.135	0.083
106	0.507	0.775	1.281	1.140	0.446	0.706	1.121	2.030	3.008	0.513	0.402
107	0.453	0.616	0.756	0.863	0.322	0.790	1.138	1.756	2.256	0.719	0.611
108	0.194	0.259	0.478	0.757	0.128	0.300	0.500	1.020	1.580	0.255	0.190
109	0.049	0.473	0.534	0.423	0.049	0.099	0.808	1.049	0.987	0.099	0.049
110	0.079	0.136	0.458	0.733	0.079	0.147	0.288	0.953	1.622	0.147	0.079

Table C.4 (continued) Ground motion parameters for the 9-story building.

ID #	Sa(T1)	Sa(T2)	Sa(T3)	Sa(T4)	SaI(T1)	Ai(T1)	Ai(T2)	Ai(T3)	Ai(T4)	AiI(T1)	AaI(T1)
111	0.035	0.203	0.246	0.492	0.035	0.064	0.309	0.483	1.068	0.064	0.035
112	0.022	0.142	0.185	0.233	0.022	0.037	0.209	0.334	0.474	0.037	0.022
113	0.042	0.058	0.234	0.473	0.042	0.077	0.142	0.573	1.147	0.077	0.042
114	0.123	0.571	1.085	2.160	0.104	0.199	0.821	1.935	5.287	0.194	0.123
115	0.139	0.628	1.051	1.657	0.144	0.204	0.950	1.916	3.664	0.198	0.134
116	0.114	0.377	1.176	2.365	0.115	0.184	0.660	2.297	4.211	0.180	0.113
117	0.090	0.372	0.705	0.547	0.090	0.121	0.510	1.121	1.196	0.121	0.090
118	0.168	0.283	0.500	0.757	0.171	0.424	0.760	1.148	1.966	0.430	0.262
119	0.186	0.398	1.087	1.478	0.148	0.386	0.711	2.187	2.815	0.353	0.213
120	0.233	0.950	0.814	0.612	0.307	0.450	1.887	2.104	1.440	0.456	0.315
121	0.236	0.309	0.662	1.211	0.222	0.396	0.739	1.338	2.524	0.480	0.388
122	0.105	0.383	1.239	1.056	0.105	0.153	0.800	2.076	2.349	0.157	0.104
123	0.115	0.176	0.201	0.208	0.126	0.178	0.326	0.457	0.608	0.191	0.130
124	0.074	0.319	0.302	0.467	0.074	0.138	0.551	0.538	1.366	0.138	0.074
125	0.109	0.371	0.688	0.747	0.109	0.185	0.687	1.083	1.636	0.194	0.115
126	0.101	0.311	0.470	0.458	0.101	0.214	0.637	1.041	1.119	0.210	0.105
127	0.039	0.176	0.355	1.131	0.039	0.077	0.349	0.861	2.384	0.077	0.039
128	0.068	0.498	0.906	1.877	0.068	0.123	0.693	2.033	4.563	0.123	0.068
129	0.085	0.918	0.985	2.379	0.085	0.161	2.005	1.956	4.930	0.161	0.085
130	0.248	0.485	0.555	0.432	0.282	0.459	0.995	1.082	1.197	0.352	0.274
131	0.209	1.035	2.068	2.781	0.164	0.336	1.448	3.181	4.549	0.328	0.240
132	0.137	0.427	0.583	0.518	0.149	0.237	0.769	1.376	1.528	0.232	0.161
133	0.139	0.794	0.614	0.823	0.165	0.272	1.594	1.411	2.103	0.287	0.171
134	0.173	0.328	0.326	0.644	0.144	0.256	0.604	0.870	1.753	0.263	0.167
135	0.203	0.368	0.506	0.698	0.152	0.374	0.980	1.409	2.000	0.346	0.216
136	0.223	0.371	0.439	0.393	0.191	0.454	0.897	0.783	1.253	0.441	0.336
137	0.281	0.934	1.059	0.765	0.231	0.542	1.645	2.111	3.195	0.524	0.421
138	0.130	0.352	0.585	0.483	0.118	0.210	0.677	1.509	1.168	0.203	0.133
139	0.063	0.187	0.350	0.708	0.063	0.098	0.345	0.673	1.303	0.098	0.063
140	0.215	0.355	0.449	0.536	0.178	0.346	0.742	1.062	1.383	0.307	0.227

Table C.4 (continued) Ground motion parameters for the 9-story building.

ID #	Sa(T1)	Sa(T2)	Sa(T3)	Sa(T4)	SaI(T1)	Ai(T1)	Ai(T2)	Ai(T3)	Ai(T4)	AiI(T1)	AaI(T1)
1	0.020	0.207	0.250	0.287	0.020	0.029	0.431	0.386	0.558	0.029	0.020
2	0.037	0.272	0.661	0.458	0.037	0.051	0.478	0.819	0.698	0.051	0.037
3	0.021	0.275	0.738	0.720	0.021	0.044	0.456	1.512	1.620	0.044	0.021
4	0.059	0.567	1.557	1.658	0.059	0.077	0.753	1.837	2.001	0.076	0.056
5	0.037	0.204	0.422	0.759	0.037	0.062	0.327	0.747	1.126	0.062	0.037
6	0.016	0.261	0.907	0.666	0.016	0.035	0.339	1.339	0.938	0.035	0.016
7	0.037	0.180	0.713	1.226	0.037	0.056	0.285	0.899	1.838	0.056	0.037
8	0.015	0.103	0.196	0.229	0.015	0.025	0.232	0.348	0.425	0.025	0.015
9	0.041	0.855	0.710	0.881	0.041	0.060	1.488	0.942	1.513	0.061	0.041
10	0.037	0.125	0.099	0.096	0.037	0.059	0.314	0.243	0.258	0.059	0.037
11	0.043	0.219	0.386	0.576	0.043	0.059	0.364	0.773	1.101	0.059	0.043
12	0.035	0.148	0.306	0.428	0.035	0.058	0.299	0.513	0.757	0.058	0.035
13	0.030	0.216	0.301	0.533	0.030	0.040	0.367	0.436	0.760	0.040	0.030
14	0.033	0.153	0.768	0.773	0.033	0.050	0.299	1.125	1.408	0.050	0.033
15	0.011	0.050	0.075	0.069	0.011	0.018	0.088	0.150	0.152	0.018	0.011
16	0.017	0.205	0.335	0.432	0.017	0.029	0.366	0.554	0.718	0.029	0.017
17	0.040	0.203	0.399	0.559	0.040	0.058	0.383	0.791	1.034	0.058	0.040
18	0.056	0.255	0.517	0.926	0.056	0.088	0.535	0.992	1.917	0.085	0.056
19	0.047	0.665	1.349	0.973	0.047	0.063	0.880	1.931	1.533	0.064	0.047
20	0.013	0.068	0.132	0.269	0.013	0.020	0.124	0.275	0.517	0.020	0.013
21	0.043	0.451	1.345	1.731	0.043	0.063	0.587	1.930	2.618	0.064	0.043
22	0.048	0.350	1.198	2.013	0.044	0.093	0.527	1.653	3.701	0.093	0.049
23	0.103	0.709	0.942	1.608	0.060	0.172	0.980	1.718	2.741	0.142	0.102
24	0.170	0.197	0.378	0.577	0.114	0.259	0.367	0.730	1.044	0.196	0.163
25	0.043	0.618	1.038	1.579	0.043	0.077	1.110	1.556	2.449	0.078	0.043
26	0.059	0.754	2.048	2.844	0.066	0.122	1.457	2.900	4.284	0.127	0.073
27	0.109	0.781	0.766	0.846	0.129	0.156	1.097	1.183	1.559	0.134	0.102
28	0.131	0.756	0.837	1.204	0.140	0.181	1.054	1.439	2.345	0.147	0.112
29	0.081	0.543	1.737	3.754	0.130	0.142	1.264	3.351	6.197	0.152	0.103
30	0.207	0.386	0.300	0.290	0.146	0.301	0.539	0.783	0.832	0.226	0.189
31	0.063	0.239	0.506	0.950	0.068	0.107	0.386	1.136	1.942	0.114	0.083
32	0.438	1.236	1.475	1.797	0.305	0.616	1.540	2.468	3.315	0.329	0.253
33	0.274	0.333	0.327	0.568	0.285	0.458	0.692	0.794	1.117	0.280	0.236
34	0.132	0.385	0.795	1.117	0.117	0.166	0.640	1.360	2.044	0.174	0.145
35	0.551	0.723	0.906	0.776	0.399	0.695	1.098	1.504	1.918	0.352	0.284
36	0.614	0.635	1.031	1.360	0.426	0.749	1.175	2.135	2.750	0.386	0.307
37	0.746	0.813	1.162	1.327	0.493	0.960	1.177	2.269	2.609	0.396	0.303
38	0.557	0.971	2.592	1.679	0.397	0.774	1.352	3.665	3.708	0.350	0.270
39	0.339	0.534	0.832	1.513	0.264	0.447	0.891	1.198	2.583	0.293	0.247
40	0.287	0.571	0.900	1.515	0.249	0.404	0.869	1.394	2.150	0.305	0.257
41	0.321	0.538	0.697	0.661	0.333	0.480	0.838	1.221	1.423	0.288	0.240
42	0.327	0.414	0.765	0.934	0.357	0.470	0.631	1.496	2.028	0.275	0.226
43	0.117	0.228	0.265	0.380	0.101	0.163	0.328	0.553	0.855	0.151	0.119
44	0.021	0.403	0.831	1.137	0.021	0.049	0.722	1.253	2.114	0.049	0.021
45	0.327	1.993	1.790	2.034	0.244	0.454	2.947	3.159	4.424	0.361	0.281
46	0.116	0.679	0.724	0.837	0.123	0.198	1.101	1.042	1.617	0.195	0.162
47	0.139	1.131	1.043	2.452	0.110	0.255	1.691	1.938	4.737	0.201	0.153
48	0.095	0.689	1.425	2.662	0.091	0.129	1.070	1.932	4.481	0.133	0.095
49	0.500	1.453	1.743	1.251	0.274	0.619	1.850	3.121	2.643	0.350	0.274
50	0.347	1.867	3.384	4.298	0.331	0.473	3.106	4.268	6.586	0.298	0.229
51	0.166	1.148	1.622	2.287	0.151	0.266	2.127	2.779	4.147	0.247	0.189
52	0.308	2.366	4.305	4.101	0.308	0.399	4.011	6.020	5.721	0.311	0.218
53	0.171	0.785	2.157	1.805	0.117	0.236	1.204	3.969	3.532	0.238	0.186
54	0.470	1.730	3.810	2.557	0.451	0.653	3.313	6.437	4.936	0.431	0.320
55	0.368	0.932	2.752	1.918	0.367	0.496	1.485	4.829	3.122	0.315	0.242

Table C.5 Ground motion parameters for the 20-story building.

ID #	Sa(T1)	Sa(T2)	Sa(T3)	Sa(T4)	SaI(T1)	Ai(T1)	Ai(T2)	Ai(T3)	Ai(T4)	AiI(T1)	AaI(T1)
56	0.306	1.752	1.531	1.594	0.324	0.425	2.612	2.896	3.132	0.324	0.244
57	0.219	1.657	5.082	3.365	0.135	0.352	2.525	7.020	5.378	0.279	0.200
58	0.048	0.837	1.235	2.449	0.047	0.099	1.594	2.300	4.076	0.100	0.049
59	0.109	0.819	2.208	1.840	0.081	0.163	1.071	4.243	3.113	0.151	0.102
60	0.059	0.696	0.503	0.721	0.054	0.093	1.082	0.744	1.054	0.092	0.060
61	0.154	0.771	1.476	1.077	0.162	0.236	1.110	2.351	2.249	0.220	0.173
62	0.182	0.860	2.651	3.217	0.177	0.244	1.230	3.661	5.450	0.209	0.159
63	0.313	0.604	1.960	1.572	0.319	0.565	1.005	2.900	3.100	0.428	0.360
64	0.151	0.867	1.368	1.175	0.124	0.225	1.741	3.543	3.119	0.224	0.167
65	0.072	0.491	0.509	1.399	0.059	0.134	0.933	1.258	2.336	0.128	0.081
66	0.095	0.306	0.715	0.985	0.076	0.151	0.468	1.414	2.099	0.137	0.106
67	0.403	1.297	3.033	2.590	0.397	0.538	2.224	6.137	4.787	0.459	0.363
68	0.070	0.172	0.387	0.275	0.055	0.092	0.279	0.634	0.598	0.088	0.068
69	0.419	0.440	0.925	1.610	0.405	0.585	0.896	1.744	2.523	0.331	0.283
70	0.412	1.336	1.152	1.337	0.193	0.567	2.118	2.153	2.799	0.379	0.325
71	0.019	0.069	0.223	0.455	0.019	0.030	0.145	0.485	0.982	0.030	0.019
72	0.045	0.149	0.289	0.242	0.045	0.075	0.302	0.507	0.543	0.075	0.045
73	0.006	0.019	0.034	0.066	0.006	0.011	0.034	0.061	0.134	0.011	0.006
74	0.008	0.107	0.142	0.188	0.008	0.014	0.213	0.255	0.442	0.014	0.008
75	0.024	0.119	0.142	0.127	0.024	0.041	0.225	0.312	0.343	0.041	0.024
76	0.009	0.147	0.258	0.298	0.009	0.018	0.255	0.448	0.530	0.018	0.009
77	0.017	0.258	0.376	0.296	0.017	0.031	0.534	0.732	0.579	0.031	0.017
78	0.018	0.262	0.307	0.265	0.018	0.038	0.589	0.625	0.435	0.038	0.018
79	0.017	0.262	0.408	0.349	0.017	0.038	0.589	0.764	0.565	0.038	0.017
80	0.017	0.258	0.396	0.385	0.017	0.037	0.544	0.789	0.689	0.037	0.017
81	0.017	0.290	0.394	0.321	0.017	0.034	0.579	0.603	0.679	0.034	0.017
82	0.028	0.082	0.189	0.147	0.028	0.045	0.159	0.339	0.318	0.045	0.028
83	0.004	0.019	0.027	0.058	0.004	0.008	0.035	0.056	0.112	0.008	0.004
84	0.020	0.152	0.252	0.225	0.020	0.032	0.273	0.361	0.489	0.032	0.020
85	0.018	0.136	0.135	0.115	0.018	0.026	0.230	0.220	0.260	0.026	0.018
86	0.046	0.423	0.568	0.638	0.046	0.065	0.701	1.006	1.354	0.066	0.045
87	0.055	1.017	1.685	1.160	0.047	0.110	1.415	2.676	2.167	0.115	0.063
88	0.030	0.264	0.657	0.800	0.030	0.056	0.408	1.349	1.355	0.056	0.030
89	0.020	0.216	0.350	0.557	0.020	0.039	0.317	0.744	1.165	0.039	0.020
90	0.018	0.227	0.313	0.277	0.018	0.029	0.338	0.678	0.430	0.029	0.018
91	0.027	0.321	0.703	0.579	0.027	0.047	0.581	1.043	1.010	0.047	0.027
92	0.017	0.104	0.183	0.226	0.017	0.026	0.178	0.316	0.324	0.026	0.017
93	0.017	0.101	0.170	0.251	0.017	0.025	0.173	0.300	0.542	0.025	0.017
94	0.070	0.161	0.215	0.239	0.083	0.103	0.289	0.392	0.579	0.125	0.095
95	0.061	0.263	0.812	0.927	0.083	0.125	0.737	2.016	2.811	0.128	0.081
96	0.119	0.609	1.291	1.753	0.100	0.191	1.029	2.707	2.737	0.153	0.114
97	0.050	0.149	0.315	0.397	0.050	0.079	0.312	0.768	0.822	0.077	0.052
98	0.145	0.390	0.945	0.957	0.144	0.314	1.056	2.382	2.947	0.305	0.240
99	0.061	0.105	0.158	0.245	0.049	0.101	0.193	0.364	0.532	0.094	0.062
100	0.087	0.266	0.304	0.390	0.087	0.139	0.510	0.787	0.859	0.136	0.106
101	0.056	0.236	0.233	0.327	0.048	0.076	0.496	0.484	0.753	0.084	0.055
102	0.014	0.044	0.077	0.137	0.014	0.021	0.070	0.150	0.294	0.021	0.014
103	0.029	0.064	0.084	0.152	0.029	0.045	0.113	0.193	0.379	0.045	0.029
104	0.174	0.173	0.239	0.247	0.170	0.259	0.322	0.489	0.694	0.235	0.203
105	0.028	0.164	0.308	0.375	0.028	0.044	0.282	0.485	0.681	0.044	0.028
106	0.159	0.885	0.929	1.234	0.116	0.310	1.147	1.539	2.010	0.232	0.189
107	0.166	0.673	0.623	0.771	0.101	0.314	1.325	1.232	1.617	0.249	0.198
108	0.123	0.195	0.255	0.308	0.112	0.167	0.335	0.435	0.698	0.128	0.108
109	0.014	0.191	0.501	0.530	0.014	0.032	0.290	0.982	0.866	0.032	0.014
110	0.043	0.066	0.160	0.257	0.043	0.057	0.144	0.318	0.513	0.057	0.043

Table C.5 (continued) Ground motion parameters for the 20-story building.

ID #	Sa(T1)	Sa(T2)	Sa(T3)	Sa(T4)	SaI(T1)	Ai(T1)	Ai(T2)	Ai(T3)	Ai(T4)	AiI(T1)	AaI(T1)
111	0.018	0.052	0.209	0.208	0.018	0.028	0.112	0.299	0.425	0.028	0.018
112	0.014	0.035	0.144	0.144	0.014	0.021	0.080	0.217	0.290	0.021	0.014
113	0.042	0.068	0.091	0.101	0.042	0.061	0.126	0.200	0.279	0.061	0.042
114	0.050	0.241	0.577	1.088	0.050	0.072	0.381	0.931	1.744	0.072	0.049
115	0.046	0.308	0.559	1.002	0.048	0.080	0.425	0.909	1.978	0.079	0.047
116	0.032	0.280	0.447	1.031	0.032	0.047	0.404	0.949	1.812	0.047	0.032
117	0.020	0.252	0.424	0.756	0.020	0.036	0.334	0.567	1.075	0.036	0.020
118	0.195	0.237	0.322	0.311	0.085	0.351	0.613	0.753	0.846	0.259	0.191
119	0.115	0.175	0.486	1.053	0.090	0.264	0.405	1.120	1.774	0.233	0.177
120	0.266	0.381	1.215	0.980	0.090	0.509	0.960	2.046	2.248	0.296	0.243
121	0.104	0.322	0.328	0.455	0.128	0.166	0.608	0.731	1.139	0.188	0.154
122	0.043	0.294	0.658	1.624	0.043	0.061	0.530	1.195	3.032	0.063	0.043
123	0.051	0.228	0.187	0.339	0.052	0.073	0.325	0.337	0.607	0.078	0.051
124	0.047	0.110	0.316	0.427	0.046	0.071	0.258	0.557	0.762	0.070	0.047
125	0.060	0.346	0.375	0.737	0.062	0.084	0.563	0.605	1.276	0.081	0.058
126	0.058	0.208	0.709	0.720	0.060	0.082	0.320	1.328	1.518	0.079	0.057
127	0.034	0.198	0.236	0.256	0.034	0.050	0.356	0.446	0.628	0.050	0.034
128	0.051	0.205	0.397	0.530	0.048	0.075	0.416	0.660	1.110	0.074	0.051
129	0.051	0.502	0.832	0.735	0.051	0.081	0.833	1.621	1.631	0.080	0.050
130	0.137	0.316	0.438	0.379	0.087	0.175	0.480	0.815	0.933	0.134	0.109
131	0.048	0.788	1.019	1.228	0.055	0.095	1.573	1.433	2.117	0.100	0.053
132	0.165	0.222	0.569	0.565	0.101	0.251	0.393	1.076	0.996	0.178	0.146
133	0.073	0.424	0.607	0.544	0.064	0.132	0.815	1.249	1.256	0.138	0.097
134	0.134	0.159	0.329	0.456	0.123	0.238	0.371	0.678	0.911	0.178	0.138
135	0.096	0.323	0.342	0.515	0.102	0.197	0.823	0.855	1.224	0.180	0.126
136	0.050	0.237	0.372	0.491	0.053	0.099	0.581	0.925	0.908	0.100	0.051
137	0.172	1.051	0.874	0.944	0.182	0.257	1.822	1.693	1.887	0.262	0.223
138	0.056	0.221	0.327	0.349	0.047	0.077	0.342	0.612	0.902	0.083	0.059
139	0.036	0.145	0.280	0.324	0.036	0.051	0.204	0.427	0.526	0.051	0.036
140	0.043	0.482	0.291	0.418	0.044	0.076	0.713	0.626	0.868	0.078	0.043

Table C.5 (continued) Ground motion parameters for the 20-story building.

ID #	IDR1	IDR2	IDR3	RDR	AIDR	MIDR
1	0.0116	0.0148	0.0122	0.0126	0.0129	0.0148
2	0.0218	0.0299	0.0257	0.0258	0.0258	0.0299
3	0.0114	0.0157	0.0183	0.0138	0.0151	0.0183
4	0.0313	0.0405	0.0358	0.0344	0.0358	0.0405
5	0.0102	0.0129	0.0126	0.0110	0.0119	0.0129
6	0.0174	0.0238	0.0220	0.0195	0.0211	0.0238
7	0.0108	0.0154	0.0157	0.0135	0.0140	0.0157
8	0.0070	0.0078	0.0111	0.0071	0.0086	0.0111
9	0.0287	0.0393	0.0347	0.0341	0.0343	0.0393
10	0.0041	0.0054	0.0050	0.0048	0.0049	0.0054
11	0.0119	0.0166	0.0192	0.0148	0.0159	0.0192
12	0.0125	0.0159	0.0149	0.0137	0.0144	0.0159
13	0.0144	0.0154	0.0218	0.0131	0.0172	0.0218
14	0.0099	0.0128	0.0166	0.0118	0.0131	0.0166
15	0.0022	0.0025	0.0029	0.0022	0.0025	0.0029
16	0.0092	0.0103	0.0105	0.0088	0.0100	0.0105
17	0.0095	0.0122	0.0135	0.0103	0.0117	0.0135
18	0.0225	0.0320	0.0292	0.0278	0.0279	0.0320
19	0.0281	0.0403	0.0366	0.0349	0.0350	0.0403
20	0.0061	0.0032	0.0111	0.0034	0.0068	0.0111
21	0.0271	0.0347	0.0294	0.0298	0.0304	0.0347
22	0.0230	0.0273	0.0355	0.0220	0.0286	0.0355
23	0.0409	0.0605	0.0597	0.0529	0.0537	0.0605
24	0.0069	0.0096	0.0094	0.0084	0.0086	0.0096
25	0.0414	0.0535	0.0518	0.0457	0.0489	0.0535
26	0.0662	0.0868	0.0821	0.0747	0.0784	0.0868
27	0.0234	0.0315	0.0344	0.0284	0.0298	0.0344
28	0.0162	0.0230	0.0217	0.0202	0.0203	0.0230
29	0.0278	0.0358	0.0444	0.0311	0.0360	0.0444
30	0.0112	0.0149	0.0144	0.0132	0.0135	0.0149
31	0.0161	0.0197	0.0182	0.0164	0.0180	0.0197
32	0.0252	0.0339	0.0317	0.0292	0.0303	0.0339
33	0.0107	0.0141	0.0152	0.0125	0.0133	0.0152
34	0.0136	0.0166	0.0187	0.0149	0.0163	0.0187
35	0.0297	0.0410	0.0431	0.0366	0.0379	0.0431
36	0.0435	0.0585	0.0550	0.0505	0.0523	0.0585
37	0.0247	0.0331	0.0338	0.0293	0.0305	0.0338
38	0.0363	0.0510	0.0457	0.0441	0.0443	0.0510
39	0.0184	0.0220	0.0204	0.0180	0.0203	0.0220
40	0.0191	0.0285	0.0314	0.0248	0.0263	0.0314
41	0.0108	0.0132	0.0127	0.0113	0.0122	0.0132
42	0.0238	0.0283	0.0354	0.0262	0.0292	0.0354
43	0.0089	0.0118	0.0128	0.0102	0.0112	0.0128
44	0.0184	0.0197	0.0263	0.0162	0.0215	0.0263
45	0.0522	0.0708	0.0621	0.0617	0.0617	0.0708
46	0.0208	0.0275	0.0252	0.0233	0.0245	0.0275
47	0.0254	0.0375	0.0339	0.0322	0.0323	0.0375
48	0.0363	0.0424	0.0387	0.0350	0.0391	0.0424
49	0.0688	0.0956	0.0843	0.0828	0.0829	0.0956
50	0.0671	0.0974	0.0990	0.0851	0.0878	0.0990
51	0.0391	0.0561	0.0591	0.0489	0.0514	0.0591
52	0.1052	0.1438	0.1247	0.1229	0.1246	0.1438
53	0.0369	0.0488	0.0472	0.0422	0.0443	0.0488
54	0.0947	0.1273	0.1140	0.1110	0.1120	0.1273
55	0.0458	0.0508	0.0574	0.0431	0.0513	0.0574

Table C.6 Drift ratio demands for the *elastic* 3-story building model.

ID #	IDR1	IDR2	IDR3	RDR	AIDR	MIDR
56	0.0557	0.0627	0.0740	0.0558	0.0641	0.0740
57	0.0931	0.1287	0.1257	0.1124	0.1159	0.1287
58	0.0243	0.0309	0.0297	0.0262	0.0283	0.0309
59	0.0260	0.0362	0.0351	0.0313	0.0324	0.0362
60	0.0131	0.0166	0.0185	0.0141	0.0161	0.0185
61	0.0437	0.0590	0.0577	0.0519	0.0535	0.0590
62	0.0384	0.0597	0.0598	0.0514	0.0526	0.0598
63	0.0334	0.0379	0.0454	0.0340	0.0389	0.0454
64	0.0263	0.0310	0.0307	0.0267	0.0294	0.0310
65	0.0171	0.0232	0.0239	0.0206	0.0214	0.0239
66	0.0134	0.0199	0.0209	0.0178	0.0180	0.0209
67	0.0352	0.0513	0.0535	0.0441	0.0467	0.0535
68	0.0064	0.0098	0.0099	0.0076	0.0087	0.0099
69	0.0205	0.0299	0.0361	0.0272	0.0288	0.0361
70	0.0215	0.0275	0.0269	0.0242	0.0253	0.0275
71	0.0061	0.0085	0.0071	0.0071	0.0072	0.0085
72	0.0067	0.0085	0.0096	0.0077	0.0083	0.0096
73	0.0010	0.0011	0.0014	0.0009	0.0011	0.0014
74	0.0034	0.0046	0.0041	0.0040	0.0040	0.0046
75	0.0047	0.0069	0.0065	0.0060	0.0060	0.0069
76	0.0062	0.0090	0.0085	0.0077	0.0079	0.0090
77	0.0085	0.0117	0.0120	0.0102	0.0107	0.0120
78	0.0085	0.0121	0.0115	0.0105	0.0107	0.0121
79	0.0083	0.0123	0.0124	0.0108	0.0110	0.0124
80	0.0094	0.0125	0.0126	0.0110	0.0115	0.0126
81	0.0091	0.0115	0.0104	0.0098	0.0104	0.0115
82	0.0063	0.0092	0.0088	0.0081	0.0081	0.0092
83	0.0012	0.0011	0.0017	0.0008	0.0013	0.0017
84	0.0031	0.0040	0.0060	0.0037	0.0044	0.0060
85	0.0036	0.0045	0.0039	0.0039	0.0040	0.0045
86	0.0255	0.0344	0.0305	0.0296	0.0301	0.0344
87	0.0680	0.0984	0.0901	0.0854	0.0855	0.0984
88	0.0196	0.0276	0.0253	0.0241	0.0242	0.0276
89	0.0167	0.0253	0.0258	0.0224	0.0226	0.0258
90	0.0075	0.0103	0.0093	0.0089	0.0090	0.0103
91	0.0299	0.0432	0.0428	0.0380	0.0386	0.0432
92	0.0056	0.0059	0.0074	0.0050	0.0063	0.0074
93	0.0043	0.0066	0.0066	0.0058	0.0058	0.0066
94	0.0068	0.0089	0.0086	0.0077	0.0081	0.0089
95	0.0197	0.0252	0.0262	0.0223	0.0237	0.0262
96	0.0246	0.0318	0.0312	0.0277	0.0292	0.0318
97	0.0065	0.0093	0.0096	0.0083	0.0085	0.0096
98	0.0211	0.0245	0.0227	0.0212	0.0228	0.0245
99	0.0055	0.0069	0.0067	0.0060	0.0064	0.0069
100	0.0107	0.0150	0.0136	0.0130	0.0131	0.0150
101	0.0059	0.0075	0.0062	0.0064	0.0065	0.0075
102	0.0017	0.0022	0.0021	0.0019	0.0020	0.0022
103	0.0021	0.0020	0.0026	0.0017	0.0022	0.0026
104	0.0036	0.0049	0.0049	0.0044	0.0045	0.0049
105	0.0116	0.0161	0.0135	0.0137	0.0137	0.0161
106	0.0198	0.0243	0.0272	0.0213	0.0238	0.0272
107	0.0155	0.0217	0.0204	0.0192	0.0192	0.0217
108	0.0102	0.0121	0.0150	0.0109	0.0124	0.0150
109	0.0167	0.0222	0.0196	0.0191	0.0195	0.0222
110	0.0059	0.0074	0.0083	0.0061	0.0072	0.0083

Table C.6 (continued) Drift ratio demands for the *elastic* 3-story building model.

ID #	IDR1	IDR2	IDR3	RDR	AIDR	MIDR
111	0.0051	0.0068	0.0070	0.0060	0.0063	0.0070
112	0.0034	0.0047	0.0048	0.0042	0.0043	0.0048
113	0.0041	0.0030	0.0061	0.0027	0.0044	0.0061
114	0.0109	0.0120	0.0156	0.0090	0.0128	0.0156
115	0.0163	0.0212	0.0210	0.0189	0.0195	0.0212
116	0.0127	0.0170	0.0220	0.0154	0.0172	0.0220
117	0.0097	0.0130	0.0149	0.0117	0.0125	0.0149
118	0.0118	0.0168	0.0181	0.0142	0.0156	0.0181
119	0.0094	0.0144	0.0143	0.0122	0.0127	0.0144
120	0.0237	0.0329	0.0292	0.0285	0.0286	0.0329
121	0.0090	0.0118	0.0119	0.0102	0.0109	0.0119
122	0.0118	0.0162	0.0188	0.0145	0.0156	0.0188
123	0.0062	0.0085	0.0075	0.0073	0.0074	0.0085
124	0.0092	0.0124	0.0111	0.0106	0.0109	0.0124
125	0.0148	0.0202	0.0219	0.0174	0.0189	0.0219
126	0.0053	0.0070	0.0075	0.0061	0.0066	0.0075
127	0.0092	0.0112	0.0118	0.0084	0.0107	0.0118
128	0.0225	0.0239	0.0259	0.0192	0.0241	0.0259
129	0.0246	0.0329	0.0348	0.0284	0.0308	0.0348
130	0.0153	0.0214	0.0207	0.0188	0.0191	0.0214
131	0.0336	0.0457	0.0504	0.0405	0.0432	0.0504
132	0.0102	0.0158	0.0158	0.0139	0.0139	0.0158
133	0.0257	0.0351	0.0318	0.0305	0.0309	0.0351
134	0.0057	0.0070	0.0072	0.0060	0.0066	0.0072
135	0.0189	0.0245	0.0208	0.0212	0.0214	0.0245
136	0.0163	0.0224	0.0191	0.0192	0.0193	0.0224
137	0.0284	0.0369	0.0305	0.0312	0.0319	0.0369
138	0.0059	0.0084	0.0087	0.0068	0.0077	0.0087
139	0.0069	0.0098	0.0101	0.0086	0.0089	0.0101
140	0.0097	0.0122	0.0105	0.0103	0.0108	0.0122

Table C.6 (continued) Drift ratio demands for the *elastic* 3-story building model.

ID #	IDR1	IDR2	IDR3	RDR	AIDR	MIDR
1	0.0102	0.0123	0.0097	0.0102	0.0107	0.0123
2	0.0128	0.0160	0.0152	0.0137	0.0147	0.0160
3	0.0094	0.0138	0.0198	0.0123	0.0143	0.0198
4	0.0256	0.0304	0.0322	0.0262	0.0294	0.0322
5	0.0095	0.0116	0.0124	0.0099	0.0112	0.0124
6	0.0139	0.0181	0.0210	0.0153	0.0177	0.0210
7	0.0083	0.0147	0.0147	0.0124	0.0126	0.0147
8	0.0070	0.0078	0.0110	0.0071	0.0086	0.0110
9	0.0190	0.0219	0.0197	0.0193	0.0202	0.0219
10	0.0041	0.0054	0.0050	0.0047	0.0048	0.0054
11	0.0101	0.0141	0.0183	0.0125	0.0142	0.0183
12	0.0102	0.0131	0.0114	0.0111	0.0115	0.0131
13	0.0102	0.0136	0.0183	0.0115	0.0140	0.0183
14	0.0088	0.0104	0.0166	0.0098	0.0119	0.0166
15	0.0022	0.0025	0.0029	0.0022	0.0025	0.0029
16	0.0092	0.0100	0.0101	0.0085	0.0098	0.0101
17	0.0089	0.0118	0.0129	0.0102	0.0112	0.0129
18	0.0169	0.0232	0.0259	0.0206	0.0220	0.0259
19	0.0268	0.0364	0.0365	0.0328	0.0332	0.0365
20	0.0060	0.0032	0.0111	0.0034	0.0068	0.0111
21	0.0191	0.0241	0.0219	0.0206	0.0217	0.0241
22	0.0229	0.0237	0.0231	0.0221	0.0232	0.0237
23	0.0256	0.0323	0.0370	0.0280	0.0316	0.0370
24	0.0069	0.0096	0.0094	0.0083	0.0086	0.0096
25	0.0171	0.0199	0.0278	0.0177	0.0216	0.0278
26	0.0298	0.0480	0.0610	0.0428	0.0463	0.0610
27	0.0239	0.0271	0.0239	0.0245	0.0250	0.0271
28	0.0195	0.0236	0.0208	0.0208	0.0213	0.0236
29	0.0212	0.0278	0.0417	0.0257	0.0302	0.0417
30	0.0120	0.0162	0.0136	0.0137	0.0139	0.0162
31	0.0119	0.0192	0.0194	0.0159	0.0168	0.0194
32	0.0526	0.0550	0.0490	0.0521	0.0522	0.0550
33	0.0114	0.0155	0.0161	0.0134	0.0143	0.0161
34	0.0131	0.0167	0.0178	0.0144	0.0159	0.0178
35	0.0542	0.0523	0.0491	0.0505	0.0519	0.0542
36	0.0403	0.0468	0.0468	0.0440	0.0446	0.0468
37	0.0442	0.0431	0.0391	0.0405	0.0421	0.0442
38	0.0638	0.0698	0.0709	0.0671	0.0682	0.0709
39	0.0155	0.0206	0.0211	0.0164	0.0191	0.0211
40	0.0158	0.0219	0.0254	0.0197	0.0210	0.0254
41	0.0103	0.0128	0.0126	0.0106	0.0119	0.0128
42	0.0228	0.0237	0.0214	0.0217	0.0226	0.0237
43	0.0083	0.0116	0.0127	0.0100	0.0109	0.0127
44	0.0119	0.0174	0.0230	0.0136	0.0174	0.0230
45	0.0659	0.0794	0.0731	0.0711	0.0728	0.0794
46	0.0161	0.0205	0.0189	0.0175	0.0185	0.0205
47	0.0224	0.0284	0.0326	0.0243	0.0278	0.0326
48	0.0236	0.0305	0.0336	0.0275	0.0292	0.0336
49	0.0530	0.0557	0.0526	0.0520	0.0538	0.0557
50	0.0387	0.0506	0.0667	0.0476	0.0520	0.0667
51	0.0396	0.0414	0.0394	0.0373	0.0401	0.0414
52	0.0801	0.0815	0.0693	0.0671	0.0769	0.0815
53	0.0470	0.0569	0.0527	0.0490	0.0522	0.0569
54	0.0889	0.0953	0.0904	0.0884	0.0915	0.0953
55	0.0569	0.0552	0.0500	0.0501	0.0540	0.0569

Table C.7 Drift ratio demands for the *ductile* 3-story building model.

ID #	IDR1	IDR2	IDR3	RDR	AIDR	MIDR
56	0.0646	0.0618	0.0595	0.0599	0.0620	0.0646
57	0.0594	0.0772	0.0979	0.0724	0.0782	0.0979
58	0.0173	0.0234	0.0283	0.0202	0.0230	0.0283
59	0.0327	0.0381	0.0413	0.0355	0.0374	0.0413
60	0.0127	0.0162	0.0189	0.0136	0.0159	0.0189
61	0.0268	0.0356	0.0341	0.0319	0.0322	0.0356
62	0.0529	0.0564	0.0599	0.0530	0.0564	0.0599
63	0.0279	0.0318	0.0352	0.0294	0.0316	0.0352
64	0.0255	0.0280	0.0257	0.0258	0.0264	0.0280
65	0.0129	0.0173	0.0211	0.0153	0.0171	0.0211
66	0.0104	0.0172	0.0183	0.0153	0.0153	0.0183
67	0.0904	0.0911	0.0765	0.0808	0.0860	0.0911
68	0.0064	0.0098	0.0099	0.0077	0.0087	0.0099
69	0.0182	0.0240	0.0280	0.0208	0.0234	0.0280
70	0.0365	0.0422	0.0404	0.0389	0.0397	0.0422
71	0.0061	0.0084	0.0071	0.0071	0.0072	0.0084
72	0.0067	0.0085	0.0096	0.0077	0.0083	0.0096
73	0.0010	0.0011	0.0014	0.0009	0.0012	0.0014
74	0.0034	0.0046	0.0041	0.0040	0.0040	0.0046
75	0.0047	0.0069	0.0064	0.0060	0.0060	0.0069
76	0.0062	0.0090	0.0085	0.0077	0.0079	0.0090
77	0.0086	0.0118	0.0114	0.0103	0.0106	0.0118
78	0.0083	0.0122	0.0115	0.0105	0.0107	0.0122
79	0.0080	0.0125	0.0125	0.0109	0.0110	0.0125
80	0.0091	0.0126	0.0127	0.0112	0.0115	0.0127
81	0.0091	0.0116	0.0105	0.0098	0.0104	0.0116
82	0.0063	0.0092	0.0088	0.0081	0.0081	0.0092
83	0.0012	0.0011	0.0017	0.0008	0.0013	0.0017
84	0.0031	0.0040	0.0060	0.0037	0.0043	0.0060
85	0.0036	0.0045	0.0039	0.0040	0.0040	0.0045
86	0.0157	0.0201	0.0170	0.0174	0.0176	0.0201
87	0.0346	0.0382	0.0372	0.0350	0.0367	0.0382
88	0.0157	0.0207	0.0200	0.0176	0.0188	0.0207
89	0.0113	0.0173	0.0185	0.0148	0.0157	0.0185
90	0.0075	0.0103	0.0092	0.0088	0.0090	0.0103
91	0.0188	0.0231	0.0204	0.0202	0.0207	0.0231
92	0.0056	0.0059	0.0074	0.0050	0.0063	0.0074
93	0.0043	0.0066	0.0066	0.0058	0.0058	0.0066
94	0.0068	0.0089	0.0086	0.0077	0.0081	0.0089
95	0.0159	0.0219	0.0211	0.0191	0.0196	0.0219
96	0.0194	0.0259	0.0274	0.0229	0.0243	0.0274
97	0.0065	0.0093	0.0096	0.0083	0.0085	0.0096
98	0.0126	0.0169	0.0229	0.0144	0.0175	0.0229
99	0.0055	0.0069	0.0067	0.0060	0.0064	0.0069
100	0.0099	0.0134	0.0116	0.0113	0.0116	0.0134
101	0.0059	0.0075	0.0062	0.0065	0.0065	0.0075
102	0.0017	0.0022	0.0020	0.0019	0.0020	0.0022
103	0.0021	0.0020	0.0026	0.0017	0.0022	0.0026
104	0.0036	0.0049	0.0049	0.0043	0.0045	0.0049
105	0.0097	0.0140	0.0116	0.0114	0.0118	0.0140
106	0.0245	0.0295	0.0278	0.0252	0.0273	0.0295
107	0.0157	0.0201	0.0170	0.0175	0.0176	0.0201
108	0.0091	0.0115	0.0142	0.0104	0.0116	0.0142
109	0.0120	0.0175	0.0138	0.0143	0.0144	0.0175
110	0.0058	0.0074	0.0083	0.0061	0.0072	0.0083

Table C.7 (continued) Drift ratio demands for the *ductile* 3-story building model.

ID #	IDR1	IDR2	IDR3	RDR	AIDR	MIDR
111	0.0051	0.0068	0.0070	0.0060	0.0063	0.0070
112	0.0034	0.0047	0.0048	0.0041	0.0043	0.0048
113	0.0041	0.0030	0.0061	0.0027	0.0044	0.0061
114	0.0106	0.0122	0.0148	0.0096	0.0125	0.0148
115	0.0161	0.0171	0.0177	0.0147	0.0170	0.0177
116	0.0113	0.0151	0.0162	0.0125	0.0142	0.0162
117	0.0096	0.0128	0.0140	0.0108	0.0121	0.0140
118	0.0090	0.0144	0.0158	0.0126	0.0131	0.0158
119	0.0088	0.0141	0.0150	0.0119	0.0126	0.0150
120	0.0131	0.0211	0.0203	0.0177	0.0182	0.0211
121	0.0089	0.0118	0.0118	0.0101	0.0108	0.0118
122	0.0102	0.0135	0.0167	0.0119	0.0135	0.0167
123	0.0062	0.0085	0.0075	0.0073	0.0074	0.0085
124	0.0090	0.0118	0.0105	0.0103	0.0105	0.0118
125	0.0099	0.0146	0.0160	0.0127	0.0135	0.0160
126	0.0053	0.0070	0.0075	0.0061	0.0066	0.0075
127	0.0090	0.0112	0.0118	0.0085	0.0107	0.0118
128	0.0123	0.0178	0.0177	0.0135	0.0159	0.0178
129	0.0136	0.0220	0.0307	0.0196	0.0221	0.0307
130	0.0126	0.0164	0.0130	0.0140	0.0140	0.0164
131	0.0318	0.0428	0.0440	0.0393	0.0395	0.0440
132	0.0097	0.0142	0.0142	0.0122	0.0127	0.0142
133	0.0180	0.0221	0.0191	0.0192	0.0197	0.0221
134	0.0057	0.0070	0.0072	0.0060	0.0066	0.0072
135	0.0144	0.0189	0.0145	0.0158	0.0159	0.0189
136	0.0115	0.0159	0.0133	0.0131	0.0136	0.0159
137	0.0207	0.0278	0.0284	0.0252	0.0256	0.0284
138	0.0059	0.0084	0.0087	0.0068	0.0077	0.0087
139	0.0069	0.0098	0.0101	0.0086	0.0090	0.0101
140	0.0098	0.0124	0.0105	0.0103	0.0109	0.0124

Table C.7 (continued) Drift ratio demands for the *ductile* 3-story building model.

ID #	IDR1	IDR2	IDR3	RDR	AIDR	MIDR
1	0.0102	0.0123	0.0097	0.0102	0.0107	0.0123
2	0.0128	0.0160	0.0152	0.0137	0.0147	0.0160
3	0.0094	0.0138	0.0198	0.0123	0.0143	0.0198
4	0.0256	0.0309	0.0288	0.0261	0.0284	0.0309
5	0.0095	0.0116	0.0124	0.0099	0.0112	0.0124
6	0.0139	0.0181	0.0210	0.0153	0.0177	0.0210
7	0.0083	0.0147	0.0147	0.0124	0.0126	0.0147
8	0.0070	0.0078	0.0110	0.0071	0.0086	0.0110
9	0.0190	0.0219	0.0197	0.0193	0.0202	0.0219
10	0.0041	0.0054	0.0050	0.0047	0.0048	0.0054
11	0.0101	0.0141	0.0183	0.0125	0.0142	0.0183
12	0.0102	0.0131	0.0114	0.0111	0.0115	0.0131
13	0.0102	0.0136	0.0183	0.0115	0.0140	0.0183
14	0.0088	0.0104	0.0166	0.0098	0.0119	0.0166
15	0.0022	0.0025	0.0029	0.0022	0.0025	0.0029
16	0.0092	0.0100	0.0101	0.0085	0.0098	0.0101
17	0.0089	0.0118	0.0129	0.0102	0.0112	0.0129
18	0.0169	0.0232	0.0259	0.0206	0.0220	0.0259
19	0.0272	0.0392	0.0365	0.0337	0.0343	0.0392
20	0.0060	0.0032	0.0111	0.0034	0.0068	0.0111
21	0.0191	0.0241	0.0219	0.0206	0.0217	0.0241
22	0.0229	0.0237	0.0231	0.0221	0.0232	0.0237
23	0.0218	0.0338	0.0381	0.0286	0.0312	0.0381
24	0.0069	0.0096	0.0094	0.0083	0.0086	0.0096
25	0.0171	0.0199	0.0278	0.0177	0.0216	0.0278
26	0.0506	0.0752	0.0849	0.0699	0.0702	0.0849
27	0.0239	0.0271	0.0239	0.0245	0.0250	0.0271
28	0.0195	0.0236	0.0208	0.0208	0.0213	0.0236
29	0.0147	0.0270	0.0477	0.0280	0.0298	0.0477
30	0.0120	0.0162	0.0136	0.0137	0.0139	0.0162
31	0.0119	0.0192	0.0194	0.0159	0.0168	0.0194
32	0.0623	0.0807	0.0823	0.0746	0.0751	0.0823
33	0.0114	0.0155	0.0161	0.0134	0.0143	0.0161
34	0.0131	0.0167	0.0178	0.0144	0.0159	0.0178
35	0.0712	0.0888	0.0946	0.0838	0.0849	0.0946
36	0.0524	0.0703	0.0742	0.0650	0.0656	0.0742
37	0.0867	0.1077	0.1129	0.1020	0.1025	0.1129
38	0.1572	0.1828	0.1901	0.1765	0.1767	0.1901
39	0.0155	0.0206	0.0211	0.0164	0.0191	0.0211
40	0.0158	0.0219	0.0254	0.0197	0.0210	0.0254
41	0.0103	0.0128	0.0126	0.0106	0.0119	0.0128
42	0.0228	0.0237	0.0214	0.0217	0.0226	0.0237
43	0.0083	0.0116	0.0127	0.0100	0.0109	0.0127
44	0.0119	0.0174	0.0230	0.0136	0.0174	0.0230
45	0.1376	0.1678	0.1754	0.1586	0.1602	0.1754
46	0.0161	0.0205	0.0189	0.0175	0.0185	0.0205
47	0.0224	0.0284	0.0326	0.0243	0.0278	0.0326
48	0.0236	0.0305	0.0336	0.0275	0.0292	0.0336
49	0.0888	0.1086	0.1129	0.1030	0.1034	0.1129
50	0.1075	0.1484	0.1578	0.1376	0.1379	0.1578
51	0.1462	0.1767	0.1808	0.1677	0.1679	0.1808
52	0.0822	0.0934	0.0775	0.0696	0.0844	0.0934
53	0.1083	0.1439	0.1544	0.1353	0.1356	0.1544
54	0.1959	0.2490	0.2457	0.2300	0.2302	0.2490
55	0.1160	0.1365	0.1366	0.1291	0.1297	0.1366

Table C.8 Drift ratio demands for the *brittle* 3-story building model.

ID #	IDR1	IDR2	IDR3	RDR	AIDR	MIDR
56	0.0569	0.0838	0.1060	0.0766	0.0822	0.1060
57	0.1658	0.2321	0.2541	0.2147	0.2173	0.2541
58	0.0173	0.0234	0.0283	0.0202	0.0230	0.0283
59	0.0425	0.0604	0.0674	0.0563	0.0568	0.0674
60	0.0127	0.0162	0.0189	0.0136	0.0159	0.0189
61	0.0456	0.0637	0.0690	0.0594	0.0595	0.0690
62	0.1024	0.1289	0.1453	0.1240	0.1255	0.1453
63	0.0384	0.0510	0.0531	0.0470	0.0475	0.0531
64	0.0255	0.0287	0.0257	0.0258	0.0266	0.0287
65	0.0129	0.0173	0.0211	0.0153	0.0171	0.0211
66	0.0104	0.0172	0.0183	0.0153	0.0153	0.0183
67	0.2101	0.2474	0.2540	0.2367	0.2372	0.2540
68	0.0064	0.0098	0.0099	0.0077	0.0087	0.0099
69	0.0182	0.0240	0.0280	0.0208	0.0234	0.0280
70	0.0726	0.0920	0.0966	0.0869	0.0871	0.0966
71	0.0061	0.0084	0.0071	0.0071	0.0072	0.0084
72	0.0067	0.0085	0.0096	0.0077	0.0083	0.0096
73	0.0010	0.0011	0.0014	0.0009	0.0012	0.0014
74	0.0034	0.0046	0.0041	0.0040	0.0040	0.0046
75	0.0047	0.0069	0.0064	0.0060	0.0060	0.0069
76	0.0062	0.0090	0.0085	0.0077	0.0079	0.0090
77	0.0086	0.0118	0.0114	0.0103	0.0106	0.0118
78	0.0083	0.0122	0.0115	0.0105	0.0107	0.0122
79	0.0080	0.0125	0.0125	0.0109	0.0110	0.0125
80	0.0091	0.0126	0.0127	0.0112	0.0115	0.0127
81	0.0091	0.0116	0.0105	0.0098	0.0104	0.0116
82	0.0063	0.0092	0.0088	0.0081	0.0081	0.0092
83	0.0012	0.0011	0.0017	0.0008	0.0013	0.0017
84	0.0031	0.0040	0.0060	0.0037	0.0043	0.0060
85	0.0036	0.0045	0.0039	0.0040	0.0040	0.0045
86	0.0157	0.0201	0.0170	0.0174	0.0176	0.0201
87	0.1007	0.1203	0.1233	0.1145	0.1147	0.1233
88	0.0157	0.0207	0.0200	0.0176	0.0188	0.0207
89	0.0113	0.0173	0.0185	0.0148	0.0157	0.0185
90	0.0075	0.0103	0.0092	0.0088	0.0090	0.0103
91	0.0188	0.0231	0.0204	0.0202	0.0207	0.0231
92	0.0056	0.0059	0.0074	0.0050	0.0063	0.0074
93	0.0043	0.0066	0.0066	0.0058	0.0058	0.0066
94	0.0068	0.0089	0.0086	0.0077	0.0081	0.0089
95	0.0159	0.0219	0.0211	0.0191	0.0196	0.0219
96	0.0194	0.0259	0.0274	0.0229	0.0243	0.0274
97	0.0065	0.0093	0.0096	0.0083	0.0085	0.0096
98	0.0126	0.0169	0.0229	0.0144	0.0175	0.0229
99	0.0055	0.0069	0.0067	0.0060	0.0064	0.0069
100	0.0099	0.0134	0.0116	0.0113	0.0116	0.0134
101	0.0059	0.0075	0.0062	0.0065	0.0065	0.0075
102	0.0017	0.0022	0.0020	0.0019	0.0020	0.0022
103	0.0021	0.0020	0.0026	0.0017	0.0022	0.0026
104	0.0036	0.0049	0.0049	0.0043	0.0045	0.0049
105	0.0097	0.0140	0.0116	0.0114	0.0118	0.0140
106	0.0245	0.0299	0.0248	0.0251	0.0264	0.0299
107	0.0157	0.0201	0.0170	0.0175	0.0176	0.0201
108	0.0091	0.0115	0.0142	0.0104	0.0116	0.0142
109	0.0120	0.0175	0.0138	0.0143	0.0144	0.0175
110	0.0058	0.0074	0.0083	0.0061	0.0072	0.0083

Table C.8 (continued) Drift ratio demands for the *brittle* 3-story building model.

ID #	IDR1	IDR2	IDR3	RDR	AIDR	MIDR
111	0.0051	0.0068	0.0070	0.0060	0.0063	0.0070
112	0.0034	0.0047	0.0048	0.0041	0.0043	0.0048
113	0.0041	0.0030	0.0061	0.0027	0.0044	0.0061
114	0.0106	0.0122	0.0148	0.0096	0.0125	0.0148
115	0.0161	0.0171	0.0177	0.0147	0.0170	0.0177
116	0.0113	0.0151	0.0162	0.0125	0.0142	0.0162
117	0.0096	0.0128	0.0140	0.0108	0.0121	0.0140
118	0.0090	0.0144	0.0158	0.0126	0.0131	0.0158
119	0.0088	0.0141	0.0150	0.0119	0.0126	0.0150
120	0.0131	0.0211	0.0203	0.0177	0.0182	0.0211
121	0.0089	0.0118	0.0118	0.0101	0.0108	0.0118
122	0.0102	0.0135	0.0167	0.0119	0.0135	0.0167
123	0.0062	0.0085	0.0075	0.0073	0.0074	0.0085
124	0.0090	0.0118	0.0105	0.0103	0.0105	0.0118
125	0.0099	0.0146	0.0160	0.0127	0.0135	0.0160
126	0.0053	0.0070	0.0075	0.0061	0.0066	0.0075
127	0.0090	0.0112	0.0118	0.0085	0.0107	0.0118
128	0.0123	0.0178	0.0177	0.0135	0.0159	0.0178
129	0.0136	0.0220	0.0307	0.0196	0.0221	0.0307
130	0.0126	0.0164	0.0130	0.0140	0.0140	0.0164
131	0.0584	0.0785	0.0854	0.0737	0.0741	0.0854
132	0.0097	0.0142	0.0142	0.0122	0.0127	0.0142
133	0.0180	0.0221	0.0191	0.0192	0.0197	0.0221
134	0.0057	0.0070	0.0072	0.0060	0.0066	0.0072
135	0.0144	0.0189	0.0145	0.0158	0.0159	0.0189
136	0.0115	0.0159	0.0133	0.0131	0.0136	0.0159
137	0.0207	0.0278	0.0284	0.0252	0.0256	0.0284
138	0.0059	0.0084	0.0087	0.0068	0.0077	0.0087
139	0.0069	0.0098	0.0101	0.0086	0.0090	0.0101
140	0.0098	0.0124	0.0105	0.0103	0.0109	0.0124

Table C.8 (continued) Drift ratio demands for the *brittle* 3-story building model.

ID #	IDR1	IDR2	IDR3	IDR4	IDR5	IDR6	IDR7	IDR8	IDR9	RDR	AIDR	MIDR
1	0.0065	0.0058	0.0055	0.0054	0.0057	0.0056	0.0080	0.0094	0.0080	0.0050	0.0066	0.0094
2	0.0164	0.0142	0.0126	0.0118	0.0128	0.0141	0.0173	0.0191	0.0158	0.0121	0.0149	0.0191
3	0.0145	0.0112	0.0076	0.0081	0.0104	0.0115	0.0150	0.0219	0.0208	0.0075	0.0134	0.0219
4	0.0246	0.0181	0.0154	0.0156	0.0167	0.0191	0.0239	0.0293	0.0285	0.0110	0.0212	0.0293
5	0.0078	0.0068	0.0066	0.0081	0.0078	0.0065	0.0068	0.0091	0.0095	0.0048	0.0077	0.0095
6	0.0112	0.0075	0.0054	0.0063	0.0065	0.0088	0.0128	0.0186	0.0181	0.0051	0.0106	0.0186
7	0.0105	0.0088	0.0082	0.0082	0.0078	0.0092	0.0107	0.0153	0.0155	0.0066	0.0105	0.0155
8	0.0067	0.0059	0.0060	0.0062	0.0060	0.0058	0.0067	0.0076	0.0068	0.0053	0.0064	0.0076
9	0.0095	0.0082	0.0099	0.0111	0.0126	0.0127	0.0139	0.0157	0.0147	0.0093	0.0120	0.0157
10	0.0054	0.0050	0.0049	0.0049	0.0048	0.0051	0.0062	0.0067	0.0053	0.0049	0.0054	0.0067
11	0.0099	0.0083	0.0086	0.0097	0.0109	0.0113	0.0106	0.0106	0.0113	0.0083	0.0101	0.0113
12	0.0059	0.0042	0.0038	0.0040	0.0045	0.0054	0.0059	0.0073	0.0080	0.0040	0.0054	0.0080
13	0.0085	0.0071	0.0064	0.0075	0.0074	0.0074	0.0091	0.0085	0.0081	0.0061	0.0078	0.0091
14	0.0137	0.0108	0.0109	0.0121	0.0130	0.0125	0.0135	0.0167	0.0180	0.0090	0.0135	0.0180
15	0.0021	0.0018	0.0018	0.0018	0.0018	0.0017	0.0019	0.0024	0.0027	0.0016	0.0020	0.0027
16	0.0052	0.0038	0.0044	0.0056	0.0055	0.0044	0.0052	0.0060	0.0055	0.0038	0.0051	0.0060
17	0.0124	0.0106	0.0096	0.0107	0.0111	0.0106	0.0106	0.0111	0.0095	0.0097	0.0107	0.0124
18	0.0105	0.0064	0.0075	0.0104	0.0118	0.0109	0.0105	0.0164	0.0183	0.0054	0.0114	0.0183
19	0.0145	0.0097	0.0081	0.0088	0.0092	0.0135	0.0189	0.0278	0.0263	0.0075	0.0152	0.0278
20	0.0031	0.0021	0.0027	0.0036	0.0027	0.0038	0.0034	0.0043	0.0069	0.0015	0.0036	0.0069
21	0.0133	0.0108	0.0117	0.0123	0.0111	0.0127	0.0169	0.0229	0.0240	0.0078	0.0151	0.0240
22	0.0214	0.0170	0.0139	0.0147	0.0185	0.0202	0.0216	0.0305	0.0329	0.0122	0.0212	0.0329
23	0.0248	0.0210	0.0193	0.0165	0.0162	0.0207	0.0294	0.0378	0.0340	0.0149	0.0244	0.0378
24	0.0231	0.0206	0.0200	0.0207	0.0201	0.0191	0.0200	0.0200	0.0155	0.0197	0.0199	0.0231
25	0.0157	0.0118	0.0100	0.0163	0.0183	0.0161	0.0173	0.0230	0.0233	0.0106	0.0169	0.0233
26	0.0287	0.0184	0.0169	0.0241	0.0285	0.0259	0.0244	0.0344	0.0361	0.0139	0.0264	0.0361
27	0.0271	0.0254	0.0264	0.0283	0.0272	0.0227	0.0248	0.0279	0.0238	0.0204	0.0260	0.0283
28	0.0354	0.0323	0.0327	0.0341	0.0311	0.0331	0.0409	0.0479	0.0415	0.0299	0.0365	0.0479
29	0.0265	0.0243	0.0251	0.0252	0.0240	0.0271	0.0336	0.0386	0.0324	0.0209	0.0285	0.0386
30	0.0254	0.0223	0.0213	0.0212	0.0191	0.0183	0.0209	0.0219	0.0173	0.0188	0.0209	0.0254
31	0.0105	0.0089	0.0077	0.0076	0.0081	0.0077	0.0090	0.0100	0.0132	0.0063	0.0092	0.0132
32	0.0791	0.0695	0.0666	0.0688	0.0678	0.0657	0.0711	0.0726	0.0561	0.0642	0.0686	0.0791
33	0.0277	0.0241	0.0245	0.0257	0.0244	0.0223	0.0230	0.0250	0.0201	0.0231	0.0241	0.0277
34	0.0147	0.0122	0.0134	0.0167	0.0177	0.0154	0.0158	0.0192	0.0194	0.0113	0.0161	0.0194
35	0.0394	0.0342	0.0365	0.0399	0.0387	0.0373	0.0397	0.0398	0.0302	0.0357	0.0373	0.0399
36	0.0604	0.0530	0.0517	0.0550	0.0563	0.0550	0.0582	0.0601	0.0491	0.0508	0.0554	0.0604
37	0.0619	0.0530	0.0498	0.0535	0.0540	0.0513	0.0507	0.0491	0.0396	0.0483	0.0514	0.0619
38	0.0594	0.0495	0.0456	0.0507	0.0537	0.0578	0.0712	0.0788	0.0648	0.0526	0.0590	0.0788
39	0.0264	0.0231	0.0239	0.0239	0.0240	0.0240	0.0265	0.0263	0.0201	0.0225	0.0242	0.0265
40	0.0354	0.0300	0.0321	0.0339	0.0300	0.0261	0.0327	0.0377	0.0325	0.0264	0.0323	0.0377
41	0.0312	0.0269	0.0260	0.0256	0.0261	0.0252	0.0273	0.0321	0.0292	0.0255	0.0277	0.0321
42	0.0276	0.0230	0.0212	0.0209	0.0202	0.0197	0.0217	0.0251	0.0197	0.0174	0.0221	0.0276
43	0.0138	0.0126	0.0128	0.0138	0.0131	0.0108	0.0122	0.0140	0.0121	0.0109	0.0128	0.0140
44	0.0135	0.0092	0.0095	0.0082	0.0090	0.0134	0.0183	0.0214	0.0237	0.0060	0.0140	0.0237
45	0.0927	0.0814	0.0769	0.0796	0.0819	0.0828	0.0950	0.1029	0.0850	0.0810	0.0865	0.1029
46	0.0143	0.0113	0.0120	0.0124	0.0122	0.0130	0.0161	0.0199	0.0190	0.0097	0.0145	0.0199
47	0.0501	0.0451	0.0464	0.0472	0.0442	0.0447	0.0518	0.0540	0.0446	0.0404	0.0475	0.0540
48	0.0296	0.0236	0.0238	0.0270	0.0285	0.0265	0.0275	0.0360	0.0358	0.0233	0.0287	0.0360
49	0.0880	0.0790	0.0770	0.0775	0.0734	0.0680	0.0698	0.0725	0.0569	0.0711	0.0736	0.0880
50	0.0397	0.0312	0.0345	0.0399	0.0402	0.0385	0.0446	0.0668	0.0664	0.0320	0.0446	0.0668
51	0.0672	0.0589	0.0549	0.0533	0.0519	0.0498	0.0547	0.0588	0.0495	0.0469	0.0554	0.0672
52	0.0788	0.0650	0.0630	0.0610	0.0650	0.0760	0.0943	0.1124	0.0970	0.0588	0.0792	0.1124
53	0.0425	0.0362	0.0349	0.0373	0.0349	0.0384	0.0530	0.0688	0.0646	0.0362	0.0456	0.0688
54	0.1034	0.0902	0.0869	0.0826	0.0695	0.0740	0.0905	0.0970	0.0816	0.0706	0.0862	0.1034
55	0.0709	0.0626	0.0590	0.0546	0.0482	0.0539	0.0654	0.0790	0.0678	0.0455	0.0624	0.0790

Table C.9 Drift ratio demands for the *elastic* 9-story building model.

ID #	IDR1	IDR2	IDR3	IDR4	IDR5	IDR6	IDR7	IDR8	IDR9	RDR	AIDR	MIDR
56	0.1081	0.0939	0.0954	0.0992	0.0942	0.0864	0.0941	0.1020	0.0847	0.0863	0.0953	0.1081
57	0.0720	0.0566	0.0435	0.0407	0.0541	0.0665	0.0881	0.1028	0.0973	0.0490	0.0691	0.1028
58	0.0165	0.0147	0.0128	0.0150	0.0157	0.0147	0.0185	0.0212	0.0209	0.0114	0.0167	0.0212
59	0.0239	0.0216	0.0212	0.0193	0.0185	0.0197	0.0291	0.0356	0.0305	0.0160	0.0244	0.0356
60	0.0169	0.0132	0.0132	0.0160	0.0168	0.0152	0.0142	0.0173	0.0166	0.0125	0.0155	0.0173
61	0.0392	0.0341	0.0317	0.0326	0.0314	0.0306	0.0411	0.0446	0.0343	0.0306	0.0355	0.0446
62	0.0602	0.0508	0.0442	0.0440	0.0474	0.0521	0.0622	0.0714	0.0623	0.0385	0.0549	0.0714
63	0.0452	0.0360	0.0335	0.0318	0.0345	0.0363	0.0377	0.0404	0.0370	0.0281	0.0369	0.0452
64	0.0244	0.0224	0.0224	0.0231	0.0222	0.0210	0.0226	0.0234	0.0226	0.0219	0.0227	0.0244
65	0.0154	0.0132	0.0125	0.0124	0.0124	0.0138	0.0169	0.0186	0.0153	0.0125	0.0145	0.0186
66	0.0135	0.0111	0.0094	0.0093	0.0109	0.0130	0.0171	0.0199	0.0175	0.0090	0.0135	0.0199
67	0.0887	0.0736	0.0683	0.0590	0.0558	0.0684	0.0816	0.0895	0.0775	0.0544	0.0736	0.0895
68	0.0078	0.0060	0.0047	0.0042	0.0044	0.0054	0.0072	0.0087	0.0077	0.0041	0.0062	0.0087
69	0.0419	0.0371	0.0356	0.0351	0.0366	0.0377	0.0418	0.0441	0.0364	0.0364	0.0385	0.0441
70	0.0381	0.0336	0.0314	0.0309	0.0324	0.0349	0.0408	0.0428	0.0344	0.0308	0.0355	0.0428
71	0.0041	0.0037	0.0035	0.0033	0.0036	0.0037	0.0040	0.0057	0.0059	0.0028	0.0042	0.0059
72	0.0081	0.0074	0.0073	0.0074	0.0070	0.0072	0.0080	0.0082	0.0066	0.0069	0.0075	0.0082
73	0.0012	0.0011	0.0011	0.0010	0.0010	0.0010	0.0011	0.0012	0.0014	0.0010	0.0011	0.0014
74	0.0022	0.0017	0.0014	0.0018	0.0021	0.0020	0.0022	0.0028	0.0026	0.0013	0.0021	0.0028
75	0.0071	0.0062	0.0057	0.0062	0.0065	0.0068	0.0079	0.0082	0.0064	0.0062	0.0068	0.0082
76	0.0049	0.0034	0.0022	0.0030	0.0035	0.0035	0.0038	0.0069	0.0075	0.0018	0.0043	0.0075
77	0.0047	0.0045	0.0044	0.0039	0.0030	0.0039	0.0056	0.0070	0.0060	0.0025	0.0048	0.0070
78	0.0042	0.0034	0.0031	0.0033	0.0036	0.0038	0.0050	0.0058	0.0063	0.0029	0.0043	0.0063
79	0.0043	0.0035	0.0031	0.0031	0.0035	0.0040	0.0057	0.0068	0.0063	0.0028	0.0045	0.0068
80	0.0057	0.0048	0.0041	0.0046	0.0041	0.0048	0.0067	0.0082	0.0078	0.0030	0.0056	0.0082
81	0.0049	0.0042	0.0043	0.0041	0.0033	0.0041	0.0057	0.0067	0.0061	0.0032	0.0048	0.0067
82	0.0049	0.0044	0.0043	0.0041	0.0041	0.0044	0.0054	0.0063	0.0055	0.0041	0.0048	0.0063
83	0.0009	0.0007	0.0008	0.0008	0.0008	0.0007	0.0010	0.0012	0.0013	0.0006	0.0009	0.0013
84	0.0075	0.0063	0.0058	0.0069	0.0074	0.0074	0.0084	0.0084	0.0066	0.0061	0.0072	0.0084
85	0.0056	0.0050	0.0047	0.0050	0.0053	0.0054	0.0058	0.0058	0.0047	0.0049	0.0053	0.0058
86	0.0097	0.0076	0.0076	0.0079	0.0076	0.0082	0.0113	0.0135	0.0114	0.0075	0.0094	0.0135
87	0.0211	0.0174	0.0143	0.0156	0.0181	0.0202	0.0271	0.0326	0.0284	0.0157	0.0216	0.0326
88	0.0152	0.0121	0.0126	0.0142	0.0138	0.0126	0.0158	0.0205	0.0186	0.0118	0.0150	0.0205
89	0.0074	0.0063	0.0069	0.0070	0.0067	0.0074	0.0076	0.0088	0.0089	0.0057	0.0074	0.0089
90	0.0068	0.0060	0.0059	0.0060	0.0060	0.0058	0.0068	0.0074	0.0060	0.0056	0.0063	0.0074
91	0.0130	0.0116	0.0105	0.0086	0.0104	0.0136	0.0184	0.0207	0.0176	0.0101	0.0138	0.0207
92	0.0056	0.0047	0.0047	0.0051	0.0047	0.0046	0.0045	0.0048	0.0059	0.0040	0.0050	0.0059
93	0.0069	0.0058	0.0057	0.0064	0.0067	0.0066	0.0067	0.0068	0.0058	0.0057	0.0064	0.0069
94	0.0088	0.0078	0.0079	0.0086	0.0089	0.0091	0.0104	0.0108	0.0085	0.0086	0.0090	0.0108
95	0.0145	0.0114	0.0099	0.0087	0.0097	0.0115	0.0178	0.0226	0.0206	0.0086	0.0141	0.0226
96	0.0134	0.0124	0.0138	0.0139	0.0130	0.0149	0.0191	0.0204	0.0188	0.0114	0.0155	0.0204
97	0.0061	0.0049	0.0042	0.0049	0.0052	0.0053	0.0060	0.0071	0.0069	0.0045	0.0056	0.0071
98	0.0176	0.0142	0.0141	0.0137	0.0144	0.0161	0.0202	0.0219	0.0225	0.0127	0.0172	0.0225
99	0.0070	0.0061	0.0063	0.0066	0.0059	0.0055	0.0059	0.0059	0.0058	0.0052	0.0061	0.0070
100	0.0137	0.0117	0.0116	0.0129	0.0132	0.0132	0.0141	0.0140	0.0116	0.0124	0.0129	0.0141
101	0.0074	0.0064	0.0064	0.0070	0.0071	0.0068	0.0073	0.0077	0.0059	0.0065	0.0069	0.0077
102	0.0031	0.0027	0.0026	0.0027	0.0026	0.0025	0.0026	0.0029	0.0028	0.0024	0.0027	0.0031
103	0.0026	0.0024	0.0023	0.0021	0.0021	0.0019	0.0020	0.0024	0.0022	0.0018	0.0022	0.0026
104	0.0188	0.0167	0.0163	0.0164	0.0152	0.0140	0.0147	0.0146	0.0112	0.0143	0.0153	0.0188
105	0.0072	0.0061	0.0063	0.0069	0.0076	0.0082	0.0092	0.0106	0.0100	0.0065	0.0080	0.0106
106	0.0394	0.0351	0.0353	0.0359	0.0324	0.0321	0.0371	0.0395	0.0321	0.0308	0.0354	0.0395
107	0.0345	0.0314	0.0309	0.0311	0.0291	0.0272	0.0281	0.0278	0.0213	0.0278	0.0290	0.0345
108	0.0157	0.0138	0.0135	0.0142	0.0134	0.0123	0.0123	0.0123	0.0097	0.0122	0.0130	0.0157
109	0.0074	0.0054	0.0049	0.0047	0.0056	0.0072	0.0086	0.0125	0.0122	0.0043	0.0076	0.0125
110	0.0070	0.0063	0.0062	0.0063	0.0060	0.0056	0.0063	0.0071	0.0073	0.0059	0.0065	0.0073

Table C.9 (continued) Drift ratio demands for the *elastic* 9-story building model.

ID #	IDR1	IDR2	IDR3	IDR4	IDR5	IDR6	IDR7	IDR8	IDR9	RDR	AIDR	MIDR
111	0.0034	0.0026	0.0027	0.0028	0.0028	0.0031	0.0037	0.0045	0.0048	0.0024	0.0034	0.0048
112	0.0019	0.0015	0.0015	0.0016	0.0016	0.0017	0.0023	0.0034	0.0034	0.0015	0.0021	0.0034
113	0.0034	0.0030	0.0029	0.0034	0.0037	0.0036	0.0035	0.0037	0.0040	0.0031	0.0035	0.0040
114	0.0124	0.0108	0.0096	0.0093	0.0098	0.0102	0.0137	0.0162	0.0128	0.0084	0.0116	0.0162
115	0.0139	0.0115	0.0091	0.0098	0.0114	0.0111	0.0141	0.0182	0.0161	0.0091	0.0128	0.0182
116	0.0115	0.0099	0.0084	0.0094	0.0100	0.0107	0.0107	0.0141	0.0136	0.0071	0.0109	0.0141
117	0.0076	0.0067	0.0075	0.0076	0.0075	0.0082	0.0090	0.0117	0.0119	0.0046	0.0086	0.0119
118	0.0156	0.0131	0.0132	0.0139	0.0131	0.0120	0.0128	0.0136	0.0109	0.0120	0.0131	0.0156
119	0.0153	0.0138	0.0141	0.0149	0.0146	0.0136	0.0138	0.0134	0.0133	0.0135	0.0141	0.0153
120	0.0223	0.0182	0.0167	0.0167	0.0173	0.0181	0.0249	0.0323	0.0297	0.0154	0.0218	0.0323
121	0.0180	0.0156	0.0166	0.0177	0.0172	0.0166	0.0197	0.0226	0.0202	0.0163	0.0182	0.0226
122	0.0118	0.0093	0.0095	0.0095	0.0079	0.0078	0.0095	0.0117	0.0130	0.0059	0.0100	0.0130
123	0.0092	0.0082	0.0081	0.0082	0.0079	0.0077	0.0085	0.0089	0.0074	0.0073	0.0082	0.0092
124	0.0072	0.0065	0.0061	0.0059	0.0056	0.0055	0.0061	0.0075	0.0075	0.0053	0.0064	0.0075
125	0.0078	0.0065	0.0069	0.0078	0.0074	0.0072	0.0075	0.0095	0.0090	0.0055	0.0077	0.0095
126	0.0104	0.0094	0.0091	0.0091	0.0084	0.0084	0.0095	0.0103	0.0083	0.0082	0.0092	0.0104
127	0.0038	0.0036	0.0034	0.0033	0.0034	0.0037	0.0039	0.0045	0.0047	0.0027	0.0038	0.0047
128	0.0094	0.0071	0.0059	0.0084	0.0102	0.0105	0.0102	0.0135	0.0130	0.0052	0.0098	0.0135
129	0.0167	0.0123	0.0095	0.0080	0.0098	0.0151	0.0238	0.0304	0.0271	0.0079	0.0169	0.0304
130	0.0232	0.0207	0.0197	0.0188	0.0178	0.0193	0.0236	0.0262	0.0217	0.0180	0.0212	0.0262
131	0.0218	0.0175	0.0177	0.0162	0.0184	0.0179	0.0217	0.0232	0.0206	0.0139	0.0194	0.0232
132	0.0097	0.0087	0.0089	0.0102	0.0100	0.0090	0.0097	0.0121	0.0114	0.0089	0.0100	0.0121
133	0.0120	0.0094	0.0077	0.0087	0.0093	0.0108	0.0123	0.0140	0.0127	0.0082	0.0108	0.0140
134	0.0123	0.0109	0.0107	0.0112	0.0107	0.0098	0.0101	0.0115	0.0097	0.0102	0.0107	0.0123
135	0.0151	0.0135	0.0130	0.0134	0.0133	0.0131	0.0136	0.0146	0.0124	0.0131	0.0135	0.0151
136	0.0183	0.0161	0.0158	0.0158	0.0161	0.0161	0.0178	0.0182	0.0141	0.0156	0.0165	0.0183
137	0.0235	0.0211	0.0206	0.0208	0.0198	0.0193	0.0227	0.0262	0.0229	0.0186	0.0219	0.0262
138	0.0138	0.0115	0.0098	0.0101	0.0102	0.0090	0.0098	0.0120	0.0102	0.0081	0.0107	0.0138
139	0.0053	0.0045	0.0044	0.0043	0.0043	0.0050	0.0055	0.0057	0.0062	0.0036	0.0050	0.0062
140	0.0160	0.0145	0.0148	0.0155	0.0155	0.0152	0.0156	0.0160	0.0130	0.0140	0.0151	0.0160

Table C.9 (continued) Drift ratio demands for the *elastic* 9-story building model.

ID #	IDR1	IDR2	IDR3	IDR4	IDR5	IDR6	IDR7	IDR8	IDR9	RDR	AIDR	MIDR
1	0.0065	0.0058	0.0055	0.0053	0.0057	0.0056	0.0081	0.0095	0.0081	0.0051	0.0067	0.0095
2	0.0132	0.0116	0.0095	0.0097	0.0097	0.0102	0.0144	0.0166	0.0124	0.0092	0.0119	0.0166
3	0.0089	0.0076	0.0055	0.0066	0.0096	0.0106	0.0127	0.0174	0.0179	0.0051	0.0107	0.0179
4	0.0166	0.0176	0.0178	0.0166	0.0162	0.0178	0.0233	0.0259	0.0198	0.0108	0.0191	0.0259
5	0.0078	0.0069	0.0065	0.0080	0.0077	0.0065	0.0069	0.0090	0.0093	0.0049	0.0076	0.0093
6	0.0079	0.0062	0.0054	0.0063	0.0051	0.0082	0.0127	0.0184	0.0152	0.0039	0.0095	0.0184
7	0.0095	0.0082	0.0075	0.0077	0.0070	0.0084	0.0109	0.0159	0.0158	0.0070	0.0101	0.0159
8	0.0067	0.0059	0.0061	0.0063	0.0060	0.0057	0.0066	0.0075	0.0066	0.0053	0.0064	0.0075
9	0.0080	0.0082	0.0100	0.0115	0.0131	0.0127	0.0154	0.0174	0.0125	0.0092	0.0121	0.0174
10	0.0054	0.0049	0.0049	0.0049	0.0048	0.0052	0.0063	0.0068	0.0054	0.0049	0.0054	0.0068
11	0.0099	0.0083	0.0085	0.0096	0.0109	0.0113	0.0104	0.0105	0.0115	0.0082	0.0101	0.0115
12	0.0059	0.0042	0.0039	0.0040	0.0046	0.0054	0.0060	0.0071	0.0079	0.0040	0.0054	0.0079
13	0.0086	0.0072	0.0065	0.0076	0.0075	0.0074	0.0092	0.0086	0.0081	0.0062	0.0078	0.0092
14	0.0117	0.0096	0.0096	0.0106	0.0109	0.0107	0.0123	0.0141	0.0166	0.0078	0.0118	0.0166
15	0.0020	0.0018	0.0017	0.0017	0.0017	0.0016	0.0018	0.0022	0.0026	0.0015	0.0019	0.0026
16	0.0052	0.0038	0.0044	0.0055	0.0054	0.0044	0.0053	0.0061	0.0056	0.0039	0.0051	0.0061
17	0.0116	0.0101	0.0093	0.0103	0.0104	0.0099	0.0100	0.0109	0.0094	0.0096	0.0102	0.0116
18	0.0091	0.0060	0.0064	0.0099	0.0104	0.0106	0.0120	0.0159	0.0175	0.0059	0.0109	0.0175
19	0.0088	0.0079	0.0081	0.0089	0.0086	0.0097	0.0171	0.0241	0.0208	0.0062	0.0127	0.0241
20	0.0031	0.0021	0.0026	0.0036	0.0026	0.0038	0.0033	0.0042	0.0067	0.0014	0.0036	0.0067
21	0.0115	0.0111	0.0119	0.0126	0.0104	0.0091	0.0150	0.0251	0.0256	0.0078	0.0147	0.0256
22	0.0128	0.0102	0.0106	0.0125	0.0144	0.0143	0.0164	0.0299	0.0381	0.0107	0.0177	0.0381
23	0.0144	0.0125	0.0093	0.0115	0.0156	0.0168	0.0173	0.0279	0.0301	0.0088	0.0173	0.0301
24	0.0154	0.0151	0.0140	0.0135	0.0115	0.0111	0.0128	0.0132	0.0104	0.0114	0.0130	0.0154
25	0.0112	0.0094	0.0088	0.0112	0.0142	0.0160	0.0194	0.0203	0.0232	0.0108	0.0149	0.0232
26	0.0181	0.0146	0.0138	0.0201	0.0238	0.0195	0.0287	0.0358	0.0389	0.0150	0.0237	0.0389
27	0.0197	0.0243	0.0267	0.0233	0.0159	0.0152	0.0194	0.0238	0.0191	0.0137	0.0208	0.0267
28	0.0249	0.0254	0.0254	0.0255	0.0268	0.0236	0.0218	0.0243	0.0192	0.0210	0.0241	0.0268
29	0.0149	0.0138	0.0162	0.0168	0.0153	0.0133	0.0200	0.0299	0.0360	0.0141	0.0196	0.0360
30	0.0264	0.0309	0.0320	0.0288	0.0202	0.0135	0.0154	0.0167	0.0120	0.0189	0.0218	0.0320
31	0.0104	0.0089	0.0076	0.0075	0.0079	0.0076	0.0087	0.0099	0.0134	0.0061	0.0091	0.0134
32	0.1061	0.1014	0.0915	0.0832	0.0387	0.0223	0.0177	0.0215	0.0183	0.0507	0.0556	0.1061
33	0.0271	0.0316	0.0335	0.0296	0.0210	0.0140	0.0123	0.0140	0.0125	0.0194	0.0217	0.0335
34	0.0144	0.0119	0.0121	0.0168	0.0177	0.0138	0.0176	0.0209	0.0207	0.0129	0.0162	0.0209
35	0.1249	0.1179	0.0916	0.0757	0.0472	0.0320	0.0235	0.0269	0.0246	0.0615	0.0627	0.1249
36	0.1463	0.1386	0.1098	0.0910	0.0461	0.0243	0.0258	0.0280	0.0238	0.0670	0.0704	0.1463
37	0.1321	0.1271	0.1028	0.0843	0.0431	0.0278	0.0268	0.0329	0.0314	0.0673	0.0676	0.1321
38	0.0664	0.0728	0.0739	0.0718	0.0549	0.0436	0.0367	0.0365	0.0305	0.0493	0.0541	0.0739
39	0.0373	0.0381	0.0346	0.0285	0.0182	0.0120	0.0194	0.0259	0.0222	0.0219	0.0262	0.0381
40	0.0572	0.0559	0.0516	0.0431	0.0327	0.0228	0.0166	0.0180	0.0168	0.0314	0.0350	0.0572
41	0.0388	0.0401	0.0356	0.0284	0.0179	0.0117	0.0163	0.0207	0.0162	0.0221	0.0251	0.0401
42	0.0258	0.0279	0.0282	0.0263	0.0191	0.0125	0.0236	0.0268	0.0190	0.0152	0.0232	0.0282
43	0.0121	0.0114	0.0131	0.0142	0.0117	0.0095	0.0102	0.0128	0.0115	0.0096	0.0118	0.0142
44	0.0108	0.0074	0.0082	0.0080	0.0077	0.0097	0.0135	0.0188	0.0183	0.0055	0.0114	0.0188
45	0.0319	0.0355	0.0482	0.0533	0.0470	0.0381	0.0366	0.0401	0.0412	0.0344	0.0413	0.0533
46	0.0125	0.0112	0.0135	0.0139	0.0121	0.0118	0.0164	0.0178	0.0169	0.0093	0.0140	0.0178
47	0.0417	0.0437	0.0433	0.0418	0.0345	0.0222	0.0219	0.0265	0.0199	0.0275	0.0328	0.0437
48	0.0177	0.0166	0.0213	0.0242	0.0209	0.0144	0.0231	0.0290	0.0270	0.0154	0.0216	0.0290
49	0.0450	0.0492	0.0472	0.0414	0.0329	0.0281	0.0330	0.0347	0.0290	0.0341	0.0379	0.0492
50	0.0441	0.0441	0.0468	0.0458	0.0394	0.0368	0.0333	0.0438	0.0425	0.0318	0.0418	0.0468
51	0.0357	0.0352	0.0364	0.0405	0.0389	0.0349	0.0320	0.0306	0.0240	0.0280	0.0343	0.0405
52	0.0913	0.0909	0.0687	0.0568	0.0315	0.0283	0.0406	0.0402	0.0384	0.0424	0.0541	0.0913
53	0.0240	0.0265	0.0258	0.0244	0.0195	0.0216	0.0401	0.0424	0.0378	0.0234	0.0291	0.0424
54	0.1449	0.1350	0.0999	0.0776	0.0509	0.0338	0.0503	0.0485	0.0426	0.0607	0.0759	0.1449
55	0.0703	0.0671	0.0575	0.0517	0.0294	0.0264	0.0326	0.0334	0.0312	0.0331	0.0444	0.0703

Table C.10 Drift ratio demands for the *ductile* 9-story building model.

ID #	IDR1	IDR2	IDR3	IDR4	IDR5	IDR6	IDR7	IDR8	IDR9	RDR	AIDR	MIDR
56	0.0659	0.0619	0.0515	0.0517	0.0373	0.0373	0.0428	0.0443	0.0361	0.0312	0.0477	0.0659
57	0.0452	0.0463	0.0453	0.0391	0.0308	0.0315	0.0466	0.0480	0.0435	0.0355	0.0418	0.0480
58	0.0125	0.0108	0.0133	0.0162	0.0128	0.0118	0.0192	0.0191	0.0199	0.0088	0.0151	0.0199
59	0.0130	0.0151	0.0157	0.0157	0.0137	0.0138	0.0230	0.0316	0.0277	0.0108	0.0188	0.0316
60	0.0121	0.0109	0.0123	0.0183	0.0199	0.0150	0.0124	0.0142	0.0125	0.0113	0.0142	0.0199
61	0.0365	0.0366	0.0305	0.0245	0.0196	0.0158	0.0376	0.0417	0.0342	0.0194	0.0308	0.0417
62	0.0446	0.0505	0.0493	0.0451	0.0389	0.0353	0.0319	0.0330	0.0276	0.0324	0.0396	0.0505
63	0.0218	0.0256	0.0289	0.0281	0.0213	0.0210	0.0225	0.0279	0.0223	0.0173	0.0244	0.0289
64	0.0184	0.0203	0.0186	0.0143	0.0116	0.0154	0.0274	0.0303	0.0248	0.0158	0.0201	0.0303
65	0.0121	0.0109	0.0116	0.0128	0.0120	0.0116	0.0150	0.0161	0.0124	0.0116	0.0127	0.0161
66	0.0118	0.0098	0.0084	0.0087	0.0099	0.0106	0.0157	0.0201	0.0157	0.0087	0.0123	0.0201
67	0.0786	0.0779	0.0736	0.0684	0.0468	0.0303	0.0291	0.0381	0.0379	0.0489	0.0534	0.0786
68	0.0078	0.0060	0.0047	0.0041	0.0044	0.0055	0.0073	0.0087	0.0075	0.0040	0.0062	0.0087
69	0.0372	0.0349	0.0321	0.0339	0.0295	0.0257	0.0237	0.0224	0.0152	0.0240	0.0283	0.0372
70	0.0334	0.0392	0.0383	0.0358	0.0285	0.0185	0.0188	0.0267	0.0233	0.0252	0.0292	0.0392
71	0.0041	0.0037	0.0035	0.0033	0.0037	0.0037	0.0039	0.0056	0.0057	0.0027	0.0041	0.0057
72	0.0081	0.0074	0.0073	0.0073	0.0071	0.0072	0.0081	0.0084	0.0065	0.0070	0.0075	0.0084
73	0.0012	0.0011	0.0010	0.0010	0.0010	0.0010	0.0010	0.0010	0.0013	0.0009	0.0011	0.0013
74	0.0022	0.0017	0.0014	0.0017	0.0020	0.0019	0.0023	0.0026	0.0024	0.0012	0.0020	0.0026
75	0.0071	0.0061	0.0057	0.0062	0.0065	0.0069	0.0080	0.0083	0.0066	0.0063	0.0068	0.0083
76	0.0048	0.0033	0.0021	0.0029	0.0036	0.0036	0.0039	0.0070	0.0077	0.0019	0.0043	0.0077
77	0.0047	0.0045	0.0044	0.0039	0.0029	0.0039	0.0057	0.0071	0.0061	0.0024	0.0048	0.0071
78	0.0042	0.0033	0.0030	0.0033	0.0036	0.0039	0.0049	0.0059	0.0061	0.0030	0.0043	0.0061
79	0.0043	0.0034	0.0030	0.0031	0.0035	0.0040	0.0057	0.0069	0.0063	0.0028	0.0045	0.0069
80	0.0056	0.0047	0.0040	0.0045	0.0041	0.0049	0.0068	0.0081	0.0076	0.0030	0.0056	0.0081
81	0.0048	0.0041	0.0043	0.0041	0.0034	0.0041	0.0056	0.0066	0.0060	0.0031	0.0048	0.0066
82	0.0048	0.0043	0.0042	0.0041	0.0040	0.0044	0.0054	0.0062	0.0054	0.0040	0.0047	0.0062
83	0.0009	0.0006	0.0008	0.0009	0.0008	0.0007	0.0009	0.0011	0.0011	0.0006	0.0009	0.0011
84	0.0075	0.0064	0.0059	0.0068	0.0073	0.0074	0.0083	0.0082	0.0065	0.0061	0.0071	0.0083
85	0.0055	0.0049	0.0046	0.0049	0.0053	0.0054	0.0057	0.0057	0.0046	0.0048	0.0052	0.0057
86	0.0095	0.0075	0.0076	0.0079	0.0075	0.0081	0.0108	0.0127	0.0105	0.0076	0.0091	0.0127
87	0.0141	0.0134	0.0128	0.0174	0.0215	0.0247	0.0313	0.0386	0.0398	0.0170	0.0237	0.0398
88	0.0130	0.0117	0.0113	0.0133	0.0114	0.0089	0.0132	0.0179	0.0153	0.0090	0.0129	0.0179
89	0.0075	0.0062	0.0068	0.0070	0.0067	0.0073	0.0075	0.0090	0.0087	0.0056	0.0074	0.0090
90	0.0068	0.0060	0.0058	0.0060	0.0060	0.0058	0.0069	0.0073	0.0059	0.0055	0.0063	0.0073
91	0.0113	0.0087	0.0070	0.0074	0.0094	0.0110	0.0181	0.0235	0.0191	0.0090	0.0128	0.0235
92	0.0055	0.0047	0.0047	0.0051	0.0046	0.0045	0.0045	0.0050	0.0060	0.0040	0.0050	0.0060
93	0.0070	0.0058	0.0057	0.0064	0.0067	0.0065	0.0066	0.0067	0.0056	0.0056	0.0063	0.0070
94	0.0087	0.0078	0.0079	0.0085	0.0088	0.0090	0.0103	0.0106	0.0083	0.0086	0.0089	0.0106
95	0.0110	0.0092	0.0074	0.0071	0.0076	0.0082	0.0137	0.0182	0.0152	0.0070	0.0108	0.0182
96	0.0126	0.0122	0.0123	0.0135	0.0129	0.0115	0.0176	0.0217	0.0200	0.0110	0.0149	0.0217
97	0.0061	0.0050	0.0043	0.0048	0.0052	0.0053	0.0059	0.0071	0.0067	0.0044	0.0056	0.0071
98	0.0143	0.0148	0.0162	0.0162	0.0131	0.0122	0.0153	0.0215	0.0204	0.0120	0.0160	0.0215
99	0.0069	0.0060	0.0062	0.0065	0.0058	0.0055	0.0059	0.0060	0.0059	0.0053	0.0061	0.0069
100	0.0131	0.0121	0.0113	0.0118	0.0110	0.0105	0.0126	0.0134	0.0104	0.0104	0.0118	0.0134
101	0.0074	0.0063	0.0064	0.0070	0.0070	0.0067	0.0073	0.0078	0.0060	0.0064	0.0069	0.0078
102	0.0030	0.0027	0.0027	0.0028	0.0027	0.0024	0.0025	0.0028	0.0027	0.0023	0.0027	0.0030
103	0.0026	0.0024	0.0023	0.0021	0.0020	0.0019	0.0019	0.0022	0.0021	0.0018	0.0022	0.0026
104	0.0149	0.0157	0.0153	0.0139	0.0111	0.0107	0.0109	0.0111	0.0087	0.0115	0.0125	0.0157
105	0.0071	0.0060	0.0064	0.0070	0.0075	0.0082	0.0092	0.0106	0.0098	0.0064	0.0080	0.0106
106	0.0236	0.0301	0.0336	0.0297	0.0205	0.0134	0.0133	0.0183	0.0192	0.0178	0.0224	0.0336
107	0.0174	0.0208	0.0211	0.0202	0.0149	0.0134	0.0180	0.0198	0.0141	0.0147	0.0178	0.0211
108	0.0139	0.0136	0.0121	0.0123	0.0113	0.0106	0.0112	0.0118	0.0094	0.0114	0.0118	0.0139
109	0.0071	0.0054	0.0048	0.0046	0.0055	0.0071	0.0086	0.0126	0.0122	0.0043	0.0075	0.0126
110	0.0070	0.0063	0.0061	0.0062	0.0059	0.0055	0.0062	0.0070	0.0075	0.0058	0.0064	0.0075

Table C.10 (continued) Drift ratio demands for the *ductile* 9-story building model.

ID #	IDR1	IDR2	IDR3	IDR4	IDR5	IDR6	IDR7	IDR8	IDR9	RDR	AIDR	MIDR
111	0.0034	0.0026	0.0026	0.0028	0.0028	0.0030	0.0036	0.0044	0.0047	0.0025	0.0033	0.0047
112	0.0019	0.0016	0.0015	0.0016	0.0016	0.0017	0.0024	0.0033	0.0032	0.0014	0.0021	0.0033
113	0.0034	0.0029	0.0029	0.0034	0.0036	0.0036	0.0035	0.0036	0.0042	0.0030	0.0034	0.0042
114	0.0102	0.0089	0.0091	0.0093	0.0096	0.0094	0.0139	0.0173	0.0133	0.0080	0.0112	0.0173
115	0.0128	0.0108	0.0080	0.0092	0.0099	0.0098	0.0153	0.0202	0.0163	0.0090	0.0125	0.0202
116	0.0111	0.0098	0.0085	0.0094	0.0100	0.0107	0.0105	0.0132	0.0129	0.0070	0.0107	0.0132
117	0.0076	0.0067	0.0074	0.0076	0.0074	0.0082	0.0089	0.0116	0.0118	0.0045	0.0086	0.0118
118	0.0134	0.0135	0.0128	0.0128	0.0116	0.0105	0.0111	0.0113	0.0094	0.0105	0.0118	0.0135
119	0.0125	0.0117	0.0123	0.0136	0.0122	0.0111	0.0114	0.0124	0.0124	0.0110	0.0122	0.0136
120	0.0140	0.0152	0.0165	0.0164	0.0136	0.0115	0.0168	0.0234	0.0218	0.0128	0.0166	0.0234
121	0.0161	0.0158	0.0148	0.0137	0.0132	0.0130	0.0146	0.0160	0.0135	0.0122	0.0145	0.0161
122	0.0114	0.0091	0.0093	0.0093	0.0079	0.0074	0.0090	0.0113	0.0128	0.0060	0.0097	0.0128
123	0.0092	0.0082	0.0081	0.0081	0.0080	0.0077	0.0086	0.0089	0.0072	0.0073	0.0082	0.0092
124	0.0072	0.0066	0.0061	0.0059	0.0057	0.0054	0.0062	0.0074	0.0073	0.0054	0.0064	0.0074
125	0.0078	0.0066	0.0069	0.0078	0.0074	0.0072	0.0074	0.0094	0.0088	0.0056	0.0077	0.0094
126	0.0104	0.0094	0.0091	0.0090	0.0085	0.0084	0.0096	0.0104	0.0085	0.0082	0.0093	0.0104
127	0.0038	0.0036	0.0034	0.0032	0.0035	0.0037	0.0038	0.0044	0.0046	0.0026	0.0038	0.0046
128	0.0092	0.0069	0.0057	0.0082	0.0099	0.0103	0.0098	0.0125	0.0133	0.0049	0.0095	0.0133
129	0.0113	0.0081	0.0074	0.0072	0.0072	0.0097	0.0151	0.0226	0.0212	0.0057	0.0122	0.0226
130	0.0170	0.0172	0.0154	0.0148	0.0144	0.0153	0.0193	0.0186	0.0129	0.0136	0.0161	0.0193
131	0.0131	0.0132	0.0120	0.0138	0.0181	0.0166	0.0220	0.0242	0.0186	0.0117	0.0169	0.0242
132	0.0097	0.0087	0.0088	0.0100	0.0097	0.0090	0.0097	0.0120	0.0116	0.0090	0.0099	0.0120
133	0.0115	0.0092	0.0074	0.0085	0.0089	0.0103	0.0121	0.0139	0.0121	0.0079	0.0104	0.0139
134	0.0118	0.0113	0.0114	0.0119	0.0105	0.0097	0.0100	0.0114	0.0095	0.0103	0.0108	0.0119
135	0.0140	0.0134	0.0119	0.0114	0.0111	0.0105	0.0124	0.0143	0.0115	0.0109	0.0123	0.0143
136	0.0154	0.0157	0.0151	0.0135	0.0114	0.0108	0.0116	0.0116	0.0097	0.0114	0.0127	0.0157
137	0.0149	0.0148	0.0174	0.0193	0.0184	0.0225	0.0285	0.0304	0.0251	0.0184	0.0213	0.0304
138	0.0128	0.0110	0.0087	0.0096	0.0097	0.0086	0.0082	0.0103	0.0111	0.0076	0.0100	0.0128
139	0.0054	0.0045	0.0044	0.0042	0.0044	0.0050	0.0054	0.0056	0.0060	0.0037	0.0050	0.0060
140	0.0133	0.0145	0.0159	0.0163	0.0125	0.0103	0.0120	0.0128	0.0106	0.0120	0.0131	0.0163

Table C.10 (continued) Drift ratio demands for the *ductile* 9-story building model.

ID #	IDR1	IDR2	IDR3	IDR4	IDR5	IDR6	IDR7	IDR8	IDR9	RDR	AIDR	MIDR
1	0.0065	0.0058	0.0055	0.0053	0.0057	0.0056	0.0081	0.0095	0.0081	0.0051	0.0067	0.0095
2	0.0132	0.0116	0.0095	0.0097	0.0097	0.0102	0.0144	0.0166	0.0124	0.0092	0.0119	0.0166
3	0.0089	0.0076	0.0055	0.0066	0.0096	0.0106	0.0127	0.0174	0.0179	0.0051	0.0107	0.0179
4	0.0166	0.0176	0.0178	0.0166	0.0162	0.0178	0.0233	0.0259	0.0198	0.0108	0.0191	0.0259
5	0.0078	0.0069	0.0065	0.0080	0.0077	0.0065	0.0069	0.0090	0.0093	0.0049	0.0076	0.0093
6	0.0079	0.0062	0.0054	0.0063	0.0051	0.0082	0.0127	0.0184	0.0152	0.0039	0.0095	0.0184
7	0.0095	0.0082	0.0075	0.0077	0.0070	0.0084	0.0109	0.0159	0.0158	0.0070	0.0101	0.0159
8	0.0067	0.0059	0.0061	0.0063	0.0060	0.0057	0.0066	0.0075	0.0066	0.0053	0.0064	0.0075
9	0.0080	0.0082	0.0100	0.0115	0.0131	0.0127	0.0154	0.0174	0.0125	0.0092	0.0121	0.0174
10	0.0054	0.0049	0.0049	0.0049	0.0048	0.0052	0.0063	0.0068	0.0054	0.0049	0.0054	0.0068
11	0.0099	0.0083	0.0085	0.0096	0.0109	0.0113	0.0104	0.0105	0.0115	0.0082	0.0101	0.0115
12	0.0059	0.0042	0.0039	0.0040	0.0046	0.0054	0.0060	0.0071	0.0079	0.0040	0.0054	0.0079
13	0.0086	0.0072	0.0065	0.0076	0.0075	0.0074	0.0092	0.0086	0.0081	0.0062	0.0078	0.0092
14	0.0117	0.0096	0.0096	0.0106	0.0109	0.0107	0.0123	0.0141	0.0166	0.0078	0.0118	0.0166
15	0.0020	0.0018	0.0017	0.0017	0.0017	0.0016	0.0018	0.0022	0.0026	0.0015	0.0019	0.0026
16	0.0052	0.0038	0.0044	0.0055	0.0054	0.0044	0.0053	0.0061	0.0056	0.0039	0.0051	0.0061
17	0.0116	0.0101	0.0093	0.0103	0.0104	0.0099	0.0100	0.0109	0.0094	0.0096	0.0102	0.0116
18	0.0091	0.0060	0.0064	0.0099	0.0104	0.0106	0.0120	0.0159	0.0175	0.0059	0.0109	0.0175
19	0.0088	0.0079	0.0081	0.0089	0.0086	0.0097	0.0171	0.0241	0.0208	0.0062	0.0127	0.0241
20	0.0031	0.0021	0.0026	0.0036	0.0026	0.0038	0.0033	0.0042	0.0067	0.0014	0.0036	0.0067
21	0.0115	0.0111	0.0119	0.0126	0.0104	0.0091	0.0150	0.0251	0.0256	0.0078	0.0147	0.0256
22	0.0128	0.0102	0.0106	0.0125	0.0144	0.0143	0.0164	0.0299	0.0381	0.0107	0.0177	0.0381
23	0.0144	0.0125	0.0093	0.0115	0.0156	0.0168	0.0173	0.0279	0.0301	0.0088	0.0173	0.0301
24	0.0154	0.0151	0.0140	0.0135	0.0115	0.0111	0.0128	0.0132	0.0104	0.0114	0.0130	0.0154
25	0.0112	0.0094	0.0088	0.0112	0.0142	0.0160	0.0194	0.0203	0.0232	0.0108	0.0149	0.0232
26	0.0181	0.0146	0.0138	0.0201	0.0238	0.0195	0.0287	0.0358	0.0389	0.0150	0.0237	0.0389
27	0.0185	0.0284	0.0381	0.0299	0.0153	0.0152	0.0194	0.0238	0.0194	0.0137	0.0231	0.0381
28	0.0254	0.0307	0.0257	0.0213	0.0186	0.0170	0.0224	0.0245	0.0178	0.0210	0.0226	0.0307
29	0.0149	0.0138	0.0162	0.0168	0.0153	0.0133	0.0200	0.0299	0.0360	0.0141	0.0196	0.0360
30	0.0313	0.0499	0.0523	0.0425	0.0184	0.0135	0.0154	0.0167	0.0120	0.0249	0.0280	0.0523
31	0.0104	0.0089	0.0076	0.0075	0.0079	0.0076	0.0087	0.0099	0.0134	0.0061	0.0091	0.0134
32	0.2142	0.2190	0.2089	0.1892	0.0962	0.0160	0.0167	0.0215	0.0151	0.1102	0.1108	0.2190
33	0.0367	0.0513	0.0503	0.0351	0.0157	0.0124	0.0127	0.0155	0.0126	0.0224	0.0269	0.0513
34	0.0144	0.0119	0.0121	0.0168	0.0177	0.0138	0.0176	0.0209	0.0207	0.0129	0.0162	0.0209
35	######	######	######	######	######	######	######	######	######	######	######	######
36	######	######	######	######	######	######	######	######	######	7.1228	######	######
37	0.0550	0.0742	0.0780	0.0686	0.0501	0.0208	0.0190	0.0212	0.0192	0.0409	0.0451	0.0780
38	0.2143	0.2200	0.2123	0.1973	0.1421	0.0793	0.0178	0.0266	0.0305	0.1263	0.1267	0.2200
39	0.0484	0.0621	0.0593	0.0428	0.0156	0.0113	0.0174	0.0222	0.0160	0.0275	0.0328	0.0621
40	0.1049	0.1173	0.1147	0.1015	0.0639	0.0159	0.0166	0.0171	0.0122	0.0618	0.0627	0.1173
41	0.0707	0.0842	0.0804	0.0622	0.0161	0.0097	0.0100	0.0115	0.0110	0.0381	0.0395	0.0842
42	0.0290	0.0469	0.0492	0.0374	0.0151	0.0125	0.0236	0.0268	0.0190	0.0202	0.0288	0.0492
43	0.0121	0.0114	0.0131	0.0142	0.0117	0.0095	0.0102	0.0128	0.0115	0.0096	0.0118	0.0142
44	0.0108	0.0074	0.0082	0.0080	0.0077	0.0097	0.0135	0.0188	0.0183	0.0055	0.0114	0.0188
45	0.0457	0.0569	0.0559	0.0476	0.0743	0.0970	0.1311	0.1405	0.1394	0.0490	0.0876	0.1405
46	0.0125	0.0112	0.0135	0.0139	0.0121	0.0118	0.0164	0.0178	0.0169	0.0093	0.0140	0.0178
47	0.1152	0.1321	0.1359	0.1301	0.1032	0.0717	0.0234	0.0265	0.0198	0.0812	0.0842	0.1359
48	0.0177	0.0166	0.0213	0.0255	0.0195	0.0144	0.0231	0.0290	0.0280	0.0154	0.0217	0.0290
49	0.1229	0.1354	0.1328	0.1195	0.0427	0.0129	0.0222	0.0215	0.0168	0.0630	0.0696	0.1354
50	0.1446	0.1597	0.1598	0.1518	0.1128	0.0430	0.0192	0.0223	0.0260	0.0885	0.0933	0.1598
51	0.0955	0.1060	0.0991	0.0777	0.0227	0.0264	0.0340	0.0293	0.0223	0.0437	0.0570	0.1060
52	0.1792	0.1969	0.1938	0.1678	0.1052	0.0644	0.0220	0.0302	0.0346	0.1015	0.1105	0.1969
53	0.0183	0.0221	0.0266	0.0282	0.0203	0.0285	0.1021	0.1184	0.1203	0.0378	0.0539	0.1203
54	######	######	######	######	######	######	######	######	######	######	######	######
55	0.2200	0.2241	0.2133	0.1861	0.1035	0.0144	0.0192	0.0215	0.0201	0.1101	0.1136	0.2241

Table C.11 Drift ratio demands for the *brittle* 9-story building model. Note the collapses (###'s).

ID #	IDR1	IDR2	IDR3	IDR4	IDR5	IDR6	IDR7	IDR8	IDR9	RDR	AIDR	MIDR
56	0.1943	0.2039	0.1934	0.1667	0.0833	0.0173	0.0235	0.0273	0.0211	0.0978	0.1034	0.2039
57	0.1543	0.1652	0.1559	0.1456	0.1142	0.0779	0.0344	0.0405	0.0309	0.0991	0.1021	0.1652
58	0.0125	0.0108	0.0133	0.0162	0.0128	0.0118	0.0192	0.0191	0.0199	0.0088	0.0151	0.0199
59	0.0130	0.0151	0.0157	0.0157	0.0137	0.0138	0.0230	0.0316	0.0277	0.0108	0.0188	0.0316
60	0.0121	0.0109	0.0123	0.0183	0.0199	0.0150	0.0124	0.0142	0.0125	0.0113	0.0142	0.0199
61	0.1120	0.1252	0.1233	0.1098	0.0701	0.0121	0.0220	0.0281	0.0265	0.0634	0.0699	0.1252
62	0.0961	0.1058	0.1070	0.1036	0.0716	0.0238	0.0200	0.0249	0.0276	0.0597	0.0645	0.1070
63	0.0622	0.0765	0.0735	0.0556	0.0213	0.0210	0.0225	0.0279	0.0223	0.0318	0.0425	0.0765
64	0.0184	0.0203	0.0186	0.0143	0.0116	0.0154	0.0274	0.0303	0.0248	0.0158	0.0201	0.0303
65	0.0121	0.0109	0.0116	0.0128	0.0120	0.0116	0.0150	0.0161	0.0124	0.0116	0.0127	0.0161
66	0.0118	0.0098	0.0084	0.0087	0.0099	0.0106	0.0157	0.0201	0.0157	0.0087	0.0123	0.0201
67	######	######	######	######	######	######	######	######	######	######	######	######
68	0.0078	0.0060	0.0047	0.0041	0.0044	0.0055	0.0073	0.0087	0.0075	0.0040	0.0062	0.0087
69	0.0933	0.1091	0.1121	0.1052	0.0876	0.0546	0.0133	0.0168	0.0142	0.0660	0.0674	0.1121
70	0.1041	0.1175	0.1148	0.1013	0.0652	0.0161	0.0167	0.0196	0.0179	0.0613	0.0637	0.1175
71	0.0041	0.0037	0.0035	0.0033	0.0037	0.0037	0.0039	0.0056	0.0057	0.0027	0.0041	0.0057
72	0.0081	0.0074	0.0073	0.0073	0.0071	0.0072	0.0081	0.0084	0.0065	0.0070	0.0075	0.0084
73	0.0012	0.0011	0.0010	0.0010	0.0010	0.0010	0.0010	0.0010	0.0013	0.0009	0.0011	0.0013
74	0.0022	0.0017	0.0014	0.0017	0.0020	0.0019	0.0023	0.0026	0.0024	0.0012	0.0020	0.0026
75	0.0071	0.0061	0.0057	0.0062	0.0065	0.0069	0.0080	0.0083	0.0066	0.0063	0.0068	0.0083
76	0.0048	0.0033	0.0021	0.0029	0.0036	0.0036	0.0039	0.0070	0.0077	0.0019	0.0043	0.0077
77	0.0047	0.0045	0.0044	0.0039	0.0029	0.0039	0.0057	0.0071	0.0061	0.0024	0.0048	0.0071
78	0.0042	0.0033	0.0030	0.0033	0.0036	0.0039	0.0049	0.0059	0.0061	0.0030	0.0043	0.0061
79	0.0043	0.0034	0.0030	0.0031	0.0035	0.0040	0.0057	0.0069	0.0063	0.0028	0.0045	0.0069
80	0.0056	0.0047	0.0040	0.0045	0.0041	0.0049	0.0068	0.0081	0.0076	0.0030	0.0056	0.0081
81	0.0048	0.0041	0.0043	0.0041	0.0034	0.0041	0.0056	0.0066	0.0060	0.0031	0.0048	0.0066
82	0.0048	0.0043	0.0042	0.0041	0.0040	0.0044	0.0054	0.0062	0.0054	0.0040	0.0047	0.0062
83	0.0009	0.0006	0.0008	0.0009	0.0008	0.0007	0.0009	0.0011	0.0011	0.0006	0.0009	0.0011
84	0.0075	0.0064	0.0059	0.0068	0.0073	0.0074	0.0083	0.0082	0.0065	0.0061	0.0071	0.0083
85	0.0055	0.0049	0.0046	0.0049	0.0053	0.0054	0.0057	0.0057	0.0046	0.0048	0.0052	0.0057
86	0.0095	0.0075	0.0076	0.0079	0.0075	0.0081	0.0108	0.0127	0.0105	0.0076	0.0091	0.0127
87	0.0125	0.0127	0.0129	0.0174	0.0215	0.0280	0.0435	0.0457	0.0360	0.0230	0.0256	0.0457
88	0.0130	0.0117	0.0113	0.0133	0.0114	0.0089	0.0132	0.0179	0.0153	0.0090	0.0129	0.0179
89	0.0075	0.0062	0.0068	0.0070	0.0067	0.0073	0.0075	0.0090	0.0087	0.0056	0.0074	0.0090
90	0.0068	0.0060	0.0058	0.0060	0.0060	0.0058	0.0069	0.0073	0.0059	0.0055	0.0063	0.0073
91	0.0113	0.0087	0.0070	0.0074	0.0094	0.0110	0.0181	0.0235	0.0191	0.0090	0.0128	0.0235
92	0.0055	0.0047	0.0047	0.0051	0.0046	0.0045	0.0045	0.0050	0.0060	0.0040	0.0050	0.0060
93	0.0070	0.0058	0.0057	0.0064	0.0067	0.0065	0.0066	0.0067	0.0056	0.0056	0.0063	0.0070
94	0.0087	0.0078	0.0079	0.0085	0.0088	0.0090	0.0103	0.0106	0.0083	0.0086	0.0089	0.0106
95	0.0110	0.0092	0.0074	0.0071	0.0076	0.0082	0.0137	0.0182	0.0152	0.0070	0.0108	0.0182
96	0.0126	0.0122	0.0123	0.0135	0.0129	0.0115	0.0176	0.0217	0.0200	0.0110	0.0149	0.0217
97	0.0061	0.0050	0.0043	0.0048	0.0052	0.0053	0.0059	0.0071	0.0067	0.0044	0.0056	0.0071
98	0.0143	0.0148	0.0162	0.0162	0.0131	0.0122	0.0153	0.0215	0.0204	0.0120	0.0160	0.0215
99	0.0069	0.0060	0.0062	0.0065	0.0058	0.0055	0.0059	0.0060	0.0059	0.0053	0.0061	0.0069
100	0.0131	0.0121	0.0113	0.0118	0.0110	0.0105	0.0126	0.0134	0.0104	0.0104	0.0118	0.0134
101	0.0074	0.0063	0.0064	0.0070	0.0070	0.0067	0.0073	0.0078	0.0060	0.0064	0.0069	0.0078
102	0.0030	0.0027	0.0027	0.0028	0.0027	0.0024	0.0025	0.0028	0.0027	0.0023	0.0027	0.0030
103	0.0026	0.0024	0.0023	0.0021	0.0020	0.0019	0.0019	0.0022	0.0021	0.0018	0.0022	0.0026
104	0.0149	0.0157	0.0153	0.0139	0.0111	0.0107	0.0109	0.0111	0.0087	0.0115	0.0125	0.0157
105	0.0071	0.0060	0.0064	0.0070	0.0075	0.0082	0.0092	0.0106	0.0098	0.0064	0.0080	0.0106
106	0.0511	0.0639	0.0592	0.0425	0.0149	0.0114	0.0119	0.0117	0.0127	0.0281	0.0310	0.0639
107	0.0174	0.0208	0.0211	0.0202	0.0149	0.0134	0.0180	0.0198	0.0141	0.0147	0.0178	0.0211
108	0.0139	0.0136	0.0121	0.0123	0.0113	0.0106	0.0112	0.0118	0.0094	0.0114	0.0118	0.0139
109	0.0071	0.0054	0.0048	0.0046	0.0055	0.0071	0.0086	0.0126	0.0122	0.0043	0.0075	0.0126
110	0.0070	0.0063	0.0061	0.0062	0.0059	0.0055	0.0062	0.0070	0.0075	0.0058	0.0064	0.0075

Table C.11 (continued) Drift ratio demands for the *brittle* 9-story building model. Note the collapses (###'s).

ID #	IDR1	IDR2	IDR3	IDR4	IDR5	IDR6	IDR7	IDR8	IDR9	RDR	AIDR	MIDR
111	0.0034	0.0026	0.0026	0.0028	0.0028	0.0030	0.0036	0.0044	0.0047	0.0025	0.0033	0.0047
112	0.0019	0.0016	0.0015	0.0016	0.0016	0.0017	0.0024	0.0033	0.0032	0.0014	0.0021	0.0033
113	0.0034	0.0029	0.0029	0.0034	0.0036	0.0036	0.0035	0.0036	0.0042	0.0030	0.0034	0.0042
114	0.0102	0.0089	0.0091	0.0093	0.0096	0.0094	0.0139	0.0173	0.0133	0.0080	0.0112	0.0173
115	0.0128	0.0108	0.0080	0.0092	0.0099	0.0098	0.0153	0.0202	0.0163	0.0090	0.0125	0.0202
116	0.0111	0.0098	0.0085	0.0094	0.0100	0.0107	0.0105	0.0132	0.0129	0.0070	0.0107	0.0132
117	0.0076	0.0067	0.0074	0.0076	0.0074	0.0082	0.0089	0.0116	0.0118	0.0045	0.0086	0.0118
118	0.0134	0.0135	0.0128	0.0128	0.0116	0.0105	0.0111	0.0113	0.0094	0.0105	0.0118	0.0135
119	0.0125	0.0117	0.0123	0.0136	0.0122	0.0111	0.0114	0.0124	0.0124	0.0110	0.0122	0.0136
120	0.0140	0.0152	0.0165	0.0164	0.0136	0.0115	0.0168	0.0234	0.0218	0.0128	0.0166	0.0234
121	0.0161	0.0158	0.0148	0.0137	0.0132	0.0130	0.0146	0.0160	0.0135	0.0122	0.0145	0.0161
122	0.0114	0.0091	0.0093	0.0093	0.0079	0.0074	0.0090	0.0113	0.0128	0.0060	0.0097	0.0128
123	0.0092	0.0082	0.0081	0.0081	0.0080	0.0077	0.0086	0.0089	0.0072	0.0073	0.0082	0.0092
124	0.0072	0.0066	0.0061	0.0059	0.0057	0.0054	0.0062	0.0074	0.0073	0.0054	0.0064	0.0074
125	0.0078	0.0066	0.0069	0.0078	0.0074	0.0072	0.0074	0.0094	0.0088	0.0056	0.0077	0.0094
126	0.0104	0.0094	0.0091	0.0090	0.0085	0.0084	0.0096	0.0104	0.0085	0.0082	0.0093	0.0104
127	0.0038	0.0036	0.0034	0.0032	0.0035	0.0037	0.0038	0.0044	0.0046	0.0026	0.0038	0.0046
128	0.0092	0.0069	0.0057	0.0082	0.0099	0.0103	0.0098	0.0125	0.0133	0.0049	0.0095	0.0133
129	0.0113	0.0081	0.0074	0.0072	0.0072	0.0097	0.0151	0.0226	0.0212	0.0057	0.0122	0.0226
130	0.0170	0.0172	0.0154	0.0148	0.0144	0.0153	0.0193	0.0186	0.0129	0.0136	0.0161	0.0193
131	0.0131	0.0132	0.0120	0.0138	0.0181	0.0166	0.0220	0.0242	0.0186	0.0117	0.0169	0.0242
132	0.0097	0.0087	0.0088	0.0100	0.0097	0.0090	0.0097	0.0120	0.0116	0.0090	0.0099	0.0120
133	0.0115	0.0092	0.0074	0.0085	0.0089	0.0103	0.0121	0.0139	0.0121	0.0079	0.0104	0.0139
134	0.0118	0.0113	0.0114	0.0119	0.0105	0.0097	0.0100	0.0114	0.0095	0.0103	0.0108	0.0119
135	0.0140	0.0134	0.0119	0.0114	0.0111	0.0105	0.0124	0.0143	0.0115	0.0109	0.0123	0.0143
136	0.0154	0.0157	0.0151	0.0135	0.0114	0.0108	0.0116	0.0116	0.0097	0.0114	0.0127	0.0157
137	0.0149	0.0148	0.0174	0.0193	0.0184	0.0225	0.0285	0.0304	0.0251	0.0184	0.0213	0.0304
138	0.0128	0.0110	0.0087	0.0096	0.0097	0.0086	0.0082	0.0103	0.0111	0.0076	0.0100	0.0128
139	0.0054	0.0045	0.0044	0.0042	0.0044	0.0050	0.0054	0.0056	0.0060	0.0037	0.0050	0.0060
140	0.0133	0.0145	0.0159	0.0163	0.0125	0.0103	0.0120	0.0128	0.0106	0.0120	0.0131	0.0163

Table C.11 (continued) Drift ratio demands for the *brittle* 9-story building model.

ID #	IDR1	IDR2	IDR3	IDR4	IDR5	IDR6	IDR7	IDR8	IDR9	IDR10	IDR11	IDR12	IDR13	IDR14	IDR15	IDR16	IDR17	IDR18	IDR19	IDR20	RDR	AIDR	MIDR
1	0.0044	0.0042	0.0037	0.0034	0.0031	0.0027	0.0022	0.0024	0.0025	0.0027	0.0034	0.0037	0.0041	0.0045	0.0049	0.0049	0.0050	0.0049	0.0047	0.0043	0.0022	0.0038	0.0050
2	0.0057	0.0053	0.0049	0.0049	0.0047	0.0043	0.0040	0.0039	0.0036	0.0042	0.0050	0.0058	0.0064	0.0073	0.0080	0.0076	0.0072	0.0067	0.0060	0.0055	0.0036	0.0056	0.0080
3	0.0066	0.0057	0.0052	0.0046	0.0037	0.0042	0.0046	0.0052	0.0051	0.0049	0.0055	0.0058	0.0056	0.0057	0.0072	0.0075	0.0076	0.0090	0.0106	0.0102	0.0026	0.0062	0.0106
4	0.0185	0.0166	0.0129	0.0108	0.0104	0.0108	0.0110	0.0110	0.0110	0.0109	0.0113	0.0120	0.0119	0.0125	0.0148	0.0163	0.0176	0.0187	0.0218	0.0211	0.0055	0.0141	0.0218
5	0.0065	0.0064	0.0056	0.0046	0.0046	0.0047	0.0049	0.0048	0.0045	0.0048	0.0053	0.0056	0.0058	0.0065	0.0066	0.0055	0.0059	0.0059	0.0063	0.0065	0.0033	0.0056	0.0066
6	0.0054	0.0049	0.0041	0.0036	0.0037	0.0040	0.0044	0.0047	0.0049	0.0049	0.0051	0.0049	0.0042	0.0040	0.0056	0.0072	0.0088	0.0092	0.0090	0.0081	0.0023	0.0055	0.0092
7	0.0062	0.0057	0.0048	0.0047	0.0052	0.0054	0.0053	0.0054	0.0057	0.0054	0.0051	0.0051	0.0051	0.0050	0.0054	0.0059	0.0079	0.0096	0.0109	0.0102	0.0033	0.0062	0.0109
8	0.0034	0.0033	0.0029	0.0027	0.0024	0.0020	0.0021	0.0021	0.0021	0.0021	0.0026	0.0032	0.0035	0.0038	0.0040	0.0039	0.0041	0.0040	0.0038	0.0033	0.0018	0.0031	0.0041
9	0.0169	0.0162	0.0141	0.0117	0.0095	0.0073	0.0047	0.0057	0.0062	0.0082	0.0114	0.0143	0.0162	0.0184	0.0201	0.0198	0.0198	0.0190	0.0193	0.0171	0.0057	0.0138	0.0201
10	0.0046	0.0046	0.0045	0.0043	0.0041	0.0039	0.0038	0.0039	0.0040	0.0042	0.0043	0.0044	0.0044	0.0046	0.0048	0.0046	0.0046	0.0044	0.0042	0.0035	0.0035	0.0043	0.0048
11	0.0053	0.0053	0.0055	0.0063	0.0064	0.0052	0.0047	0.0051	0.0056	0.0059	0.0059	0.0057	0.0055	0.0057	0.0051	0.0058	0.0058	0.0053	0.0073	0.0076	0.0035	0.0057	0.0076
12	0.0054	0.0053	0.0049	0.0046	0.0045	0.0043	0.0042	0.0042	0.0042	0.0040	0.0040	0.0040	0.0038	0.0040	0.0042	0.0042	0.0047	0.0048	0.0050	0.0047	0.0030	0.0045	0.0054
13	0.0055	0.0053	0.0047	0.0041	0.0042	0.0044	0.0044	0.0036	0.0036	0.0041	0.0043	0.0045	0.0045	0.0050	0.0063	0.0066	0.0058	0.0054	0.0060	0.0081	0.0026	0.0050	0.0081
14	0.0078	0.0077	0.0072	0.0066	0.0060	0.0065	0.0066	0.0071	0.0077	0.0072	0.0073	0.0077	0.0070	0.0057	0.0061	0.0068	0.0083	0.0085	0.0127	0.0142	0.0027	0.0077	0.0142
15	0.0021	0.0020	0.0019	0.0017	0.0016	0.0014	0.0014	0.0014	0.0014	0.0014	0.0015	0.0015	0.0014	0.0015	0.0017	0.0018	0.0019	0.0019	0.0018	0.0016	0.0009	0.0016	0.0021
16	0.0051	0.0049	0.0043	0.0035	0.0027	0.0026	0.0028	0.0032	0.0033	0.0032	0.0033	0.0037	0.0037	0.0042	0.0048	0.0048	0.0053	0.0058	0.0061	0.0054	0.0020	0.0041	0.0061
17	0.0065	0.0060	0.0050	0.0044	0.0041	0.0048	0.0052	0.0055	0.0058	0.0059	0.0061	0.0062	0.0058	0.0056	0.0063	0.0064	0.0067	0.0070	0.0073	0.0066	0.0042	0.0059	0.0073
18	0.0086	0.0077	0.0067	0.0075	0.0083	0.0086	0.0082	0.0072	0.0059	0.0066	0.0079	0.0087	0.0085	0.0080	0.0074	0.0071	0.0071	0.0080	0.0094	0.0091	0.0048	0.0078	0.0094
19	0.0157	0.0142	0.0111	0.0094	0.0087	0.0086	0.0086	0.0085	0.0086	0.0091	0.0104	0.0114	0.0114	0.0123	0.0143	0.0150	0.0171	0.0183	0.0196	0.0178	0.0042	0.0125	0.0196
20	0.0024	0.0023	0.0020	0.0019	0.0017	0.0018	0.0018	0.0019	0.0022	0.0024	0.0026	0.0027	0.0028	0.0027	0.0023	0.0022	0.0022	0.0020	0.0024	0.0028	0.0012	0.0023	0.0028
21	0.0090	0.0091	0.0085	0.0076	0.0083	0.0087	0.0084	0.0076	0.0070	0.0073	0.0086	0.0100	0.0103	0.0104	0.0106	0.0113	0.0152	0.0185	0.0209	0.0198	0.0050	0.0109	0.0209
22	0.0093	0.0076	0.0075	0.0087	0.0094	0.0092	0.0094	0.0097	0.0090	0.0076	0.0097	0.0116	0.0115	0.0110	0.0121	0.0103	0.0103	0.0138	0.0168	0.0175	0.0044	0.0106	0.0175
23	0.0164	0.0162	0.0148	0.0137	0.0138	0.0138	0.0125	0.0117	0.0118	0.0123	0.0132	0.0136	0.0135	0.0135	0.0150	0.0168	0.0182	0.0179	0.0169	0.0157	0.0099	0.0146	0.0182
24	0.0166	0.0172	0.0172	0.0173	0.0172	0.0172	0.0171	0.0168	0.0165	0.0162	0.0163	0.0162	0.0156	0.0153	0.0146	0.0133	0.0125	0.0116	0.0108	0.0094	0.0150	0.0152	0.0173
25	0.0127	0.0115	0.0097	0.0096	0.0090	0.0075	0.0080	0.0080	0.0087	0.0094	0.0107	0.0118	0.0114	0.0123	0.0150	0.0153	0.0162	0.0178	0.0213	0.0202	0.0049	0.0123	0.0213
26	0.0203	0.0189	0.0156	0.0141	0.0133	0.0121	0.0128	0.0144	0.0145	0.0140	0.0151	0.0167	0.0164	0.0163	0.0176	0.0190	0.0235	0.0297	0.0358	0.0340	0.0074	0.0187	0.0358
27	0.0149	0.0146	0.0136	0.0124	0.0109	0.0097	0.0108	0.0117	0.0125	0.0136	0.0153	0.0171	0.0183	0.0198	0.0204	0.0188	0.0174	0.0155	0.0151	0.0152	0.0094	0.0149	0.0204
28	0.0224	0.0216	0.0191	0.0166	0.0145	0.0145	0.0155	0.0153	0.0142	0.0136	0.0162	0.0184	0.0197	0.0208	0.0210	0.0191	0.0175	0.0172	0.0179	0.0164	0.0107	0.0176	0.0224
29	0.0172	0.0165	0.0142	0.0127	0.0123	0.0116	0.0118	0.0124	0.0112	0.0112	0.0135	0.0157	0.0162	0.0159	0.0165	0.0182	0.0209	0.0225	0.0230	0.0250	0.0072	0.0159	0.0250
30	0.0203	0.0209	0.0206	0.0206	0.0203	0.0198	0.0191	0.0183	0.0178	0.0180	0.0187	0.0192	0.0189	0.0188	0.0185	0.0171	0.0161	0.0149	0.0139	0.0119	0.0170	0.0182	0.0209
31	0.0093	0.0091	0.0084	0.0076	0.0068	0.0074	0.0085	0.0096	0.0097	0.0086	0.0070	0.0072	0.0068	0.0078	0.0089	0.0085	0.0087	0.0094	0.0099	0.0100	0.0054	0.0085	0.0100
32	0.0520	0.0522	0.0493	0.0462	0.0428	0.0408	0.0427	0.0437	0.0437	0.0429	0.0425	0.0430	0.0424	0.0418	0.0395	0.0347	0.0328	0.0313	0.0296	0.0253	0.0332	0.0410	0.0522
33	0.0292	0.0301	0.0298	0.0302	0.0302	0.0302	0.0298	0.0289	0.0280	0.0272	0.0271	0.0267	0.0253	0.0243	0.0232	0.0215	0.0206	0.0192	0.0183	0.0164	0.0250	0.0258	0.0302
34	0.0177	0.0188	0.0185	0.0175	0.0157	0.0132	0.0124	0.0117	0.0117	0.0127	0.0144	0.0153	0.0149	0.0141	0.0125	0.0117	0.0124	0.0135	0.0142	0.0134	0.0093	0.0143	0.0188
35	0.0528	0.0539	0.0523	0.0516	0.0510	0.0504	0.0501	0.0493	0.0479	0.0469	0.0480	0.0489	0.0478	0.0482	0.0475	0.0435	0.0412	0.0388	0.0360	0.0307	0.0448	0.0468	0.0539

Table C.12 Drift ratio demands for the *elastic* 20-story building model.

ID #	IDR1	IDR2	IDR3	IDR4	IDR5	IDR6	IDR7	IDR8	IDR9	IDR10	IDR11	IDR12	IDR13	IDR14	IDR15	IDR16	IDR17	IDR18	IDR19	IDR20	RDR	AIDR	MIDR
36	0.0560	0.0579	0.0569	0.0561	0.0554	0.0552	0.0546	0.0532	0.0513	0.0495	0.0491	0.0480	0.0448	0.0436	0.0421	0.0388	0.0368	0.0335	0.0300	0.0265	0.0461	0.0470	0.0579
37	0.0678	0.0700	0.0691	0.0687	0.0684	0.0685	0.0680	0.0667	0.0655	0.0640	0.0636	0.0621	0.0581	0.0559	0.0537	0.0487	0.0455	0.0423	0.0392	0.0340	0.0578	0.0590	0.0700
38	0.0650	0.0654	0.0620	0.0596	0.0575	0.0565	0.0556	0.0537	0.0513	0.0498	0.0509	0.0504	0.0467	0.0438	0.0424	0.0396	0.0404	0.0403	0.0386	0.0330	0.0429	0.0501	0.0654
39	0.0367	0.0364	0.0341	0.0322	0.0317	0.0314	0.0312	0.0303	0.0304	0.0311	0.0327	0.0344	0.0341	0.0335	0.0315	0.0285	0.0278	0.0273	0.0258	0.0220	0.0277	0.0312	0.0367
40	0.0326	0.0326	0.0321	0.0325	0.0327	0.0320	0.0312	0.0294	0.0263	0.0253	0.0259	0.0253	0.0236	0.0253	0.0279	0.0272	0.0261	0.0248	0.0256	0.0235	0.0220	0.0281	0.0327
41	0.0324	0.0329	0.0321	0.0316	0.0307	0.0297	0.0291	0.0299	0.0306	0.0311	0.0324	0.0333	0.0332	0.0332	0.0324	0.0296	0.0276	0.0259	0.0244	0.0210	0.0273	0.0302	0.0333
42	0.0294	0.0303	0.0298	0.0296	0.0289	0.0287	0.0296	0.0305	0.0308	0.0305	0.0303	0.0302	0.0292	0.0283	0.0278	0.0268	0.0265	0.0251	0.0239	0.0216	0.0262	0.0284	0.0308
43	0.0114	0.0116	0.0112	0.0111	0.0112	0.0116	0.0118	0.0117	0.0114	0.0109	0.0107	0.0106	0.0107	0.0108	0.0107	0.0099	0.0093	0.0084	0.0079	0.0071	0.0100	0.0105	0.0118
44	0.0080	0.0079	0.0073	0.0067	0.0060	0.0050	0.0041	0.0044	0.0048	0.0050	0.0058	0.0072	0.0084	0.0088	0.0087	0.0084	0.0090	0.0102	0.0108	0.0103	0.0027	0.0073	0.0108
45	0.0454	0.0434	0.0379	0.0355	0.0336	0.0307	0.0329	0.0351	0.0358	0.0358	0.0385	0.0426	0.0459	0.0507	0.0549	0.0535	0.0522	0.0482	0.0429	0.0350	0.0291	0.0415	0.0549
46	0.0166	0.0165	0.0157	0.0148	0.0138	0.0129	0.0119	0.0109	0.0099	0.0109	0.0124	0.0137	0.0141	0.0150	0.0155	0.0143	0.0135	0.0124	0.0135	0.0127	0.0088	0.0135	0.0166
47	0.0293	0.0283	0.0253	0.0223	0.0207	0.0189	0.0170	0.0172	0.0181	0.0207	0.0242	0.0274	0.0284	0.0306	0.0321	0.0314	0.0310	0.0298	0.0285	0.0246	0.0172	0.0253	0.0321
48	0.0188	0.0177	0.0155	0.0137	0.0126	0.0118	0.0122	0.0122	0.0107	0.0110	0.0128	0.0144	0.0162	0.0165	0.0151	0.0138	0.0187	0.0222	0.0241	0.0232	0.0095	0.0156	0.0241
49	0.0422	0.0435	0.0424	0.0410	0.0409	0.0442	0.0472	0.0490	0.0497	0.0498	0.0505	0.0507	0.0485	0.0462	0.0417	0.0358	0.0361	0.0358	0.0360	0.0329	0.0389	0.0432	0.0507
50	0.0549	0.0537	0.0492	0.0446	0.0404	0.0363	0.0325	0.0355	0.0448	0.0529	0.0601	0.0647	0.0644	0.0648	0.0646	0.0588	0.0563	0.0538	0.0560	0.0546	0.0352	0.0521	0.0648
51	0.0343	0.0328	0.0307	0.0290	0.0269	0.0235	0.0212	0.0174	0.0182	0.0201	0.0246	0.0298	0.0331	0.0357	0.0356	0.0343	0.0322	0.0324	0.0332	0.0295	0.0153	0.0287	0.0357
52	0.0709	0.0685	0.0610	0.0530	0.0448	0.0386	0.0388	0.0388	0.0410	0.0421	0.0446	0.0515	0.0570	0.0631	0.0710	0.0741	0.0780	0.0770	0.0731	0.0616	0.0312	0.0574	0.0780
53	0.0254	0.0250	0.0241	0.0241	0.0244	0.0249	0.0262	0.0269	0.0260	0.0246	0.0224	0.0194	0.0194	0.0211	0.0222	0.0255	0.0296	0.0320	0.0333	0.0342	0.0143	0.0255	0.0342
54	0.0580	0.0581	0.0543	0.0498	0.0445	0.0480	0.0529	0.0556	0.0563	0.0554	0.0545	0.0516	0.0450	0.0490	0.0567	0.0592	0.0623	0.0612	0.0573	0.0495	0.0395	0.0540	0.0623
55	0.0424	0.0418	0.0397	0.0386	0.0377	0.0391	0.0410	0.0419	0.0420	0.0401	0.0378	0.0341	0.0346	0.0397	0.0431	0.0414	0.0421	0.0438	0.0436	0.0383	0.0323	0.0401	0.0438
56	0.0383	0.0378	0.0381	0.0382	0.0364	0.0319	0.0285	0.0291	0.0323	0.0341	0.0371	0.0403	0.0435	0.0468	0.0485	0.0476	0.0493	0.0472	0.0430	0.0371	0.0289	0.0393	0.0493
57	0.0362	0.0352	0.0345	0.0339	0.0332	0.0299	0.0287	0.0317	0.0321	0.0316	0.0335	0.0353	0.0380	0.0434	0.0486	0.0478	0.0460	0.0493	0.0539	0.0496	0.0229	0.0386	0.0539
58	0.0199	0.0193	0.0173	0.0149	0.0128	0.0103	0.0082	0.0081	0.0099	0.0114	0.0139	0.0162	0.0178	0.0198	0.0210	0.0215	0.0232	0.0229	0.0225	0.0206	0.0073	0.0166	0.0232
59	0.0226	0.0216	0.0184	0.0156	0.0136	0.0119	0.0137	0.0165	0.0199	0.0221	0.0239	0.0245	0.0231	0.0213	0.0180	0.0195	0.0249	0.0277	0.0284	0.0244	0.0100	0.0206	0.0284
60	0.0119	0.0119	0.0111	0.0101	0.0088	0.0072	0.0064	0.0071	0.0086	0.0099	0.0117	0.0135	0.0144	0.0152	0.0157	0.0150	0.0147	0.0141	0.0141	0.0126	0.0066	0.0117	0.0157
61	0.0264	0.0260	0.0239	0.0218	0.0194	0.0164	0.0166	0.0168	0.0177	0.0188	0.0200	0.0206	0.0202	0.0200	0.0219	0.0227	0.0235	0.0226	0.0209	0.0182	0.0137	0.0207	0.0264
62	0.0246	0.0220	0.0198	0.0190	0.0226	0.0263	0.0277	0.0268	0.0238	0.0226	0.0229	0.0216	0.0219	0.0243	0.0272	0.0290	0.0317	0.0317	0.0303	0.0269	0.0167	0.0251	0.0317
63	0.0360	0.0370	0.0365	0.0362	0.0356	0.0348	0.0338	0.0325	0.0328	0.0327	0.0337	0.0350	0.0341	0.0327	0.0304	0.0276	0.0289	0.0281	0.0263	0.0234	0.0277	0.0324	0.0370
64	0.0288	0.0291	0.0275	0.0255	0.0229	0.0192	0.0153	0.0151	0.0177	0.0198	0.0218	0.0230	0.0226	0.0236	0.0242	0.0235	0.0244	0.0241	0.0235	0.0199	0.0120	0.0226	0.0291
65	0.0121	0.0119	0.0110	0.0104	0.0098	0.0095	0.0090	0.0081	0.0078	0.0085	0.0096	0.0105	0.0109	0.0112	0.0120	0.0120	0.0125	0.0123	0.0118	0.0105	0.0062	0.0106	0.0125
66	0.0113	0.0111	0.0110	0.0108	0.0106	0.0104	0.0102	0.0102	0.0100	0.0096	0.0099	0.0101	0.0098	0.0099	0.0099	0.0097	0.0095	0.0091	0.0103	0.0098	0.0091	0.0102	0.0113
67	0.0483	0.0489	0.0470	0.0457	0.0460	0.0467	0.0462	0.0443	0.0423	0.0406	0.0425	0.0441	0.0416	0.0426	0.0491	0.0489	0.0472	0.0466	0.0481	0.0455	0.0323	0.0456	0.0491
68	0.0089	0.0086	0.0078	0.0071	0.0068	0.0069	0.0074	0.0075	0.0074	0.0070	0.0065	0.0058	0.0057	0.0060	0.0068	0.0066	0.0062	0.0059	0.0055	0.0052	0.0047	0.0068	0.0089
69	0.0420	0.0426	0.0416	0.0411	0.0411	0.0413	0.0408	0.0395	0.0375	0.0353	0.0348	0.0348	0.0337	0.0332	0.0321	0.0294	0.0275	0.0253	0.0236	0.0204	0.0339	0.0349	0.0426
70	0.0445	0.0459	0.0449	0.0438	0.0418	0.0388	0.0367	0.0401	0.0428	0.0450	0.0482	0.0514	0.0523	0.0535	0.0539	0.0507	0.0492	0.0463	0.0428	0.0363	0.0382	0.0454	0.0539

Table C.12 (continued) Drift ratio demands for the *elastic* 20-story building model.

ID #	IDR1	IDR2	IDR3	IDR4	IDR5	IDR6	IDR7	IDR8	IDR9	IDR10	IDR11	IDR12	IDR13	IDR14	IDR15	IDR16	IDR17	IDR18	IDR19	IDR20	RDR	AIDR	MIDR
71	0.0022	0.0021	0.0020	0.0019	0.0020	0.0022	0.0023	0.0024	0.0024	0.0023	0.0022	0.0022	0.0024	0.0026	0.0028	0.0027	0.0027	0.0029	0.0032	0.0033	0.0018	0.0024	0.0033
72	0.0051	0.0051	0.0047	0.0044	0.0043	0.0044	0.0045	0.0047	0.0048	0.0048	0.0050	0.0051	0.0050	0.0049	0.0054	0.0056	0.0059	0.0060	0.0058	0.0050	0.0038	0.0050	0.0060
73	0.0008	0.0008	0.0008	0.0008	0.0007	0.0007	0.0007	0.0007	0.0006	0.0007	0.0007	0.0007	0.0007	0.0007	0.0007	0.0006	0.0006	0.0005	0.0006	0.0007	0.0006	0.0007	0.0008
74	0.0025	0.0025	0.0022	0.0021	0.0019	0.0016	0.0014	0.0012	0.0013	0.0016	0.0019	0.0021	0.0024	0.0027	0.0030	0.0030	0.0031	0.0031	0.0031	0.0027	0.0011	0.0023	0.0031
75	0.0028	0.0029	0.0028	0.0027	0.0026	0.0026	0.0026	0.0025	0.0024	0.0025	0.0027	0.0030	0.0030	0.0031	0.0032	0.0031	0.0032	0.0031	0.0029	0.0025	0.0020	0.0028	0.0032
76	0.0038	0.0037	0.0033	0.0028	0.0023	0.0023	0.0021	0.0019	0.0022	0.0025	0.0028	0.0029	0.0030	0.0034	0.0039	0.0042	0.0046	0.0047	0.0047	0.0040	0.0015	0.0032	0.0047
77	0.0057	0.0056	0.0050	0.0044	0.0036	0.0029	0.0027	0.0027	0.0033	0.0039	0.0043	0.0046	0.0053	0.0059	0.0065	0.0066	0.0070	0.0069	0.0066	0.0056	0.0021	0.0050	0.0070
78	0.0062	0.0059	0.0052	0.0044	0.0036	0.0028	0.0025	0.0024	0.0030	0.0036	0.0042	0.0054	0.0063	0.0071	0.0078	0.0078	0.0079	0.0076	0.0072	0.0062	0.0025	0.0053	0.0079
79	0.0070	0.0066	0.0057	0.0047	0.0037	0.0032	0.0027	0.0028	0.0035	0.0040	0.0047	0.0055	0.0061	0.0068	0.0078	0.0080	0.0084	0.0084	0.0082	0.0071	0.0028	0.0057	0.0084
80	0.0053	0.0051	0.0045	0.0038	0.0032	0.0029	0.0026	0.0033	0.0039	0.0042	0.0045	0.0047	0.0050	0.0056	0.0060	0.0059	0.0064	0.0068	0.0066	0.0059	0.0024	0.0048	0.0068
81	0.0053	0.0052	0.0046	0.0039	0.0034	0.0031	0.0028	0.0025	0.0026	0.0032	0.0041	0.0051	0.0057	0.0063	0.0068	0.0066	0.0069	0.0072	0.0076	0.0068	0.0021	0.0050	0.0076
82	0.0033	0.0034	0.0034	0.0034	0.0033	0.0032	0.0031	0.0030	0.0030	0.0030	0.0032	0.0033	0.0033	0.0033	0.0033	0.0030	0.0033	0.0034	0.0035	0.0031	0.0028	0.0032	0.0035
83	0.0007	0.0006	0.0006	0.0006	0.0006	0.0006	0.0005	0.0005	0.0006	0.0006	0.0006	0.0007	0.0007	0.0007	0.0007	0.0007	0.0006	0.0006	0.0006	0.0008	0.0004	0.0006	0.0008
84	0.0037	0.0037	0.0035	0.0033	0.0033	0.0033	0.0031	0.0025	0.0026	0.0028	0.0031	0.0035	0.0038	0.0042	0.0046	0.0047	0.0048	0.0046	0.0047	0.0044	0.0022	0.0037	0.0048
85	0.0032	0.0031	0.0028	0.0025	0.0022	0.0019	0.0016	0.0018	0.0021	0.0024	0.0027	0.0032	0.0035	0.0038	0.0039	0.0038	0.0039	0.0039	0.0037	0.0031	0.0021	0.0030	0.0039
86	0.0086	0.0084	0.0075	0.0068	0.0061	0.0057	0.0054	0.0056	0.0060	0.0061	0.0062	0.0073	0.0083	0.0091	0.0097	0.0101	0.0106	0.0105	0.0103	0.0092	0.0036	0.0079	0.0106
87	0.0184	0.0185	0.0174	0.0164	0.0150	0.0129	0.0102	0.0100	0.0103	0.0121	0.0137	0.0145	0.0140	0.0164	0.0204	0.0224	0.0246	0.0251	0.0249	0.0223	0.0073	0.0170	0.0251
88	0.0062	0.0056	0.0047	0.0046	0.0044	0.0048	0.0052	0.0049	0.0054	0.0054	0.0057	0.0055	0.0050	0.0050	0.0064	0.0070	0.0073	0.0088	0.0103	0.0098	0.0028	0.0061	0.0103
89	0.0044	0.0040	0.0036	0.0035	0.0033	0.0034	0.0035	0.0033	0.0032	0.0032	0.0039	0.0044	0.0044	0.0044	0.0047	0.0049	0.0058	0.0066	0.0074	0.0069	0.0026	0.0044	0.0074
90	0.0044	0.0040	0.0033	0.0033	0.0033	0.0033	0.0031	0.0030	0.0031	0.0035	0.0039	0.0042	0.0043	0.0044	0.0047	0.0050	0.0055	0.0059	0.0062	0.0055	0.0021	0.0042	0.0062
91	0.0071	0.0066	0.0055	0.0053	0.0049	0.0048	0.0044	0.0037	0.0033	0.0033	0.0043	0.0052	0.0053	0.0061	0.0073	0.0076	0.0079	0.0082	0.0085	0.0077	0.0019	0.0058	0.0085
92	0.0022	0.0021	0.0020	0.0019	0.0020	0.0023	0.0022	0.0019	0.0022	0.0026	0.0027	0.0024	0.0026	0.0028	0.0026	0.0025	0.0031	0.0033	0.0035	0.0035	0.0016	0.0025	0.0035
93	0.0024	0.0022	0.0018	0.0018	0.0018	0.0018	0.0017	0.0017	0.0019	0.0021	0.0022	0.0023	0.0023	0.0023	0.0023	0.0022	0.0022	0.0024	0.0029	0.0029	0.0015	0.0022	0.0029
94	0.0070	0.0072	0.0069	0.0067	0.0063	0.0068	0.0070	0.0072	0.0072	0.0071	0.0069	0.0068	0.0065	0.0065	0.0064	0.0058	0.0054	0.0050	0.0047	0.0042	0.0057	0.0064	0.0072
95	0.0081	0.0081	0.0077	0.0074	0.0072	0.0066	0.0069	0.0066	0.0062	0.0067	0.0070	0.0082	0.0087	0.0088	0.0089	0.0079	0.0083	0.0082	0.0087	0.0083	0.0047	0.0077	0.0089
96	0.0176	0.0177	0.0166	0.0154	0.0144	0.0137	0.0139	0.0138	0.0134	0.0129	0.0134	0.0138	0.0143	0.0152	0.0158	0.0152	0.0160	0.0180	0.0189	0.0167	0.0107	0.0153	0.0189
97	0.0079	0.0079	0.0075	0.0071	0.0065	0.0059	0.0053	0.0050	0.0052	0.0054	0.0060	0.0066	0.0067	0.0067	0.0065	0.0063	0.0063	0.0063	0.0061	0.0051	0.0044	0.0063	0.0079
98	0.0185	0.0185	0.0175	0.0169	0.0164	0.0160	0.0160	0.0160	0.0159	0.0158	0.0161	0.0163	0.0160	0.0162	0.0167	0.0162	0.0161	0.0154	0.0144	0.0122	0.0135	0.0162	0.0185
99	0.0064	0.0066	0.0064	0.0063	0.0064	0.0065	0.0065	0.0065	0.0063	0.0062	0.0063	0.0066	0.0066	0.0066	0.0064	0.0058	0.0055	0.0054	0.0052	0.0045	0.0056	0.0061	0.0066
100	0.0099	0.0098	0.0092	0.0090	0.0087	0.0085	0.0082	0.0078	0.0073	0.0072	0.0076	0.0078	0.0085	0.0094	0.0099	0.0095	0.0095	0.0091	0.0087	0.0074	0.0068	0.0086	0.0099
101	0.0096	0.0093	0.0084	0.0078	0.0073	0.0067	0.0063	0.0060	0.0058	0.0063	0.0068	0.0072	0.0073	0.0077	0.0081	0.0081	0.0086	0.0087	0.0084	0.0072	0.0047	0.0076	0.0096
102	0.0016	0.0016	0.0015	0.0014	0.0013	0.0013	0.0014	0.0014	0.0015	0.0016	0.0017	0.0018	0.0018	0.0017	0.0016	0.0015	0.0014	0.0014	0.0015	0.0016	0.0012	0.0015	0.0018
103	0.0031	0.0031	0.0031	0.0031	0.0030	0.0030	0.0031	0.0032	0.0033	0.0033	0.0034	0.0035	0.0034	0.0033	0.0032	0.0029	0.0029	0.0028	0.0028	0.0025	0.0028	0.0031	0.0035
104	0.0185	0.0189	0.0185	0.0183	0.0180	0.0178	0.0177	0.0175	0.0169	0.0163	0.0159	0.0154	0.0143	0.0136	0.0126	0.0118	0.0114	0.0107	0.0099	0.0085	0.0144	0.0151	0.0189
105	0.0054	0.0047	0.0038	0.0036	0.0037	0.0036	0.0032	0.0033	0.0037	0.0038	0.0036	0.0035	0.0035	0.0039	0.0041	0.0044	0.0048	0.0052	0.0059	0.0058	0.0022	0.0042	0.0059

Table C.12 (continued) Drift ratio demands for the *elastic* 20-story building model.

ID #	IDR1	IDR2	IDR3	IDR4	IDR5	IDR6	IDR7	IDR8	IDR9	IDR10	IDR11	IDR12	IDR13	IDR14	IDR15	IDR16	IDR17	IDR18	IDR19	IDR20	RDR	AIDR	MIDR
106	0.0208	0.0208	0.0204	0.0201	0.0197	0.0191	0.0185	0.0177	0.0172	0.0169	0.0170	0.0173	0.0181	0.0198	0.0211	0.0205	0.0202	0.0190	0.0199	0.0191	0.0163	0.0192	0.0211
107	0.0190	0.0197	0.0194	0.0191	0.0184	0.0176	0.0167	0.0158	0.0157	0.0166	0.0179	0.0191	0.0195	0.0201	0.0213	0.0213	0.0218	0.0219	0.0216	0.0187	0.0148	0.0191	0.0219
108	0.0109	0.0115	0.0115	0.0116	0.0115	0.0117	0.0119	0.0121	0.0123	0.0122	0.0125	0.0125	0.0119	0.0117	0.0115	0.0109	0.0108	0.0105	0.0100	0.0089	0.0108	0.0114	0.0125
109	0.0039	0.0036	0.0033	0.0034	0.0033	0.0029	0.0027	0.0028	0.0029	0.0033	0.0035	0.0034	0.0033	0.0037	0.0044	0.0050	0.0055	0.0054	0.0053	0.0049	0.0018	0.0038	0.0055
110	0.0038	0.0039	0.0038	0.0039	0.0039	0.0040	0.0040	0.0041	0.0042	0.0042	0.0044	0.0044	0.0043	0.0043	0.0043	0.0041	0.0040	0.0038	0.0036	0.0030	0.0038	0.0040	0.0044
111	0.0025	0.0024	0.0022	0.0021	0.0022	0.0024	0.0024	0.0023	0.0021	0.0021	0.0022	0.0023	0.0023	0.0023	0.0022	0.0021	0.0022	0.0023	0.0026	0.0026	0.0017	0.0023	0.0026
112	0.0019	0.0019	0.0017	0.0016	0.0017	0.0018	0.0019	0.0017	0.0015	0.0015	0.0016	0.0016	0.0016	0.0016	0.0016	0.0014	0.0015	0.0016	0.0018	0.0017	0.0012	0.0017	0.0019
113	0.0043	0.0044	0.0042	0.0040	0.0039	0.0039	0.0041	0.0042	0.0041	0.0040	0.0039	0.0039	0.0038	0.0039	0.0039	0.0037	0.0037	0.0035	0.0033	0.0028	0.0032	0.0039	0.0044
114	0.0071	0.0071	0.0067	0.0062	0.0059	0.0057	0.0059	0.0065	0.0064	0.0074	0.0090	0.0094	0.0087	0.0089	0.0093	0.0081	0.0077	0.0098	0.0094	0.0116	0.0048	0.0078	0.0116
115	0.0067	0.0067	0.0069	0.0071	0.0068	0.0066	0.0058	0.0051	0.0056	0.0063	0.0065	0.0073	0.0070	0.0075	0.0083	0.0073	0.0069	0.0067	0.0101	0.0111	0.0046	0.0071	0.0111
116	0.0065	0.0059	0.0050	0.0047	0.0047	0.0059	0.0067	0.0059	0.0051	0.0048	0.0064	0.0071	0.0063	0.0070	0.0080	0.0068	0.0076	0.0091	0.0101	0.0125	0.0027	0.0068	0.0125
117	0.0044	0.0044	0.0042	0.0040	0.0036	0.0029	0.0027	0.0024	0.0028	0.0032	0.0034	0.0038	0.0045	0.0050	0.0051	0.0047	0.0054	0.0063	0.0067	0.0060	0.0021	0.0043	0.0067
118	0.0218	0.0226	0.0225	0.0225	0.0223	0.0221	0.0218	0.0212	0.0206	0.0200	0.0199	0.0196	0.0186	0.0180	0.0172	0.0156	0.0146	0.0134	0.0122	0.0105	0.0189	0.0188	0.0226
119	0.0147	0.0153	0.0152	0.0153	0.0151	0.0150	0.0148	0.0144	0.0140	0.0135	0.0135	0.0133	0.0126	0.0122	0.0116	0.0105	0.0098	0.0090	0.0090	0.0090	0.0128	0.0129	0.0153
120	0.0342	0.0352	0.0346	0.0343	0.0335	0.0331	0.0328	0.0323	0.0317	0.0311	0.0314	0.0315	0.0305	0.0300	0.0292	0.0269	0.0257	0.0239	0.0220	0.0188	0.0290	0.0301	0.0352
121	0.0137	0.0135	0.0124	0.0118	0.0114	0.0105	0.0098	0.0092	0.0090	0.0088	0.0089	0.0105	0.0115	0.0120	0.0115	0.0098	0.0099	0.0100	0.0090	0.0083	0.0078	0.0106	0.0137
122	0.0068	0.0066	0.0063	0.0057	0.0057	0.0058	0.0058	0.0053	0.0055	0.0060	0.0062	0.0069	0.0072	0.0076	0.0086	0.0088	0.0088	0.0084	0.0093	0.0088	0.0037	0.0070	0.0093
123	0.0048	0.0049	0.0047	0.0047	0.0046	0.0046	0.0044	0.0046	0.0050	0.0054	0.0059	0.0063	0.0065	0.0066	0.0065	0.0059	0.0055	0.0050	0.0045	0.0039	0.0043	0.0052	0.0066
124	0.0056	0.0057	0.0055	0.0052	0.0049	0.0047	0.0049	0.0050	0.0050	0.0051	0.0055	0.0057	0.0056	0.0055	0.0052	0.0046	0.0046	0.0048	0.0047	0.0042	0.0043	0.0051	0.0057
125	0.0074	0.0073	0.0069	0.0063	0.0058	0.0054	0.0058	0.0059	0.0064	0.0070	0.0077	0.0081	0.0081	0.0083	0.0088	0.0088	0.0088	0.0090	0.0090	0.0078	0.0055	0.0074	0.0090
126	0.0096	0.0091	0.0078	0.0070	0.0063	0.0074	0.0082	0.0085	0.0082	0.0075	0.0070	0.0067	0.0057	0.0053	0.0061	0.0076	0.0093	0.0107	0.0116	0.0105	0.0047	0.0080	0.0116
127	0.0062	0.0061	0.0057	0.0056	0.0051	0.0042	0.0034	0.0041	0.0048	0.0054	0.0062	0.0067	0.0069	0.0074	0.0077	0.0070	0.0069	0.0070	0.0073	0.0068	0.0038	0.0060	0.0077
128	0.0065	0.0067	0.0065	0.0062	0.0058	0.0053	0.0052	0.0051	0.0053	0.0059	0.0065	0.0069	0.0068	0.0070	0.0072	0.0071	0.0073	0.0076	0.0078	0.0071	0.0052	0.0065	0.0078
129	0.0125	0.0117	0.0100	0.0089	0.0098	0.0097	0.0085	0.0069	0.0074	0.0080	0.0091	0.0107	0.0115	0.0134	0.0171	0.0178	0.0173	0.0149	0.0149	0.0136	0.0061	0.0117	0.0178
130	0.0140	0.0145	0.0143	0.0141	0.0138	0.0133	0.0130	0.0127	0.0125	0.0121	0.0117	0.0111	0.0107	0.0110	0.0117	0.0117	0.0121	0.0121	0.0116	0.0099	0.0102	0.0124	0.0145
131	0.0173	0.0166	0.0144	0.0120	0.0104	0.0081	0.0071	0.0069	0.0090	0.0102	0.0128	0.0155	0.0171	0.0186	0.0198	0.0193	0.0195	0.0193	0.0191	0.0192	0.0072	0.0146	0.0198
132	0.0178	0.0184	0.0180	0.0177	0.0173	0.0168	0.0167	0.0166	0.0165	0.0164	0.0168	0.0170	0.0165	0.0163	0.0158	0.0146	0.0139	0.0131	0.0122	0.0106	0.0155	0.0160	0.0184
133	0.0108	0.0105	0.0095	0.0094	0.0095	0.0096	0.0094	0.0087	0.0087	0.0091	0.0097	0.0101	0.0098	0.0103	0.0110	0.0110	0.0112	0.0107	0.0099	0.0083	0.0067	0.0099	0.0112
134	0.0143	0.0148	0.0147	0.0148	0.0148	0.0148	0.0148	0.0147	0.0145	0.0144	0.0146	0.0148	0.0145	0.0145	0.0144	0.0135	0.0131	0.0123	0.0113	0.0096	0.0139	0.0140	0.0148
135	0.0140	0.0142	0.0139	0.0136	0.0130	0.0122	0.0113	0.0102	0.0097	0.0092	0.0095	0.0102	0.0103	0.0106	0.0106	0.0104	0.0107	0.0104	0.0099	0.0085	0.0088	0.0111	0.0142
136	0.0073	0.0073	0.0068	0.0064	0.0060	0.0057	0.0054	0.0051	0.0049	0.0052	0.0057	0.0061	0.0063	0.0066	0.0067	0.0064	0.0067	0.0071	0.0072	0.0063	0.0044	0.0063	0.0073
137	0.0298	0.0299	0.0279	0.0255	0.0226	0.0189	0.0156	0.0181	0.0207	0.0228	0.0252	0.0274	0.0286	0.0299	0.0309	0.0302	0.0308	0.0300	0.0284	0.0252	0.0182	0.0259	0.0309
138	0.0060	0.0062	0.0061	0.0060	0.0057	0.0054	0.0054	0.0054	0.0052	0.0048	0.0048	0.0055	0.0059	0.0061	0.0059	0.0054	0.0051	0.0050	0.0050	0.0045	0.0044	0.0055	0.0062
139	0.0046	0.0045	0.0042	0.0039	0.0038	0.0035	0.0036	0.0037	0.0038	0.0039	0.0042	0.0043	0.0040	0.0035	0.0034	0.0034	0.0038	0.0042	0.0046	0.0045	0.0028	0.0040	0.0046
140	0.0074	0.0069	0.0060	0.0053	0.0044	0.0036	0.0039	0.0043	0.0046	0.0050	0.0055	0.0066	0.0076	0.0084	0.0089	0.0089	0.0093	0.0093	0.0090	0.0077	0.0039	0.0066	0.0093

Table C.12 (continued) Drift ratio demands for the *elastic* 20-story building model.

ID #	IDR1	IDR2	IDR3	IDR4	IDR5	IDR6	IDR7	IDR8	IDR9	IDR10	IDR11	IDR12	IDR13	IDR14	IDR15	IDR16	IDR17	IDR18	IDR19	IDR20	RDR	AIDR	MIDR
1	0.0044	0.0042	0.0037	0.0034	0.0031	0.0027	0.0022	0.0024	0.0025	0.0027	0.0034	0.0037	0.0041	0.0045	0.0049	0.0049	0.0050	0.0049	0.0047	0.0043	0.0022	0.0038	0.0050
2	0.0057	0.0053	0.0049	0.0049	0.0047	0.0043	0.0040	0.0039	0.0036	0.0042	0.0050	0.0058	0.0064	0.0073	0.0080	0.0076	0.0072	0.0067	0.0060	0.0055	0.0036	0.0056	0.0080
3	0.0065	0.0055	0.0051	0.0045	0.0036	0.0042	0.0047	0.0051	0.0051	0.0048	0.0054	0.0057	0.0055	0.0056	0.0071	0.0074	0.0075	0.0089	0.0104	0.0098	0.0026	0.0061	0.0104
4	0.0104	0.0122	0.0119	0.0116	0.0109	0.0098	0.0093	0.0090	0.0088	0.0084	0.0088	0.0091	0.0089	0.0095	0.0117	0.0133	0.0146	0.0157	0.0129	0.0122	0.0044	0.0109	0.0157
5	0.0065	0.0064	0.0056	0.0046	0.0046	0.0047	0.0049	0.0048	0.0044	0.0048	0.0053	0.0056	0.0058	0.0065	0.0066	0.0055	0.0059	0.0059	0.0063	0.0065	0.0033	0.0056	0.0066
6	0.0054	0.0049	0.0041	0.0036	0.0037	0.0040	0.0044	0.0046	0.0048	0.0048	0.0051	0.0049	0.0042	0.0039	0.0055	0.0071	0.0088	0.0093	0.0090	0.0081	0.0022	0.0055	0.0093
7	0.0061	0.0056	0.0047	0.0047	0.0051	0.0054	0.0052	0.0053	0.0056	0.0053	0.0051	0.0051	0.0051	0.0049	0.0053	0.0057	0.0078	0.0097	0.0111	0.0102	0.0034	0.0061	0.0111
8	0.0034	0.0033	0.0029	0.0027	0.0024	0.0020	0.0021	0.0021	0.0021	0.0021	0.0026	0.0032	0.0035	0.0038	0.0040	0.0039	0.0041	0.0040	0.0038	0.0033	0.0018	0.0031	0.0041
9	0.0114	0.0134	0.0109	0.0074	0.0056	0.0044	0.0041	0.0048	0.0054	0.0061	0.0074	0.0085	0.0102	0.0117	0.0122	0.0126	0.0119	0.0122	0.0130	0.0119	0.0044	0.0093	0.0134
10	0.0046	0.0046	0.0045	0.0043	0.0041	0.0039	0.0038	0.0039	0.0040	0.0042	0.0043	0.0044	0.0044	0.0046	0.0048	0.0046	0.0046	0.0044	0.0042	0.0035	0.0035	0.0043	0.0048
11	0.0053	0.0053	0.0055	0.0063	0.0064	0.0052	0.0047	0.0051	0.0056	0.0059	0.0059	0.0057	0.0055	0.0057	0.0051	0.0058	0.0057	0.0053	0.0072	0.0075	0.0035	0.0057	0.0075
12	0.0054	0.0053	0.0049	0.0046	0.0045	0.0043	0.0042	0.0042	0.0042	0.0040	0.0040	0.0040	0.0038	0.0040	0.0042	0.0042	0.0047	0.0048	0.0050	0.0047	0.0030	0.0045	0.0054
13	0.0055	0.0053	0.0047	0.0041	0.0042	0.0044	0.0044	0.0036	0.0036	0.0041	0.0043	0.0045	0.0045	0.0050	0.0063	0.0066	0.0058	0.0054	0.0060	0.0081	0.0026	0.0050	0.0081
14	0.0078	0.0080	0.0072	0.0063	0.0056	0.0058	0.0061	0.0067	0.0072	0.0068	0.0065	0.0069	0.0063	0.0051	0.0056	0.0058	0.0073	0.0072	0.0124	0.0136	0.0030	0.0072	0.0136
15	0.0021	0.0020	0.0019	0.0017	0.0016	0.0014	0.0014	0.0014	0.0014	0.0014	0.0015	0.0015	0.0014	0.0015	0.0017	0.0018	0.0019	0.0019	0.0018	0.0016	0.0009	0.0016	0.0021
16	0.0051	0.0049	0.0043	0.0035	0.0027	0.0026	0.0028	0.0032	0.0033	0.0032	0.0033	0.0037	0.0037	0.0042	0.0048	0.0048	0.0053	0.0058	0.0061	0.0054	0.0020	0.0041	0.0061
17	0.0065	0.0060	0.0050	0.0044	0.0041	0.0048	0.0051	0.0055	0.0058	0.0059	0.0060	0.0061	0.0058	0.0056	0.0063	0.0064	0.0067	0.0070	0.0072	0.0066	0.0042	0.0058	0.0072
18	0.0081	0.0081	0.0068	0.0072	0.0080	0.0082	0.0077	0.0067	0.0055	0.0063	0.0077	0.0087	0.0084	0.0078	0.0072	0.0069	0.0069	0.0077	0.0091	0.0089	0.0048	0.0076	0.0091
19	0.0121	0.0144	0.0125	0.0096	0.0075	0.0065	0.0062	0.0061	0.0064	0.0069	0.0076	0.0082	0.0089	0.0101	0.0114	0.0127	0.0163	0.0164	0.0134	0.0128	0.0039	0.0103	0.0164
20	0.0024	0.0023	0.0020	0.0019	0.0017	0.0018	0.0018	0.0019	0.0022	0.0024	0.0026	0.0027	0.0028	0.0027	0.0023	0.0022	0.0022	0.0020	0.0024	0.0028	0.0012	0.0023	0.0028
21	0.0078	0.0074	0.0067	0.0074	0.0083	0.0085	0.0079	0.0070	0.0063	0.0067	0.0081	0.0096	0.0100	0.0098	0.0095	0.0106	0.0150	0.0220	0.0233	0.0158	0.0052	0.0104	0.0233
22	0.0079	0.0079	0.0066	0.0071	0.0073	0.0081	0.0093	0.0090	0.0073	0.0064	0.0070	0.0089	0.0095	0.0090	0.0089	0.0078	0.0089	0.0125	0.0174	0.0156	0.0048	0.0091	0.0174
23	0.0128	0.0163	0.0155	0.0152	0.0142	0.0107	0.0085	0.0080	0.0078	0.0080	0.0078	0.0094	0.0100	0.0106	0.0110	0.0121	0.0126	0.0147	0.0164	0.0123	0.0088	0.0117	0.0164
24	0.0120	0.0159	0.0173	0.0171	0.0145	0.0107	0.0101	0.0105	0.0106	0.0105	0.0110	0.0114	0.0113	0.0113	0.0111	0.0107	0.0105	0.0100	0.0092	0.0079	0.0097	0.0117	0.0173
25	0.0092	0.0087	0.0072	0.0068	0.0065	0.0062	0.0067	0.0074	0.0073	0.0072	0.0084	0.0099	0.0101	0.0103	0.0138	0.0158	0.0147	0.0120	0.0160	0.0146	0.0040	0.0099	0.0160
26	0.0130	0.0147	0.0121	0.0105	0.0087	0.0075	0.0103	0.0122	0.0108	0.0082	0.0088	0.0115	0.0133	0.0126	0.0125	0.0171	0.0199	0.0207	0.0205	0.0177	0.0052	0.0131	0.0207
27	0.0144	0.0194	0.0178	0.0140	0.0110	0.0082	0.0068	0.0074	0.0090	0.0106	0.0135	0.0165	0.0176	0.0168	0.0143	0.0119	0.0119	0.0127	0.0122	0.0101	0.0095	0.0128	0.0194
28	0.0123	0.0179	0.0209	0.0213	0.0180	0.0121	0.0096	0.0086	0.0096	0.0103	0.0104	0.0123	0.0156	0.0155	0.0131	0.0108	0.0110	0.0119	0.0118	0.0103	0.0094	0.0132	0.0213
29	0.0114	0.0165	0.0186	0.0184	0.0175	0.0164	0.0153	0.0139	0.0122	0.0103	0.0094	0.0111	0.0117	0.0105	0.0109	0.0110	0.0107	0.0144	0.0202	0.0209	0.0077	0.0141	0.0209
30	0.0137	0.0190	0.0225	0.0234	0.0209	0.0172	0.0146	0.0150	0.0170	0.0190	0.0197	0.0192	0.0173	0.0149	0.0127	0.0117	0.0111	0.0099	0.0088	0.0080	0.0128	0.0158	0.0234
31	0.0096	0.0104	0.0089	0.0077	0.0074	0.0071	0.0077	0.0088	0.0087	0.0073	0.0067	0.0064	0.0060	0.0066	0.0074	0.0069	0.0071	0.0080	0.0089	0.0100	0.0060	0.0079	0.0104
32	0.0961	0.1048	0.1040	0.0981	0.0879	0.0534	0.0353	0.0289	0.0242	0.0196	0.0146	0.0132	0.0136	0.0141	0.0155	0.0164	0.0190	0.0190	0.0171	0.0143	0.0361	0.0405	0.1048
33	0.0227	0.0339	0.0390	0.0430	0.0438	0.0408	0.0342	0.0247	0.0183	0.0136	0.0118	0.0120	0.0123	0.0121	0.0119	0.0114	0.0114	0.0110	0.0103	0.0088	0.0177	0.0213	0.0438
34	0.0134	0.0172	0.0178	0.0179	0.0140	0.0088	0.0089	0.0089	0.0083	0.0095	0.0117	0.0133	0.0120	0.0105	0.0090	0.0083	0.0088	0.0107	0.0118	0.0109	0.0078	0.0116	0.0179
35	0.1289	0.1356	0.1316	0.1226	0.1097	0.0512	0.0325	0.0223	0.0161	0.0138	0.0148	0.0158	0.0155	0.0148	0.0145	0.0149	0.0166	0.0179	0.0173	0.0144	0.0416	0.0460	0.1356

Table C.13 Drift ratio demands for the *ductile* 20-story building model.

ID #	IDR1	IDR2	IDR3	IDR4	IDR5	IDR6	IDR7	IDR8	IDR9	IDR10	IDR11	IDR12	IDR13	IDR14	IDR15	IDR16	IDR17	IDR18	IDR19	IDR20	RDR	AIDR	MIDR
36	######	######	######	######	######	######	######	######	######	######	######	######	######	######	######	######	######	######	######	######	######	######	######
37	0.0601	0.0725	0.0790	0.0818	0.0788	0.0449	0.0430	0.0379	0.0277	0.0168	0.0115	0.0129	0.0132	0.0124	0.0129	0.0123	0.0114	0.0108	0.0110	0.0093	0.0242	0.0330	0.0818
38	0.0489	0.0588	0.0630	0.0654	0.0640	0.0427	0.0286	0.0233	0.0183	0.0136	0.0143	0.0177	0.0199	0.0205	0.0202	0.0191	0.0200	0.0219	0.0221	0.0186	0.0274	0.0310	0.0654
39	0.0681	0.0762	0.0752	0.0703	0.0617	0.0411	0.0272	0.0182	0.0120	0.0105	0.0122	0.0119	0.0127	0.0136	0.0138	0.0126	0.0124	0.0124	0.0124	0.0120	0.0240	0.0293	0.0762
40	0.0362	0.0475	0.0513	0.0507	0.0457	0.0367	0.0289	0.0231	0.0201	0.0198	0.0228	0.0231	0.0218	0.0201	0.0178	0.0154	0.0150	0.0150	0.0137	0.0114	0.0244	0.0268	0.0513
41	0.0471	0.0575	0.0611	0.0611	0.0571	0.0478	0.0313	0.0220	0.0157	0.0123	0.0122	0.0129	0.0132	0.0126	0.0112	0.0104	0.0103	0.0097	0.0090	0.0082	0.0226	0.0261	0.0611
42	0.0271	0.0378	0.0450	0.0484	0.0446	0.0325	0.0232	0.0155	0.0123	0.0111	0.0111	0.0117	0.0125	0.0122	0.0130	0.0122	0.0130	0.0134	0.0135	0.0122	0.0162	0.0211	0.0484
43	0.0099	0.0119	0.0120	0.0114	0.0102	0.0093	0.0089	0.0085	0.0081	0.0080	0.0084	0.0088	0.0087	0.0087	0.0086	0.0082	0.0081	0.0077	0.0072	0.0064	0.0079	0.0089	0.0120
44	0.0079	0.0084	0.0074	0.0063	0.0055	0.0050	0.0041	0.0043	0.0047	0.0048	0.0055	0.0068	0.0080	0.0084	0.0080	0.0081	0.0083	0.0097	0.0105	0.0097	0.0026	0.0071	0.0105
45	0.0313	0.0377	0.0342	0.0339	0.0349	0.0325	0.0279	0.0248	0.0231	0.0222	0.0258	0.0266	0.0226	0.0189	0.0161	0.0148	0.0147	0.0159	0.0156	0.0123	0.0174	0.0243	0.0377
46	0.0133	0.0181	0.0185	0.0160	0.0117	0.0094	0.0091	0.0087	0.0092	0.0096	0.0100	0.0101	0.0094	0.0103	0.0103	0.0096	0.0108	0.0121	0.0134	0.0120	0.0075	0.0116	0.0185
47	0.0125	0.0162	0.0162	0.0154	0.0118	0.0106	0.0125	0.0145	0.0166	0.0192	0.0224	0.0277	0.0307	0.0298	0.0205	0.0162	0.0156	0.0149	0.0154	0.0135	0.0103	0.0176	0.0307
48	0.0108	0.0124	0.0126	0.0119	0.0098	0.0088	0.0094	0.0094	0.0088	0.0090	0.0105	0.0137	0.0147	0.0126	0.0112	0.0112	0.0160	0.0224	0.0214	0.0185	0.0092	0.0127	0.0224
49	0.0399	0.0501	0.0543	0.0562	0.0549	0.0397	0.0300	0.0194	0.0147	0.0127	0.0157	0.0187	0.0179	0.0161	0.0176	0.0198	0.0213	0.0208	0.0195	0.0163	0.0193	0.0278	0.0562
50	0.0921	0.0984	0.0942	0.0852	0.0733	0.0373	0.0241	0.0185	0.0172	0.0171	0.0203	0.0214	0.0197	0.0179	0.0146	0.0143	0.0167	0.0176	0.0168	0.0141	0.0321	0.0365	0.0984
51	0.0155	0.0204	0.0228	0.0221	0.0178	0.0135	0.0103	0.0086	0.0093	0.0101	0.0103	0.0119	0.0133	0.0151	0.0186	0.0200	0.0231	0.0225	0.0191	0.0150	0.0081	0.0160	0.0231
52	0.1071	0.1129	0.1099	0.1022	0.0904	0.0412	0.0246	0.0184	0.0163	0.0144	0.0127	0.0116	0.0141	0.0173	0.0168	0.0133	0.0141	0.0203	0.0197	0.0177	0.0326	0.0397	0.1129
53	0.0171	0.0208	0.0192	0.0171	0.0138	0.0125	0.0130	0.0138	0.0158	0.0148	0.0153	0.0140	0.0111	0.0125	0.0145	0.0167	0.0203	0.0224	0.0189	0.0191	0.0108	0.0161	0.0224
54	######	######	######	######	######	######	######	######	######	######	######	92.4960	24.3370	6.3065	1.5909	0.3510	0.0951	0.0161	0.0153	0.0662	0.1615	######	######
55	0.0997	0.1073	0.1053	0.0989	0.0889	0.0530	0.0348	0.0245	0.0174	0.0150	0.0141	0.0147	0.0145	0.0135	0.0124	0.0107	0.0128	0.0143	0.0148	0.0133	0.0351	0.0390	0.1073
56	0.0861	0.0950	0.0948	0.0897	0.0803	0.0480	0.0290	0.0213	0.0160	0.0130	0.0138	0.0172	0.0189	0.0202	0.0196	0.0189	0.0201	0.0191	0.0200	0.0180	0.0287	0.0380	0.0950
57	0.0216	0.0298	0.0313	0.0306	0.0271	0.0206	0.0168	0.0162	0.0125	0.0142	0.0165	0.0174	0.0165	0.0137	0.0140	0.0150	0.0193	0.0251	0.0267	0.0221	0.0134	0.0204	0.0313
58	0.0113	0.0133	0.0129	0.0112	0.0084	0.0055	0.0059	0.0072	0.0073	0.0072	0.0088	0.0107	0.0120	0.0129	0.0115	0.0109	0.0127	0.0149	0.0132	0.0109	0.0043	0.0104	0.0149
59	0.0122	0.0160	0.0160	0.0135	0.0095	0.0084	0.0089	0.0092	0.0090	0.0105	0.0112	0.0105	0.0103	0.0102	0.0111	0.0113	0.0120	0.0171	0.0178	0.0144	0.0066	0.0120	0.0178
60	0.0098	0.0105	0.0086	0.0065	0.0064	0.0062	0.0062	0.0063	0.0068	0.0074	0.0079	0.0096	0.0128	0.0163	0.0165	0.0129	0.0110	0.0106	0.0102	0.0088	0.0058	0.0096	0.0165
61	0.0131	0.0182	0.0206	0.0223	0.0222	0.0201	0.0177	0.0153	0.0136	0.0118	0.0103	0.0108	0.0116	0.0133	0.0129	0.0105	0.0103	0.0124	0.0125	0.0100	0.0097	0.0145	0.0223
62	0.0221	0.0319	0.0366	0.0382	0.0353	0.0278	0.0236	0.0200	0.0187	0.0182	0.0181	0.0169	0.0156	0.0170	0.0167	0.0189	0.0201	0.0211	0.0219	0.0177	0.0171	0.0228	0.0382
63	0.0292	0.0379	0.0401	0.0404	0.0382	0.0340	0.0258	0.0181	0.0144	0.0130	0.0139	0.0143	0.0132	0.0123	0.0122	0.0137	0.0160	0.0159	0.0148	0.0135	0.0156	0.0215	0.0404
64	0.0148	0.0194	0.0187	0.0184	0.0163	0.0115	0.0084	0.0080	0.0094	0.0105	0.0141	0.0156	0.0146	0.0166	0.0150	0.0131	0.0154	0.0163	0.0145	0.0138	0.0084	0.0142	0.0194
65	0.0104	0.0120	0.0114	0.0101	0.0088	0.0079	0.0074	0.0068	0.0067	0.0074	0.0084	0.0093	0.0093	0.0094	0.0093	0.0097	0.0108	0.0121	0.0121	0.0102	0.0058	0.0095	0.0121
66	0.0090	0.0097	0.0097	0.0098	0.0095	0.0086	0.0081	0.0081	0.0076	0.0078	0.0081	0.0081	0.0081	0.0083	0.0092	0.0094	0.0091	0.0090	0.0105	0.0098	0.0078	0.0089	0.0105
67	######	######	######	######	######	######	######	######	######	######	######	######	######	######	######	######	######	######	######	######	######	######	######
68	0.0092	0.0096	0.0080	0.0066	0.0068	0.0069	0.0074	0.0075	0.0074	0.0070	0.0064	0.0057	0.0057	0.0060	0.0067	0.0065	0.0062	0.0058	0.0054	0.0052	0.0047	0.0068	0.0096
69	0.0743	0.0820	0.0817	0.0767	0.0674	0.0386	0.0255	0.0169	0.0119	0.0125	0.0134	0.0131	0.0137	0.0144	0.0143	0.0154	0.0162	0.0146	0.0143	0.0119	0.0252	0.0314	0.0820
70	0.1256	0.1315	0.1276	0.1181	0.1046	0.0454	0.0228	0.0153	0.0124	0.0144	0.0155	0.0161	0.0200	0.0206	0.0154	0.0122	0.0123	0.0131	0.0132	0.0118	0.0376	0.0434	0.1315

Table C.13 (continued) Drift ratio demands for the *ductile* 20-story building model. Note the collapses (###'s).

ID #	IDR1	IDR2	IDR3	IDR4	IDR5	IDR6	IDR7	IDR8	IDR9	IDR10	IDR11	IDR12	IDR13	IDR14	IDR15	IDR16	IDR17	IDR18	IDR19	IDR20	RDR	AIDR	MIDR
71	0.0022	0.0021	0.0020	0.0019	0.0020	0.0022	0.0023	0.0024	0.0024	0.0023	0.0022	0.0022	0.0024	0.0026	0.0028	0.0027	0.0027	0.0029	0.0032	0.0033	0.0018	0.0024	0.0033
72	0.0051	0.0051	0.0047	0.0044	0.0043	0.0044	0.0045	0.0047	0.0048	0.0048	0.0050	0.0051	0.0050	0.0049	0.0054	0.0056	0.0059	0.0060	0.0058	0.0050	0.0038	0.0050	0.0060
73	0.0008	0.0008	0.0008	0.0008	0.0007	0.0007	0.0007	0.0007	0.0006	0.0007	0.0007	0.0007	0.0007	0.0007	0.0007	0.0006	0.0006	0.0005	0.0006	0.0007	0.0006	0.0007	0.0008
74	0.0025	0.0025	0.0022	0.0021	0.0019	0.0016	0.0014	0.0012	0.0013	0.0016	0.0019	0.0021	0.0024	0.0027	0.0030	0.0030	0.0031	0.0031	0.0031	0.0027	0.0011	0.0023	0.0031
75	0.0028	0.0029	0.0028	0.0027	0.0026	0.0026	0.0026	0.0025	0.0024	0.0025	0.0027	0.0030	0.0030	0.0031	0.0032	0.0031	0.0032	0.0031	0.0029	0.0025	0.0020	0.0028	0.0032
76	0.0038	0.0037	0.0033	0.0028	0.0023	0.0023	0.0021	0.0019	0.0022	0.0025	0.0028	0.0029	0.0030	0.0034	0.0039	0.0042	0.0046	0.0047	0.0047	0.0040	0.0015	0.0032	0.0047
77	0.0057	0.0056	0.0050	0.0044	0.0036	0.0029	0.0027	0.0027	0.0033	0.0039	0.0043	0.0046	0.0053	0.0059	0.0065	0.0066	0.0070	0.0069	0.0066	0.0056	0.0021	0.0050	0.0070
78	0.0062	0.0059	0.0052	0.0043	0.0036	0.0028	0.0025	0.0024	0.0030	0.0036	0.0042	0.0054	0.0063	0.0071	0.0078	0.0077	0.0079	0.0076	0.0072	0.0062	0.0025	0.0053	0.0079
79	0.0069	0.0066	0.0055	0.0045	0.0037	0.0032	0.0027	0.0028	0.0035	0.0040	0.0047	0.0054	0.0059	0.0068	0.0077	0.0080	0.0084	0.0084	0.0082	0.0071	0.0028	0.0057	0.0084
80	0.0053	0.0051	0.0045	0.0038	0.0032	0.0029	0.0026	0.0033	0.0039	0.0042	0.0045	0.0047	0.0050	0.0056	0.0060	0.0059	0.0064	0.0068	0.0066	0.0059	0.0024	0.0048	0.0068
81	0.0053	0.0052	0.0046	0.0039	0.0034	0.0031	0.0028	0.0025	0.0026	0.0032	0.0041	0.0051	0.0057	0.0063	0.0068	0.0066	0.0069	0.0072	0.0076	0.0068	0.0021	0.0050	0.0076
82	0.0033	0.0034	0.0034	0.0034	0.0033	0.0032	0.0031	0.0030	0.0030	0.0030	0.0032	0.0033	0.0033	0.0033	0.0033	0.0030	0.0033	0.0034	0.0035	0.0031	0.0028	0.0032	0.0035
83	0.0007	0.0006	0.0006	0.0006	0.0006	0.0006	0.0005	0.0005	0.0006	0.0006	0.0006	0.0007	0.0007	0.0007	0.0007	0.0007	0.0006	0.0006	0.0006	0.0008	0.0004	0.0006	0.0008
84	0.0037	0.0037	0.0035	0.0033	0.0033	0.0033	0.0031	0.0025	0.0026	0.0028	0.0031	0.0035	0.0038	0.0042	0.0046	0.0047	0.0048	0.0046	0.0047	0.0044	0.0022	0.0037	0.0048
85	0.0032	0.0031	0.0028	0.0025	0.0022	0.0019	0.0016	0.0018	0.0021	0.0024	0.0027	0.0032	0.0035	0.0038	0.0039	0.0038	0.0039	0.0039	0.0037	0.0031	0.0021	0.0030	0.0039
86	0.0078	0.0079	0.0066	0.0063	0.0060	0.0055	0.0051	0.0056	0.0059	0.0060	0.0060	0.0065	0.0075	0.0083	0.0092	0.0098	0.0103	0.0099	0.0096	0.0085	0.0033	0.0074	0.0103
87	0.0098	0.0130	0.0132	0.0110	0.0087	0.0068	0.0065	0.0067	0.0063	0.0067	0.0070	0.0083	0.0109	0.0138	0.0170	0.0191	0.0217	0.0196	0.0160	0.0124	0.0054	0.0117	0.0217
88	0.0062	0.0056	0.0047	0.0046	0.0044	0.0048	0.0052	0.0049	0.0054	0.0053	0.0057	0.0055	0.0049	0.0049	0.0064	0.0069	0.0072	0.0088	0.0104	0.0098	0.0028	0.0061	0.0104
89	0.0044	0.0040	0.0036	0.0035	0.0033	0.0034	0.0035	0.0033	0.0032	0.0032	0.0039	0.0044	0.0044	0.0044	0.0047	0.0049	0.0058	0.0066	0.0074	0.0069	0.0026	0.0044	0.0074
90	0.0044	0.0040	0.0033	0.0033	0.0033	0.0033	0.0031	0.0030	0.0031	0.0035	0.0039	0.0042	0.0043	0.0044	0.0047	0.0050	0.0055	0.0059	0.0062	0.0055	0.0021	0.0042	0.0062
91	0.0071	0.0067	0.0054	0.0053	0.0049	0.0048	0.0044	0.0037	0.0033	0.0033	0.0043	0.0052	0.0053	0.0060	0.0071	0.0074	0.0077	0.0081	0.0084	0.0076	0.0019	0.0058	0.0084
92	0.0022	0.0021	0.0020	0.0019	0.0020	0.0023	0.0022	0.0019	0.0022	0.0026	0.0027	0.0024	0.0026	0.0028	0.0026	0.0025	0.0031	0.0033	0.0035	0.0035	0.0016	0.0025	0.0035
93	0.0024	0.0022	0.0018	0.0018	0.0018	0.0018	0.0017	0.0017	0.0019	0.0021	0.0022	0.0023	0.0023	0.0023	0.0023	0.0022	0.0022	0.0024	0.0029	0.0029	0.0015	0.0022	0.0029
94	0.0069	0.0071	0.0068	0.0064	0.0062	0.0067	0.0069	0.0070	0.0071	0.0070	0.0068	0.0067	0.0065	0.0065	0.0063	0.0058	0.0053	0.0049	0.0046	0.0041	0.0056	0.0063	0.0071
95	0.0077	0.0080	0.0073	0.0066	0.0064	0.0065	0.0070	0.0068	0.0060	0.0064	0.0066	0.0074	0.0078	0.0083	0.0085	0.0079	0.0083	0.0082	0.0085	0.0077	0.0046	0.0074	0.0085
96	0.0117	0.0134	0.0109	0.0086	0.0080	0.0083	0.0088	0.0087	0.0082	0.0092	0.0106	0.0119	0.0119	0.0104	0.0107	0.0126	0.0140	0.0143	0.0150	0.0124	0.0068	0.0110	0.0150
97	0.0077	0.0081	0.0073	0.0067	0.0061	0.0055	0.0049	0.0048	0.0050	0.0053	0.0059	0.0064	0.0065	0.0065	0.0064	0.0061	0.0063	0.0063	0.0061	0.0051	0.0040	0.0061	0.0081
98	0.0129	0.0174	0.0170	0.0143	0.0104	0.0091	0.0088	0.0085	0.0085	0.0087	0.0095	0.0101	0.0102	0.0104	0.0105	0.0108	0.0132	0.0146	0.0136	0.0111	0.0073	0.0115	0.0174
99	0.0064	0.0066	0.0064	0.0063	0.0064	0.0065	0.0065	0.0065	0.0063	0.0061	0.0062	0.0066	0.0066	0.0066	0.0064	0.0058	0.0055	0.0054	0.0052	0.0045	0.0056	0.0061	0.0066
100	0.0097	0.0117	0.0113	0.0103	0.0088	0.0074	0.0070	0.0071	0.0071	0.0071	0.0072	0.0073	0.0077	0.0085	0.0094	0.0092	0.0090	0.0086	0.0080	0.0067	0.0069	0.0084	0.0117
101	0.0099	0.0108	0.0091	0.0075	0.0063	0.0055	0.0052	0.0052	0.0057	0.0062	0.0067	0.0070	0.0071	0.0076	0.0079	0.0074	0.0072	0.0069	0.0066	0.0056	0.0045	0.0071	0.0108
102	0.0016	0.0016	0.0015	0.0014	0.0013	0.0013	0.0014	0.0014	0.0015	0.0016	0.0017	0.0018	0.0018	0.0017	0.0016	0.0015	0.0014	0.0014	0.0015	0.0016	0.0012	0.0015	0.0018
103	0.0031	0.0031	0.0031	0.0031	0.0030	0.0030	0.0031	0.0032	0.0033	0.0033	0.0034	0.0035	0.0034	0.0033	0.0032	0.0029	0.0029	0.0028	0.0028	0.0025	0.0028	0.0031	0.0035
104	0.0162	0.0232	0.0241	0.0227	0.0192	0.0148	0.0117	0.0104	0.0104	0.0103	0.0104	0.0104	0.0099	0.0095	0.0089	0.0084	0.0083	0.0080	0.0076	0.0067	0.0106	0.0126	0.0241
105	0.0054	0.0047	0.0038	0.0036	0.0037	0.0036	0.0032	0.0033	0.0037	0.0038	0.0036	0.0035	0.0035	0.0039	0.0041	0.0044	0.0048	0.0052	0.0059	0.0058	0.0022	0.0042	0.0059

Table C.13 (continued) Drift ratio demands for the *ductile* 20-story building model.

ID #	IDR1	IDR2	IDR3	IDR4	IDR5	IDR6	IDR7	IDR8	IDR9	IDR10	IDR11	IDR12	IDR13	IDR14	IDR15	IDR16	IDR17	IDR18	IDR19	IDR20	RDR	AIDR	MIDR
106	0.0142	0.0206	0.0226	0.0217	0.0179	0.0126	0.0102	0.0094	0.0106	0.0124	0.0149	0.0176	0.0200	0.0213	0.0192	0.0144	0.0141	0.0135	0.0125	0.0124	0.0117	0.0156	0.0226
107	0.0115	0.0159	0.0170	0.0161	0.0144	0.0123	0.0110	0.0102	0.0098	0.0099	0.0102	0.0114	0.0134	0.0136	0.0155	0.0162	0.0158	0.0150	0.0142	0.0116	0.0089	0.0133	0.0170
108	0.0088	0.0104	0.0105	0.0103	0.0098	0.0093	0.0092	0.0093	0.0093	0.0093	0.0095	0.0101	0.0097	0.0093	0.0092	0.0086	0.0084	0.0079	0.0075	0.0073	0.0089	0.0092	0.0105
109	0.0039	0.0036	0.0033	0.0034	0.0033	0.0029	0.0027	0.0028	0.0029	0.0033	0.0035	0.0034	0.0033	0.0037	0.0044	0.0050	0.0055	0.0054	0.0053	0.0049	0.0018	0.0038	0.0055
110	0.0038	0.0039	0.0038	0.0039	0.0039	0.0040	0.0040	0.0041	0.0042	0.0042	0.0044	0.0044	0.0043	0.0043	0.0043	0.0041	0.0040	0.0038	0.0036	0.0030	0.0038	0.0040	0.0044
111	0.0025	0.0024	0.0022	0.0021	0.0022	0.0024	0.0024	0.0023	0.0021	0.0021	0.0022	0.0023	0.0023	0.0023	0.0022	0.0021	0.0022	0.0023	0.0026	0.0026	0.0017	0.0023	0.0026
112	0.0019	0.0019	0.0017	0.0016	0.0017	0.0018	0.0019	0.0017	0.0015	0.0015	0.0016	0.0016	0.0016	0.0016	0.0016	0.0014	0.0015	0.0016	0.0018	0.0017	0.0012	0.0017	0.0019
113	0.0043	0.0044	0.0042	0.0040	0.0039	0.0039	0.0041	0.0042	0.0041	0.0040	0.0039	0.0039	0.0038	0.0039	0.0039	0.0037	0.0037	0.0035	0.0033	0.0028	0.0032	0.0039	0.0044
114	0.0071	0.0072	0.0067	0.0061	0.0058	0.0055	0.0056	0.0060	0.0060	0.0070	0.0087	0.0093	0.0087	0.0086	0.0090	0.0078	0.0074	0.0094	0.0090	0.0113	0.0046	0.0076	0.0113
115	0.0066	0.0066	0.0068	0.0070	0.0066	0.0064	0.0057	0.0050	0.0056	0.0063	0.0064	0.0073	0.0070	0.0074	0.0082	0.0072	0.0068	0.0066	0.0102	0.0111	0.0045	0.0071	0.0111
116	0.0062	0.0058	0.0050	0.0047	0.0047	0.0059	0.0067	0.0059	0.0051	0.0046	0.0062	0.0069	0.0061	0.0067	0.0077	0.0066	0.0073	0.0089	0.0103	0.0126	0.0026	0.0067	0.0126
117	0.0044	0.0044	0.0042	0.0040	0.0036	0.0029	0.0027	0.0024	0.0028	0.0032	0.0034	0.0038	0.0045	0.0050	0.0051	0.0047	0.0054	0.0063	0.0067	0.0060	0.0021	0.0043	0.0067
118	0.0119	0.0156	0.0158	0.0147	0.0123	0.0099	0.0092	0.0093	0.0091	0.0090	0.0093	0.0095	0.0094	0.0093	0.0092	0.0088	0.0088	0.0083	0.0077	0.0065	0.0085	0.0102	0.0158
119	0.0104	0.0129	0.0127	0.0116	0.0101	0.0086	0.0082	0.0082	0.0081	0.0082	0.0085	0.0088	0.0086	0.0086	0.0085	0.0081	0.0080	0.0076	0.0091	0.0090	0.0082	0.0092	0.0129
120	0.0127	0.0171	0.0184	0.0191	0.0171	0.0133	0.0124	0.0120	0.0114	0.0109	0.0112	0.0115	0.0113	0.0113	0.0133	0.0142	0.0136	0.0122	0.0115	0.0101	0.0109	0.0132	0.0191
121	0.0142	0.0186	0.0196	0.0189	0.0157	0.0111	0.0093	0.0092	0.0093	0.0095	0.0100	0.0103	0.0102	0.0099	0.0093	0.0088	0.0087	0.0088	0.0081	0.0071	0.0103	0.0113	0.0196
122	0.0067	0.0066	0.0063	0.0056	0.0057	0.0058	0.0057	0.0052	0.0054	0.0060	0.0061	0.0069	0.0072	0.0075	0.0084	0.0087	0.0087	0.0085	0.0093	0.0087	0.0036	0.0070	0.0093
123	0.0048	0.0049	0.0047	0.0047	0.0046	0.0046	0.0044	0.0046	0.0050	0.0054	0.0059	0.0063	0.0065	0.0066	0.0065	0.0059	0.0055	0.0050	0.0045	0.0039	0.0043	0.0052	0.0066
124	0.0056	0.0057	0.0055	0.0052	0.0049	0.0047	0.0049	0.0050	0.0050	0.0051	0.0055	0.0057	0.0056	0.0055	0.0052	0.0046	0.0046	0.0048	0.0047	0.0042	0.0043	0.0051	0.0057
125	0.0075	0.0072	0.0065	0.0061	0.0056	0.0053	0.0057	0.0059	0.0063	0.0070	0.0077	0.0081	0.0081	0.0081	0.0086	0.0086	0.0085	0.0087	0.0086	0.0074	0.0054	0.0073	0.0087
126	0.0083	0.0087	0.0079	0.0066	0.0055	0.0065	0.0073	0.0075	0.0071	0.0063	0.0063	0.0061	0.0050	0.0048	0.0060	0.0070	0.0087	0.0099	0.0105	0.0092	0.0046	0.0073	0.0105
127	0.0062	0.0061	0.0057	0.0056	0.0051	0.0042	0.0034	0.0041	0.0048	0.0054	0.0062	0.0067	0.0069	0.0074	0.0076	0.0070	0.0069	0.0069	0.0072	0.0068	0.0038	0.0060	0.0076
128	0.0065	0.0068	0.0065	0.0061	0.0058	0.0053	0.0052	0.0051	0.0053	0.0059	0.0065	0.0069	0.0068	0.0070	0.0072	0.0071	0.0073	0.0076	0.0078	0.0071	0.0052	0.0065	0.0078
129	0.0095	0.0099	0.0084	0.0078	0.0087	0.0081	0.0066	0.0057	0.0065	0.0069	0.0072	0.0080	0.0083	0.0102	0.0135	0.0150	0.0140	0.0119	0.0121	0.0111	0.0048	0.0095	0.0150
130	0.0111	0.0154	0.0182	0.0194	0.0178	0.0135	0.0100	0.0093	0.0093	0.0095	0.0098	0.0100	0.0097	0.0092	0.0084	0.0074	0.0078	0.0076	0.0070	0.0059	0.0097	0.0108	0.0194
131	0.0125	0.0150	0.0141	0.0126	0.0099	0.0073	0.0054	0.0063	0.0074	0.0078	0.0087	0.0098	0.0122	0.0133	0.0118	0.0129	0.0150	0.0184	0.0188	0.0172	0.0056	0.0118	0.0188
132	0.0107	0.0125	0.0123	0.0112	0.0106	0.0101	0.0099	0.0097	0.0094	0.0093	0.0095	0.0098	0.0096	0.0094	0.0092	0.0089	0.0090	0.0090	0.0089	0.0080	0.0088	0.0099	0.0125
133	0.0088	0.0094	0.0088	0.0090	0.0086	0.0078	0.0077	0.0074	0.0073	0.0080	0.0088	0.0094	0.0092	0.0093	0.0094	0.0090	0.0087	0.0083	0.0083	0.0075	0.0058	0.0085	0.0094
134	0.0149	0.0205	0.0208	0.0186	0.0142	0.0094	0.0080	0.0078	0.0079	0.0082	0.0087	0.0092	0.0094	0.0097	0.0097	0.0096	0.0098	0.0097	0.0094	0.0081	0.0093	0.0112	0.0208
135	0.0121	0.0151	0.0139	0.0112	0.0092	0.0079	0.0080	0.0079	0.0078	0.0077	0.0077	0.0079	0.0078	0.0078	0.0077	0.0073	0.0074	0.0073	0.0075	0.0068	0.0072	0.0088	0.0151
136	0.0074	0.0075	0.0068	0.0064	0.0060	0.0057	0.0054	0.0051	0.0049	0.0050	0.0055	0.0059	0.0061	0.0064	0.0066	0.0063	0.0067	0.0071	0.0072	0.0063	0.0042	0.0062	0.0075
137	0.0310	0.0382	0.0370	0.0325	0.0253	0.0145	0.0116	0.0108	0.0125	0.0155	0.0178	0.0176	0.0167	0.0186	0.0191	0.0158	0.0135	0.0141	0.0140	0.0120	0.0158	0.0194	0.0382
138	0.0060	0.0062	0.0061	0.0060	0.0057	0.0054	0.0054	0.0054	0.0052	0.0048	0.0048	0.0055	0.0059	0.0061	0.0059	0.0054	0.0051	0.0050	0.0050	0.0045	0.0044	0.0055	0.0062
139	0.0046	0.0045	0.0042	0.0039	0.0038	0.0035	0.0036	0.0037	0.0038	0.0039	0.0042	0.0043	0.0040	0.0035	0.0034	0.0034	0.0038	0.0042	0.0046	0.0045	0.0028	0.0040	0.0046
140	0.0076	0.0070	0.0056	0.0050	0.0042	0.0035	0.0039	0.0043	0.0046	0.0050	0.0055	0.0066	0.0076	0.0084	0.0089	0.0089	0.0093	0.0090	0.0085	0.0073	0.0039	0.0065	0.0093

Table C.13 (continued) Drift ratio demands for the *ductile* 20-story building model.

ID #	IDR1	IDR2	IDR3	IDR4	IDR5	IDR6	IDR7	IDR8	IDR9	IDR10	IDR11	IDR12	IDR13	IDR14	IDR15	IDR16	IDR17	IDR18	IDR19	IDR20	RDR	AIDR	MIDR
1	0.0044	0.0042	0.0037	0.0034	0.0031	0.0027	0.0022	0.0024	0.0025	0.0027	0.0034	0.0037	0.0041	0.0045	0.0049	0.0049	0.0050	0.0049	0.0047	0.0043	0.0022	0.0038	0.0050
2	0.0057	0.0053	0.0049	0.0049	0.0047	0.0043	0.0040	0.0039	0.0036	0.0042	0.0050	0.0058	0.0064	0.0073	0.0080	0.0076	0.0072	0.0067	0.0060	0.0055	0.0036	0.0056	0.0080
3	0.0065	0.0055	0.0051	0.0045	0.0036	0.0042	0.0047	0.0051	0.0051	0.0048	0.0054	0.0057	0.0055	0.0056	0.0071	0.0074	0.0075	0.0089	0.0104	0.0098	0.0026	0.0061	0.0104
4	0.0104	0.0122	0.0119	0.0116	0.0109	0.0098	0.0093	0.0090	0.0088	0.0084	0.0088	0.0091	0.0089	0.0095	0.0117	0.0133	0.0146	0.0157	0.0129	0.0122	0.0044	0.0109	0.0157
5	0.0065	0.0064	0.0056	0.0046	0.0046	0.0047	0.0049	0.0048	0.0044	0.0048	0.0053	0.0056	0.0058	0.0065	0.0066	0.0055	0.0059	0.0059	0.0063	0.0065	0.0033	0.0056	0.0066
6	0.0054	0.0049	0.0041	0.0036	0.0037	0.0040	0.0044	0.0046	0.0048	0.0048	0.0051	0.0049	0.0042	0.0039	0.0055	0.0071	0.0088	0.0093	0.0090	0.0081	0.0022	0.0055	0.0093
7	0.0061	0.0056	0.0047	0.0047	0.0051	0.0054	0.0052	0.0053	0.0056	0.0053	0.0051	0.0051	0.0051	0.0049	0.0053	0.0057	0.0078	0.0097	0.0111	0.0102	0.0034	0.0061	0.0111
8	0.0034	0.0033	0.0029	0.0027	0.0024	0.0020	0.0021	0.0021	0.0021	0.0021	0.0026	0.0032	0.0035	0.0038	0.0040	0.0039	0.0041	0.0040	0.0038	0.0033	0.0018	0.0031	0.0041
9	0.0114	0.0134	0.0109	0.0074	0.0056	0.0044	0.0041	0.0048	0.0054	0.0061	0.0074	0.0085	0.0102	0.0117	0.0122	0.0126	0.0119	0.0122	0.0130	0.0119	0.0044	0.0093	0.0134
10	0.0046	0.0046	0.0045	0.0043	0.0041	0.0039	0.0038	0.0039	0.0040	0.0042	0.0043	0.0044	0.0044	0.0046	0.0048	0.0046	0.0046	0.0044	0.0042	0.0035	0.0035	0.0043	0.0048
11	0.0053	0.0053	0.0055	0.0063	0.0064	0.0052	0.0047	0.0051	0.0056	0.0059	0.0059	0.0057	0.0055	0.0057	0.0051	0.0058	0.0057	0.0053	0.0072	0.0075	0.0035	0.0057	0.0075
12	0.0054	0.0053	0.0049	0.0046	0.0045	0.0043	0.0042	0.0042	0.0042	0.0040	0.0040	0.0040	0.0038	0.0040	0.0042	0.0042	0.0047	0.0048	0.0050	0.0047	0.0030	0.0045	0.0054
13	0.0055	0.0053	0.0047	0.0041	0.0042	0.0044	0.0044	0.0036	0.0036	0.0041	0.0043	0.0045	0.0045	0.0050	0.0063	0.0066	0.0058	0.0054	0.0060	0.0081	0.0026	0.0050	0.0081
14	0.0078	0.0080	0.0072	0.0063	0.0056	0.0058	0.0061	0.0067	0.0072	0.0068	0.0065	0.0069	0.0063	0.0051	0.0056	0.0058	0.0073	0.0072	0.0124	0.0136	0.0030	0.0072	0.0136
15	0.0021	0.0020	0.0019	0.0017	0.0016	0.0014	0.0014	0.0014	0.0014	0.0014	0.0015	0.0015	0.0014	0.0015	0.0017	0.0018	0.0019	0.0019	0.0018	0.0016	0.0009	0.0016	0.0021
16	0.0051	0.0049	0.0043	0.0035	0.0027	0.0026	0.0028	0.0032	0.0033	0.0032	0.0033	0.0037	0.0037	0.0042	0.0048	0.0048	0.0053	0.0058	0.0061	0.0054	0.0020	0.0041	0.0061
17	0.0065	0.0060	0.0050	0.0044	0.0041	0.0048	0.0051	0.0055	0.0058	0.0059	0.0060	0.0061	0.0058	0.0056	0.0063	0.0064	0.0067	0.0070	0.0072	0.0066	0.0042	0.0058	0.0072
18	0.0081	0.0081	0.0068	0.0072	0.0080	0.0082	0.0077	0.0067	0.0055	0.0063	0.0077	0.0087	0.0084	0.0078	0.0072	0.0069	0.0069	0.0077	0.0091	0.0089	0.0048	0.0076	0.0091
19	0.0121	0.0144	0.0125	0.0096	0.0075	0.0065	0.0062	0.0061	0.0064	0.0069	0.0076	0.0082	0.0089	0.0101	0.0114	0.0127	0.0163	0.0164	0.0134	0.0128	0.0039	0.0103	0.0164
20	0.0024	0.0023	0.0020	0.0019	0.0017	0.0018	0.0018	0.0019	0.0022	0.0024	0.0026	0.0027	0.0028	0.0027	0.0023	0.0022	0.0022	0.0020	0.0024	0.0028	0.0012	0.0023	0.0028
21	0.0078	0.0074	0.0067	0.0074	0.0083	0.0085	0.0079	0.0070	0.0063	0.0067	0.0081	0.0096	0.0100	0.0098	0.0095	0.0106	0.0150	0.0220	0.0233	0.0158	0.0052	0.0104	0.0233
22	0.0079	0.0079	0.0066	0.0071	0.0073	0.0081	0.0093	0.0090	0.0073	0.0064	0.0070	0.0089	0.0095	0.0090	0.0089	0.0078	0.0089	0.0125	0.0174	0.0156	0.0048	0.0091	0.0174
23	0.0128	0.0163	0.0155	0.0152	0.0142	0.0107	0.0085	0.0080	0.0078	0.0080	0.0078	0.0094	0.0100	0.0106	0.0110	0.0121	0.0126	0.0147	0.0164	0.0123	0.0088	0.0117	0.0164
24	0.0120	0.0159	0.0173	0.0171	0.0145	0.0107	0.0101	0.0105	0.0106	0.0105	0.0110	0.0114	0.0113	0.0113	0.0111	0.0107	0.0105	0.0100	0.0092	0.0079	0.0097	0.0117	0.0173
25	0.0092	0.0087	0.0072	0.0068	0.0065	0.0062	0.0067	0.0074	0.0073	0.0072	0.0084	0.0099	0.0101	0.0103	0.0138	0.0158	0.0147	0.0120	0.0160	0.0146	0.0040	0.0099	0.0160
26	0.0130	0.0147	0.0121	0.0105	0.0087	0.0075	0.0103	0.0122	0.0108	0.0082	0.0088	0.0115	0.0133	0.0126	0.0125	0.0171	0.0199	0.0207	0.0205	0.0177	0.0052	0.0131	0.0207
27	0.0144	0.0194	0.0178	0.0140	0.0110	0.0082	0.0068	0.0074	0.0090	0.0106	0.0135	0.0165	0.0176	0.0168	0.0143	0.0119	0.0119	0.0127	0.0122	0.0101	0.0095	0.0128	0.0194
28	0.0123	0.0179	0.0209	0.0213	0.0180	0.0121	0.0096	0.0086	0.0096	0.0103	0.0104	0.0123	0.0156	0.0155	0.0131	0.0108	0.0110	0.0119	0.0118	0.0103	0.0094	0.0132	0.0213
29	0.0114	0.0165	0.0186	0.0184	0.0175	0.0164	0.0153	0.0139	0.0122	0.0103	0.0094	0.0111	0.0117	0.0105	0.0109	0.0110	0.0107	0.0144	0.0202	0.0209	0.0077	0.0141	0.0209
30	0.0137	0.0190	0.0225	0.0234	0.0209	0.0172	0.0146	0.0150	0.0170	0.0190	0.0197	0.0192	0.0173	0.0149	0.0127	0.0117	0.0111	0.0099	0.0088	0.0080	0.0128	0.0158	0.0234
31	0.0096	0.0104	0.0089	0.0077	0.0074	0.0071	0.0077	0.0088	0.0087	0.0073	0.0067	0.0064	0.0060	0.0066	0.0074	0.0069	0.0071	0.0080	0.0089	0.0100	0.0060	0.0079	0.0104
32	######	######	######	######	######	######	######	######	######	######	######	######	######	######	######	######	######	######	######	######	######	######	######
33	######	######	######	######	######	######	######	######	######	######	######	######	######	######	######	######	######	######	######	######	######	######	######
34	0.0134	0.0172	0.0178	0.0179	0.0140	0.0088	0.0089	0.0089	0.0083	0.0095	0.0117	0.0133	0.0120	0.0105	0.0090	0.0083	0.0088	0.0107	0.0118	0.0109	0.0078	0.0116	0.0179
35	######	######	######	######	######	######	######	######	######	######	######	######	######	######	######	######	######	######	######	######	######	######	######

Table C.14 Drift ratio demands for the *brittle* 20-story building model. Note the collapses (###'s).

ID #	IDR1	IDR2	IDR3	IDR4	IDR5	IDR6	IDR7	IDR8	IDR9	IDR10	IDR11	IDR12	IDR13	IDR14	IDR15	IDR16	IDR17	IDR18	IDR19	IDR20	RDR	AIDR	MIDR
36	######	######	######	######	######	######	######	72.4530	19.3280	5.0722	1.2867	0.3731	0.0761	0.0331	0.0120	0.0125	0.0144	0.0165	0.0167	0.0138	0.1646	######	######
37	######	######	######	######	######	######	######	######	######	######	######	######	######	######	32.9380	7.3669	1.8632	0.2436	0.2653	1.2804	0.1319	######	######
38	######	######	######	######	######	######	######	######	######	######	######	######	######	######	######	######	######	######	######	######	######	######	######
39	######	######	######	######	######	######	######	62.4390	16.5420	4.4317	1.0655	0.3288	0.0703	0.0260	0.0095	0.0083	0.0077	0.0080	0.0084	0.0078	0.1440	######	######
40	######	######	######	######	######	######	######	######	54.3140	14.3260	3.6678	1.0321	0.2442	0.0768	0.0178	0.0154	0.0150	0.0150	0.0137	0.0114	0.1541	######	######
41	######	######	######	######	######	######	######	######	34.4350	9.0642	2.3062	0.6510	0.1526	0.0503	0.0112	0.0104	0.0103	0.0097	0.0090	0.0078	0.1594	######	######
42	######	######	######	######	######	######	######	######	######	######	######	######	######	######	######	######	######	######	######	######	######	######	######
43	0.0099	0.0119	0.0120	0.0114	0.0102	0.0093	0.0089	0.0085	0.0081	0.0080	0.0084	0.0088	0.0087	0.0087	0.0086	0.0082	0.0081	0.0077	0.0072	0.0064	0.0079	0.0089	0.0120
44	0.0079	0.0084	0.0074	0.0063	0.0055	0.0050	0.0041	0.0043	0.0047	0.0048	0.0055	0.0068	0.0080	0.0084	0.0080	0.0081	0.0083	0.0097	0.0105	0.0097	0.0026	0.0071	0.0105
45	0.0555	0.0724	0.0759	0.0706	0.0537	0.0210	0.0212	0.0209	0.0211	0.0230	0.0283	0.0317	0.0297	0.0248	0.0186	0.0155	0.0156	0.0148	0.0156	0.0123	0.0144	0.0321	0.0759
46	0.0133	0.0181	0.0185	0.0160	0.0117	0.0094	0.0091	0.0087	0.0092	0.0096	0.0100	0.0101	0.0094	0.0103	0.0103	0.0096	0.0108	0.0121	0.0134	0.0120	0.0075	0.0116	0.0185
47	0.0125	0.0162	0.0162	0.0154	0.0118	0.0106	0.0125	0.0145	0.0166	0.0192	0.0224	0.0278	0.0313	0.0307	0.0191	0.0158	0.0156	0.0149	0.0154	0.0135	0.0103	0.0176	0.0313
48	0.0108	0.0124	0.0126	0.0119	0.0098	0.0088	0.0094	0.0094	0.0088	0.0090	0.0105	0.0137	0.0147	0.0126	0.0112	0.0112	0.0160	0.0224	0.0214	0.0185	0.0092	0.0127	0.0224
49	######	######	######	######	######	######	######	######	######	######	######	######	######	27.1390	6.8317	1.5313	0.3846	0.0522	0.0582	0.2621	0.1381	######	######
50	######	######	######	######	######	######	######	######	######	######	######	######	######	######	######	######	######	######	######	######	######	######	######
51	0.0155	0.0204	0.0228	0.0221	0.0178	0.0135	0.0103	0.0086	0.0093	0.0101	0.0103	0.0119	0.0133	0.0151	0.0186	0.0200	0.0231	0.0225	0.0191	0.0150	0.0081	0.0160	0.0231
52	######	######	######	######	######	######	######	######	######	######	######	######	######	######	######	######	######	######	######	######	######	######	######
53	0.0171	0.0208	0.0192	0.0171	0.0138	0.0125	0.0130	0.0138	0.0158	0.0148	0.0153	0.0140	0.0111	0.0125	0.0145	0.0167	0.0203	0.0224	0.0189	0.0191	0.0108	0.0161	0.0224
54	######	######	######	######	######	######	######	######	######	######	######	######	######	######	######	######	######	######	######	######	######	######	######
55	######	######	######	######	######	######	######	######	######	######	######	######	######	######	######	######	######	######	######	######	######	######	######
56	######	######	######	######	######	######	######	######	######	######	######	######	######	######	######	######	######	######	######	######	######	######	######
57	0.0379	0.0563	0.0621	0.0588	0.0483	0.0177	0.0165	0.0162	0.0125	0.0142	0.0165	0.0174	0.0165	0.0137	0.0140	0.0150	0.0193	0.0251	0.0257	0.0205	0.0155	0.0262	0.0621
58	0.0113	0.0133	0.0129	0.0112	0.0084	0.0055	0.0059	0.0072	0.0073	0.0072	0.0088	0.0107	0.0120	0.0129	0.0115	0.0109	0.0127	0.0149	0.0132	0.0109	0.0043	0.0104	0.0149
59	0.0122	0.0160	0.0160	0.0135	0.0095	0.0084	0.0089	0.0092	0.0090	0.0105	0.0112	0.0105	0.0103	0.0102	0.0111	0.0113	0.0120	0.0171	0.0178	0.0144	0.0066	0.0120	0.0178
60	0.0098	0.0105	0.0086	0.0065	0.0064	0.0062	0.0062	0.0063	0.0068	0.0074	0.0079	0.0096	0.0128	0.0163	0.0165	0.0129	0.0110	0.0106	0.0102	0.0088	0.0058	0.0096	0.0165
61	0.0131	0.0182	0.0206	0.0223	0.0222	0.0201	0.0177	0.0153	0.0136	0.0118	0.0103	0.0108	0.0116	0.0133	0.0129	0.0105	0.0103	0.0124	0.0125	0.0100	0.0097	0.0145	0.0223
62	0.0616	0.0807	0.0876	0.0863	0.0765	0.0350	0.0181	0.0140	0.0129	0.0127	0.0134	0.0148	0.0156	0.0170	0.0167	0.0189	0.0201	0.0211	0.0219	0.0177	0.0271	0.0331	0.0876
63	######	######	######	######	######	######	######	######	38.9470	10.3660	2.5904	0.7397	0.1783	0.0532	0.0096	0.0103	0.0100	0.0101	0.0101	0.0098	0.1451	######	######
64	0.0148	0.0194	0.0187	0.0184	0.0163	0.0115	0.0084	0.0080	0.0094	0.0105	0.0141	0.0156	0.0146	0.0166	0.0150	0.0131	0.0154	0.0163	0.0145	0.0138	0.0084	0.0142	0.0194
65	0.0104	0.0120	0.0114	0.0101	0.0088	0.0079	0.0074	0.0068	0.0067	0.0074	0.0084	0.0093	0.0093	0.0094	0.0093	0.0097	0.0108	0.0121	0.0121	0.0102	0.0058	0.0095	0.0121
66	0.0090	0.0097	0.0097	0.0098	0.0095	0.0086	0.0081	0.0081	0.0076	0.0078	0.0081	0.0081	0.0081	0.0083	0.0092	0.0094	0.0091	0.0090	0.0105	0.0098	0.0078	0.0089	0.0105
67	######	######	######	######	######	######	######	######	######	######	######	######	######	######	######	######	######	######	######	######	######	######	######
68	0.0092	0.0096	0.0080	0.0066	0.0068	0.0069	0.0074	0.0075	0.0074	0.0070	0.0064	0.0057	0.0057	0.0060	0.0067	0.0065	0.0062	0.0058	0.0054	0.0052	0.0047	0.0068	0.0096
69	2.0131	0.9851	0.7065	0.3312	0.1835	0.6747	0.6994	0.3806	0.1770	0.0215	0.0169	0.0131	0.0137	0.0144	0.0143	0.0154	0.0162	0.0146	0.0143	0.0119	0.1352	0.3159	2.0131
70	######	######	######	######	######	######	######	######	39.7320	10.6230	2.6227	0.7579	0.1846	0.0511	0.0125	0.0116	0.0114	0.0115	0.0111	0.0093	0.1451	######	######

Table C.14 (continued) Drift ratio demands for the *brittle* 20-story building model. Note the collapses (###'s).

ID #	IDR1	IDR2	IDR3	IDR4	IDR5	IDR6	IDR7	IDR8	IDR9	IDR10	IDR11	IDR12	IDR13	IDR14	IDR15	IDR16	IDR17	IDR18	IDR19	IDR20	RDR	AIDR	MIDR
71	0.0022	0.0021	0.0020	0.0019	0.0020	0.0022	0.0023	0.0024	0.0024	0.0023	0.0022	0.0022	0.0024	0.0026	0.0028	0.0027	0.0027	0.0029	0.0032	0.0033	0.0018	0.0024	0.0033
72	0.0051	0.0051	0.0047	0.0044	0.0043	0.0044	0.0045	0.0047	0.0048	0.0048	0.0050	0.0051	0.0050	0.0049	0.0054	0.0056	0.0059	0.0060	0.0058	0.0050	0.0038	0.0050	0.0060
73	0.0008	0.0008	0.0008	0.0008	0.0007	0.0007	0.0007	0.0007	0.0006	0.0007	0.0007	0.0007	0.0007	0.0007	0.0007	0.0006	0.0006	0.0005	0.0006	0.0007	0.0006	0.0007	0.0008
74	0.0025	0.0025	0.0022	0.0021	0.0019	0.0016	0.0014	0.0012	0.0013	0.0016	0.0019	0.0021	0.0024	0.0027	0.0030	0.0030	0.0031	0.0031	0.0031	0.0027	0.0011	0.0023	0.0031
75	0.0028	0.0029	0.0028	0.0027	0.0026	0.0026	0.0026	0.0025	0.0024	0.0025	0.0027	0.0030	0.0030	0.0031	0.0032	0.0031	0.0032	0.0031	0.0029	0.0025	0.0020	0.0028	0.0032
76	0.0038	0.0037	0.0033	0.0028	0.0023	0.0023	0.0021	0.0019	0.0022	0.0025	0.0028	0.0029	0.0030	0.0034	0.0039	0.0042	0.0046	0.0047	0.0047	0.0040	0.0015	0.0032	0.0047
77	0.0057	0.0056	0.0050	0.0044	0.0036	0.0029	0.0027	0.0027	0.0033	0.0039	0.0043	0.0046	0.0053	0.0059	0.0065	0.0066	0.0070	0.0069	0.0066	0.0056	0.0021	0.0050	0.0070
78	0.0062	0.0059	0.0052	0.0043	0.0036	0.0028	0.0025	0.0024	0.0030	0.0036	0.0042	0.0054	0.0063	0.0071	0.0078	0.0077	0.0079	0.0076	0.0072	0.0062	0.0025	0.0053	0.0079
79	0.0069	0.0066	0.0055	0.0045	0.0037	0.0032	0.0027	0.0028	0.0035	0.0040	0.0047	0.0054	0.0059	0.0068	0.0077	0.0080	0.0084	0.0084	0.0082	0.0071	0.0028	0.0057	0.0084
80	0.0053	0.0051	0.0045	0.0038	0.0032	0.0029	0.0026	0.0033	0.0039	0.0042	0.0045	0.0047	0.0050	0.0056	0.0060	0.0059	0.0064	0.0068	0.0066	0.0059	0.0024	0.0048	0.0068
81	0.0053	0.0052	0.0046	0.0039	0.0034	0.0031	0.0028	0.0025	0.0026	0.0032	0.0041	0.0051	0.0057	0.0063	0.0068	0.0066	0.0069	0.0072	0.0076	0.0068	0.0021	0.0050	0.0076
82	0.0033	0.0034	0.0034	0.0034	0.0033	0.0032	0.0031	0.0030	0.0030	0.0030	0.0032	0.0033	0.0033	0.0033	0.0033	0.0030	0.0033	0.0034	0.0035	0.0031	0.0028	0.0032	0.0035
83	0.0007	0.0006	0.0006	0.0006	0.0006	0.0006	0.0005	0.0005	0.0006	0.0006	0.0006	0.0007	0.0007	0.0007	0.0007	0.0007	0.0006	0.0006	0.0006	0.0008	0.0004	0.0006	0.0008
84	0.0037	0.0037	0.0035	0.0033	0.0033	0.0033	0.0031	0.0025	0.0026	0.0028	0.0031	0.0035	0.0038	0.0042	0.0046	0.0047	0.0048	0.0046	0.0047	0.0044	0.0022	0.0037	0.0048
85	0.0032	0.0031	0.0028	0.0025	0.0022	0.0019	0.0016	0.0018	0.0021	0.0024	0.0027	0.0032	0.0035	0.0038	0.0039	0.0038	0.0039	0.0039	0.0037	0.0031	0.0021	0.0030	0.0039
86	0.0078	0.0079	0.0066	0.0063	0.0060	0.0055	0.0051	0.0056	0.0059	0.0060	0.0060	0.0065	0.0075	0.0083	0.0092	0.0098	0.0103	0.0099	0.0096	0.0085	0.0033	0.0074	0.0103
87	0.0098	0.0130	0.0132	0.0110	0.0087	0.0068	0.0065	0.0067	0.0063	0.0067	0.0070	0.0083	0.0109	0.0138	0.0170	0.0191	0.0217	0.0196	0.0160	0.0124	0.0054	0.0117	0.0217
88	0.0062	0.0056	0.0047	0.0046	0.0044	0.0048	0.0052	0.0049	0.0054	0.0053	0.0057	0.0055	0.0049	0.0049	0.0064	0.0069	0.0072	0.0088	0.0104	0.0098	0.0028	0.0061	0.0104
89	0.0044	0.0040	0.0036	0.0035	0.0033	0.0034	0.0035	0.0033	0.0032	0.0032	0.0039	0.0044	0.0044	0.0044	0.0047	0.0049	0.0058	0.0066	0.0074	0.0069	0.0026	0.0044	0.0074
90	0.0044	0.0040	0.0033	0.0033	0.0033	0.0033	0.0031	0.0030	0.0031	0.0035	0.0039	0.0042	0.0043	0.0044	0.0047	0.0050	0.0055	0.0059	0.0062	0.0055	0.0021	0.0042	0.0062
91	0.0071	0.0067	0.0054	0.0053	0.0049	0.0048	0.0044	0.0037	0.0033	0.0033	0.0043	0.0052	0.0053	0.0060	0.0071	0.0074	0.0077	0.0081	0.0084	0.0076	0.0019	0.0058	0.0084
92	0.0022	0.0021	0.0020	0.0019	0.0020	0.0023	0.0022	0.0019	0.0022	0.0026	0.0027	0.0024	0.0026	0.0028	0.0026	0.0025	0.0031	0.0033	0.0035	0.0035	0.0016	0.0025	0.0035
93	0.0024	0.0022	0.0018	0.0018	0.0018	0.0018	0.0017	0.0017	0.0019	0.0021	0.0022	0.0023	0.0023	0.0023	0.0023	0.0022	0.0022	0.0024	0.0029	0.0029	0.0015	0.0022	0.0029
94	0.0069	0.0071	0.0068	0.0064	0.0062	0.0067	0.0069	0.0070	0.0071	0.0070	0.0068	0.0067	0.0065	0.0065	0.0063	0.0058	0.0053	0.0049	0.0046	0.0041	0.0056	0.0063	0.0071
95	0.0077	0.0080	0.0073	0.0066	0.0064	0.0065	0.0070	0.0068	0.0060	0.0064	0.0066	0.0074	0.0078	0.0083	0.0085	0.0079	0.0083	0.0082	0.0085	0.0077	0.0046	0.0074	0.0085
96	0.0117	0.0134	0.0109	0.0086	0.0080	0.0083	0.0088	0.0087	0.0082	0.0092	0.0106	0.0119	0.0119	0.0104	0.0107	0.0126	0.0140	0.0143	0.0150	0.0124	0.0068	0.0110	0.0150
97	0.0077	0.0081	0.0073	0.0067	0.0061	0.0055	0.0049	0.0048	0.0050	0.0053	0.0059	0.0064	0.0065	0.0065	0.0064	0.0061	0.0063	0.0063	0.0061	0.0051	0.0040	0.0061	0.0081
98	0.0129	0.0174	0.0170	0.0143	0.0104	0.0091	0.0088	0.0085	0.0085	0.0087	0.0095	0.0101	0.0102	0.0104	0.0105	0.0108	0.0132	0.0146	0.0136	0.0111	0.0073	0.0115	0.0174
99	0.0064	0.0066	0.0064	0.0063	0.0064	0.0065	0.0065	0.0065	0.0063	0.0061	0.0062	0.0066	0.0066	0.0066	0.0064	0.0058	0.0055	0.0054	0.0052	0.0045	0.0056	0.0061	0.0066
100	0.0097	0.0117	0.0113	0.0103	0.0088	0.0074	0.0070	0.0071	0.0071	0.0071	0.0072	0.0073	0.0077	0.0085	0.0094	0.0092	0.0090	0.0086	0.0080	0.0067	0.0069	0.0084	0.0117
101	0.0099	0.0108	0.0091	0.0075	0.0063	0.0055	0.0052	0.0052	0.0057	0.0062	0.0067	0.0070	0.0071	0.0076	0.0079	0.0074	0.0072	0.0069	0.0066	0.0056	0.0045	0.0071	0.0108
102	0.0016	0.0016	0.0015	0.0014	0.0013	0.0013	0.0014	0.0014	0.0015	0.0016	0.0017	0.0018	0.0018	0.0017	0.0016	0.0015	0.0014	0.0014	0.0015	0.0016	0.0012	0.0015	0.0018
103	0.0031	0.0031	0.0031	0.0031	0.0030	0.0030	0.0031	0.0032	0.0033	0.0033	0.0034	0.0035	0.0034	0.0033	0.0032	0.0029	0.0029	0.0028	0.0028	0.0025	0.0028	0.0031	0.0035
104	0.0162	0.0232	0.0241	0.0227	0.0192	0.0148	0.0117	0.0104	0.0104	0.0103	0.0104	0.0104	0.0099	0.0095	0.0089	0.0084	0.0083	0.0080	0.0076	0.0067	0.0106	0.0126	0.0241
105	0.0054	0.0047	0.0038	0.0036	0.0037	0.0036	0.0032	0.0033	0.0037	0.0038	0.0036	0.0035	0.0035	0.0039	0.0041	0.0044	0.0048	0.0052	0.0059	0.0058	0.0022	0.0042	0.0059

Table C.14 (continued) Drift ratio demands for the *brittle* 20-story building model.

ID #	IDR1	IDR2	IDR3	IDR4	IDR5	IDR6	IDR7	IDR8	IDR9	IDR10	IDR11	IDR12	IDR13	IDR14	IDR15	IDR16	IDR17	IDR18	IDR19	IDR20	RDR	AIDR	MIDR
106	0.0142	0.0206	0.0226	0.0217	0.0179	0.0126	0.0102	0.0094	0.0106	0.0124	0.0149	0.0176	0.0200	0.0213	0.0192	0.0144	0.0141	0.0135	0.0125	0.0124	0.0117	0.0156	0.0226
107	0.0115	0.0159	0.0170	0.0161	0.0144	0.0123	0.0110	0.0102	0.0098	0.0099	0.0102	0.0114	0.0134	0.0136	0.0155	0.0162	0.0158	0.0150	0.0142	0.0116	0.0089	0.0133	0.0170
108	0.0088	0.0104	0.0105	0.0103	0.0098	0.0093	0.0092	0.0093	0.0093	0.0093	0.0095	0.0101	0.0097	0.0093	0.0092	0.0086	0.0084	0.0079	0.0075	0.0073	0.0089	0.0092	0.0105
109	0.0039	0.0036	0.0033	0.0034	0.0033	0.0029	0.0027	0.0028	0.0029	0.0033	0.0035	0.0034	0.0033	0.0037	0.0044	0.0050	0.0055	0.0054	0.0053	0.0049	0.0018	0.0038	0.0055
110	0.0038	0.0039	0.0038	0.0039	0.0039	0.0040	0.0040	0.0041	0.0042	0.0042	0.0044	0.0044	0.0043	0.0043	0.0043	0.0041	0.0040	0.0038	0.0036	0.0030	0.0038	0.0040	0.0044
111	0.0025	0.0024	0.0022	0.0021	0.0022	0.0024	0.0024	0.0023	0.0021	0.0021	0.0022	0.0023	0.0023	0.0023	0.0022	0.0021	0.0022	0.0023	0.0026	0.0026	0.0017	0.0023	0.0026
112	0.0019	0.0019	0.0017	0.0016	0.0017	0.0018	0.0019	0.0017	0.0015	0.0015	0.0016	0.0016	0.0016	0.0016	0.0016	0.0014	0.0015	0.0016	0.0018	0.0017	0.0012	0.0017	0.0019
113	0.0043	0.0044	0.0042	0.0040	0.0039	0.0039	0.0041	0.0042	0.0041	0.0040	0.0039	0.0039	0.0038	0.0039	0.0039	0.0037	0.0037	0.0035	0.0033	0.0028	0.0032	0.0039	0.0044
114	0.0071	0.0072	0.0067	0.0061	0.0058	0.0055	0.0056	0.0060	0.0060	0.0070	0.0087	0.0093	0.0087	0.0086	0.0090	0.0078	0.0074	0.0094	0.0090	0.0113	0.0046	0.0076	0.0113
115	0.0066	0.0066	0.0068	0.0070	0.0066	0.0064	0.0057	0.0050	0.0056	0.0063	0.0064	0.0073	0.0070	0.0074	0.0082	0.0072	0.0068	0.0066	0.0102	0.0111	0.0045	0.0071	0.0111
116	0.0062	0.0058	0.0050	0.0047	0.0047	0.0059	0.0067	0.0059	0.0051	0.0046	0.0062	0.0069	0.0061	0.0067	0.0077	0.0066	0.0073	0.0089	0.0103	0.0126	0.0026	0.0067	0.0126
117	0.0044	0.0044	0.0042	0.0040	0.0036	0.0029	0.0027	0.0024	0.0028	0.0032	0.0034	0.0038	0.0045	0.0050	0.0051	0.0047	0.0054	0.0063	0.0067	0.0060	0.0021	0.0043	0.0067
118	0.0119	0.0156	0.0158	0.0147	0.0123	0.0099	0.0092	0.0093	0.0091	0.0090	0.0093	0.0095	0.0094	0.0093	0.0092	0.0088	0.0088	0.0083	0.0077	0.0065	0.0085	0.0102	0.0158
119	0.0104	0.0129	0.0127	0.0116	0.0101	0.0086	0.0082	0.0082	0.0081	0.0082	0.0085	0.0088	0.0086	0.0086	0.0085	0.0081	0.0080	0.0076	0.0091	0.0090	0.0082	0.0092	0.0129
120	0.0127	0.0171	0.0184	0.0191	0.0171	0.0133	0.0124	0.0120	0.0114	0.0109	0.0112	0.0115	0.0113	0.0113	0.0133	0.0142	0.0136	0.0122	0.0115	0.0101	0.0109	0.0132	0.0191
121	0.0142	0.0186	0.0196	0.0189	0.0157	0.0111	0.0093	0.0092	0.0093	0.0095	0.0100	0.0103	0.0102	0.0099	0.0093	0.0088	0.0087	0.0088	0.0081	0.0071	0.0103	0.0113	0.0196
122	0.0067	0.0066	0.0063	0.0056	0.0057	0.0058	0.0057	0.0052	0.0054	0.0060	0.0061	0.0069	0.0072	0.0075	0.0084	0.0087	0.0087	0.0085	0.0093	0.0087	0.0036	0.0070	0.0093
123	0.0048	0.0049	0.0047	0.0047	0.0046	0.0046	0.0044	0.0046	0.0050	0.0054	0.0059	0.0063	0.0065	0.0066	0.0065	0.0059	0.0055	0.0050	0.0045	0.0039	0.0043	0.0052	0.0066
124	0.0056	0.0057	0.0055	0.0052	0.0049	0.0047	0.0049	0.0050	0.0050	0.0051	0.0055	0.0057	0.0056	0.0055	0.0052	0.0046	0.0046	0.0048	0.0047	0.0042	0.0043	0.0051	0.0057
125	0.0075	0.0072	0.0065	0.0061	0.0056	0.0053	0.0057	0.0059	0.0063	0.0070	0.0077	0.0081	0.0081	0.0081	0.0086	0.0086	0.0085	0.0087	0.0086	0.0074	0.0054	0.0073	0.0087
126	0.0083	0.0087	0.0079	0.0066	0.0055	0.0065	0.0073	0.0075	0.0071	0.0063	0.0063	0.0061	0.0050	0.0048	0.0060	0.0070	0.0087	0.0099	0.0105	0.0092	0.0046	0.0073	0.0105
127	0.0062	0.0061	0.0057	0.0056	0.0051	0.0042	0.0034	0.0041	0.0048	0.0054	0.0062	0.0067	0.0069	0.0074	0.0076	0.0070	0.0069	0.0069	0.0072	0.0068	0.0038	0.0060	0.0076
128	0.0065	0.0068	0.0065	0.0061	0.0058	0.0053	0.0052	0.0051	0.0053	0.0059	0.0065	0.0069	0.0068	0.0070	0.0072	0.0071	0.0073	0.0076	0.0078	0.0071	0.0052	0.0065	0.0078
129	0.0095	0.0099	0.0084	0.0078	0.0087	0.0081	0.0066	0.0057	0.0065	0.0069	0.0072	0.0080	0.0083	0.0102	0.0135	0.0150	0.0140	0.0119	0.0121	0.0111	0.0048	0.0095	0.0150
130	0.0111	0.0154	0.0182	0.0194	0.0178	0.0135	0.0100	0.0093	0.0093	0.0095	0.0098	0.0100	0.0097	0.0092	0.0084	0.0074	0.0078	0.0076	0.0070	0.0059	0.0097	0.0108	0.0194
131	0.0125	0.0150	0.0141	0.0126	0.0099	0.0073	0.0054	0.0063	0.0074	0.0078	0.0087	0.0098	0.0122	0.0133	0.0118	0.0129	0.0150	0.0184	0.0188	0.0172	0.0056	0.0118	0.0188
132	0.0107	0.0125	0.0123	0.0112	0.0106	0.0101	0.0099	0.0097	0.0094	0.0093	0.0095	0.0098	0.0096	0.0094	0.0092	0.0089	0.0090	0.0090	0.0089	0.0080	0.0088	0.0099	0.0125
133	0.0088	0.0094	0.0088	0.0090	0.0086	0.0078	0.0077	0.0074	0.0073	0.0080	0.0088	0.0094	0.0092	0.0093	0.0094	0.0090	0.0087	0.0083	0.0083	0.0075	0.0058	0.0085	0.0094
134	0.0149	0.0205	0.0208	0.0186	0.0142	0.0094	0.0080	0.0078	0.0079	0.0082	0.0087	0.0092	0.0094	0.0097	0.0097	0.0096	0.0098	0.0097	0.0094	0.0081	0.0093	0.0112	0.0208
135	0.0121	0.0151	0.0139	0.0112	0.0092	0.0079	0.0080	0.0079	0.0078	0.0077	0.0077	0.0079	0.0078	0.0078	0.0077	0.0073	0.0074	0.0073	0.0075	0.0068	0.0072	0.0088	0.0151
136	0.0074	0.0075	0.0068	0.0064	0.0060	0.0057	0.0054	0.0051	0.0049	0.0050	0.0055	0.0059	0.0061	0.0064	0.0066	0.0063	0.0067	0.0071	0.0072	0.0063	0.0042	0.0062	0.0075
137	######	######	######	######	######	######	######	######	######	######	######	######	33.8980	8.7960	2.2013	0.5058	0.1157	0.0243	0.0254	0.0803	0.1407	######	######
138	0.0060	0.0062	0.0061	0.0060	0.0057	0.0054	0.0054	0.0054	0.0052	0.0048	0.0048	0.0055	0.0059	0.0061	0.0059	0.0054	0.0051	0.0050	0.0050	0.0045	0.0044	0.0055	0.0062
139	0.0046	0.0045	0.0042	0.0039	0.0038	0.0035	0.0036	0.0037	0.0038	0.0039	0.0042	0.0043	0.0040	0.0035	0.0034	0.0034	0.0038	0.0042	0.0046	0.0045	0.0028	0.0040	0.0046
140	0.0076	0.0070	0.0056	0.0050	0.0042	0.0035	0.0039	0.0043	0.0046	0.0050	0.0055	0.0066	0.0076	0.0084	0.0089	0.0089	0.0093	0.0090	0.0085	0.0073	0.0039	0.0065	0.0093

Table C.14 (continued) Drift ratio demands for the *brittle* 20-story building model. Note the collapses (###'s).